

NATURAL GAS AND ELECTRICITY OPTIMAL POWER FLOW

By

SEUNGWON AN

Bachelor of Engineering
Korea Maritime University
Pusan, Korea
February, 1991

Master of Engineering
Oklahoma State University
Stillwater, Oklahoma
May, 1999

Submitted to the Faculty of the
Graduate College of the
Oklahoma State University
in partial fulfillment of
the requirements for
the Degree of
DOTOR OF PHILOSOPHY
May, 2004

NATURAL GAS AND ELECTRICITY OPTIMAL POWER FLOW

Thesis Approved:

Thesis Advisor

Dean of the Graduate College

Acknowledgment

I would like to express my sincere appreciation to my advisor Dr. Thomas W. Gedra for his intelligent supervision, friendship and confidence in me. I wish to thank the other members of my doctoral committee, Dr. Ramakumar, Dr. Yen and Dr. Misawa for their assistance throughout this work. I would like to give very special thanks to Dr. Ramakumar for his continuous guidance during my study at OSU.

I wish to take this opportunity to express my gratitude to Mr. Lee Clark for his assistance and encouragement in all aspects of my work. I wish to express my sincere gratitude to the School of Electrical and Computer Engineering for providing me with this research opportunity and generous financial support.

I am deeply indebted to all members of the Korean Catholic Community at Stillwater for their spiritual support. Especially, I would like to thank Mr. Hyunwoong Hong and Mrs. Eunjoo Kang for their brotherhood.

I am deeply grateful to my wife, Misook Kim, for her patience and to our twin boys, Clemens and Martino for their existence. My final appreciation goes to my parents and brothers for their enduring love, support and encouragement.

TABLE OF CONTENTS

1	INTRODUCTION	1
2	AC LOADFLOW	6
2.1	Flows on Transmission Systems	6
2.2	Loadflow Problem Statement	10
2.3	Newton-Raphson Method	13
3	ECONOMIC DISPATCH	17
3.1	Lossless Economic Dispatch	18
3.2	Economic Dispatch with Transmission Losses	22
4	OPTIMAL POWER FLOW AND SOLUTION METHODS	25
4.1	OPF by Newton's Method	27
4.2	Primal-Dual Interior-Point (PDIP) Method	31
5	NATURAL GAS FLOW MODELING	39
5.1	Elements of Natural Gas Transmission Network	40
5.2	Network Topology	41
5.3	Matrix Representations of Network	43
5.4	Flow Equation	43
5.5	Compressor Horsepower Equation	45
5.6	Conservation of Mass Flow	46
6	NATURAL GAS LOADFLOW	49
6.1	Loadflow Problem Statement	50
6.2	Loadflow without Compressors	52
6.3	Loadflow with Compressors	53

7	UPFC MODELING FOR STEADY-STATE ANALYSIS	57
7.1	Operating Principles	58
7.2	Uncoupled Model	59
7.3	Ideal Transformer Model	62
7.4	UPFC in a Transmission Line	65
8	GAS AND ELECTRICITY OPTIMAL POWER FLOW	69
8.1	Gas and Electric Combined Network	69
8.2	Gas and Electricity Optimal Power Flow	70
8.2.1	Cost, Benefit, and Social Welfare	71
8.2.2	Constraints	74
9	OPTIMAL LOCATION OF A UPFC IN A POWER SYSTEM	79
9.1	Optimal Power Flow with UPFC	79
9.2	First-Order Sensitivity Analysis	81
9.3	Second-Order Sensitivity Analysis	84
9.4	Estimation of Incremental Value	87
10	RESULTS	88
10.1	Result of Sensitivity Analysis	88
10.2	Result of GEOPF	92
10.2.1	Test System I	93
10.2.2	Test System II	95
11	CONCLUSIONS AND FUTURE WORK	101
	BIBLIOGRAPHY	104
A	DERIVATIVES REQUIRED FOR GEOPF	108
A.1	Electric Networks	108
A.2	Gas Network	115
A.3	Objective Function of GEOPF	119
B	DERIVATIVES REQUIRED FOR UPFC SENSITIVITIES	120

C	INPUT DATA FILE FORMAT	130
C.1	IEEE Common Data Format	130
C.2	Generator Data	133
C.3	Electricity Load Data	134
C.4	Natural Gas Common Data Format	135
C.5	Natural Gas Load Data	137
C.6	Natural Gas Source Data	138
D	MATLAB CODE	146
D.1	GEOPF	146
D.2	Base Case OPF with Sensitivity Analysis	157
D.3	OPF with a UPFC	167

LIST OF FIGURES

1.1	Monthly natural gas price trends at AECO hub in Canada	2
1.2	Average Virginia mine coal price (1975-2000, Virginia)	3
2.1	Bus i and connection to transmission system	7
4.1	Effect of barrier term	33
4.2	Graphical representation of central path	37
5.1	Pipeline network representation	40
5.2	Graph of the gas network	41
7.1	General UPFC scheme	58
7.2	Proposed UPFC model in a transmission line	59
7.3	Phasor diagram of UPFC input-output voltages and currents	60
7.4	Uncoupled UPFC model in a transmission line.	61
7.5	UPFC ideal transformer model	62
7.6	Simplified UPFC circuit	64
7.7	Cascaded transmission line with a UPFC	66
8.1	Combined natural gas and electricity network	70
10.1	Diagram of 5-bus subset of IEEE 14-bus system	88
10.2	Marginal and incremental values for 5-bus system	89
10.3	Marginal and incremental values for IEEE 14-bus system	90
10.4	Marginal and incremental values for IEEE 30-bus system	91

10.5 Combined gas and electric network	92
10.6 SW losses due to non-integrated operation for test system I	96
10.7 Combined gas and electric network	97
10.8 SW losses due to non-integrated operation for test system II	98

LIST OF TABLES

10.1	Real power generation, line loss and incremental value	89
10.2	GEOPF results for test system I	99
10.3	GEOPF results for test system II	100

CHAPTER 1

INTRODUCTION

Restructuring of natural gas and electric industries, both known as network industries, and deregulation of their products have been undertaken in the U.S. to minimize the social inefficiency incurred by regulated monopolies when natural monopoly has disappeared from their technologies [1]. Due to the successful deregulation of the natural gas market, the wellhead price of natural gas declined by 44 % between 1983 and 1997.

Electric power generation technologies utilizing natural gas are generally less capital-intensive and often more technically efficient than other alternatives. Thus, natural gas is playing an important role in electric power generation since 1990 partially due to incentives of the Clean Air Act Amendments (CAAA) of 1990. Since 1997, more than 120 GW of new capacity has been added by merchant energy companies at a lower cost per installed MW and with shorter construction times than in the past [2]. Most of this new generation is fueled by natural gas. However, due to the lack of financial instruments to lock in future prices to reduce price risk, the large increase in natural gas prices, and excess reserve margins, more than 110 GW of installed capacity belongs to entities that have below-investment-grade credit ratings (*i.e.*, junk bonds) [2]. Thus, we have been experiencing large price volatility in major natural gas markets while price volatility in electric markets has declined steadily over the past three years [2]. In addition, the floor price for natural gas in summer

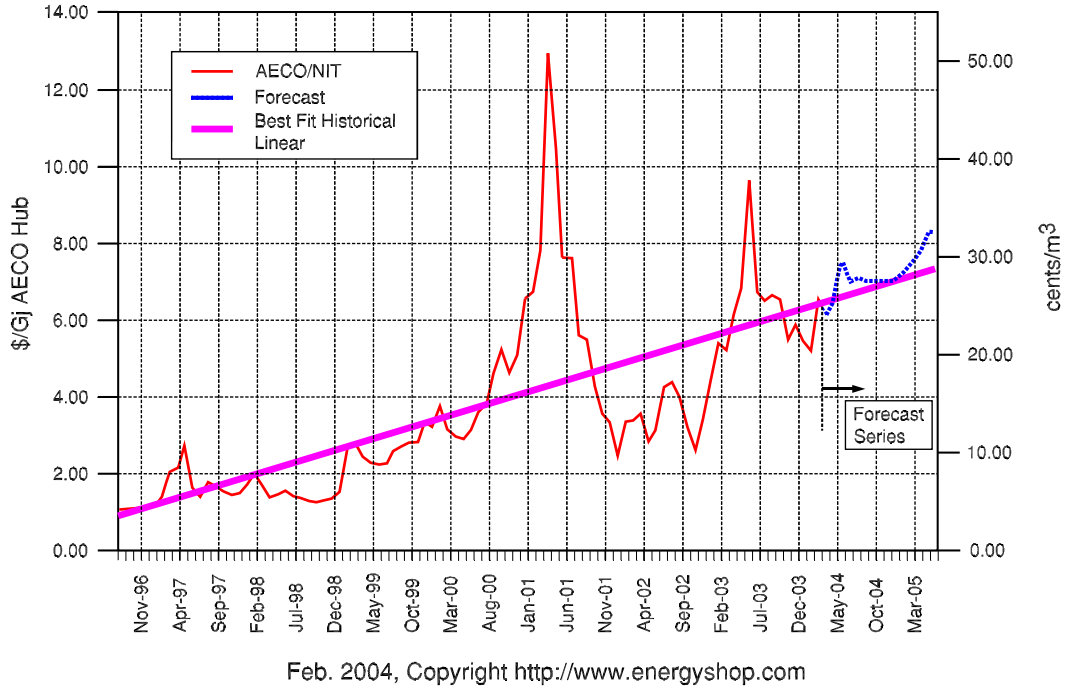


Figure 1.1: Monthly natural gas price trends at AECO hub in Canada

2003 reached over U.S. \$4.00 per MMBTU, as shown in Figure 1.1 (on the basis of 1 U.S. \$ = 0.75 nominal Canadian \$ in December 2003).

In the meantime, due to regulatory uncertainties posed by the restructuring of electric industries and environmental concerns, baseload units such as coal-fired power plants have been rarely built since 1990. The amount of electric energy generated by coal-fired generators has been almost constant since that time, resulting in decreases in coal price as illustrated in Figure 1.2. With increasing gas prices and with a diverging price gap between coal and natural gas, generation using natural gas may be no longer competitive with coal-fired generation. Consequently, a significant amount of planned natural gas generation capacity addition using natural gas has been cancelled or postponed in 2003 [2].

The exposure to price volatility and price risk should be better understood in competitive energy markets to promote efficient use and expansion of electric transmission and gas transportation networks, and to facilitate effective competition in power generation and gas supply [3]. The large-scale construction of gas-fired elec-

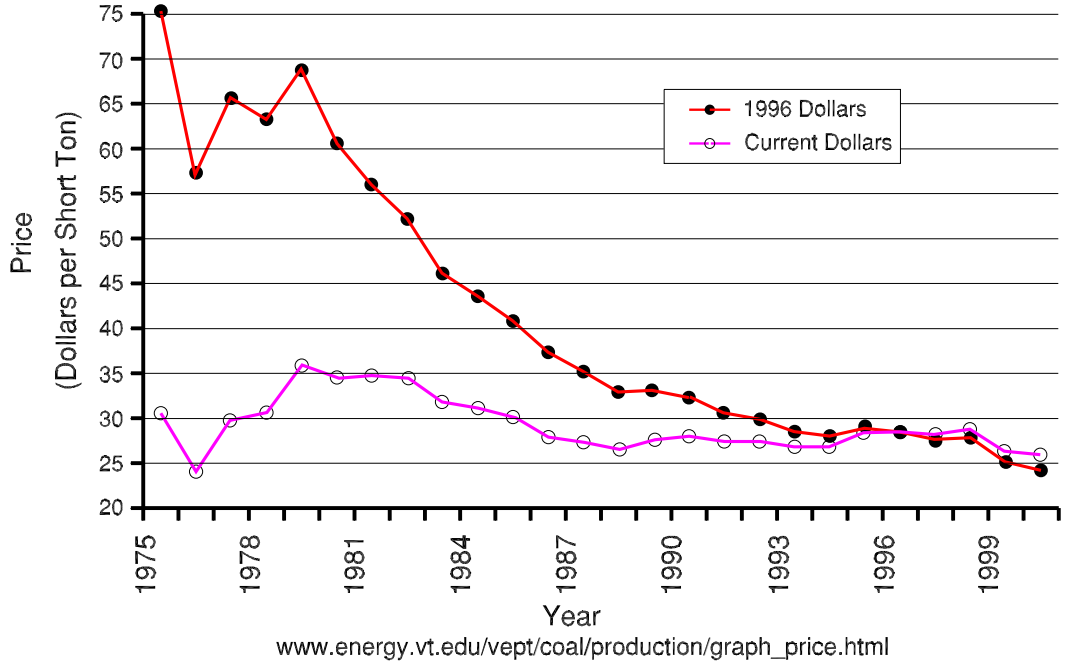


Figure 1.2: Average Virginia mine coal price (1975-2000, Virginia)

tric generation, combined with electric power restructuring, is expected to create an even greater convergence between electricity and natural gas markets. Lack of fuel diversity (*i.e.*, excessive dependence on natural gas with volatile prices, as opposed to coal, especially newer “clean coal” technology) will likely increase volatility of gas and electric prices, even if the price of coal is lower and less volatile. Therefore, viewing these markets separately without recognizing their increasing convergence is myopic at best, and disastrous at worst.

Economic forces in energy markets have been driving not only the optimal operation of energy networks but also efficient price-based system planning. The unified power flow controller (UPFC) is one of the most technically promising devices in the Flexible AC Transmission System (FACTS) family [4, 5, 6, 7]. It has the capability to control both voltage magnitude and phase angle, and can also independently provide (positive or negative) reactive power injections. However, it cannot be installed in all possible transmission lines due to its high capital cost. Thus, a need exists for developing a cost-benefit analysis technique to determine if installation of a UPFC

would be beneficial and the best location to install the UPFC. In principle, determining the optimal location for a UPFC is simple. For each possible location, we place a UPFC in the power system model and calculate the cost savings with respect to a base case (with no new UPFC installed). The operating cost at each time throughout the year and for each potential location is determined using an optimal power flow (OPF) program. However, the computational burden of evaluating this annual value for every possible line is immense because an OPF problem must be solved for each possible UPFC location and at each of several time periods. Therefore, an efficient screening technique is desired to identify the most promising locations so that at each point in time throughout the year, the exhaustive calculations described above do not have to be carried out for every location that is a candidate for installing the UPFC.

In this research, we introduce fundamental natural gas modeling for steady-state analysis, and propose general formulations to solve a combined natural gas and electric optimal power flow (GEOPF). In addition, a screening technique is developed for greatly reducing the computation involved in determining the optimal UPFC location in a large power system. This technique requires running only one optimal power flow (OPF) to obtain UPFC sensitivities for all possible transmission lines. To implement the screening technique, we develop a new mathematical model of UPFC under steady-state, consisting of an ideal transformer with a complex turns ratio and a variable shunt admittance.

We begin by reviewing basic concepts which describe power flows in power systems. Economic dispatch is discussed next, followed by the introduction of the optimal power flow concept and its solution methodology. A GEOPF model is described in detail after the introduction of natural gas network modeling. A screening technique based on sensitivity analysis is discussed next and a new UPFC model is described. The GEOPF model has been successfully applied to two test cases: a 15-node gas network with (i) a 5-bus electric network and (ii) a 9-bus electric network. The

screening technique (electricity only) has also been implemented in a 5-bus system and IEEE 14- and 30-bus systems. Discussions of results are presented in Chapter 10.

CHAPTER 2

AC LOADFLOW

Electric loadflow problems are solved routinely to study power systems under both normal operating conditions and under various contingencies using predicted data or to analyze “what if” scenarios. It is also of great importance in power system planning for future expansion. The principal information obtained from loadflow analysis is the magnitude and phase angle of the voltage at each bus. Using these values, we can calculate real and reactive power flows in transmission lines and transformers, and line losses.

In this chapter, we describe the formulation of the bus admittance ($\bar{\mathbf{Y}}_{\text{bus}}$) matrix, which represents a transmission line network, and explain how complex power injections into a network are related to the bus voltage magnitudes and angles. Then, we construct the loadflow problem and discuss some of its characteristics.

2.1 Flows on Transmission Systems

Consider a network of transmission lines connecting a set of buses in a power transmission system. We will find out the relationship between complex power and current injections into the transmission system and the phasor voltages at each bus. Figure 2.1 [8] shows connections to a transmission system at bus i . The double-subscript notation \bar{S}_{ik} and \vec{I}_{ik} , for $k \neq i$, indicates complex power or phasor current (respec-

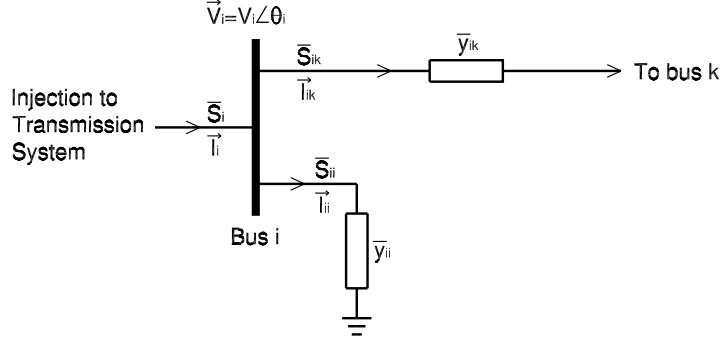


Figure 2.1: Bus i and connection to transmission system [8]

tively) flowing from bus i towards bus k along line ik . For $i = k$, the double subscript notations \bar{S}_{ii} and \vec{I}_{ii} indicate complex power and phasor current flowing to ground through the shunt element at bus i . The single subscript notations \bar{S}_i and \vec{I}_i indicate total complex power and phasor current injection into the transmission system at bus i . Generally, the complex power injected at bus i will consist of power generated by any generator(s) at bus i , minus any power consumed at bus i , or

$$\bar{S}_i = \bar{S}_{G_i} - \bar{S}_{D_i}. \quad (2.1)$$

If a line exists between bus i and bus k , and has a series impedance of \bar{z}_{ik} , the series admittance of the line will be defined as

$$\bar{y}_{ik} = \frac{1}{\bar{z}_{ik}}. \quad (2.2)$$

If bus i and bus k are not directly connected, then $\bar{y}_{ik} = 0$. In a similar way, we define the admittance of any shunt element connecting bus i to ground as \bar{y}_{ii} , which includes transmission line capacitive susceptance $jb/2$. The current flowing from bus i towards bus k is

$$\vec{I}_{ik} = \frac{1}{\bar{z}_{ik}}(\vec{V}_i - \vec{V}_k) = \bar{y}_{ik}(\vec{V}_i - \vec{V}_k), \quad (2.3)$$

while the current flowing through the shunt element \bar{y}_{ii} from bus i to ground is

$$\vec{I}_{ii} = \bar{y}_{ii}\vec{V}_i, \quad (2.4)$$

where \vec{V}_i denotes the phasor voltage at bus i . If the total number of buses is n , the total current injected into the power transmission system at bus i is

$$\vec{I}_i = \bar{y}_{ii}\vec{V}_i + \sum_{\substack{k=1 \\ k \neq i}}^n \bar{y}_{ik} (\vec{V}_i - \vec{V}_k), \quad (2.5)$$

or, collecting the \vec{V}_i terms,

$$\vec{I}_i = \vec{V}_i \sum_{k=1}^n \bar{y}_{ik} - \sum_{\substack{k=1 \\ k \neq i}}^n \bar{y}_{ik} \vec{V}_k. \quad (2.6)$$

The right side of the above equation motivates the following definition:

$$\bar{Y}_{ii} = \sum_{k=1}^n \bar{y}_{ik}, \quad (2.7)$$

$$\bar{Y}_{ik} = -\bar{y}_{ik}, \quad i \neq k. \quad (2.8)$$

With this definition, we can write

$$\vec{I}_i = \sum_{k=1}^n \bar{Y}_{ik} \vec{V}_k. \quad (2.9)$$

In matrix form, the definitions in equations (2.7) and (2.8) can be written as

$$\bar{\mathbf{Y}}_{\text{bus}} = \begin{bmatrix} \bar{y}_{11} + \cdots \bar{y}_{1n} & -\bar{y}_{12} & \cdots & -\bar{y}_{1n} \\ -\bar{y}_{21} & \bar{y}_{21} + \cdots \bar{y}_{2n} & \cdots & -\bar{y}_{2n} \\ \vdots & & \ddots & \vdots \\ -\bar{y}_{n1} & -\bar{y}_{n2} & \cdots & \bar{y}_{n1} + \cdots \bar{y}_{nn} \end{bmatrix}.$$

In words, the diagonal element ii of the $\bar{\mathbf{Y}}_{\text{bus}}$ matrix consists of the sum of all admittances connected to bus i (whether they are series admittances connecting to another bus or are shunt admittances), while the off-diagonal element ik is the negative of the series admittance connecting bus i to bus k . In the case that there is no transmission line connecting bus i with bus k , $\bar{y}_{ik} = 0$ as mentioned above. Likewise, $\bar{y}_{ii} = 0$ if no shunt element is present between bus i and ground. Note that, since the series admittance \bar{y}_{ik} connecting bus i to bus k is the same as that connecting bus k to bus i ,

we have $\bar{y}_{ik} = \bar{y}_{ki}$, so that the matrix $\bar{\mathbf{Y}}_{\text{bus}}$ is symmetrical, assuming no phase-shifting elements, which we have implicitly done.

If we define the bus voltage and bus current injection vectors as

$$\vec{\mathbf{V}} = \begin{bmatrix} \vec{V}_1 \\ \vec{V}_2 \\ \vdots \\ \vec{V}_n \end{bmatrix} \quad \text{and} \quad \vec{\mathbf{I}} = \begin{bmatrix} \vec{I}_1 \\ \vec{I}_2 \\ \vdots \\ \vec{I}_n \end{bmatrix},$$

then we can write equation (2.9) in matrix-vector form as

$$\vec{\mathbf{I}} = \bar{\mathbf{Y}}_{\text{bus}} \vec{\mathbf{V}}. \quad (2.10)$$

The matrix $\bar{\mathbf{Y}}_{\text{bus}}$ is called the bus admittance matrix, since it relates the bus voltages and the bus current injections.

The complex power injection at bus i can be written in terms of $\bar{\mathbf{Y}}_{\text{bus}}$ matrix elements as

$$\begin{aligned} \bar{S}_i &= \vec{V}_i \vec{I}_i^* = \vec{V}_i \sum_{k=1}^n \bar{Y}_{ik}^* \vec{V}_k^*, \\ &= V_i \sum_{k=1}^n V_k Y_{ik} e^{j(\theta_i - \theta_k - \delta_{ik})}, \end{aligned} \quad (2.11)$$

where

$$\begin{aligned} \vec{V}_i &= V_i \angle \theta_i, \quad \vec{V}_k = V_k \angle \theta_k, \quad \text{and} \\ \bar{Y}_{ik} &= G_{ik} + jB_{ik} = Y_{ik} \angle \delta_{ik}. \end{aligned}$$

We can split equation (2.12) into real and reactive parts, in terms of the bus voltage magnitudes $\{V_i, i = 1, \dots, n\}$ and bus voltage angles $\{\theta_i, i = 1, \dots, n\}$. Then the real and imaginary parts of equation (2.12) become

$$P_i(\vec{\mathbf{V}}) = \sum_{k=1}^n V_i V_k Y_{ik} \cos(\theta_i - \theta_k - \delta_{ik}), \quad (2.12)$$

$$Q_i(\vec{\mathbf{V}}) = \sum_{k=1}^n V_i V_k Y_{ik} \sin(\theta_i - \theta_k - \delta_{ik}). \quad (2.13)$$

The real and reactive power injections at bus i need to satisfy the following conditions:

$$P_{G_i} - P_{L_i} = P_i(\vec{\mathbf{V}}), \quad i = 1, \dots, n, \quad (2.14)$$

$$Q_{G_i} - Q_{L_i} = Q_i(\vec{\mathbf{V}}), \quad i = 1, \dots, n, \quad (2.15)$$

where

$$P_{G_i} = \text{real power generation at bus } i,$$

$$P_{L_i} = \text{real power load at bus } i,$$

$$Q_{G_i} = \text{reactive power generation at bus } i,$$

$$Q_{L_i} = \text{reactive power load at bus } i.$$

We can rewrite equations (2.12), (2.12) and (2.13) in matrix form as

$$\bar{\mathbf{S}} = \begin{bmatrix} \bar{S}_1 \\ \bar{S}_2 \\ \vdots \\ \bar{S}_n \end{bmatrix} = \begin{bmatrix} \vec{V}_1 \vec{I}_1^* \\ \vec{V}_2 \vec{I}_2^* \\ \vdots \\ \vec{V}_n \vec{I}_n^* \end{bmatrix} = \text{diag}\{\vec{\mathbf{V}}\} \vec{\mathbf{I}}^* = \text{diag}\{\vec{\mathbf{I}}^*\} \vec{\mathbf{V}}, \quad (2.16)$$

$$\mathbf{P} = \text{real}(\bar{\mathbf{S}}), \quad (2.17)$$

$$\mathbf{Q} = \text{imag}(\bar{\mathbf{S}}), \quad (2.18)$$

where $\text{diag}\{\vec{\mathbf{V}}\}$ denotes the diagonal matrix with the elements of the vector $\vec{\mathbf{V}}$ on its diagonal.

2.2 Loadflow Problem Statement

Since the loadflow solution is a prerequisite for many other analytical studies, it is necessary to mathematically state the problem to prepare the ground for the establishment of its links to economic dispatch and optimal power flow. The loadflow problem is stated below [8, 9, 10]:

- Given a power system described by a $\bar{\mathbf{Y}}_{\text{bus}}$ matrix, and given a subset of bus voltage magnitudes, bus voltage angles, and real and reactive power bus injections,
- Determine the other voltage magnitudes and angles and real and reactive power injections.

More precisely, two of the four quantities V_i , θ_i , P_i , and Q_i at each bus are specified, and the other two are to be determined. Each bus is classified based on the two known quantities, as follows:

- **PV bus**, or generator bus, or voltage-controlled bus. For a bus i of this type, we assume that we know the real power injection P_i and the voltage magnitude V_i . This is because the real power generation can be controlled by adjusting the prime mover input, and the voltage magnitude can be controlled by adjusting the generator field current. However, certain buses without generators may have some means of voltage support at that bus (such as a synchronous condenser, capacitor banks, or a static VAR compensator).
- **PQ bus**, or load bus. For a non-generator bus i , we assume that we know the real and reactive power injections P_i and Q_i , and the bus voltage magnitude V_i and angle θ_i are to be determined. In practice, only real power load is known and the reactive power load is calculated based on an assumed power factor by

$$Q_i = Q_{G_i} - \frac{P_{L_i}}{\text{p.f.}_i} \sqrt{1 - \text{p.f.}_i^2}.$$

We assume that a load is characterized by its constant complex power demand (which does not depend on the bus voltage V_i , as opposed to assuming that the load is a constant current or constant impedance load in which case the complex power demand would depend on the bus voltage V_i .)

In fact, solving the loadflow problem with buses of only these two types is not in general possible. The first reason is that, in the loadflow equations, the bus voltage angles never appear by themselves, but instead appear only as angle differences of the form $\theta_i - \theta_k$. Therefore, adding an angle to every bus voltage angle, will not change the values of real or reactive power injections in equations (2.12) and (2.13). Since phasor voltages are always expressed with respect to some reference voltage, we must decide on some reference phasor and refer all other phase angles to that reference. In fact, therefore, there are only $n - 1$ angles which influence the loadflows. We therefore pick one bus, say bus 1, to serve as our phasor reference, and set $\theta_1 = 0^\circ$.

Another reason is that solving a loadflow for a system containing only *PV* and *PQ* buses would imply that we know the real power injections at every single bus. In fact, we cannot specify all n real power injections, since we do not know all n real power injections until we solve the loadflow. Mathematically, the loadflow is overdetermined if we suppose we know all n real power injections. Specifying the injections at all buses is the same as specifying the real losses of the power system, which we cannot know until the loadflow is solved. Instead, we must pick one bus, and allow the real power injection at that bus to be whatever value is required to solve the loadflow equations. Thus, in addition to the *PV* and *PQ* bus types, we have a third bus type:

- **Slack Bus**, or $V\theta$, or reference, or swing bus. Typically it is a generator bus, and the voltage angle of the slack bus serves as a reference for the angles of all other bus voltages. We assume that we know V_1 and θ_1 , but we do not know P_1 and Q_1 . The usual practice is to set $\theta_1 = 0^\circ$ and $V_1 = 1$ although other values of V_1 are fine too.

2.3 Newton-Raphson Method

Equations (2.14) and (2.15) are in the form of the vector nonlinear equation $\mathbf{y} = \mathbf{f}(\mathbf{x})$, which can be solved by Newton-Raphson method [8, 9, 10]. The Newton-Raphson method is based on Taylor series expansion of $\mathbf{f}(\mathbf{x})$ about an operating point \mathbf{x}_o .

$$\mathbf{y} = \mathbf{f}(\mathbf{x}_o) + \left. \frac{\partial \mathbf{f}}{\partial \mathbf{x}} \right|_{\mathbf{x}=\mathbf{x}_o} (\mathbf{x} - \mathbf{x}_o) + \text{H.O.T.} \quad (2.19)$$

Neglecting the higher order terms in equation (2.19) and solving for \mathbf{x} , we have

$$\mathbf{x} = \mathbf{x}_o + \left[\left. \frac{\partial \mathbf{f}}{\partial \mathbf{x}} \right|_{\mathbf{x}=\mathbf{x}_o} \right]^{-1} \cdot (\mathbf{y} - \mathbf{f}(\mathbf{x}_o)). \quad (2.20)$$

The Newton-Raphson method replaces \mathbf{x}_o by the old value \mathbf{x}^k and \mathbf{x} by the new value \mathbf{x}^{k+1} for the iterative solution as shown below

$$\mathbf{x}^{k+1} = \mathbf{x}^k + \mathbf{J}^{-1} \cdot \Delta \mathbf{f}, \quad (2.21)$$

where

$$\begin{aligned} \mathbf{J} &= \left. \frac{\partial \mathbf{f}}{\partial \mathbf{x}} \right|_{\mathbf{x}=\mathbf{x}^k}, \\ \Delta \mathbf{f} &= (\mathbf{y} - \mathbf{f}(\mathbf{x}^k)). \end{aligned}$$

Equation (2.21) is repeated until the mismatches $\Delta \mathbf{f}$ are less than a specified tolerance, or the algorithm diverges.

Now, let us construct a mathematical formulation to solve the AC loadflow problem using the Newton-Raphson method. Assume that there are g generators. We assume that bus 1 is the slack bus, and buses 2 through g are *PV* buses. The $n - g$ buses will be assumed to be *PQ* buses. Then the problem becomes:

$$\begin{array}{ll} \text{Given} : & \begin{array}{ccccccc} \theta_1 & P_2 & \cdots & P_g & P_{g+1} & \cdots & P_n \\ V_1 & V_2 & \cdots & V_g & Q_{g+1} & \cdots & Q_n \end{array} \\ \text{Determine} : & \begin{array}{ccccccc} P_1 & \theta_2 & \cdots & \theta_g & \theta_{g+1} & \cdots & \theta_n \\ Q_1 & Q_2 & \cdots & Q_g & V_{g+1} & \cdots & V_n \end{array} \end{array}$$

Note that finding P_1 and Q_1 through Q_g is trivial, once all the voltage magnitudes and angles are known. The difficult part is to find $n-1$ unknown angles and the $n-g$ unknown voltage magnitudes. Let us define the \mathbf{x} , \mathbf{y} , and \mathbf{f} vectors for the loadflow problem as

$$\mathbf{x} = \begin{bmatrix} \theta \\ \mathbf{V} \end{bmatrix} = \begin{bmatrix} \theta_2 \\ \vdots \\ \theta_n \\ V_{g+1} \\ \vdots \\ V_n \end{bmatrix}, \quad \mathbf{y} = \begin{bmatrix} P_2 \\ \vdots \\ P_n \\ Q_{g+1} \\ \vdots \\ Q_n \end{bmatrix}, \quad \mathbf{f}(\mathbf{x}) = \begin{bmatrix} P_2(\mathbf{x}) \\ \vdots \\ P_n(\mathbf{x}) \\ Q_{g+1}(\mathbf{x}) \\ \vdots \\ Q_n(\mathbf{x}) \end{bmatrix}.$$

Note that there are $2n-g-1$ nonlinear equations, and there are $2n-1-g$ unknown voltages and angles. So we have exactly the right number of variables to force all the mismatches to zero. We will guess the unknown voltage magnitudes and angles of \mathbf{x}^k , and compare the calculated values of $\mathbf{P}(\mathbf{x}^k)$ and $\mathbf{Q}(\mathbf{x}^k)$ to the known values of \mathbf{P} and \mathbf{Q} . Then, we can evaluate the mismatches by

$$\Delta \mathbf{f} = \begin{bmatrix} \Delta P_2 \\ \vdots \\ \Delta P_n \\ \Delta Q_{g+1} \\ \vdots \\ \Delta Q_n \end{bmatrix} = \begin{bmatrix} P_2 - P_2(\mathbf{x}^k) \\ \vdots \\ P_n - P_n(\mathbf{x}^k) \\ Q_{g+1} - Q_{g+1}(\mathbf{x}^k) \\ \vdots \\ Q_n - Q_n(\mathbf{x}^k) \end{bmatrix}. \quad (2.22)$$

In this set of equations, the functions $P_i(\mathbf{x}^k)$ and $Q_i(\mathbf{x}^k)$ are those obtained from equations (2.12) and (2.13), or (2.17) and (2.18), while the numbers P_i and Q_i are the known values of real and reactive power injections at the buses where the injections are known. The resulting quantities ΔP_i and ΔQ_i are known as the real and reactive mismatch terms, because they represent the difference between the known injections and the values calculated based on our guesses.

To solve the AC loadflow problem, we need to update the Jacobian at each iteration. Many authors [9, 10] derived the Jacobian directly from equations (2.12) and (2.13). Even though this method is straightforward, it requires at least two *for* loop routines in Matlab. To avoid the *for* loop command, and to improve the speed of each iteration, we present an efficient technique to construct the Jacobian.

Let us define \mathbf{J}_{S_V} by

$$\mathbf{J}_{S_V} = \begin{bmatrix} \frac{\partial \bar{S}_1}{\partial V_1} & \frac{\partial \bar{S}_1}{\partial V_2} & \cdots & \frac{\partial \bar{S}_1}{\partial V_n} \\ \frac{\partial \bar{S}_2}{\partial V_1} & \frac{\partial \bar{S}_2}{\partial V_2} & \cdots & \frac{\partial \bar{S}_2}{\partial V_n} \\ \vdots & \vdots & \ddots & \vdots \\ \frac{\partial \bar{S}_n}{\partial V_1} & \frac{\partial \bar{S}_n}{\partial V_2} & \cdots & \frac{\partial \bar{S}_n}{\partial V_n} \end{bmatrix}.$$

The diagonal and off-diagonal elements of \mathbf{J}_{S_V} are given by

$$\frac{\partial \bar{S}_i}{\partial V_i} = e^{j\theta_i} \left[\sum_{k=1}^n \bar{Y}_{ik} \bar{V}_k \right]^* + \bar{V}_i \bar{Y}_{ii}^* e^{-j\theta_i}, \quad (2.23)$$

$$\frac{\partial \bar{S}_i}{\partial V_k} = \bar{V}_i \bar{Y}_{ik}^* e^{-j\theta_k}, \quad i \neq k \quad (2.24)$$

By noticing similarities in the above two equations, we can rewrite \mathbf{J}_{S_V} in compact form to be used in Matlab by

$$\mathbf{J}_{S_V} = \text{diag}(\vec{\mathbf{V}}) * \text{conj}(\vec{\mathbf{Y}}_{\text{bus}}) * \text{conj}(\text{diag}(\exp^{j\theta})) + \underbrace{\text{diag}(\exp^{j\theta}) * \text{conj}(\vec{\mathbf{I}})}_{\text{element to element multiplication}}. \quad (2.25)$$

Now, let us define \mathbf{J}_{S_θ} by

$$\mathbf{J}_{S_\theta} = \begin{bmatrix} \frac{\partial \bar{S}_1}{\partial \theta_1} & \frac{\partial \bar{S}_1}{\partial \theta_2} & \cdots & \frac{\partial \bar{S}_1}{\partial \theta_n} \\ \frac{\partial \bar{S}_2}{\partial \theta_1} & \frac{\partial \bar{S}_2}{\partial \theta_2} & \cdots & \frac{\partial \bar{S}_2}{\partial \theta_n} \\ \vdots & \vdots & \ddots & \vdots \\ \frac{\partial \bar{S}_n}{\partial \theta_1} & \frac{\partial \bar{S}_n}{\partial \theta_2} & \cdots & \frac{\partial \bar{S}_n}{\partial \theta_n} \end{bmatrix}.$$

The diagonal and off-diagonal elements of \mathbf{J}_{S_θ} are given by

$$\frac{\partial \bar{S}_i}{\partial \theta_i} = j\bar{S}_i - j\bar{V}_i \bar{Y}_{ii}^* \bar{V}_i^*, \quad (2.26)$$

$$\frac{\partial \bar{S}_i}{\partial \theta_k} = -j\bar{V}_i \bar{Y}_{ik}^* \bar{V}_k^*, \quad i \neq k. \quad (2.27)$$

In a similar way, \mathbf{J}_{S_θ} can be expressed in compact form by

$$\mathbf{J}_{S_\theta} = -j \text{diag}(\vec{\mathbf{V}}) * \text{conj}(\vec{\mathbf{Y}}_{\text{bus}}) * \text{conj}(\text{diag}(\vec{\mathbf{V}})) + \text{diag}(j\vec{\mathbf{S}}). \quad (2.28)$$

We can split the Jacobian into real and reactive parts as follows:

$$\begin{aligned} \mathbf{P}_{S_\theta} &= \text{real}(\mathbf{J}_{S_\theta}), & \mathbf{P}_{S_V} &= \text{real}(\mathbf{J}_{S_V}), \\ \mathbf{Q}_{S_\theta} &= \text{imag}(\mathbf{J}_{S_\theta}), & \mathbf{Q}_{S_V} &= \text{imag}(\mathbf{J}_{S_V}). \end{aligned}$$

Then, the full Jacobian \mathbf{J} is constructed as

$$\mathbf{J} = \begin{bmatrix} \mathbf{P}_{S_\theta} & \mathbf{P}_{S_V} \\ \mathbf{Q}_{S_\theta} & \mathbf{Q}_{S_V} \end{bmatrix}.$$

Since the voltage magnitudes at *PV* buses and the angle at the slack bus are known, their corresponding columns will be truncated from the Jacobian \mathbf{J} . In addition, since the real power injection at the slack bus, and the reactive power injections at *PV* buses and at the slack bus are unknown, their corresponding rows are removed from the Jacobian \mathbf{J} . Then, the modified Jacobian \mathbf{J}_m at the k th iteration becomes

$$\mathbf{J}_m = \begin{bmatrix} \frac{\partial P_2(\mathbf{x}^k)}{\partial \theta_2} & \dots & \frac{\partial P_2(\mathbf{x}^k)}{\partial \theta_n} & \frac{\partial P_2(\mathbf{x}^k)}{\partial V_{g+1}} & \dots & \frac{\partial P_2(\mathbf{x}^k)}{\partial V_n} \\ \vdots & \ddots & \vdots & \vdots & \ddots & \vdots \\ \frac{\partial P_n(\mathbf{x}^k)}{\partial \theta_2} & \dots & \frac{\partial P_n(\mathbf{x}^k)}{\partial \theta_n} & \frac{\partial P_n(\mathbf{x}^k)}{\partial V_{g+1}} & \dots & \frac{\partial P_n(\mathbf{x}^k)}{\partial V_n} \\ \frac{\partial Q_{g+1}(\mathbf{x}^k)}{\partial \theta_2} & \dots & \frac{\partial Q_{g+1}(\mathbf{x}^k)}{\partial \theta_n} & \frac{\partial Q_{g+1}(\mathbf{x}^k)}{\partial V_{g+1}} & \dots & \frac{\partial Q_{g+1}(\mathbf{x}^k)}{\partial V_n} \\ \vdots & \ddots & \vdots & \vdots & \ddots & \vdots \\ \frac{\partial Q_n(\mathbf{x}^k)}{\partial \theta_2} & \dots & \frac{\partial Q_n(\mathbf{x}^k)}{\partial \theta_n} & \frac{\partial Q_n(\mathbf{x}^k)}{\partial V_{g+1}} & \dots & \frac{\partial Q_n(\mathbf{x}^k)}{\partial V_n} \end{bmatrix}.$$

By using the mismatches in equation (2.22) and the modified Jacobian \mathbf{J}_m , we will update the unknown variables \mathbf{x} by equation (2.21).

Finally, once we have forced all the real and reactive mismatches to reasonably small values, by finding the unknown values of voltage magnitude and angle, we can now go back and find the unknown real and reactive injections.

CHAPTER 3

ECONOMIC DISPATCH

The economic dispatch problem is defined as the process of providing the required real power load demand and line losses by allocating generation among a set of on-line generating units such that total generation cost is minimized [8, 11, 12].

Let C be the generating cost in \$/hr, and it is often modelled analytically as a quadratic function of the power generated [8]. The cost function is derived from the generator heat rate curve. Analytically, the heat rate curve with a unit of BTU/kWh is represented in the following form:

$$H(P_G) = \frac{a}{P_G} + b + cP_G, \quad (3.1)$$

where P_G is the unit's real power generation level measured in kW. Given the heat rate curve, the next important function is the fuel rate, which is simply the rate, in BTU/hr, of consumption of fuel energy. So

$$F(P_G) = P_G H(P_G) = a + bP_G + cP_G^2. \quad (3.2)$$

If the cost of fuel is known as k \$/BTU, then the cost function with a unit of \$/hr becomes

$$C(P_G) = kF(P_G) = ka + kbP_G + kcP_G^2 = \alpha + \beta P_G + \gamma P_G^2. \quad (3.3)$$

In classic economic dispatch problems, the essential constraint on the operation is that the sum of the output powers must equal the load demand plus losses. In

addition, there are two inequality constraints that must be satisfied for each of the generator units. That is, the power output of each unit must be greater than or equal to the minimum power permitted and must also be less than or equal to the maximum power permitted on that particular unit.

3.1 Lossless Economic Dispatch

We assume that the utility is responsible for supplying its customers' load. The utility's objective is to minimize the total cost of generation, assuming that transmission losses are neglected. Then, the ideal economic dispatch problem is stated in terms of minimizing total generation cost subject to satisfying the total load demand. Mathematical formulation of lossless economic dispatch problem can be expressed as

$$\min_{\{P_{G_1}, \dots, P_{G_n}\}} \sum_{i=1}^n C_i(P_{G_i}) \quad (3.4)$$

subject to:

$$\sum_{i=1}^n P_{G_i} = P_D \quad (3.5)$$

$$\text{and} \quad P_{G_i}^{\min} \leq P_{G_i} \leq P_{G_i}^{\max}, \quad i = 1, \dots, n \quad (3.6)$$

where

$$P_D = \sum_{i=1}^n P_{D_i}$$

is the total system load.

We will ignore the constraints in equation (3.6) on generator limits, assuming that these limits are not binding. Considering only constraint (3.5), the Lagrangian is

$$\mathcal{L} = \sum_{i=1}^n C_i(P_{G_i}) - \lambda \left[\sum_{i=1}^n P_{G_i} - P_D \right]. \quad (3.7)$$

Differentiating with respect to P_{G_i} , we obtain the first-order conditions

$$0 = \frac{\partial \mathcal{L}}{\partial P_{G_i}} = \text{MC}_i - \lambda, \quad i = 1, \dots, n \quad (3.8)$$

or

$$\text{MC}_i = \lambda, \quad i = 1, \dots, n$$

where

$$\text{MC}_i = \frac{\partial C_i}{\partial P_{G_i}}.$$

The quantity λ , the Lagrange multiplier, associated with the energy balance constraint in equation (3.5), is universally called the “system lambda” and is the price associated with generating slightly more energy. Thus, the criterion for optimal economic distribution of load among n generators is that all generators should generate output at the same marginal operating cost, sometimes called *incremental cost*. That is

$$\frac{\partial C_1}{\partial P_{G_1}} = \frac{\partial C_2}{\partial P_{G_2}} = \dots = \frac{\partial C_n}{\partial P_{G_n}}. \quad (3.9)$$

In the case of quadratic cost functions, the solution to the economic dispatch problem can be calculated analytically, as follows [8]. We have, for each unit,

$$\lambda = \text{MC}_i = \beta_i + 2\gamma_i P_{G_i}, \quad (3.10)$$

which can be solved for P_{G_i} to give

$$P_{G_i} = \frac{\lambda - \beta_i}{2\gamma_i}. \quad (3.11)$$

The total generation at this λ is obtained by summing over all the units. Setting this total equal to the load P_D , we obtain

$$P_D = \sum_{i=1}^n P_{G_i} = \sum_{i=1}^n \frac{\lambda - \beta_i}{2\gamma_i} = \lambda \sum_{i=1}^n \frac{1}{2\gamma_i} - \sum_{i=1}^n \frac{\beta_i}{2\gamma_i}, \quad (3.12)$$

which can be solved to obtain the λ required for a given P_D :

$$\lambda = \frac{\left[P_D + \sum_{i=1}^n \frac{\beta_i}{2\gamma_i} \right]}{\sum_{i=1}^n \frac{1}{2\gamma_i}} \quad (3.13)$$

Finally, this value of λ can be substituted back into the expression for P_{G_k} to obtain

$$P_{G_k} = \frac{\frac{1}{2\gamma_k}}{\sum_{i=1}^n \frac{1}{2\gamma_i}} \left[P_D + \sum_{i=1}^n \frac{\beta_i}{2\gamma_i} \right] - \frac{\beta_k}{2\gamma_k}, \quad (3.14)$$

which gives the dispatch for unit k directly in terms of the total load P_D . We define the “participation factor” for unit k as

$$K_k = \frac{\frac{1}{2\gamma_k}}{\sum_{i=1}^n \frac{1}{2\gamma_i}}.$$

We can see from the definition that

$$\sum_{i=1}^n K_i = 1.$$

Generally, the meaning of the participation factor is

$$K_k = \frac{dP_{G_k}}{dP_D}.$$

Thus, if the load were to increase by a small increment (say 1MW), unit k would supply the fraction K_k of the increase. The fact that the participation factors sum to 1 simply means that any increase in load is met exactly by an increase in generation.

We can include the generator limit constraints (3.6) in one of two ways. Traditionally, we ignore the limits, perform economic dispatch, and check to see if any limits are violated. If the limit for one generator is violated, we set the generator to its limit, remove it from the set of generators included in economic dispatch, and subtract the limit from the total load P_D . In other words, we take the generator “off of economic dispatch” and then proceed to treat it as a negative load¹.

More formally, we can just include the generation limits in the Lagrangian function. Let μ_i^{\min} be the Lagrange multiplier for the lower limit of unit i , and μ_i^{\max} be

¹This may result in “cycling” of the set of active constraints, especially if there are many diverse generators. Other optimization techniques, such as a primal-dual interior-point (PDIP) method [13] can be used to avoid this problem.

the multiplier for the generator's upper limit. Then, the Lagrangian becomes

$$\begin{aligned}\mathcal{L} = & \sum_{i=1}^n C_i(P_{G_i}) - \lambda \left[\sum_{i=1}^n P_{G_i} - P_D \right] \\ & + \sum_{i=1}^n \mu_i^{\min} [P_{G_i}^{\min} - P_{G_i}] + \sum_{i=1}^n \mu_i^{\max} [P_{G_i} - P_{G_i}^{\max}].\end{aligned}\quad (3.15)$$

Now, taking the derivative of \mathcal{L} with respect to each P_{G_i} , and setting to zero, we obtain

$$0 = \frac{\partial \mathcal{L}}{\partial P_{G_i}} = MC_i - \lambda - \mu_i^{\min} + \mu_i^{\max}, \quad i = 1, \dots, n \quad (3.16)$$

or

$$MC_i = \lambda + \mu_i^{\min} - \mu_i^{\max}, \quad i = 1, \dots, n \quad (3.17)$$

We also have the complementary slackness conditions on the inequality constraints:

$$\begin{aligned}\mu_i^{\min} [P_{G_i}^{\min} - P_{G_i}] &= 0, \quad \text{and} \\ \mu_i^{\max} [P_{G_i} - P_{G_i}^{\max}] &= 0.\end{aligned}$$

But P_{G_i} cannot be at its upper and lower limits simultaneously, so there are only three possibilities for each generator:

$$\begin{aligned}P_{G_i} = P_{G_i}^{\max} &\Rightarrow \mu_i^{\max} \geq 0, \quad \mu_i^{\min} = 0, \\ P_{G_i}^{\min} \leq P_{G_i} \leq P_{G_i}^{\max} &\Rightarrow \mu_i^{\max} = 0, \quad \mu_i^{\min} = 0, \\ P_{G_i} = P_{G_i}^{\min} &\Rightarrow \mu_i^{\max} = 0, \quad \mu_i^{\min} \geq 0.\end{aligned}$$

If the limits on some generators are binding, the generators may not be able to generate output at the system incremental cost λ . Suppose that none of generators reach their limits, and all generators participate in economic dispatch. As the load increases by a small increment, each generator will supply the fraction of the load increase, which is determined by the participation factor. If a generator hits its maximum limit, the generator cannot participate in economic dispatch even though it has a lower incremental cost than the system incremental cost λ .

On the other hand, suppose that the load decreases and one of generators hits its minimum limit. Since the generator must generate the required minimum capacity in order to stay on-line, the generator cannot participate in economic dispatch for the load decrements. Thus, if the load decreases further, the incremental cost of the generator hit its minimum limit is greater than or equal to the system incremental cost λ . The optimal criterion for lossless economic dispatch with generator limits can be summarized as [11]

$$\begin{aligned} P_{G_i} = P_{G_i}^{\max} &\Rightarrow \frac{dC_i}{dP_{G_i}} \leq \lambda, \\ P_{G_i}^{\min} \leq P_{G_i} \leq P_{G_i}^{\max} &\Rightarrow \frac{dC_i}{dP_{G_i}} = \lambda, \\ P_{G_i} = P_{G_i}^{\min} &\Rightarrow \frac{dC_i}{dP_{G_i}} \geq \lambda. \end{aligned}$$

3.2 Economic Dispatch with Transmission Losses

We now wish to include the effect of transmission losses on economic dispatch [8, 12]. In lossless dispatch, the location of individual loads did not matter, but when transmission losses are considered, the solution depends both on the load locations and on the outputs of individual generators around the system.

If we know the load P_{D_i} , and generation P_{G_i} at each bus in the system, we can calculate the real power injections P_2, \dots, P_n using $P_i = P_{G_i} - P_{D_i}$. From loadflow, we can then calculate the power injection at the slack bus, $P_1 = P_{G_1} - P_{D_1}$. From this information, we can calculate losses as

$$\begin{aligned} P_L(P_{G_2}, \dots, P_{G_n}, P_{D_2}, \dots, P_{D_n}) &= \sum_{i=2}^n (P_{G_i} - P_{D_i}) \\ &+ P_1(P_{G_2}, \dots, P_{G_n}, P_{D_2}, \dots, P_{D_n}). \end{aligned} \quad (3.18)$$

Note that in our formulation, we do not consider P_L to be a function of P_{G_1} , since the slack bus generation P_{G_1} is completely determined by the injections at other buses and the slack bus demand P_{D_1} .

Now our problem becomes

$$\min_{\{P_{G_1}, \dots, P_{G_n}\}} \sum_{i=1}^n C_i(P_{G_i}) \quad (3.19)$$

subject to:

$$\sum_{i=1}^n P_{G_i} = P_D + P_L(P_{G_2}, \dots, P_{G_n}) \quad (3.20)$$

$$\text{and} \quad P_{G_i}^{\min} \leq P_{G_i} \leq P_{G_i}^{\max}, \quad i = 1, \dots, n \quad (3.21)$$

where we have suppressed the dependence of P_L on the loads $\{P_{D_i}\}$, which are assumed to be fixed. The Lagrangian for the problem now becomes

$$\mathcal{L} = \sum_{i=1}^n C_i(P_{G_i}) - \lambda \left[\sum_{i=1}^n P_{G_i} - P_D - P_L(P_{G_2}, \dots, P_{G_n}) \right]. \quad (3.22)$$

Differentiating and setting to zero yields

$$\begin{aligned} 0 &= \frac{\partial \mathcal{L}}{\partial P_{G_1}} = \text{MC}_1 - \lambda, \quad \text{and} \\ 0 &= \frac{\partial \mathcal{L}}{\partial P_{G_i}} = \text{MC}_i - \lambda \left(1 - \frac{\partial P_L}{\partial P_{G_i}} \right), \quad i = 2, \dots, n \end{aligned}$$

or

$$\begin{aligned} \lambda &= \text{MC}_1, \quad \text{and} \\ \lambda &= \text{MC}_i \frac{1}{1 - \frac{\partial P_L}{\partial P_{G_i}}}, \quad i = 2, \dots, n \end{aligned}$$

Finally, let us define the *loss-penalty factors*

$$\begin{aligned} L_1 &= 1, \quad \text{and} \\ L_i &= \frac{1}{1 - \frac{\partial P_L}{\partial P_{G_i}}}, \quad i = 2, \dots, n \end{aligned} \quad (3.23)$$

Then we can write our condition for economic dispatch as

$$\lambda = \text{MC}_i \cdot L_i, \quad i = 1, \dots, n \quad (3.24)$$

The idea behind the loss penalty factors can be explained as follows. If increasing a generator's output increases system losses, then that generator's entire increment of

generation is not available to the system. So, if a generator's output increases by 1MW but losses increase by 0.1MW, the generator has only provided a net increase in system generation of 0.9MW. Thus, the cost of this increment is not the generator's marginal cost but $MC/0.9$ instead, or $MC_i \cdot L_i$. Similarly, an increase in a generator's output could result in a decrease in system losses. Such a generator would have a loss penalty factor $L_i < 1$, since the effective cost of incremental generation from such a generator would be less than its actual marginal cost.

The loss penalty factors can either be obtained as the result of running a loadflow, or they can be obtained from a quadratic approximation to the loss function, called B-matrix formula [11].

CHAPTER 4

OPTIMAL POWER FLOW AND SOLUTION METHODS

Note that the classic economic dispatch (ED) problem does not strictly take into account power flows in the transmission system. Typically, one would solve the economic dispatch problem, then the loadflow problem, and repeat the process. The most recent loadflow provides the loss-penalty factors for the current operating state, then the ED changes the state slightly to minimize cost, and so on [8]. Provided no transmission lines are overloaded, and no voltages are outside of the allowable range, this works well. However, if the result of the economic dispatch is fed into the loadflow, and the result indicates that transmission line loading is excessive, or that bus voltage magnitudes are outside of the allowable range (typically 95% to 105% of the nominal value), no information is given by the loadflow to indicate how to redispatch generation to alleviate the overloads or restore acceptable voltage levels. Often, the system dispatcher, being extremely familiar with the system, will take some units off of economic dispatch and manually re-dispatch them to remove the line overload. There is no guarantee that such a procedure will result in the minimum cost subject to operating limits although sometimes they do fairly well.

Similarly, economic dispatch does not consider reactive flows or bus voltages, whereas loadflow considers these quantities as given or to be found from other voltages and reactive injections [8]. Neither problem considers the adjustment of bus voltages to help to minimize cost, even though reactive power flows can contribute significantly

to real power losses and thus to overall cost.

However, we can reformulate our optimization problem by including economic dispatch, voltage and reactive injections as decision variables, and various operational limits. The optimal power flow (OPF) combines economic dispatch and loadflow into a single problem, which can be written in very general terms as

$$\min_Y C(Y) \tag{4.1}$$

subject to:

$$\begin{aligned} h_i(Y) &= 0, & i &= 1, \dots, n, \\ g_i(Y) &\leq 0, & i &= 1, \dots, m, \end{aligned}$$

where

- Y : a vector of control and state variables,
- $C(Y)$: an objective function,
- $h(Y)$: a set of equality constraints, which are power flow equations,
- $g(Y)$: a set of inequality constraints, such as voltage limits, generator capacity limits, and line flow limits.

Tap-changing transformers and/or Flexible AC Transmission System (FACTS) devices also can be incorporated in the OPF problem [9, 14].

The OPF has been used as a tool to improve power system planning, and operation by adjusting the objective function and/or the constraints. From the power system planning point of view, the OPF can be used to determine the optimal types, sizes, settings, capital costs, and optimal locations of resources, such as generators, transmission lines, and FACTS devices [14, 15].

Another application of the OPF is to determine various system marginal costs. It can be used to determine short-run electric pricing (*i.e.* spot pricing), transmission

line pricing, and pricing ancillary services such as voltage support through MVAR support.

Since the work in this research is based on solving the proposed optimization problem by a primal-dual interior-point (PDIP) method using logarithmic barrier function, the PDIP will be discussed in detail after a brief introduction of Newton's method.

4.1 OPF by Newton's Method

Newton-Raphson method has been the standard solution algorithm for the economic dispatch and loadflow problems for several decades [11, 12]. Newton's method is a very powerful algorithm because of its rapid convergence near the solution. This property is especially beneficial for power system applications because an initial guess close to the solution is easily obtained [16]. For example, voltage magnitude at each bus is presumably near the rated system value, generator outputs can be estimated from historical data, and transformer tap ratios are near 1.0 p.u. during steady-state operation.

The solution of the constrained optimization problem stated in (4.1) requires the mathematical formation of the Lagrangian by

$$\mathcal{L}(Y, \lambda, \mu) = C(Y) + \sum_{i=1}^n \lambda_i h_i(Y) + \sum_{i \in \mathcal{A}} \mu_i g_i(Y), \quad (4.2)$$

where λ_i is the *Lagrange multiplier* for the i^{th} equality constraint. Assuming that we know which inequality constraints are binding, and have put them in the set \mathcal{A} , then the inequality constraints can now be enforced as equality constraints. Thus the μ_i 's in equation (4.2) have the same property as λ_i 's and they are the Lagrange multipliers for *binding* inequality constraints. However, we need $\mu_i \geq 0$ for every i [8]. We can ignore the inequality constraints that are not binding since their μ 's are

known to be zero by *complementary slackness* condition [8]. That is

$$g_i(Y) \leq 0 \Rightarrow \mu_i = 0,$$

$$g_i(Y) = 0 \Rightarrow \mu_i \geq 0.$$

Therefore, only binding inequality constraints are included in the Lagrangian function (4.2) with corresponding nonzero μ 's.

Solution of a constrained optimization problem can be solved by adjusting control and state variables, and Lagrange multipliers to satisfy the following *first-order necessary optimality conditions* :

$$1) \quad \frac{\partial \mathcal{L}}{\partial Y_i} = 0, \tag{4.3}$$

$$2) \quad \frac{\partial \mathcal{L}}{\partial \lambda_i} = 0, \tag{4.4}$$

$$3) \quad \frac{\partial \mathcal{L}}{\partial \mu_i} = g_i = 0, \tag{4.5}$$

$$4) \quad \mu_i \geq 0 \text{ and } \mu_i g_i = 0. \tag{4.6}$$

The above equations are also called the *Karush-Kuhn-Tucker* (KKT) conditions.

Let us define

$$\omega(z) = \nabla_z \mathcal{L}(z) = \left[\frac{\partial \mathcal{L}}{\partial Y} \quad \frac{\partial \mathcal{L}}{\partial \lambda} \quad \frac{\partial \mathcal{L}}{\partial \mu_{\mathcal{A}}} \right]^T = 0, \tag{4.7}$$

where z is a vector of $[Y^T \quad \lambda^T \quad \mu_{\mathcal{A}}^T]^T$, and \mathcal{A} represents the binding inequality constraints.

To solve the KKT conditions, Newton's method is applied by using the Taylor's series expansion around a current point z^p as:

$$\omega(z) = \omega(z^p) + \frac{\partial \omega(z)}{\partial z} \bigg|_{z=z^p} \cdot (z - z^p) + \underbrace{\frac{1}{2} (z - z^p)^T \cdot \frac{\partial^2 \omega(z)}{\partial z^2} \bigg|_{z=z^p} \cdot (z - z^p)}_{\text{H.O.T}} + \dots = 0,$$

The current point z^p can either be an initial guess in the first iteration of the computation, or the estimate solution from the prior iteration. Recall that we want $\omega(z) = 0$. By ignoring the high order terms (H.O.T) and defining $\Delta z = z - z^p$, the

above equation can be rewritten as:

$$\left. \frac{\partial \omega(z)}{\partial z} \right|_{z=z^p} \cdot \Delta z = -\omega(z^p). \quad (4.8)$$

The quantity Δz is the update vector, or the *Newton step*, and it tells how far and in which direction the variables and multipliers should move from this current point z^p to get closer to the solution. Since $\omega(z)$ is the gradient of the Lagrangian function $\mathcal{L}(z)$, equation (4.8) can be written in terms of the Lagrangian function $\mathcal{L}(z)$ as:

$$\left. \frac{\partial^2 \mathcal{L}(z)}{\partial z^2} \right|_{z=z^p} \cdot \Delta z = - \left. \frac{\partial \mathcal{L}(z)}{\partial z} \right|_{z=z^p}. \quad (4.9)$$

Or, simply

$$W \cdot \Delta z = -\omega(z), \quad (4.10)$$

where W denotes the second order derivatives (or the *Hessian matrix*) and ω is the gradient, both of the Lagrangian function with respect to z evaluated at the current point. Equation (4.10) can be written in matrix form as

$$\begin{bmatrix} H_Y & J^T & A^T \\ J & 0 & 0 \\ A & 0 & 0 \end{bmatrix} \begin{bmatrix} \Delta Y \\ \Delta \lambda \\ \Delta \mu_A \end{bmatrix} = - \begin{bmatrix} \nabla_Y \mathcal{L} \\ \nabla_\lambda \mathcal{L} \\ \nabla_{\mu_A} \mathcal{L} \end{bmatrix}, \quad (4.11)$$

where the Hessian matrix H_Y and Jacobian matrices J and A are given as follows:

$$\begin{aligned} H_Y &= \frac{\partial^2 \mathcal{L}(z)}{\partial Y^2}, \\ J &= \frac{\partial^2 \mathcal{L}(z)}{\partial \lambda \partial Y} = \frac{\partial h(Y)}{\partial Y}, \\ A &= \frac{\partial^2 \mathcal{L}(z)}{\partial \mu_A \partial Y} = \frac{\partial g_A(Y)}{\partial Y}, \end{aligned}$$

where g_A is a set of binding inequality constraints. The Newton step can be obtained by solving (4.10). Then a vector of estimated solution for the next iteration is updated as:

$$z^{p+1} = z^p + \alpha \Delta z, \quad (4.12)$$

where α is usually 1, but can be adjusted to values above or below 1 to speed up convergence or cause convergence in a divergent case. It is important that special attention be paid to the inequality constraints. Equation (4.2) only includes binding inequality constraints being enforced as equality constraints. Thus, after obtaining an updated set of variables and multipliers, a new set of binding inequality constraints (or what we think is the active set) should be determined as follows [12]:

- If the updated μ 's of the constraint functions in the current active set are zero or have become negative, then the corresponding constraints must be released from the current active set because $\mu_i < 0$ implies that $g_i = 0$ keeps the trial solution at the edge of the feasible region instead of allowing the trial solution to move into the interior of the feasible region.
- If other constraint functions evaluated at the updated variables violate their limits, then those constraints must be included in the new active set. The variable α may be chosen to prevent constraint violations, but $\alpha < 1$ to avoid infeasibility implies that the constraint would otherwise be violated.

As a result, if μ_i is positive, continued enforcement will result in an improvement of the objective function, and enforcement is maintained. If μ_i is negative, then enforcement will result in an decrease of the objective function, and enforcement is stopped.

Once the active set has been updated, $\omega(z^{p+1})$ is checked for convergence. There are several criteria for checking convergence of Newton's method. The convergent tolerance may be set on the maximum absolute value of elements in $\omega(z)$, or on its norm. If the updated z^{p+1} does not satisfy the desired convergence criterion, the Newton step calculation is repeated.

4.2 Primal-Dual Interior-Point (PDIP) Method

One of disadvantages of Newton's method is to identify a set of binding inequality constraints, or active constraints. Among several methods to avoid the difficulty associated with guessing the correct active set, the PDIP method has been acknowledged as one of the most successful [12, 17, 18]. Interior point methods for optimization have been widely known since the publication of Karmarkar's seminal paper in 1984 [19]. Barrier function methods were proposed much earlier in Russia but little attention was paid because the algorithm was so slow in implementation. Later, this method was shown to be equivalent to the interior point methods. Karmarkar's method results in numerical ill-conditioning although this problem is not so bad with the PDIP method.

The method uses a barrier function that is continuous in the interior of the feasible set, and becomes unbounded as the boundary of the set is approached from its interior. Two examples of such a function [13, 20] are the logarithmic function, as shown in Figure 4.1

$$\phi(Y) = -\sum_{i=1}^m \ln(-g_i(Y)), \quad (4.13)$$

and the inverse of the inequality function

$$\phi'(Y) = \sum_{i=1}^m \frac{1}{-g_i(Y)}, \quad (4.14)$$

where

$$g_i(Y) \leq 0.$$

The barrier method generates a sequence of strictly feasible iterates that converge to a solution of the problem from the interior of the feasible region [13, 20].

To apply the primal-dual interior point algorithm to the OPF problem that has equality and inequality constraints, we construct the nonlinear equality and

inequality-constrained optimization problem as

$$\min_Y f(Y) \tag{4.15}$$

subject to

$$\begin{aligned} h_i(Y) &= 0, & i &= 1, \dots, n, \\ g_i(Y) &\leq 0, & i &= 1, \dots, m. \end{aligned}$$

To solve the problem, we first form the *logarithmic barrier function* as

$$B = f(Y) - \nu \sum_{i=1}^m \ln(-g_i(Y)), \tag{4.16}$$

where the parameter ν is referred to as the barrier parameter, a positive number that is reduced to approach to zero as the algorithm converges to the optimum. Then we solve a sequence of constrained minimization problems of the form

$$\min_{(Y, \lambda, \nu)} B(Y, \lambda, \nu) \tag{4.17}$$

subject to

$$h_i(Y) = 0, \quad i = 1, \dots, n,$$

for a sequence $\{\nu_k\}$ of positive barrier parameters that decrease monotonically to zero. The solution of this problem by Newton's method requires the formulation of the Lagrangian function

$$\mathcal{L} = f(Y) - \sum_{i=1}^n \lambda_i h_i(Y) - \nu \sum_{i=1}^m \ln(-g_i(Y)). \tag{4.18}$$

Because the barrier term is infinite on the boundary of the feasible region, as shown in Fig. 4.1, it acts as a repelling force that drives the current trial solution away from the boundary into the interior of the feasible region. As the barrier parameter ν is decreased, the effect of the barrier term is diminished, so that the iterates can gradually approach the constraint boundaries of the feasible region for those constraints which eventually turn out to be binding.

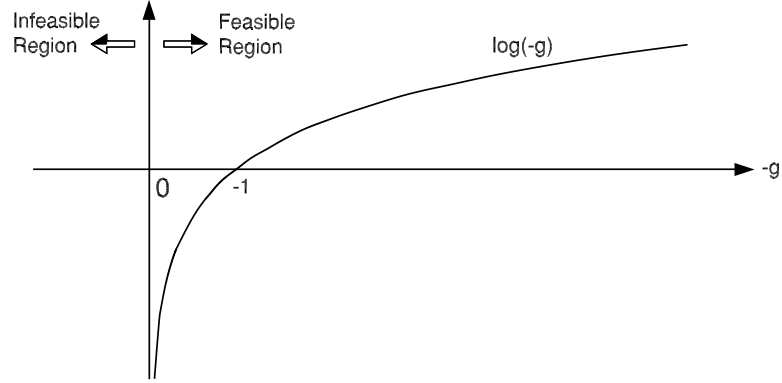


Figure 4.1: Effect of barrier term

To solve equation (4.17), we need to find the gradient of \mathcal{L} with respect to Y :

$$\begin{aligned}
\nabla_Y \mathcal{L} &= \nabla_Y f(Y) - \sum_{i=1}^n \lambda_i \nabla_Y h_i(Y) + \nu \sum_{i=1}^m \frac{1}{-g_i(Y)} \nabla_Y g_i(Y) \\
&= \nabla_Y f(Y) - \sum_{i=1}^n \lambda_i \nabla_Y h_i(Y) + \nu \sum_{i=1}^m \frac{1}{s_i} \nabla_Y g_i(Y) \\
&= \nabla_Y f(Y) - \sum_{i=1}^n \lambda_i \nabla_Y h_i(Y) + \sum_{i=1}^m \mu_i \nabla_Y g_i(Y) \\
&= \nabla_Y f(Y) - h_Y^T \lambda + g_Y^T \mu,
\end{aligned} \tag{4.19}$$

where

$$\begin{aligned}
-g_i(Y) &= s_i, & i &= 1, \dots, m, \\
\mu_i s_i &= \nu, & i &= 1, \dots, m,
\end{aligned}$$

h_Y^T is a matrix consisting of the gradient $\nabla_Y h_i(Y)$ as columns, and g_Y^T is a matrix consisting of the gradient $\nabla_Y g_i(Y)$ as columns, or

$$\begin{aligned}
h_Y^T &= \begin{bmatrix} \nabla_Y h_1(Y) & \nabla_Y h_2(Y) & \cdots & \nabla_Y h_n(Y) \end{bmatrix}, \\
g_Y^T &= \begin{bmatrix} \nabla_Y g_1(Y) & \nabla_Y g_2(Y) & \cdots & \nabla_Y g_m(Y) \end{bmatrix}.
\end{aligned}$$

Also, λ is a vector containing the elements λ_i , and μ is a vector containing the elements

μ_i . The set of equations we must solve is

$$\nabla_Y f - \sum_{i=1}^n \lambda_i \nabla h_i + \sum_{i=1}^m \mu_i \nabla g_i = 0, \quad (4.20)$$

$$h_i(Y) = 0, \quad i = 1, \dots, n \quad (4.21)$$

$$g_i(Y) + s_i = 0, \quad i = 1, \dots, m \quad (4.22)$$

$$\mu_i s_i - \nu = 0, \quad i = 1, \dots, m \quad (4.23)$$

$$s_i > 0, \quad i = 1, \dots, m \quad (4.24)$$

$$\mu_i > 0, \quad i = 1, \dots, m \quad (4.25)$$

These equations can be solved using the Newton iterative method. Our four sets of variables for which we must solve are Y , λ , μ and s . The equation for a first order approximation of a Taylor series of a function, F , whose independent variables are Y , λ , μ and s is

$$F(Y, \lambda, \mu, s) \cong F(Y_o, \lambda_o, \mu_o, s_o) + \frac{\partial F}{\partial Y} \Delta Y + \frac{\partial F}{\partial \lambda} \Delta \lambda + \frac{\partial F}{\partial \mu} \Delta \mu + \frac{\partial F}{\partial s} \Delta s. \quad (4.26)$$

We want to find the values of Y , λ , μ and s where the expressions on the left side of the equations we want to solve evaluate to zero. We use Newton-Raphson to do so.

Taking the first order approximation to the Taylor series for each of the four expressions given in equations (4.20)-(4.23) and setting them equal to zero (the desired value for each) give us

$$\begin{aligned} (\nabla_Y f - h_Y^T \lambda + g_Y^T \mu) + (\nabla_Y^2 f - \sum_{i=1}^n \lambda_i \nabla_Y^2 h_i + \sum_{i=1}^m \mu_i \nabla_Y^2 g_i) \Delta Y \\ - h_Y^T \Delta \lambda + g_Y^T \Delta \mu = 0, \end{aligned} \quad (4.27)$$

$$h + h_Y \Delta Y = 0, \quad (4.28)$$

$$(g + s) + g_Y \Delta Y + I \Delta s = 0, \quad (4.29)$$

$$(MSe - \nu e) + S \Delta \mu + M \Delta s = 0, \quad (4.30)$$

where

- I : an identity matrix,
- S : a diagonal matrix constructed from (s_1, s_2, \dots, s_m) ,
- M : a diagonal matrix constructed from $(\mu_1, \mu_2, \dots, \mu_m)$,
- e : a column vector with all elements 1.

The above equations can be organized in matrix form as

$$\begin{bmatrix} H_Y & h_Y^T & g_Y^T & 0 \\ h_Y & 0 & 0 & 0 \\ g_Y & 0 & 0 & I \\ 0 & 0 & S & M \end{bmatrix} \begin{bmatrix} \Delta Y \\ \Delta \lambda \\ \Delta \mu \\ \Delta s \end{bmatrix} = \begin{bmatrix} -\nabla_Y f + h_Y^T \lambda - g_Y^T \mu \\ -h \\ -g - s \\ \nu e - M S e \end{bmatrix}, \quad (4.31)$$

or

$$W \Delta z = \Delta F, \quad (4.32)$$

where

$$H_Y = \nabla_Y^2 f - \sum_{i=1}^n \lambda_i \nabla_Y^2 h_i + \sum_{i=1}^m \mu_i \nabla_Y^2 g_i.$$

We initially set ν to some relatively large number, such as 10. Starting with an initial guess

$$z_o = \begin{bmatrix} Y_o \\ \lambda_o \\ \mu_o \\ s_o \end{bmatrix},$$

we calculate the W matrix and the ΔF vector. If all the elements of ΔF are sufficiently close to zero, we have found the solution z_o . Otherwise we must solve for Δz by

$$\Delta z = W^{-1} \Delta F. \quad (4.33)$$

Then the original z is updated by

$$z = z_o + \alpha \Delta z. \quad (4.34)$$

However, following conditions need to be satisfied when updating z :

$$\mu_i > 0,$$

$$s_i > 0.$$

Therefore, when calculating the updated μ and s , we must make sure that each μ_i and each s_i is still strictly greater than zero when $\Delta\mu_i$ and Δs_i are added to it, respectively. If adding $\Delta\mu_i$ or Δs_i violates this condition, all $\Delta\mu_i$ and all Δs_i must be scaled by some factor α less than one before adding them as in (4.34).

Now that we have a new guess for z , the W matrix and ΔF vector are calculated again. If the elements of the ΔF vector are sufficiently close to zero, we have found the z which solves our problem. Otherwise we solve for Δz and update z again. This process is repeated until we find the z which makes ΔF very close to zero.

After we solve for z , we reduce the barrier parameter ν by some factor κ . For example, if $\kappa = 0.4$, the barrier parameter ν is updated by letting the new ν be 0.4 times the old ν . Using the value of z obtained using the old ν as an initial guess z_o , we use the iterative procedure described above to solve for the value of z which makes ΔF approximately zero for the new barrier parameter. The process of solving for z , decreasing ν , and then solving for z again is repeated until ν becomes a very small number, such as 10^{-10} . This process is illustrated in Figure 4.2. When ν gets this small, we have found the z that solves our problem. When solving for z given a particular ν , it is not necessary to force ΔF to be zero. What we really want to know is how close we are to the central path. The central path is defined by a sequence of solutions $\{Y(\nu), \lambda(\nu), \mu(\nu), s(\nu)\}$ which make ΔF evaluate to zero for every possible value of ν . One way of measuring how close we are to the central path is by checking to see how close each product $\mu_i s_i$ is to the barrier parameter ν . One

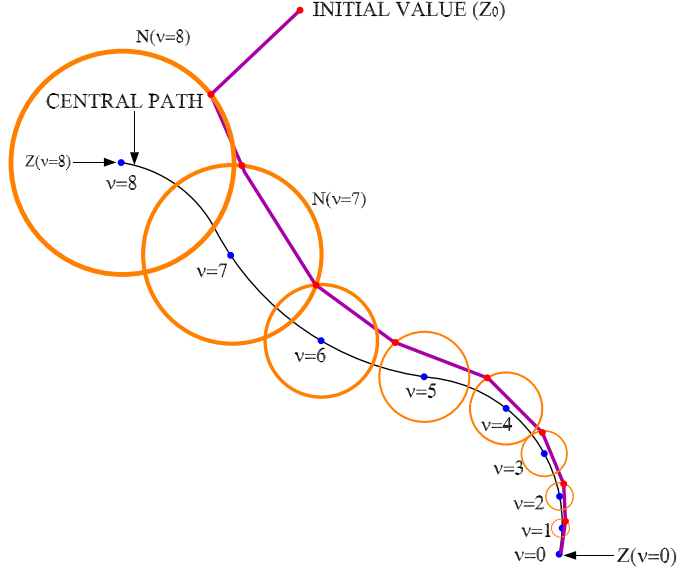


Figure 4.2: Graphical representation of central path

proposed way of doing this is by first calculating the average value of $\mu_i s_i$, also known as the *duality factor* [13], by

$$\hat{\nu} = \sum_{i=1}^m \frac{\mu_i s_i}{m}, \quad (4.35)$$

which evaluates to zero when each product $\mu_i s_i$ is equal to ν . Instead of checking to see if ΔF is sufficiently close to zero, we check to see when the following is true:

$$\left\| \begin{array}{c} \mu_1 s_1 - \hat{\nu} \\ \mu_2 s_2 - \hat{\nu} \\ \vdots \\ \mu_m s_m - \hat{\nu} \end{array} \right\|_2 \leq \tau \nu \quad (4.36)$$

where

$$0 < \tau < 1.$$

When this logical statement becomes true, we are sufficiently close to the central path, and we can reduce ν .

Despite several attractive features of the PDIP method, it has an inherent disadvantage that the size of problem is much bigger than the Newton active set method since the PDIP method includes all inequality constraints. This problem becomes

even more involved when we consider a large scale natural gas and power system network.

CHAPTER 5

NATURAL GAS FLOW MODELING

Natural gas is transported from gas producers to customers at various locations. A typical natural gas transmission system today consists of a large number of gas producers, various customers, storage, many compressor stations, thousands of pipelines, and many other devices such as valves and regulators, including midstream gas processing (between well and pipeline)

A typical pipeline network for transporting natural gas consumes a significant amount of fuel per day to operate compressors pumping natural gas. This is because there is a gas pressure loss due to friction between gas and pipe inner walls. Moreover, energy is lost by heat transfer between gas and its environment. To compensate for these losses of energy and to keep the gas flowing, compressor stations are installed in the network, which consume a part of the transported gas resulting in economic losses¹.

The purpose of this chapter is to provide the underlying mathematical modeling of natural gas transmission networks. It will include gas flow equations, compressor horsepower equation, and matrix representations of natural gas networks.

¹Losses often refer to leakage of natural gas from the pipeline system, which is negligible if there is no theft problem. We will use the term “losses” only for the gas required to power the compressors.

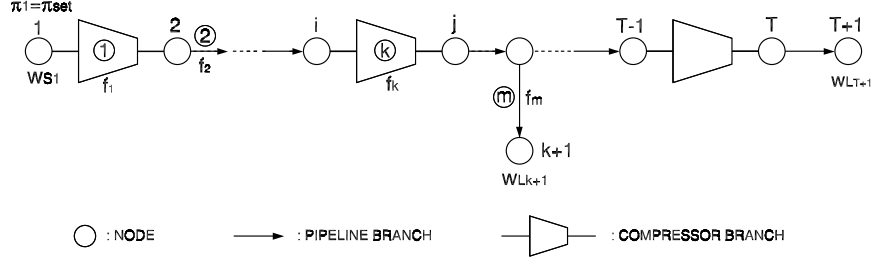


Figure 5.1: Pipeline network representation

5.1 Elements of Natural Gas Transmission Network

Three basic types of entities are considered for the modeling of a natural gas transmission network: pipelines, compressor stations, both of which are represented by branches, and interconnection points, represented by nodes.

For simulation of a network, we assume that nodes represent pipeline connections while branches represent pipelines and compressor stations, which have flow directions assigned. We also have different types of nodes. A source node represents a gas production or storage facility. A load node represents a place where gas is to be taken out of the system, either for consumption or storage.

Each compressor branch defines two more node types technically referred to as suction and discharge nodes. Likewise, each pipeline branch has two types of nodes, a sending end node and a receiving end node. We define f_{kij} (or f_k for simple notation) as the flow rate through a branch, say number k , which begins at node i and ends at node j .

Figure 5.1 shows an example of a natural gas network. It is a simple tree-structure pipeline network, which consists of one source at node 1, two loads at nodes $T + 1$ & $K + 1$, and several pipeline and compressor branches. w_{S1} is the amount of gas supplied at the source node, and w_{LT+1} & w_{Lk+1} are the amounts of gas consumed at the load nodes, respectively.

For a given gas network, there are three types of relevant decision variables: the flow rate through a pipeline, the flow rate through a compressor, and the pressure at each node. For a compressor, these variables are further restricted by a set of constraints that depend on the operating attributes of the compressor.

5.2 Network Topology

Analysis of natural gas pipeline networks is relatively complex, particularly if the network consists of a large number of pipelines, several compressors, and various suppliers and consumers [21]. Matrix notation is a simple and useful way of representing a network. In gas network analysis, matrices turn out to be the natural way of expressing the problem [22]. A gas pipeline system can be described by a set of matrices based on the topology of the network. Consider the gas network represented by the graph in Figure 5.2 [22]. This network consists of one source at node 1, three loads at nodes 2, 3 & 4 and five pipeline branches ①, ②, ③, ④ & ⑤.

For network analysis it is necessary to select at least one reference node. Mathematically, the reference node is also referred to as an independent node, and all nodal and branch quantities are dependent on it. The pressure at the reference node is

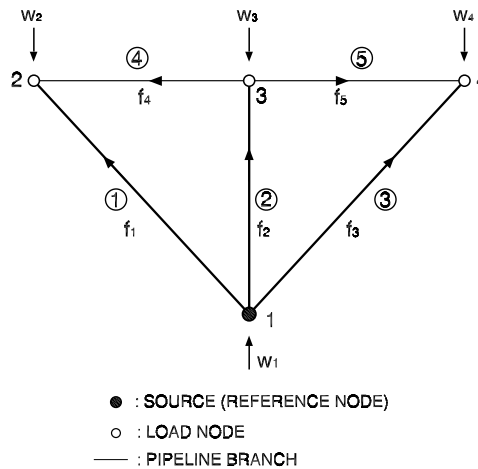


Figure 5.2: Graph of the gas network [22]

known. A network may contain several pressure-defined nodes and these form a set of reference nodes for the network.

A gas injection node is a point where gas is injected into the network, which may be positive, negative, or zero. Negative injection represents a load demand for gas from the network. This node may be supplying domestic or commercial consumers, charging gas storages, or even accounting for leakage in the network. A positive injection represents a supply of gas to the network. It may take gas from storage, source or another network. A zero injection is assigned to nodes that do not have a load or source but are used to represent a point of change in the network topology, such as a junction of several branches. Then, the vector of gas injections w at each node for Figure 5.2 is defined as

$$\begin{aligned} w &= \begin{bmatrix} w_1 & w_2 & w_3 & w_4 \end{bmatrix}^T, \\ &= \begin{bmatrix} w_{S_1} & -w_{L_2} & -w_{L_3} & -w_{L_4} \end{bmatrix}^T, \end{aligned}$$

where

$$w_i = w_{S_i} - w_{L_i},$$

$$w_{S_i} = \text{gas injection at node } i,$$

$$w_{L_i} = \text{gas removed at node } i.$$

At steady-state conditions, the total load on the network is balanced by the supply into the network at the source node.

To define the network topology completely, it is necessary to assign a direction to each branch. Each branch direction is assigned arbitrarily and is assumed to be the positive direction of flow in the branch. If the flow has a negative value, then the direction of flow is opposite to the branch direction. References such as Osiadacz's book [22] may be consulted for further detail.

5.3 Matrix Representations of Network

The interconnection of a network can be described by the branch-nodal incidence matrix \mathbf{A} . This matrix is rectangular, with the number of rows N_N equal to the number of nodes (including reference nodes), and the number of columns N_P equal to the number of pipeline and compressor branches in the network. The element A_{ij} of the matrix \mathbf{A} corresponds to node i and branch j , and is defined as

$$A_{ij} = \begin{cases} +1, & \text{if pipeline branch } j \text{ enters node } i, \\ -1, & \text{if pipeline branch } j \text{ leaves node } i, \\ 0, & \text{if pipeline branch } j \text{ is not connected to node } i. \end{cases}$$

For the network in Figure 5.2, the branch-nodal incidence matrix is

$$\mathbf{A} = \begin{bmatrix} -1 & -1 & -1 & 0 & 0 \\ 1 & 0 & 0 & 1 & 0 \\ 0 & 1 & 0 & -1 & -1 \\ 0 & 0 & 1 & 0 & 1 \end{bmatrix},$$

where $N_N = 4$ nodes and $N_P = 5$ branches. One important thing to note is that the sum of all rows in the matrix \mathbf{A} becomes zero due to the definition of each element of the matrix \mathbf{A} . Thus, the matrix \mathbf{A} is always rank-1 deficient, and therefore the matrix $\mathbf{A}\mathbf{A}^T$ is singular. This problem can be avoided by removing the rows of the matrix \mathbf{A} corresponding to known-pressure nodes, which will be discussed in next chapter.

5.4 Flow Equation

For isothermal gas flow in a long horizontal pipeline, say number k , which begins at node i and ends at node j , the general steady-state flow rate (in standard ft^3/hr , or SCF/hr at $T_0 = 520^\circ R$ and $P_0 = 14.65$ psia) is often expressed by the following

formula [22, 23] derived from energy balance:

$$f_{kij} = \mathcal{S}_{ij} \times 3.22 \frac{T_0}{\pi_0} \sqrt{\mathcal{S}_{ij} \frac{(\pi_i^2 - \pi_j^2) D_k^5}{F_k G L_k T_{ka} Z_a}}, \quad (5.1)$$

where

$$\begin{aligned} f_{kij} &= \text{pipeline flowrate (SCF/hr),} \\ \mathcal{S}_{ij} &= \begin{cases} +1 & \text{if } \pi_i - \pi_j > 0, \\ -1 & \text{if } \pi_i - \pi_j < 0, \end{cases} \\ F_k &= \text{pipeline friction factor,} \\ D_k &= \text{internal diameter of pipe between nodes (inch),} \\ G &= \text{gas specific gravity (air=1.0, gas=0.6),} \\ L_k &= \text{pipeline length between nodes (miles),} \\ \pi_i &= \text{pressure at node } i \text{ (psia),} \\ \pi_j &= \text{pressure at node } j \text{ (psia),} \\ \pi_0 &= \text{standard pressure (psia),} \\ T_0 &= \text{standard temperature (}^\circ\text{R),} \\ T_{ka} &= \text{average gas temperature (}^\circ\text{R),} \\ Z_a &= \text{average gas compressibility factor.} \end{aligned}$$

There are several different flow equations in use in the natural gas transmission industry [22, 24]. The differences are mainly due to the empirical expression assumed for the friction factor, F_k , and in some cases the rigorous consideration of the deviation of the behavior of natural gas from that of an ideal gas. The change of flow changing from partial turbulence to full turbulence is referred as the transition region. The Reynolds number, a measure of the ratio of the inertia force on an element of fluid to the viscous force on an element, at which this transition occurs is dependent on the diameter of the pipeline and its roughness, and is typically about 10^7 [22]. The extent of the transition region is dependent on the system considered, and within this region

the frictional resistance depends on both the Reynolds number and the pipe characteristics. However, in the fully-turbulent flow region for high-pressure networks, the friction factor F_k is strictly dependent on pipeline diameter [22], [25]. That is

$$F_k = \frac{0.032}{D_k^{1/3}}. \quad (5.2)$$

Then, equation (5.1) becomes

$$f_k = f_{kij} = \mathcal{S}_{ij} M_k \sqrt{\mathcal{S}_{ij} (\pi_i^2 - \pi_j^2)}, \quad \text{SCF/hr} \quad (5.3)$$

where

$$\begin{aligned} M_k &= \epsilon \frac{18.062 T_0 D_k^{8/3}}{\pi_0 \sqrt{G L_k T_{ka} Z_a}}, \\ \epsilon &= \text{pipeline efficiency.} \end{aligned}$$

As indicated in equation (5.3), gas flow can be determined once π_i and π_j are known for given conditions. Equation (5.3), known as Weymouth flow equation, is most satisfactory for large diameter (≥ 10 inches) lines with high pressures [23].

5.5 Compressor Horsepower Equation

During transportation of gas in pipelines, gas flow loses a part of its initial energy due to frictional resistance which results in a loss of pressure. To compensate the loss of energy and to move the gas, compressor stations are installed in the network. In general, the nature of the compressor work function is very complex and depends also on consideration such as the number of compressors running within the compressor station, how the compressor units are configured (*i.e.* in series, in parallel, combination of both, *etc.*), physical properties of the compressor units, and type of compressor unit [22]. One of the most common configurations implemented in practice is that of compressor stations consisting of identical centrifugal compressor units operating in parallel. Centrifugal compressors are versatile, compact, and generally used in the

range of 1,000 to 100,000 inlet ft³/min for process and pipeline compression applications [24]. In a centrifugal compressor, work is done on the gas by an impeller. Gas is discharged at a high velocity into a diffuser. The velocity of gas is reduced and its kinetic energy is converted to static pressure.

A key characteristic of the centrifugal compressor is the horsepower consumption, which is a function of the amount of gas that flows through the compressor and the relative boost ratio between the suction and the discharge pressures.

After empirical modification to account for deviation from ideal gas behavior, the actual adiabatic (zero heat transfer) compressor horsepower equation [23] at $T_o = 60^\circ\text{F}$ ($= 520^\circ\text{R}$) and $\pi_o = 14.65$ psia becomes

$$H_k = H_{kij} = B_k f_k \left[\left(\frac{\pi_j}{\pi_i} \right)^{Z_{ki} \left(\frac{\alpha-1}{\alpha} \right)} - 1 \right], \quad \text{HP} \quad (5.4)$$

where

$$\begin{aligned} B_k &= \frac{3554.58 T_{ki}}{\eta_k} \left(\frac{\alpha}{\alpha - 1} \right), \\ f_k &= \text{flow rate through compressor (SCF/hr)}, \\ \pi_i &= \text{compressor suction pressure (psia)}, \\ \pi_j &= \text{compressor discharge pressure (psia)}, \\ Z_{ki} &= \text{gas compressibility factor at compressor inlet}, \\ T_{ki} &= \text{compressor suction temperature } (^\circ\text{R}), \\ \alpha &= \text{specific heat ratio } (c_p/c_V), \\ \eta_k &= \text{compressor efficiency.} \end{aligned}$$

5.6 Conservation of Mass Flow

The mass-flow balance equation at each node can be written in matrix form as

$$(\mathbf{A} + \mathbf{U})f + w - \mathbf{T}\tau = 0, \quad (5.5)$$

where

$$\begin{aligned}
\mathbf{A} &= \text{a branch-nodal incidence matrix,} \\
U_{ik} &= \begin{cases} +1, & \text{if the } k\text{th unit has its outlet at node } i, \\ -1, & \text{if the } k\text{th unit has its inlet at node } i, \\ 0, & \text{otherwise.} \end{cases} \\
T_{ik} &= \begin{cases} +1, & \text{if the } k\text{th turbine gets gas from node } i, \\ 0, & \text{otherwise.} \end{cases} \\
f &= \text{a vector of mass flow rates through branches,} \\
w &= \text{a vector of gas injections at each node.}
\end{aligned}$$

In addition to the matrix \mathbf{A} , which represents the interconnection of pipelines and nodes, we define the matrix \mathbf{U} , which describes the connection of units (compressors) and nodes. The vector of gas injections w is obtained by

$$w = w_S - w_L, \quad (5.6)$$

where

$$\begin{aligned}
w_S &= \text{a vector of gas supplies at each node,} \\
w_L &= \text{a vector of gas demands at each node.}
\end{aligned}$$

Thus, a negative gas injection means that gas is taken out of the network.

The matrix \mathbf{T} and the vector τ represent where gas is withdrawn to power a gas turbine to operate the compressor. So if a gas compressor, say k , between nodes i and j , is driven by a gas-fired turbine, and the gas is tapped from the suction pipeline i , we have the following representation:

$$T_{ik} = +1, \quad T_{jk} = 0, \quad \text{and } \tau_k = \text{amount tapped.}$$

Conversely, if the gas were tapped at the compressor outlet, we would have

$$T_{ik} = 0, \quad T_{jk} = +1, \quad \text{and } \tau_k = \text{amount tapped.}$$

Analytically, we will assume that τ_k can be approximated as

$$\tau_k = \alpha_{Tk} + \beta_{Tk}H_{kij} + \gamma_{Tk}H_{kij}^2, \quad (5.7)$$

where $H_k = H_{kij}$ is the horsepower required for the gas compressor k in equation (5.4).

CHAPTER 6

NATURAL GAS LOADFLOW

The problem of simulation of a gas network with N_N nodes in steady state, known as *loadflow*, is usually that of computing the values of node pressures and flow rates in the individual branches for known values of N_S source pressures ($N_S \geq 1$) and of gas injections in all other nodes.

Gas loadflow analyses are required operationally whenever significant changes in demands or supplies are expected to occur. It is also used for system planning purposes. For example, when a gas-fired generator is located in the gas network, we need to see whether the network has enough capability to carry the required amount of gas to the generator while satisfying various network constraints, such as pressure limits at each node and compressor operation limits.

In this chapter, we state the loadflow problem in a general way, and construct a mathematical formation. We present a loadflow problem for a network without compressors. Then we introduce a general loadflow analysis with compressors. We formulate the gas loadflow problem in a way similar to the electric loadflow problem, and include the gas consumption rates at compressor stations.

However, we omit gas storage to avoid inter - temporal linkages-we only attempt to solve the gas loadflow at a single time-a “snapshot”.

6.1 Loadflow Problem Statement

The gas loadflow problem is stated below:

- Given a natural gas system described by a branch-nodal incidence matrix \mathbf{A} , a unit-nodal incidence matrix \mathbf{U} , a gas turbine-nodal incidence matrix \mathbf{T} , and given a set of gas injections except at the N_S known-pressure sources (injections at these nodes initially unknown), and each unit's operating condition (such as the compression ratio, the flow rate through the compressor, or the suction or discharge pressure),
- determine all other pressures, and calculate the flow rates in all branches and the gas consumptions at compressor stations.

Simply speaking, one of two quantities, nodal pressure π_i and gas injection w_i at each node, and one compressor operating condition are specified, and other values are to be determined. Specified quantities are chosen based on the following conditions:

Nodes:

- **Known-Injection Node:** For a node i of this type, we assume that we know a gas injection w_i , and the pressure π_i is to be determined. Generally, source and load nodes, and junctions with no gas injections belong to this node. Electrically, this is analogous to a “load bus.”

In fact, solving the loadflow problem with only this type of node is not in general possible. The first reason is that, in the flow equation (5.1), the pressures never appear by themselves, but instead appear only as a squared-pressure difference of the form $\pi_i^2 - \pi_j^2$. Therefore, there are only $N_N - 1$ pressures which affect the loadflow. We therefore pick $N_S \geq 1$ nodes to provide reference pressures. These nodes are generally the external gas sources supplying our system.

Another reason is that with is that solving a loadflow for a network containing only known-injection nodes would imply that we know the gas injections at every single node. In fact, we cannot mathematically specify all N_N gas injections, as it may not be possible to find a solution to the loadflow equations. Specifying the injections at all nodes is the same as specifying the gas supplies to gas turbines driving gas compressors, which we cannot know until the loadflow is solved. Instead, we must pick at least one node, allowing the set of gas injection(s) to be whatever is required to solve the loadflow equations. Thus, we have to specify another node type:

- **Known-Pressure Node:** Each is typically one of the source nodes, and the pressures of such nodes serve as references for all other pressures. We assume that we know $\{\pi_i, i = 1, \dots, N_S\}$, but we do not know the corresponding gas injections. Electrically this is analogous to a (possibly distributed) “slack bus.”

In addition to nodes, the other main components are **branches**, which connect the nodes.

Branches:

- **Pipelines:** Pipeline flow modelling has already been discussed in the previous chapter. Other than the physical characteristics of the pipeline, the only variables that the flow $f_k = f_{kij}$ on pipeline k depends on are the pressures π_i and π_j at the two ends of the pipeline.
- **Compressors:** The other key component we will model in a gas network is a compressor (also called a unit). The connection between the unit’s inlet and outlet nodes is not defined by the branch-nodal incidence matrix \mathbf{A} , but by \mathbf{U} . The compression ratio between the compressor inlet and outlet, and the flow rate through the compressor are governed by the horsepower equation (5.4), not by the flow equation (5.1). Compressor data (other than the physical characteristics of the compressor) can be specified in several ways [22] for compressor

k : relative boost $R_k = R_{kij} = \pi_j/\pi_i$, or absolute boost $\pi_j - \pi_i$, or mass-flow rate f_{kij} . The inlet pressure π_i or the outlet pressure π_j could also be specified.

6.2 Loadflow without Compressors

We will first consider a gas network with only pipelines to explain the Newton-nodal method. Assume that node 1 is the known-pressure node, and all other nodes are the known-injection nodes. Since we do not have compressors, the unit's inlet-outlet nodes are not defined. Then the loadflow problem is described as follows:

$$\begin{array}{ll} \text{Given} & : \quad \pi_1 \quad w_2 \quad \dots \quad w_{N_N} \\ \text{Determine} & : \quad w_1 \quad \pi_2 \quad \dots \quad \pi_{N_N} \end{array}$$

It appears that we have $N_N - 1$ quantities known, and $N_N - 1$ quantities unknown. The set of nodal flow equations that describes a gas network with only pipelines is given by

$$\bar{w} = \mathbf{A}_1 \cdot f(\bar{\pi}, \tilde{\pi}), \quad (6.1)$$

where

\mathbf{A}_1 = a branch-nodal incidence matrix except the known-pressure nodes,

\bar{w} = $\bar{w}_s - \bar{w}_L$,

f = a vector of flow rates through pipelines.

We used $\bar{\pi}$ to indicate the part of π we know, and $\tilde{\pi}$ for unknown part. Likewise for \bar{w} . Flow equation (5.3) is used to get each pipeline branch flow as

$$f_{kij} = \mathcal{S}_{ij} M_k \sqrt{\mathcal{S}_{ij} (\pi_i^2 - \pi_j^2)}, \quad \text{SCF/hr} \quad (6.2)$$

In the Newton-nodal method [22], an initial approximation is made to the nodal pressures. This approximation is then iteratively corrected until the final solution is

reached. At each iteration the right-hand side of equation (6.1) is not equal to zero. The pressures are only approximations of their true values and the flows calculated from these pressures are not balanced at each node. The imbalance at a node is the nodal error which is a function of all the nodal pressures (except the known-pressure nodes). The Newton-nodal method solves the set of equations (6.1) iteratively until the nodal flow errors are small enough to be insignificant. The iterative scheme for correcting the approximations to the nodal pressures is

$$\tilde{\pi}^{k+1} = \tilde{\pi}^k + \Delta\tilde{\pi}^k, \quad (6.3)$$

where k = the number of iterations. Term $\Delta\tilde{\pi}$ is computed from the following equation:

$$\mathbf{J}^k \cdot \Delta\tilde{\pi}^k = -(\mathbf{A}_1 \cdot f(\tilde{\pi}, \tilde{\pi}) - \bar{w})^k, \quad (6.4)$$

where the matrix \mathbf{J} is the nodal Jacobian matrix and is given by [22]

$$\mathbf{J} = -\mathbf{A}_1 \mathbf{D} \mathbf{A}_1^T \mathbf{\Pi}_1, \quad (6.5)$$

and

$$\mathbf{D} = \text{diag} \left(\frac{f_{kij}}{\pi_i^2 - \pi_j^2} \right), \quad k = 1, \dots, N_P$$

$$\mathbf{\Pi}_1 = \text{diag}(\tilde{\pi}).$$

Since the matrix $\mathbf{A}_1 \mathbf{D} \mathbf{A}_1^T$ is symmetric and positive definite, and $\mathbf{\Pi}_1$ is a diagonal matrix, Newton-Raphson algorithm can be implemented with a great computational efficiency [26], [21].

6.3 Loadflow with Compressors

We assume that the pressures at the N_S known-pressure nodes are known, and that the injections at the known-injection nodes are specified. Also, some operating parameter for each compressor, say (for purposes of illustration) the relative boost

$R_k = R_{kij}$, is specified, and let's say there are N_P branches in the system, of which N_C are compressors. We can state the loadflow problem this way:

Given :

$$\pi_1 \cdots \pi_{N_S} \quad w_{N_S+1} \cdots w_{N_N} \quad R_1 \cdots R_{N_C}$$

Find :

$$w_1 \cdots w_{N_S} \quad \pi_{N_S+1} \cdots \pi_{N_N} \quad f_1 \cdots f_{N_C} \quad f_{N_C+1} \cdots f_{N_P}$$

It appears that there are $N_N + N_C$ quantities given, while $N_N + N_P$ must be found.

It is clear that

$$N_C < N_P.$$

This inequality is strict, unless we have no pipelines at all, only N_P compressors connected to each other without any intervening pipelines – a silly situation. So since $N_N + N_C < N_N + N_P$, the system appears to be undetermined. Note, however, that from (6.2), the flow f_k depends only on the pressures π_i and π_j of the nodes it connects. Likewise, the horsepower H_k required by the compressor depends only on the flow f_k and the ratio $R_k = \pi_j/\pi_i$, and therefore only depends on the pressures π_i and π_j . The tap-off loss τ_k depends only on H_k and thus on the nodal pressures. So, if we knew $\{\pi_i, i = 1, \dots, N_N\}$, we would know all other quantities we have discussed. But we only know them for $i = 1, \dots, N_S$. Let's use $\bar{\pi}$ to indicate the part of π we know, and $\tilde{\pi}$ for the unknown part. Likewise for \bar{w} and \tilde{w} . The objective, then, is to calculate $\tilde{\pi}$, giving us the entire vector π , from which all other quantities can be calculated.

We can use the mass-balance equation (5.5) to write

$$\bar{w} = \tilde{\mathbf{T}}\tau(\bar{\pi}, \tilde{\pi}) - (\tilde{\mathbf{A}} + \tilde{\mathbf{U}})f(\bar{\pi}, \tilde{\pi}),$$

where $\tilde{\mathbf{A}}$, $\tilde{\mathbf{U}}$, and $\tilde{\mathbf{T}}$ are obtained from \mathbf{A} , \mathbf{U} , and \mathbf{T} as in equation (5.5) after we have removed the rows corresponding to the N_S nodes (the known-pressure nodes with unknown injections), that is, we have dropped the first N_S equations of (5.5)

corresponding to \tilde{w} . This gives us $N_N - N_S$ equations (for the elements of \bar{w}) in $N_N - N_S$ unknowns (the elements of $\tilde{\pi}$). At this point, standard Newton-Raphson or other iterative methods can be employed to drive the “mismatch” $\Delta\bar{w}$ (the difference between the values of \bar{w} computed from above and the true values of \bar{w} given as part of the data) to zero by correcting our current guess for the correct value of $\tilde{\pi}$.

We have shown that the dimension of the load flow problem with compressors is $N_N - N_S$. However, it is convenient to add new equations and new variables if they make the problem easier to implement. Since the compressor horsepower in equation (5.4) and the gas consumption rate in equation (5.7) are functions of horsepowers, compressor flow rates, and gas consumption rates as well as the specified relative boost rates, we will add three extra decision variables for each compressor station. Then the new decision variables become

$$\mathbf{x} = \begin{bmatrix} \tilde{\pi}^T & H^T & \tau^T & f_C^T \end{bmatrix}^T,$$

where

H = a vector of horsepowers at each compressor,

τ = a vector of gas consumptions at each compressor,

f_C = a vector of compressor branch flow rates.

Since there are $N_N - N_S + 3N_C$ decision variables, we need to define extra $3N_C$ equations. The mass-flow balance equations \mathbf{F}_1 in matrix form are given by

$$\mathbf{F}_1 = (\tilde{\mathbf{A}} + \tilde{\mathbf{U}}) \cdot \begin{bmatrix} f_C \\ f_P(\tilde{\pi}, \tilde{\pi}) \end{bmatrix} + \bar{w} - \tilde{\mathbf{T}} \cdot \tau = 0, \quad (6.6)$$

where $f_P(\tilde{\pi}, \tilde{\pi})$ is a vector of mass flow rates through pipelines, which are obtained by flow equation (6.2). Note that the size of the vector \mathbf{F}_1 is $N_N - N_S$. Assuming that the compression ratio R_{kij} is given, and gas compressor k located between nodes i and j is driven by a gas-fired turbine, the extra $3N_C$ equations related with compressor

operation are

$$F_{2_k} = \tau_k - \alpha_{Tk} - \beta_{Tk} H_{kij} - \gamma_{Tk} H_{kij}^2 = 0, \quad k = 1, \dots, N_C \quad (6.7)$$

$$F_{3_k} = H_{kij} - B_k f_{C_k} \left[\left(\frac{\pi_j}{\pi_i} \right)^{Z_{ki} \left(\frac{\alpha-1}{\alpha} \right)} - 1 \right] = 0, \quad k = 1, \dots, N_C \quad (6.8)$$

$$F_{4_k} = \left(\frac{\pi_j}{\pi_i} \right) - R_{kij} = 0, \quad k = 1, \dots, N_C \quad (6.9)$$

Let us define the vector of error functions $\mathbf{F}(\mathbf{x})$ by

$$\mathbf{F}(\mathbf{x}) = \begin{bmatrix} \mathbf{F}_1(\mathbf{x}) \\ \mathbf{F}_2(\mathbf{x}) \\ \mathbf{F}_3(\mathbf{x}) \\ \mathbf{F}_4(\mathbf{x}) \end{bmatrix}.$$

Note that there are $N_N - N_S + 3N_C$ equations and $N_N - N_S + 3N_C$ unknown decision variables. So we have the right number of variables to force all the mismatches to zero by using Newton-Raphson or other iterative methods. The iteration will be repeated until the mismatches become small enough to be insignificant.

CHAPTER 7

UPFC MODELING FOR STEADY-STATE ANALYSIS

Modeling UPFC for steady-state analysis has been considered by several researchers and an injection model [6] and an uncoupled model [14] have been proposed. These models can be easily incorporated into steady-state loadflow or optimal power flow studies. However, these models employ four UPFC control variables that depend on the UPFC input and output currents and voltages and both models require adding two additional buses to the loadflow or OPF problem formulation. The voltage and current relationships between UPFC input and output need to be included explicitly. In addition, a constraint on real power conservation needs to be added, thereby reducing the degrees of freedom four to three. Since electricity prices at the UPFC input and output buses, which are the dual variables (or “shadow” prices) associated with real and reactive power injections, are meaningless when no power is bought or sold at these fictitious buses, their addition to the problem only serves to increase the size of the problem. Therefore, these models are undesirable for our UPFC sensitivity analysis.

To overcome these problems, a new steady-state mathematical model for a UPFC, the UPFC ideal transformer model, is proposed. In this model, UPFC control variables do not depend on UPFC input and output voltages and currents, and therefore addition of fictitious input and output buses are not necessary. This model is easily combined with transmission line models using ABCD two-port representations,

which can then be converted to Y-parameter representations. Thus, UPFC model is embedded in the $\bar{\mathbf{Y}}_{\text{bus}}$ matrix, and so the size of the $\bar{\mathbf{Y}}_{\text{bus}}$ matrix is not changed.

7.1 Operating Principles

The Unified Power Flow Controller (UPFC) is one of the most technologically promising devices in the FACTS family [4, 5, 6, 7]. It has the capability to control voltage magnitude and phase angle, and can also independently provide (positive or negative) reactive power injections. A UPFC consists of a shunt transformer, a series transformer, power electronic switching devices and a DC link, as shown in Figure 7.1 [7]. Inverter 1 is functionally a static VAR compensator assuming that inverter 2 is not connected. It injects reactive power in the form of current at the shunt transformer, and the current phasor \vec{I}_T is in quadrature to the input voltage \vec{V}_I . Inverter 2 by itself represents the so-called advanced controllable series compensator (ACSC) assuming that inverter 1 is not connected. It injects reactive power by adding voltage through the series transformer. The injected voltage \vec{V}_T is in quadrature to the receiving end

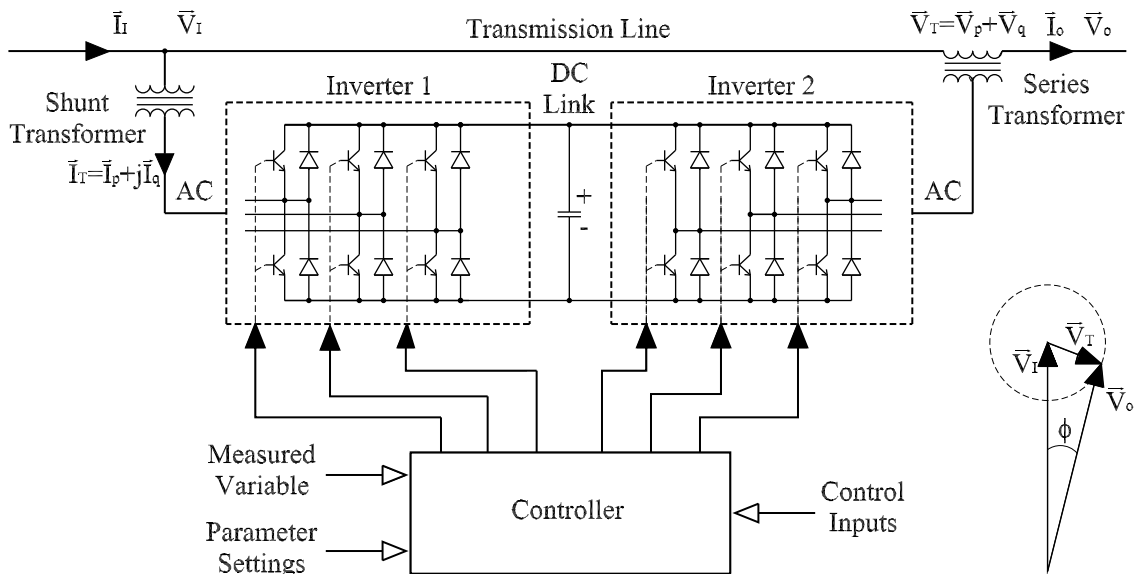


Figure 7.1: General UPFC scheme [7]

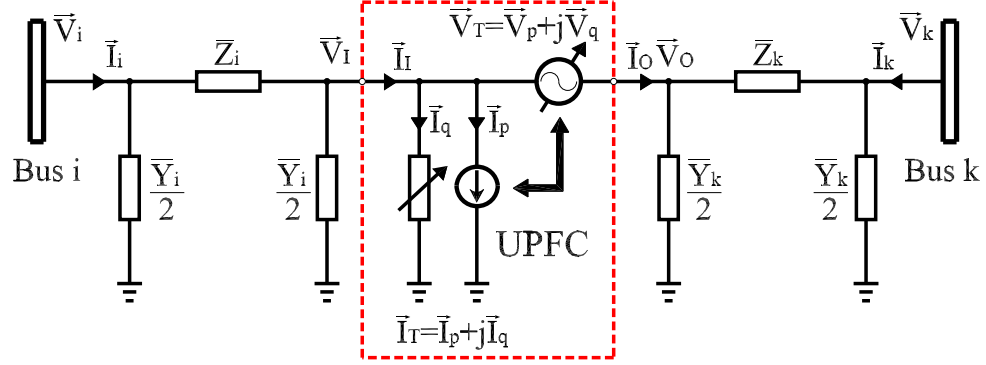


Figure 7.2: Proposed UPFC model in a transmission line

current \vec{I}_o . Now if we connect inverter 1 to inverter 2 through a DC link, inverter 1 can provide real power to inverter 2. Therefore the UPFC can independently control real and reactive power injections through the series transformer, but the real power injected at the series transformer is provided by the shunt transformer through the DC link. Inverter 1 must provide the real power used by inverter 2 via the DC link, but can also independently inject reactive power (positive or negative) through the shunt transformer.

In summary, note that the UPFC conserves real power but can still generate (or sink) reactive power at either transformer or both.

7.2 Uncoupled Model

Figure 7.2 shows a basic UPFC model, where the UPFC is located between buses i and k . Each part of the transmission line is represented as an equivalent Π circuit. Figure 7.3 shows a phasor diagram illustrating UPFC input-output voltage and current relationships. The injected series voltage \vec{V}_T can be resolved into in-phase component V_p and quadrature component V_q with respect to the UPFC output current \vec{I}_o , and can be expressed as

$$\vec{V}_T = (V_p + jV_q) e^{j\delta_o}. \quad (7.1)$$

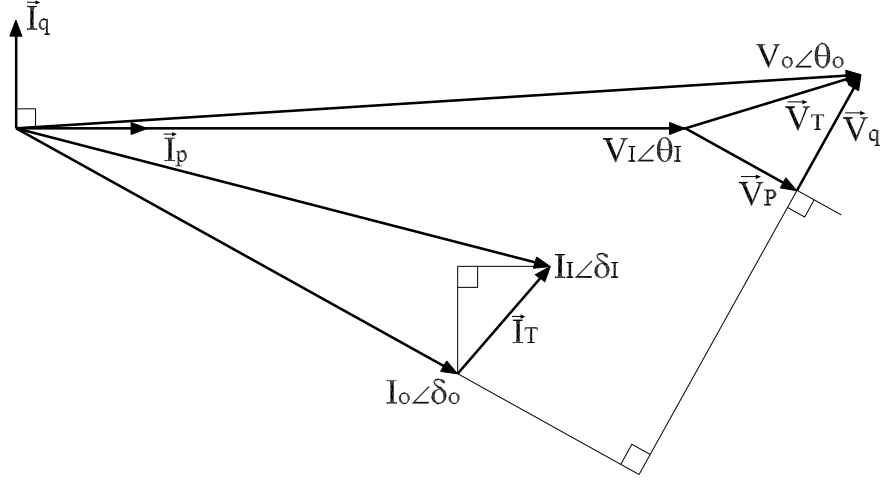


Figure 7.3: Phasor diagram of UPFC input-output voltages and currents

Since \vec{V}_T is dependent on the UPFC output current phase angle δ_o , it requires adding an extra bus for the UPFC output terminal. The current I_T injected by the shunt transformer contains a real component I_p , which is in phase or in opposite phase with the input voltage. It also has a reactive component I_q , which is in quadrature with the input voltage. Then the injected current \vec{I}_T can be written by

$$\vec{I}_T = (I_p + jI_q) e^{j\theta_I}, \quad (7.2)$$

where θ_I is the UPFC input voltage phase angle. Thus, a second extra bus is required for the UPFC input terminal.

The UPFC input-output voltage and current can be represented by

$$\vec{V}_o = \vec{V}_I + \vec{V}_T = V_I e^{j\theta_I} + V_p e^{j\delta_o} + jV_q e^{j\delta_o}, \quad (7.3)$$

$$\vec{I}_o = \vec{I}_I - \vec{I}_T = I_I e^{j\delta_I} - I_p e^{j\theta_I} - jI_q e^{j\theta_I}, \quad (7.4)$$

where δ_I is the UPFC input current phase angle. Then, the complex power injected into the transmission line by the series transformer can be resolved into the real and reactive power in simple form as

$$S_T = \vec{V}_T \cdot \vec{I}_o^* = \underbrace{V_p \cdot I_o}_{P_T} + j \underbrace{V_q \cdot I_o}_{Q_T}. \quad (7.5)$$

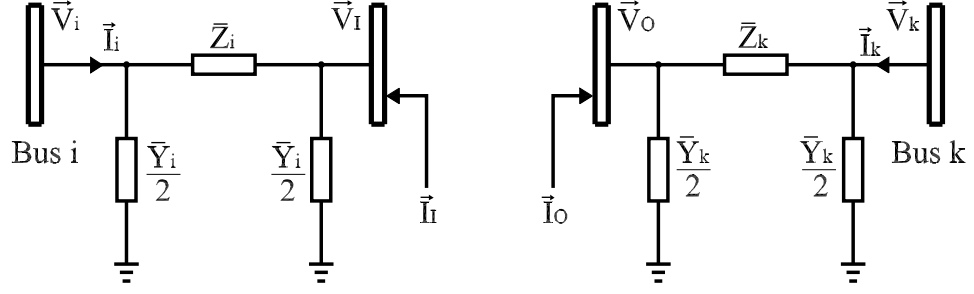


Figure 7.4: Uncoupled UPFC model in a transmission line.

The in-phase voltage V_p is associated with a real power supply and the quadrature voltage V_q with an inductive or capacitive reactance in series with the transmission line.

Since the real power P_T (which may be negative) is provided by the current I_p in the shunt transformer, we can derive the following relationship:

$$V_p \cdot I_o - V_I \cdot I_p = 0. \quad (7.6)$$

or the real power input equals the real power output. Due to (7.6), the number of degrees of freedom for the UPFC is reduced to three.

Now that two extra buses for the UPFC input and output terminals are added, and the UPFC voltage and current relationships (7.3, 7.4) and real power flow equation (7.6) are established, we can represent the UPFC uncoupled model as shown in Figure 7.4. The currents injected into the UPFC input and output buses are

$$\vec{I}_I = \left(\frac{Y_i}{2} + \frac{1}{Z_i} \right) \vec{V}_I - \frac{1}{Z_i} \vec{V}_i, \quad (7.7)$$

$$\vec{I}_o = \left(\frac{Y_k}{2} + \frac{1}{Z_k} \right) \vec{V}_o - \frac{1}{Z_k} \vec{V}_k. \quad (7.8)$$

The magnitudes of the injected voltage V_T and current I_T are limited by the maximum voltage and current ratings of the inverters and their associated transformers, which need to be included as inequality constraints in OPF.

7.3 Ideal Transformer Model

Since the UPFC conserves real power, and generates or consumes reactive power, it can be modelled using an ideal transformer and a shunt branch, as shown in Figure 7.5 [27]. The advantage of this model is that the ideal transformer turns ratio and the variable shunt susceptance are independent variables, which are not directly associated with the UPFC input-output voltages and currents. We define the UPFC variables as follows:

T = transformer voltage magnitude turns ratio (real),

ϕ = phase shifting angle,

ρ = shunt susceptance,

and the ideal transformer turns ratio can be written by

$$\bar{T} = Te^{j\phi}.$$

It is important to note that the ideal transformer does not generate real and reactive power, and the reactive power is generated (or consumed) by the shunt admittance only.

Since the UPFC input-output voltage and current relationship can be expressed

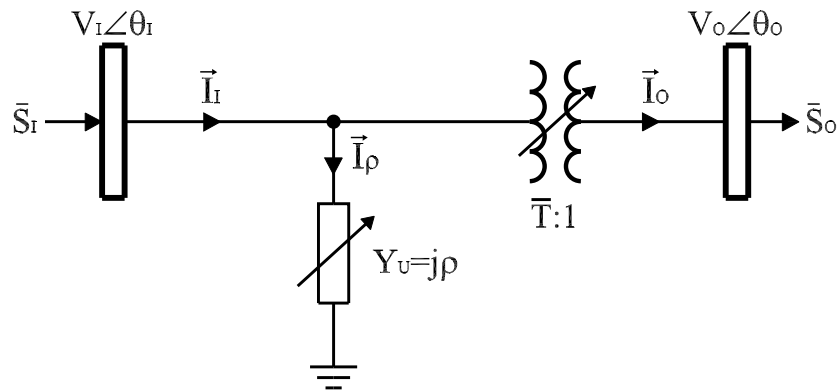


Figure 7.5: UPFC ideal transformer model

as

$$\vec{V}_I = \vec{V}_o T \angle \phi, \quad (7.9)$$

$$\vec{I}_I = j\bar{T}\rho\vec{V}_o + \frac{1}{\bar{T}^*}\vec{I}_o, \quad (7.10)$$

the UPFC can be represented by an ABCD matrix as

$$\begin{bmatrix} \vec{V}_I \\ \vec{I}_I \end{bmatrix} = ABCD_U \cdot \begin{bmatrix} \vec{V}_o \\ \vec{I}_o \end{bmatrix}, \quad (7.11)$$

where

$$ABCD_U = \begin{bmatrix} \bar{T} & 0 \\ j\bar{T}\rho & \frac{1}{\bar{T}^*} \end{bmatrix}. \quad (7.12)$$

Note that equation (7.11) is not bilateral unless $\bar{T} = 1 \angle 0$.

Now, we will show that this ideal transformer model represents the UPFC by comparing the complex power injections at the UPFC input and output. Using (7.11), the complex power injection at the UPFC input can be obtained by

$$\begin{aligned} \bar{S}_I &= \vec{V}_I \vec{I}_I^*, \\ &= \bar{T} \vec{V}_o \left(j\bar{T}\rho\vec{V}_o + \frac{1}{\bar{T}^*}\vec{I}_o \right)^*, \\ &= \vec{V}_o \vec{I}_o^* - j|\bar{T}|^2 \cdot |\vec{V}_o|^2 \rho, \\ &= \bar{S}_o - j|\bar{T}|^2 \cdot |\vec{V}_o|^2 \rho, \end{aligned} \quad (7.13)$$

and the real and reactive power injections can be obtained by

$$\begin{aligned} P_I &= \text{Real}(\bar{S}_I), & Q_I &= \text{Imag}(\bar{S}_I), \\ P_o &= \text{Real}(\bar{S}_o), & Q_o &= \text{Imag}(\bar{S}_o). \end{aligned}$$

Thus, we can derive the following relationships between the UPFC input and output:

$$P_I = P_o, \quad (7.14)$$

$$Q_o = Q_I + |\bar{T}|^2 \cdot |\vec{V}_o|^2 \rho. \quad (7.15)$$

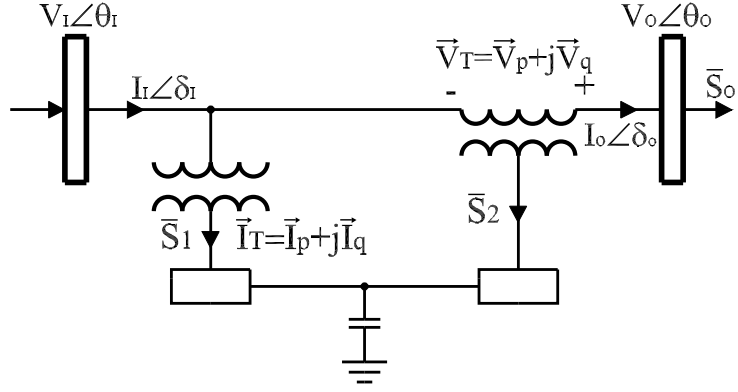


Figure 7.6: Simplified UPFC circuit

Equations (7.14) and (7.15) mean that the ideal transformer model conserves real power and generates or consumes (for $\rho < 0$) reactive power.

To determine how much real and reactive power is injected in the series and shunt transformers, we will map the complex turns ratio \bar{T} in the ideal transformer and the shunt susceptance ρ to the injected voltage \vec{V}_T and current \vec{I}_T in the UPFC uncoupled model. Since the UPFC input voltage and current are expressed as

$$\vec{V}_I = \vec{V}_o - \vec{V}_T = \vec{V}_o \left(1 - \frac{\vec{V}_T}{\vec{V}_o} \right) = \vec{V}_o T \angle \phi, \quad (7.16)$$

$$\vec{I}_I = \vec{I}_o + \vec{I}_T = \vec{I}_o + \left(\frac{1}{T} \angle \phi - 1 \right) \vec{I}_o + j\rho \vec{V}_I, \quad (7.17)$$

the injected voltage \vec{V}_T and current \vec{I}_T can be obtained by

$$\vec{V}_T = (1 - T \angle \phi) \vec{V}_o, \quad (7.18)$$

$$\vec{I}_T = \left(\frac{1}{T} \angle \phi - 1 \right) \vec{I}_o + j\rho \vec{V}_I. \quad (7.19)$$

Then, the power flows through each inverter, as shown in Figure 7.6, can be obtained

by

$$\begin{aligned}
\bar{S}_1 &= \vec{V}_I \vec{I}_T^*, \\
&= \vec{V}_o T \angle \phi \left[\left(\frac{1}{T} \angle \phi - 1 \right) \vec{I}_o + j\rho \vec{V}_o T \angle \phi \right]^*, \\
&= (1 - T \angle \phi) \bar{S}_o - j\rho |\bar{T}|^2 |\vec{V}_o|^2,
\end{aligned} \tag{7.20}$$

$$\begin{aligned}
\bar{S}_2 &= -\vec{V}_T \vec{I}_o^*, \\
&= (T \angle \phi - 1) \vec{V}_o \vec{I}_o^*, \\
&= (T \angle \phi - 1) \bar{S}_o.
\end{aligned} \tag{7.21}$$

Thus,

$$\bar{S}_1 + \bar{S}_2 = -j\rho |\bar{T}|^2 |\vec{V}_o|^2, \tag{7.22}$$

which verifies that the UPFC conserves real power and can generate (or consume) reactive power.

Since the UPFC is modelled using passive circuit elements only, non-ideal UPFC characteristics, such as shunt and series transformer reactances can be easily incorporated into this framework.

7.4 UPFC in a Transmission Line

A two-port ABCD matrix is the most convenient method to represent cascaded networks [9]. Let us divide a transmission line between buses i and k with a UPFC into three cascaded networks, a UPFC input transmission line, a UPFC, and a UPFC output transmission line, as shown in Figure 7.7. The UPFC input transmission line, and the UPFC output transmission line are easily represented by two-port ABCD matrices since the transmission lines are modelled using Π equivalent circuits. We call ABCD_i and ABCD_k as the ABCD matrices for each transmission line, and defined

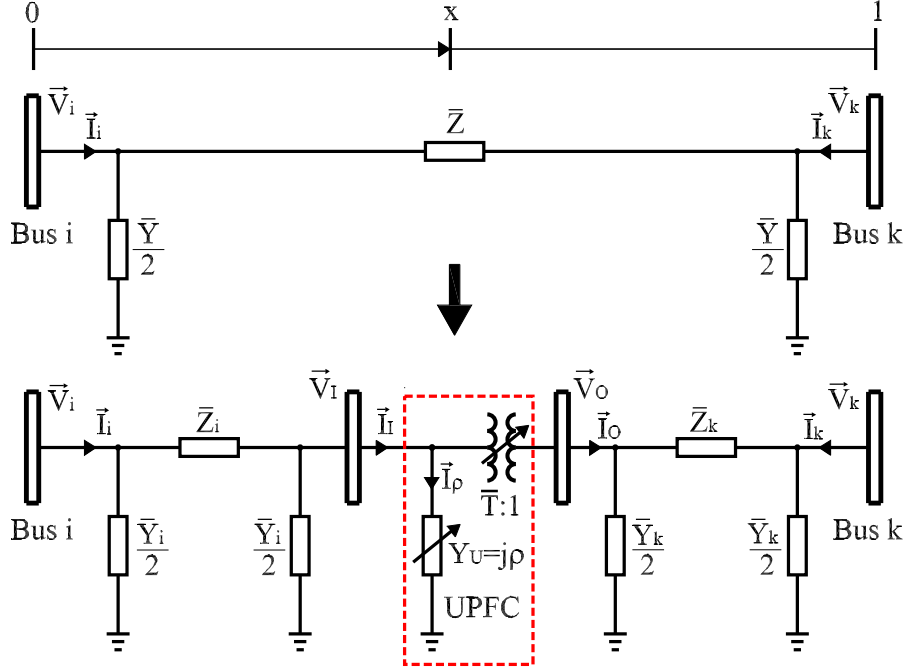


Figure 7.7: Cascaded transmission line with a UPFC

by

$$ABCD_i = \begin{bmatrix} A_i & B_i \\ C_i & D_i \end{bmatrix} \text{ and } ABCD_k = \begin{bmatrix} A_k & B_k \\ C_k & D_k \end{bmatrix},$$

where each element is defined by

$$\begin{aligned} A_i &= D_i = 1 + \frac{Y_i Z_i}{2}, & B_i &= Z_i, & C_i &= Y_i \left(1 + \frac{Y_i Z_i}{4}\right), \\ A_k &= D_k = 1 + \frac{Y_k Z_k}{2}, & B_k &= Z_k, & C_k &= Y_k \left(1 + \frac{Y_k Z_k}{4}\right). \end{aligned}$$

The ABCD parameters of each transmission line can be obtained after we identify the propagation constant γ and the characteristic impedance Z_c . Since we are using IEEE test cases with no knowledge of γ or Z_c , we compute these values using the expressions

$$\gamma = \frac{1}{l} \cosh^{-1} \left(1 + \frac{YZ}{2}\right), \quad (7.23)$$

$$Z_c = \frac{Z}{\sinh(\gamma l)}, \quad (7.24)$$

where l is the distance between buses i and k measured in kilometers. Then, assuming the UPFC is installed in x ($0 < x < 1$), Π equivalent circuit values for each section

of the transmission line can be found by

$$\begin{aligned}
Z_i &= Z_c \sinh(\gamma l \cdot x), \\
Y_i &= \frac{2}{Z_i} (\cosh(\gamma l \cdot x) - 1), \\
Z_k &= Z_c \sinh(\gamma l \cdot (1 - x)), \\
Y_k &= \frac{2}{Z_k} (\cosh(\gamma l \cdot (1 - x)) - 1).
\end{aligned}$$

Now, the three cascaded networks are combined to obtain

$$\begin{aligned}
\begin{bmatrix} \vec{V}_i \\ \vec{I}_i \end{bmatrix} &= ABCD_i \cdot ABCD_U \cdot ABCD_k \begin{bmatrix} \vec{V}_k \\ -\vec{I}_k \end{bmatrix}, \\
&= \begin{bmatrix} A_{ik} & B_{ik} \\ C_{ik} & D_{ik} \end{bmatrix} \begin{bmatrix} \vec{V}_k \\ -\vec{I}_k \end{bmatrix},
\end{aligned} \tag{7.25}$$

where $ABCD_U$ is given in (7.12). So

$$\begin{aligned}
A_{ik} &= \bar{T} A_i A_k + j \bar{T} B_i A_k \rho + \frac{1}{\bar{T}^*} B_i C_k, \\
B_{ik} &= \bar{T} A_i B_k + j \bar{T} B_i B_k \rho + \frac{1}{\bar{T}^*} B_i D_k, \\
C_{ik} &= \bar{T} C_i A_k + j \bar{T} D_i A_k \rho + \frac{1}{\bar{T}^*} D_i C_k, \\
D_{ik} &= \bar{T} C_i B_k + j \bar{T} D_i B_k \rho + \frac{1}{\bar{T}^*} D_i D_k.
\end{aligned}$$

By rearranging (7.25) and solving for I_i and I_k , we have

$$\begin{bmatrix} \vec{I}_i \\ \vec{I}_k \end{bmatrix} = \bar{\mathbf{Y}}_{\text{bus}_{ik}} \begin{bmatrix} \vec{V}_i \\ \vec{V}_k \end{bmatrix}, \tag{7.26}$$

where

$$\bar{\mathbf{Y}}_{\text{bus}_{ik}} = \begin{bmatrix} \frac{D_{ik}}{B_{ik}} & C_{ik} - \frac{A_{ik} D_{ik}}{B_{ik}} \\ -\frac{1}{B_{ik}} & \frac{A_{ik}}{B_{ik}} \end{bmatrix}.$$

In general,

$$\det \left(\begin{bmatrix} A_{ik} & B_{ik} \\ C_{ik} & D_{ik} \end{bmatrix} \right) = 1 \angle 2\phi, \tag{7.27}$$

If $\phi = 0$, that is, complex \bar{T} is real, this determinant is one at angle zero, and complex $\bar{\mathbf{Y}}_{\text{bus}_{ik}}$ becomes symmetrical. Note that equation (7.25) represents a bilateral two port network only if $\bar{T} = 1\angle 0$.

As seen in (7.26), since the UPFC is embedded in the $\bar{\mathbf{Y}}_{\text{bus}}$ matrix, the size of the $\bar{\mathbf{Y}}_{\text{bus}}$ matrix is not changed, so UPFC sensitivity analysis can be performed using this ideal transformer model.

CHAPTER 8

GAS AND ELECTRICITY OPTIMAL POWER FLOW

The purpose of this chapter is to construct a mathematical formulation to solve natural gas and electricity optimal power flow problems. To do this we present a simple combined gas and electric network, and synthesize an optimal gas flow (OGF) and an optimal electric power flow (OPF) into a single natural gas and electricity optimal power flow (GEOPF) problem. Though this integration of gas and electric system is based upon deterministic prices of gas in source nodes, we will certainly need this GEOPF algorithm for stochastic cases for future studies where the price will be a stochastic variable. For our purposes, gas and electricity storage are neglected.

8.1 Gas and Electric Combined Network

For an integrated gas and electric network, even though the gas network and electric network are physically overlapped, we represent the two systems separately. One example is shown in Figure 8.1. Electric generator buses which are coincident with any gas nodes can be used to integrate the gas and electric networks. The generators in the combined nodes are assumed to be driven by gas-powered turbines.

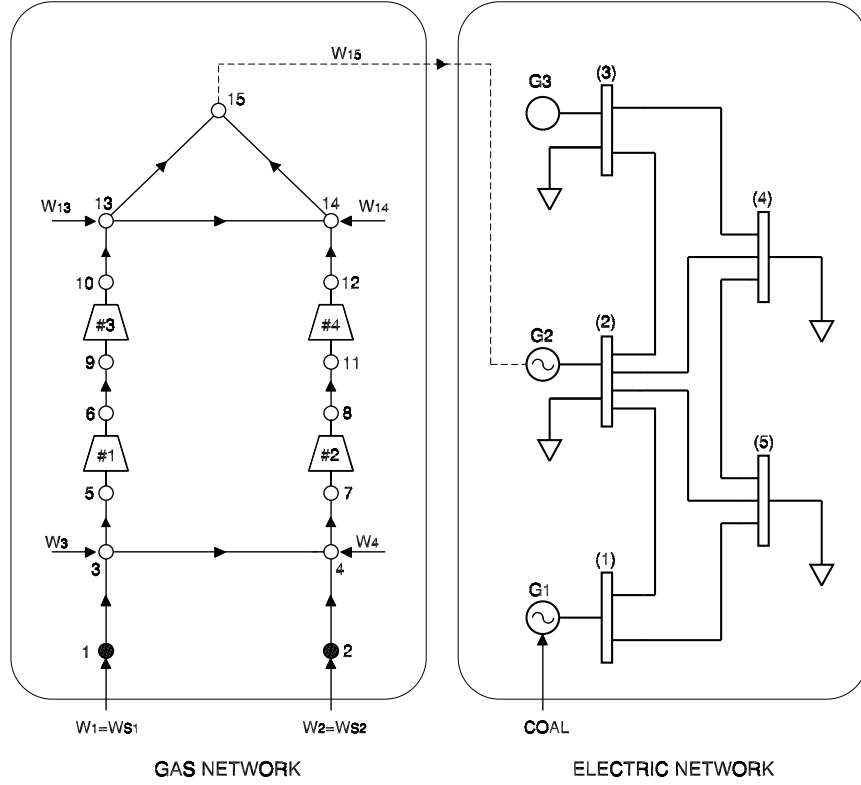


Figure 8.1: Combined natural gas and electricity network

8.2 Gas and Electricity Optimal Power Flow

The mathematical formulation of the GEOPF can be expressed as

$$\min_Y C(Y) - B(Y) \quad (8.1)$$

subject to:

$$h_i(Y) = 0, \quad i = 1, \dots, n \quad (8.2)$$

$$g_j(Y) \leq 0, \quad j = 1, \dots, m \quad (8.3)$$

where

- $C(Y)$ is total cost of system operation, and $B(Y)$ is the total benefit to society and is treated as a negative cost. $SW = B(Y) - C(Y)$ is the social welfare, which is the total benefit $B(Y)$ to society, less the cost of combined system operation, and thus is the negative of the *net* cost of system operation to society. So minimizing net cost $C(Y) - B(Y)$ is the same as maximizing social welfare.

- Y is a vector of decision variables (*i.e.* the voltage magnitude and angle at each bus, real and reactive power generations, real and reactive power consumptions, nodal pressures, flow rates through pipelines, flow rates through compressors, gas consumptions by gas turbines, *etc.*).
- h is a set of equality constraints, such as the real and reactive power balance at each bus, pipeline branch flow rates, the mass flow balance at each node, *etc.*.
- g is a set of inequality constraints, such as line flow limits, voltage limits, generation limits, relative boost limits, nodal pressure limits, *etc.*.

Then the Lagrangian for the GEOPF problem can be written

$$\mathcal{L}(Y) = -SW(Y) - \sum_{i=1}^n \lambda_i h_i(Y) + \sum_{j=1}^m \mu_j g_j(Y). \quad (8.4)$$

Here, the objective of the GEOPF is to maximize the social welfare, while satisfying n equality constraints and m inequality constraints.

8.2.1 Cost, Benefit, and Social Welfare

In the “Poolco” environment, central dispatch sets the price of gas or electricity in the system to optimize a network-wide non-discriminatory service, while consumers and producers contract competitively [8, 1]. The type of problem that the system operator wishes to solve is an optimal power flow (OPF) problem in electricity and an optimal gas flow (OGF) problem in natural gas, but doing so simultaneously in an integrated manner.

The objective function to be maximized that we will use in the GEOPF problem is social welfare [8]. To understand the concept of the social welfare, we introduce the fact that there are two types of market participants, producers and consumers. A producer is a supplier of some type of goods. Of course, there is a cost to produce the good. Let’s say we know the cost of producing the good as a function of the amount

of the good that is produced. In our case, the electricity producer is supplying electric power, so its cost is a function of the amount of real power P_G it produces. The total cost of real power generation is then (assuming quadratic cost curves)

$$\begin{aligned} C_E &= \sum_{\substack{i=1 \\ i \notin \mathcal{G}}}^{N_G} C_{E_i}(P_{G_i}), \\ &= \sum_{\substack{i=1 \\ i \notin \mathcal{G}}}^{N_G} [\alpha_{G_i} + \beta_{G_i} P_{G_i} + \gamma_{G_i} P_{G_i}^2], \end{aligned} \quad (8.5)$$

where

$$\begin{aligned} N_G &= \text{total number of real power generators,} \\ \alpha_{G_i}, \beta_{G_i}, \gamma_{G_i} &= \text{cost coefficients of real power generator } i, \\ \mathcal{G} &= \text{electric nodes with gas-fired generators.} \end{aligned}$$

For the combined node, it is important to note that the electric generation cost is not included in the equation (8.5). This is because the combined nodes simply transform gas energy into electric energy.

For the gas supplier, its production cost is a function of the amount of gas produced. Then, the total production cost becomes

$$C_G = \sum_{i=1}^{N_S} c_i w_{S_i} 10^6 \times \text{GHV}, \quad (8.6)$$

where

$$\begin{aligned} N_S &= \text{total number of source nodes,} \\ c_i &= \text{gas production cost at source node } i \text{ (\$/MMBTU),} \\ \text{GHV} &= \text{gas gross heating value (BTU/SCF).} \end{aligned}$$

A consumer purchases a good because he receives some benefit from using the good. Let us say that this benefit that he/she receives can be measured in dollars and is a quadratic function of the amount of the goods purchased. For the electric

power consumer, the benefit B_E in dollars is a function of the amount of real power P_L consumed. The total benefit received from the consumption of real power (assuming quadratic benefits) by loads is obtained by

$$\begin{aligned} B_E &= \sum_{i=1}^{N_{EL}} B_{E_i}(P_{L_i}), \\ &= \sum_{i=1}^{N_{EL}} [\beta_{EL_i} P_{L_i} + \gamma_{EL_i} P_{L_i}^2], \end{aligned} \quad (8.7)$$

where

N_{EL} = total number of electric consumers,

$\beta_{EL_i}, \gamma_{EL_i}$ = benefit coefficients of real power consumer i .

For a gas consumer, his benefit B_G is a function of the amount of gas consumed. Then, the total benefit received from the consumption of gas is expressed as

$$\begin{aligned} B_G &= \sum_{\substack{i=1 \\ i \notin \mathcal{G}}}^{N_{GL}} B_{G_i}(w_{L_i}), \\ &= \sum_{\substack{i=1 \\ i \notin \mathcal{G}}}^{N_{GL}} [\beta_{GL_i} w_{L_i} + \gamma_{GL_i} w_{L_i}^2], \end{aligned} \quad (8.8)$$

where

N_{GL} = total number of gas consumers,

$\beta_{GL_i}, \gamma_{GL_i}$ = benefit coefficients of gas consumer i .

Note again that the gas consumer's benefit at the combined node is not included since this node is simply converting gas energy to electric energy.

Now we define the meaning of social welfare. It is the total benefit received by society due to the production and consumption of the good. In the case of a combined gas and electric network, the social welfare is defined as

$$\begin{aligned} SW &= B_E + B_G - C_E - C_G \\ &= \sum_{i=1}^{N_{EL}} B_{E_i}(P_{L_i}) + \sum_{\substack{i=1 \\ i \notin \mathcal{G}}}^{N_{GL}} B_{G_i}(w_{L_i}) - \sum_{\substack{i=1 \\ i \notin \mathcal{G}}}^{N_G} C_{E_i}(P_{G_i}) - \sum_{i=1}^{N_S} C_{G_i}(w_{s_i}), \end{aligned} \quad (8.9)$$

and it is the objective function of the GEOPF which we want to maximize, or the negative of that which we wish to minimize.

8.2.2 Constraints

The GEOPF is a constrained optimization problem, which must satisfy various equality and inequality constraints at the optimum.

- **Equality Constraints**

- **Electric Network**

Kirchoff's laws must be satisfied at each electric bus, resulting in the standard power flow (power balance) equations at each bus

$$P_{G_i} - P_{L_i} = P_i(V, \theta), \quad i = 1, \dots, N_B \quad (8.10)$$

$$Q_{G_i} - Q_{L_i} = Q_i(V, \theta), \quad i = 1, \dots, N_B \quad (8.11)$$

The above two equations are conventional power flow equations, and tell that the real and reactive power injection at each bus is a function of the system bus voltage magnitudes and phase angles, or $P_i(V, \theta)$ and $Q_i(V, \theta)$. In our notation, V is the vector of system bus voltage magnitudes, and θ is the vector of bus voltage phase angles. The amount of reactive power consumed by the load, Q_L , is not considered a variable since it will be assumed that the load has a fixed power factor where the power factor is defined as

$$\text{p.f.} = \frac{P_L}{\sqrt{P_L^2 + Q_L^2}}. \quad (8.12)$$

This assumption is not critical to our formulation, and is made for simplicity and concreteness only. Then Q_L is a linear function of the real power

consumed, or

$$Q_L(P_L) = \frac{P_L}{\text{p.f.}} \sqrt{1 - \text{p.f.}^2} . \quad (8.13)$$

The real and reactive injection at bus i can be obtained by

$$\begin{aligned} S_i(V, \theta) &= \vec{V}_i \vec{I}_i^*, & i = 1, \dots, N_B \\ P_i(V, \theta) &= \text{Re}(\bar{S}_i), \\ Q_i(V, \theta) &= \text{Im}(\bar{S}_i), \end{aligned} \quad (8.14)$$

where the vector of current injections at each bus is obtained by

$$\vec{I} = \bar{\mathbf{Y}}_{\text{bus}} \cdot \vec{V}.$$

– Gas Network

There are two sets of steady-state network flow equations, which must be satisfied as equality constraints. The first equality constraint says that the amount of gas at node i transported from and to other nodes must be the same as that of gas injected at that node. This is known as a mass flow balance equation. The set of mass flow equations that describe a gas network is given by

$$(\mathbf{A} + \mathbf{U})f + w - \mathbf{T}\tau = 0, \quad (8.15)$$

where units of f , w and τ are SCF/hr, hence equivalent to conversation of mass. Note that the flow rates to the compressor inlet and from the compressor outlet are different if the compressor is driven by a gas-fired turbine. τ_k is the amount of gas supplied to gas-fired turbine k measured in SCF/hr. For simplicity, we assume

$$\tau_k = \alpha_{Tk} + \beta_{Tk} H_k + \gamma_{Tk} H_k^2, \quad k = 1, \dots, N_C \quad (8.16)$$

where H_k is the horsepower required for compressor k , and defined by

$$H_k = B_k f_k \left[\left(\frac{\pi_j}{\pi_i} \right)^{Z_{ki} \left(\frac{\alpha-1}{\alpha} \right)} - 1 \right]. \quad k = 1, \dots, N_C \quad (8.17)$$

The other equality constraint which is described by equation (5.3) is the pipeline gas flow rate through each pipeline, and it is stated by

$$\pi_i^2 - \pi_j^2 = \frac{1}{M_k^2} \mathcal{S}_{ij} f_{kij}^2, \quad i, j = 1, \dots, N_N \quad (8.18)$$

Note that while the nodal flow equation (8.15) is linear, the pipeline branch flow equation (8.18) is quadratic, and we need to take into account the fact that the flow direction must be explicitly accounted for (by \mathcal{S}_{ij}).

– Gas and Electricity Combined Node

This is the location of an actual or planned gas-fired generation facility, which would be located where a gas node and an electric power bus have a common location. The gas node may have other loads or input injections, as may the electrical node the generator is connected to. Let us suppose that the electrical bus in question is i , which is fed gas from gas node j_i . Then

$$w_{j_i} = w_{j_i, \text{other}} - (a_{G_i} + b_{G_i} P_{G_i} + c_{G_i} P_{G_i}^2) \frac{1}{\text{GHV}}, \quad i \in \mathcal{G} \quad (8.19)$$

where

GHV = gas gross heating value (BTU/SCF),

$a_{G_i}, b_{G_i}, c_{G_i}$ = gas fuel rate coefficients at node i ,

\mathcal{G} = electric nodes with gas-fired generators.

• Inequality Constraints

– Electric Network

The system operating constraints include maximum and minimum limits

on the voltage magnitude at each bus and the magnitude of the line current flowing on each line. These can be written as

$$V_{\min_i} \leq V_i \leq V_{\max_i}, \quad i = 1, \dots, N_B \quad (8.20)$$

for the voltage magnitude at bus i , and

$$I_{ik\max}^2 \geq \left| \vec{I}_{ik} \right|^2 = \vec{I}_{ik} \cdot \vec{I}_{ik}^*, \quad i, k = 1, \dots, N_B \quad (8.21)$$

where

$$\vec{I}_{ik} = \left(\vec{V}_i - \vec{V}_k \right) \bar{y}_{ik} + \vec{V}_i \bar{y}_{\text{shunt}_{ik}}$$

for the magnitude of the line current from bus i to bus k . Equation (8.21) is called a transmission thermal limit. Since the voltage magnitude at each bus is changed, we use the line current instead of the apparent power flowing on each line for the thermal limit, although an apparent power constraint could be used instead. Also, if voltage drop or the steady state stability limits real power flow, these constraints could be used instead.

There are also limits on the amount of real and reactive power produced by each generator. There may also be a limit on the amount of real power consumed by each load. This gives us an additional set of inequality constraints.

$$P_{G\min_i} \leq P_{G_i} \leq P_{G\max_i}, \quad i \in N_{PG} \quad (8.22)$$

$$Q_{G\min_i} \leq Q_{G_i} \leq Q_{G\max_i}, \quad i \in N_{QG} \quad (8.23)$$

$$P_{L\min_i} \leq P_{L_i} \leq P_{L\max_i}, \quad i \in N_{EL} \quad (8.24)$$

The tap magnitude and the tap angle of a regulating transformer, the voltage magnitude and the angle drop along a transmission line, MW interchange transactions, shunt reactors or capacitors, *etc.* can be also included as inequality constraints if required [11].

– **Gas Network**

The system operating constraints include maximum and minimum limits on the pressure at each node and maximum relative boost limits for each compressor. These can be written as

$$\pi_{\min_k} \leq \pi_k \leq \pi_{\max_k}, \quad k = 1, \dots, N_N \quad (8.25)$$

for the pressure π_i at node i , and

$$1 \leq \left(\frac{\pi_j}{\pi_i} \right)_k \leq R_{\max_k}, \quad k = 1, \dots, N_C \quad (8.26)$$

for the relative boost rate between the inlet pressure π_i and the outlet pressure π_j at compressor station k . There are also limits on the amount of gas supplied at each source node. There may also be limits on the amount of gas consumed by gas consumers. This gives us an additional set of inequality constraints.

$$w_{\min_{S_i}} \leq w_{S_i} \leq w_{\max_{S_i}}, \quad i = 1, \dots, N_S \quad (8.27)$$

$$w_{\min_{L_i}} \leq w_{L_i} \leq w_{\max_{L_i}}, \quad i = 1, \dots, N_{GL} \quad (8.28)$$

CHAPTER 9

OPTIMAL LOCATION OF A UPFC IN A POWER SYSTEM

This chapter presents a screening technique for greatly reducing the computation involved in determining the optimal location and estimation of the generation cost saving when a UPFC is installed and operated optimally. An technique to obtain the first- and second-order sensitivities of the generation cost with respect to UPFC control parameters is described. The sensitivity analysis attempts to estimate the UPFC value without having to run the OPF with the UPFC several times. This sensitivity technique can be used to optimally locate a UPFC in a large power system by ignoring the transmission lines with low marginal value (MV) and low estimated incremental value (IV), and running a full OPF only for the lines with higher estimated IV to obtain actual IV. Thus, this technique can greatly reduce the computational burden of determining the optimal location of the UPFC in a large power system.

9.1 Optimal Power Flow with UPFC

Suppose that a UPFC is installed in transmission line ik . The mathematical formulation of the OPF with the UPFC can be expressed as

$$\min_{y, x_{ik}} C(y, x_{ik}) \tag{9.1}$$

subject to:

$$h_i(y, x_{ik}) = 0, \quad i = 1, \dots, n \quad (9.2)$$

$$g_j(y, x_{ik}) \leq 0, \quad j = 1, \dots, m \quad (9.3)$$

where

- $C(y, x_{ik})$ is the total generation cost.
- y is a vector of decision variables.
- $x_{ik} = [T_{ik} \ \phi_{ik} \ \rho_{ik}]^T$ is a vector of the UPFC control variables in line ik .
- $\{h_i : i = 1, \dots, n\}$ is the set of equality constraint functions.
- $\{g_j : j = 1, \dots, m\}$ is the set of inequality constraint functions.

We use the UPFC ideal transformer model to construct the equations for OPF with a UPFC. It is important to note that the number of equality constraints is the same as that of the base case OPF with no UPFC. This is because the UPFC control variables do not depend on UPFC input and output voltages and currents, and the UPFC model is embedded in the $\bar{\mathbf{Y}}_{\text{bus}}$ matrix, and because we ignore UPFC operation limits.

Now, let us construct the Lagrange for the OPF problem as

$$\mathcal{L}_o(y, \lambda, \mu, x_{ik}) = C(y, x_{ik}) + \sum_{i=1}^n \lambda_i h_i(y, x_{ik}) + \sum_{j=1}^m \mu_j g_j(y, x_{ik}), \quad (9.4)$$

where λ_i and μ_j are the Lagrange multipliers for the equality and inequality constraints, respectively. To solve the proposed OPF problem with inequality constraints, we use the primal-dual interior-point method. At the optimum, the last term of (9.4) must satisfy the complementary slackness condition such that $\mu_j g_j = 0$ for each $j = 1, \dots, m$. Therefore, if an inequality constraint is binding in (9.4), we could treat it as an equality constraint, and we could ignore it if it is not binding.

Since we are using interior-point methods – not active-set methods – we do not have to distinguish between active and inactive constraints until the OPF problem is solved [20]. This avoids “cycling” behavior in the active set associated with “active-set” methods such as Newton’s. Then, to derive the first-order sensitivities, we rewrite (9.4) as

$$\mathcal{L}_o(y, \lambda, x_{ik}) = C(y, x_{ik}) + \sum_{j \in \mathcal{A}} \lambda_j h_j(y, x_{ik}), \quad (9.5)$$

where \mathcal{A} is the set of active constraints, which are known once the base-case OPF is solved.

9.2 First-Order Sensitivity Analysis

We consider the case where the UPFC is inserted in line ik , and the UPFC ideal transformer model is used for the analysis.

The marginal values(MVs) of the UPFC, to be installed in line ik , are simply the amounts by which the total cost of system operation could be changed by allowing a small change of the UPFC control variables in line ik . We can obtain the MVs by assuming that there is a UPFC in line ik , but that the UPFC is not operating. So we add three extra constraints

$$T_{ik} = T, \quad \phi_{ik} = \phi, \quad \rho_{ik} = \rho$$

to the original OPF problem, and for simplicity, we denote the constraints as $x_{ik} = x$. Then, the new Lagrangian can be written

$$\mathcal{L}_{ik}(y, \lambda, x_{ik}, \lambda_x) = C(y, x_{ik}) + \sum_{j \in \mathcal{A}} \lambda_j h_j(y, x_{ik}) + \lambda_x^T (x - x_{ik}), \quad (9.6)$$

where

$$\lambda_x = [\lambda_T \ \lambda_\phi \ \lambda_\rho]^T.$$

We define the function $\lambda_x^*(x)$ to be the optimal value of the Lagrange multiplier on the constraint $x_{ik} = x$. Here, we are most interested in $\lambda_x^*(x = x_0)$, which is associated

with the constraints:

$$T_{ik} = 1, \quad \phi_{ik} = 0, \quad \rho_{ik} = 0.$$

This is because the OPF problem when solved with the UPFC control parameters $x = x_0$ yields the same result for y and λ as the base case where there is no UPFC in line ik .

Using the first-order conditions for the solution of the OPF problem for $x_{ik} = x_0$,

$$\frac{\partial \mathcal{L}_{ik}}{\partial x_{ik}} = 0, \quad (9.7)$$

we can solve for $\lambda_x^*(x_0)$ to obtain

$$\lambda_x^*(x_0) = \left[\frac{\partial C(y^*, x_{ik})}{\partial x_{ik}} + \sum_{j \in A} \lambda_j^* \frac{\partial h_j(y^*, x_{ik})}{\partial x_{ik}} \right] \bigg|_{x_{ik}=x_0}. \quad (9.8)$$

Note that

$$\frac{\partial C(y^*, x_{ik})}{\partial x_{ik}} \text{ and } \lambda_j^* \frac{\partial h_j(y^*, x_{ik})}{\partial x_{ik}} \bigg|_{x_{ik}=x_0}$$

are easy to compute. Equation (9.8) indicates that the marginal value $\lambda_x^*(x_0)$ can be determined once we know y^* and λ^* , which are obtained from the base case OPF with no UPFC. Thus, if we know y^* and λ^* , we can obtain the first-order sensitivities of cost with respect to UPFC control variables x for each possible transmission line by solving **only** the base-case OPF.

Now, we will give the desired interpretation for the Lagrange multiplier λ_x by essentially re-deriving the envelope theorem for our case. The Lagrangian in (9.6) can be rewritten as

$$\mathcal{L}_{ik}(z, \lambda_z) = C(z) + \lambda_z^T h_z(z), \quad (9.9)$$

where $z = [y \ x_{ik}]^T$, $\lambda_z = [\lambda \ \lambda_x]^T$ and $h_z = [h \ x - x_{ik}]^T$. Let the solution of the OPF with the UPFC be denoted by $C^*(x)$, and let the optimal values of z and λ_z be denoted by $z^*(x)$ and $\lambda_z^*(x)$, respectively. Then

$$C^*(x) = \mathcal{L}_{ik}(z^*(x), \lambda_z^*(x), x). \quad (9.10)$$

We differentiate $C^*(x)$ with respect to x to obtain

$$\begin{aligned}
\frac{d}{dx}C^*(x) &= \frac{d}{dx}\mathcal{L}_{ik}(z^*(x), \lambda_z^*(x), x) \\
&= \frac{d}{dx} [C(z^*(x), x) + \lambda_z^{*T}(x)h_z(z^*(x), x)] \\
&= \underbrace{\left[\frac{\partial}{\partial z}C + \lambda_z^{*T}(x)\frac{\partial}{\partial z}h_z \right]}_0 \frac{dz^*(x)}{dx} + \underbrace{[h_z^T(z^*(x), x)]}_0 \frac{d\lambda_z^*(x)}{dx} \\
&\quad + \frac{\partial C}{\partial x}(z^*(x), x) + \lambda_z^{*T}(x)\frac{\partial h_z}{\partial x}(z^*(x), x) \\
&= \frac{\partial C}{\partial x}(z^*(x), x) + \lambda_z^{*T}(x)\frac{\partial h_z}{\partial x}(z^*(x), x),
\end{aligned} \tag{9.11}$$

where the two terms in square brackets are equal to zero by virtue of the KKT first-order optimality conditions. Equation (9.11) indicates that the change in the system generation cost results from the change in C due to the change in x and the change in h_z due to the change in x , as the envelope theorem says.

The interpretation of λ_x can be obtained by considering the constraint $(x - x_{ik})$ and writing

$$C(z^*(x)) = C(z^*(x), x) \tag{9.12}$$

and

$$h(z^*(x), x) = h(z^*(x)) + [0 \ \cdots \ 0 \ x - x_{ik}]^T. \tag{9.13}$$

Then the envelope theorem [8, 28] says that

$$\frac{d}{dx}C^*(x) = \lambda_x^{*T}(x). \tag{9.14}$$

For any value of the parameter x , the interpretation of the multiplier $\lambda_x^*(x)$ is the marginal change in the total generation cost as the constraint $x_{ik} = x$ is changed slightly. If such a change is allowed, it would be made to improve the objective function. The sign of λ_x^* determines the desired direction of the change in components of x_{ik} . Therefore, only the absolute value of the multiplier matters. As we vary x from x_0 to the set of optimal values x_{ik}^* , the multiplier will vary from the marginal

value $\lambda_x^*(x_0)$ to the value $\lambda_x^*(x_{ik}^*) = 0$. This is because, if we constrain x_{ik} to be equal to its unconstrained optimal value, the multiplier for this constraint must be zero.

Since the UPFC model is embedded in the $\bar{\mathbf{Y}}_{\text{bus}}$ matrix, as explained in (7.26), the first-order UPFC sensitivity analysis is only associated with complex power injections at buses i and k , and the thermal limit of transmission line ik if it is binding. If transmission flow is limited by steady-state stability, such constraints ($|P_{ik}| \leq P_{\text{max}}$, or $|\theta_i - \theta_k| \leq \theta_{\text{max}}$) can be included as well.

9.3 Second-Order Sensitivity Analysis

The second-order sensitivity we wish to obtain is

$$H_x = \left. \frac{d^2 C^*(x_{ik})}{dx^2} \right|_{x_{ik}=x_o} = \left. \frac{d\lambda_x^*(x_{ik})}{dx} \right|_{x_{ik}=x_o}. \quad (9.15)$$

As in the first order sensitivity analysis, we artificially insert the UPFC between bus i and bus k , but then constrain $x_{ik} = x$, where we are primarily interested in the case where $x = x_0$, since it represents the base case OPF with no UPFC installed. Rather than including the additional control variable x_{ik} in the vector of decision variables y , and the additional multipliers λ_x in the vector of multipliers λ , we keep these two variables separate for clarity.

By the first-order conditions for optimality, the Lagrange function (9.6) must satisfy the following condition:

$$\begin{aligned} \omega(u, x) &= \nabla_u \mathcal{L}_{ik} \\ &= \begin{bmatrix} \nabla_y \mathcal{L}_{ik} \\ \nabla_\lambda \mathcal{L}_{ik} \\ \nabla_{x_{ik}} \mathcal{L}_{ik} \\ \nabla_{\lambda_x} \mathcal{L}_{ik} \end{bmatrix} = \begin{bmatrix} \nabla_y \mathcal{L}_{ik} \\ h(y, x_{ik}) \\ \nabla_{x_{ik}} \mathcal{L}_{ik} \\ (x - x_{ik}) \end{bmatrix} = 0, \end{aligned} \quad (9.16)$$

where

$$u = \begin{bmatrix} y \\ \lambda \\ x_{ik} \\ \lambda_x \end{bmatrix}.$$

Note that x occurs only in the term $\lambda_x^T (x - x_{ik})$ of the Lagrangian in (9.6), so that mixed partials involving y and x , λ and x , and x_{ik} and x are zero. Thus we have

$$\frac{\partial \omega}{\partial x} = \begin{bmatrix} 0 \\ 0 \\ 0 \\ +I \end{bmatrix}, \quad (9.17)$$

where I is an identity matrix with the size of x_{ik} .

As the vector x of the UPFC parameters changes, so will the optimal value of u . Let us denote the optimal value by $u^*(x)$. Then for each x , it must satisfy the condition (9.16):

$$\omega(u^*(x), x) = 0, \quad \forall x \quad (9.18)$$

Since optimality is maintained as we change x , it must satisfy

$$\frac{d}{dx} \omega(u^*(x), x) = 0. \quad (9.19)$$

If we expand (9.19) by the chain rule, then we have

$$\frac{\partial \omega}{\partial u} \cdot \frac{du^*(x)}{dx} + \frac{\partial \omega}{\partial x} = 0. \quad (9.20)$$

The first term of (9.20) can be expressed as

$$\begin{aligned} \frac{\partial \omega}{\partial u} &= W_{ik}(u^*(x), x) \\ &= \begin{bmatrix} H_y & J_y^T & \nabla_y \nabla_{x_{ik}}^T \mathcal{L}_{ik} & 0 \\ J_y & 0 & J_{x_{ik}} & 0 \\ \nabla_{x_{ik}} \nabla_y^T \mathcal{L}_{ik} & J_{x_{ik}}^T & H_{x_{ik}} & -I \\ 0 & 0 & -I & 0 \end{bmatrix}, \end{aligned} \quad (9.21)$$

where H_y and $H_{x_{ik}}$ are the Hessians of the Lagrangian, and J_y and $J_{x_{ik}}$ are the Jacobians of constraints in the active set \mathcal{A} with respect to y and x_{ik} , respectively. Using $W_{ik}(u^*(x), x)$, we can rewrite (9.20) in simple form as

$$W_{ik} \frac{du^*(x)}{dx} = -\frac{\partial \omega}{\partial x}. \quad (9.22)$$

Then, (9.22) becomes

$$W_{ik} \cdot \begin{bmatrix} \frac{dy^*(x)}{dx} \\ \frac{d\lambda^*(x)}{dx} \\ \frac{dx_{ik}^*(x)}{dx} \\ \frac{d\lambda_x^*(x)}{dx} \end{bmatrix} = \begin{bmatrix} 0 \\ 0 \\ 0 \\ -I \end{bmatrix}. \quad (9.23)$$

In equation (9.23), we can see that $dx_{ik}^*/dx = I$, an obvious result since we have constrained $x_{ik} = x$. The first two equations can be combined and rearranged to obtain

$$\begin{bmatrix} \frac{dy^*(x)}{dx} \\ \frac{d\lambda^*(x)}{dx} \end{bmatrix} = -W^{-1} \cdot \begin{bmatrix} \nabla_y \nabla_{x_{ik}}^T \mathcal{L}_{ik} \\ J_{x_{ik}} \end{bmatrix}, \quad (9.24)$$

where

$$W = \begin{bmatrix} H_y & J_y^T \\ J_y & 0 \end{bmatrix}.$$

Once this is found, the third equation can be rearranged to yield

$$\left. \frac{d\lambda_x^*(x)}{dx} \right|_{x=x_0} = \begin{bmatrix} \nabla_{x_{ik}} \nabla_y^T \mathcal{L}_{ik} & J_{x_{ik}}^T \end{bmatrix} \cdot \left. \begin{bmatrix} \frac{dy^*(x)}{dx} \\ \frac{d\lambda^*(x)}{dx} \end{bmatrix} \right|_{x=x_0} + H_{x_{ik}}. \quad (9.25)$$

The matrix W is not affected by the UPFC since we set $x = x_0$. Thus, to calculate $d\lambda_x^*/dx$ for $x = x_0$, we already have available W matrix in factored form, so only single forward substitution and back substitution are required in (9.24).

9.4 Estimation of Incremental Value using First- and Second-Order Sensitivities

Now, we will estimate the incremental value of the UPFC using the first- and second-order sensitivities. We approximate $\lambda_x(x)$ as a linear function of x . Let us expand $C(z^*(x), x)$ at the optimum with respect to x . Then, we have

$$\begin{aligned} C(z^*(x), x) &= C(x) \\ &= C(x_0) + \lambda_x^{*T}(x_0)\Delta x + \frac{1}{2}\Delta x^T H_x(x_0)\Delta x + H.O.T, \end{aligned} \quad (9.26)$$

where

$$\Delta x = x - x_0.$$

Neglecting the high order terms in (9.26) and differentiating with respect to x yield

$$\nabla_x C(x) \cong \lambda_x^*(x_0) + H_x(x_0)\Delta x. \quad (9.27)$$

Since $\nabla_x C(x) = 0$ at the optimum, the estimated optimal value of x is obtained as

$$\hat{x}^* = -H_x^{-1}(x_0)\lambda_x^*(x_0) + x_0. \quad (9.28)$$

The estimated incremental value (\widehat{IV}) at the estimated optimum \hat{x}^* is then calculated as

$$\begin{aligned} \widehat{IV} &= C(x_0) - C(\hat{x}^*), \\ &= -\lambda_x^{*T}(x_0)(\hat{x}^* - x_0) - \frac{1}{2}(\hat{x}^* - x_0)^T H_x(x_0)(\hat{x}^* - x_0), \\ &= \lambda_x^{*T}(x_0)H_x^{-1}(x_0)\lambda_x^*(x_0) - \frac{1}{2}\lambda_x^{*T}(x_0)H_x^{-T}(x_0)H_x(x_0)H_x^{-1}(x_0)\lambda_x^*(x_0), \\ &= \frac{1}{2}\lambda_x^{*T}(x_0)H_x^{-1}(x_0)\lambda_x^*(x_0) \geq 0. \end{aligned} \quad (9.29)$$

Although IV is by definition nonnegative, nonnegativity of \widehat{IV} is guaranteed only if H_x is positive semidefinite (which is not guaranteed).

The accuracy of \widehat{IV} depends also on the fact that \mathcal{A} does not change in (9.5) since this would change (9.16), the fundamental equation for the sensitivity analysis.

CHAPTER 10

RESULTS

10.1 Result of Sensitivity Analysis

The proposed sensitivity methods are tested on a 5-bus system derived from the IEEE 14-bus system, and IEEE 14- and 30-bus systems to establish their effectiveness. These systems have 7, 20, 41 transmission lines, respectively. Figure 10.1 shows the 5-bus system [15]. The system consists of two generators at buses 1 & 2 and one synchronous condenser at bus 3. We assume that generator 2 has higher generation cost than generator 1, and UPFCs are installed in the middle of each transmission line. Loads are assigned such that the current flow constraint in line 1 is binding (we assume that thermal constraints limit line flow for this example).

The marginal values ($|\lambda_T|$, $|\lambda_\phi|$ and $|\lambda_\rho|$), estimated incremental values (\widehat{IV}) and

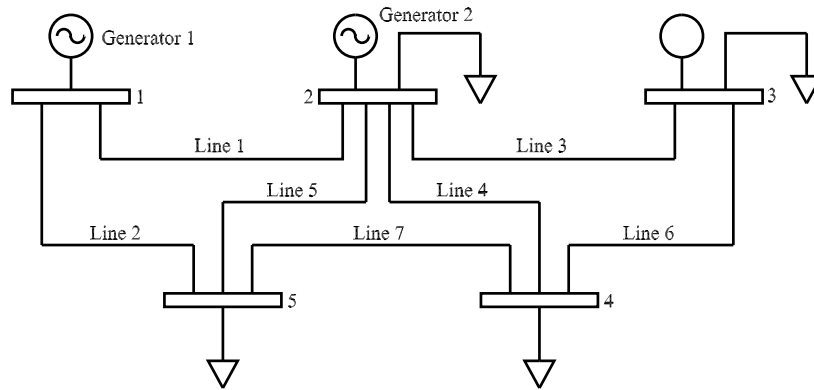


Figure 10.1: Diagram of 5-bus subset of IEEE 14-bus system [15]

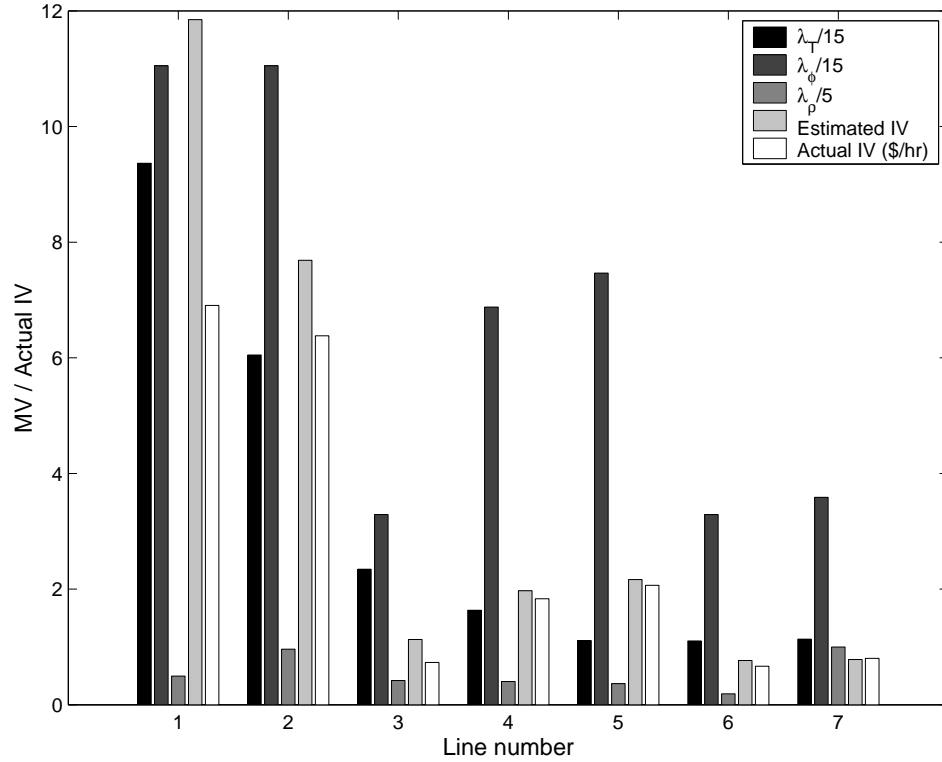


Figure 10.2: Normalized marginal and incremental values for 5-bus system.

actual incremental values (IV) for the 5-bus system are shown in Figure 10.2. It shows that the lines with high MVs usually produce high estimated IVs. The UPFC location in line 1 produces high MVs for $|\lambda_T|$ and $|\lambda_\phi|$, and the highest estimated IV. In general, it is more economical to locate the UPFC in heavily-loaded high voltage

UPFC Location	P_{G1}	P_{G2}	P_{loss}	Est. IV	Actual IV
	MW	MW	MW	\$/hr	\$/hr
Without UPFC	198.18	71.60	10.51	0	0
Line 1	219.31	51.18	11.64	11.85	6.90
Line 2	224.56	46.19	11.90	7.69	6.38
Line 3	196.85	72.77	10.77	1.13	0.73
Line 4	202.45	67.40	10.99	1.97	1.83
Line 5	204.52	65.44	11.11	2.17	2.07
Line 6	196.85	72.73	10.73	0.75	0.67
Line 7	202.59	67.22	10.95	0.78	0.80

Table 10.1: Real power generation, line loss and total generation cost for 5-bus system

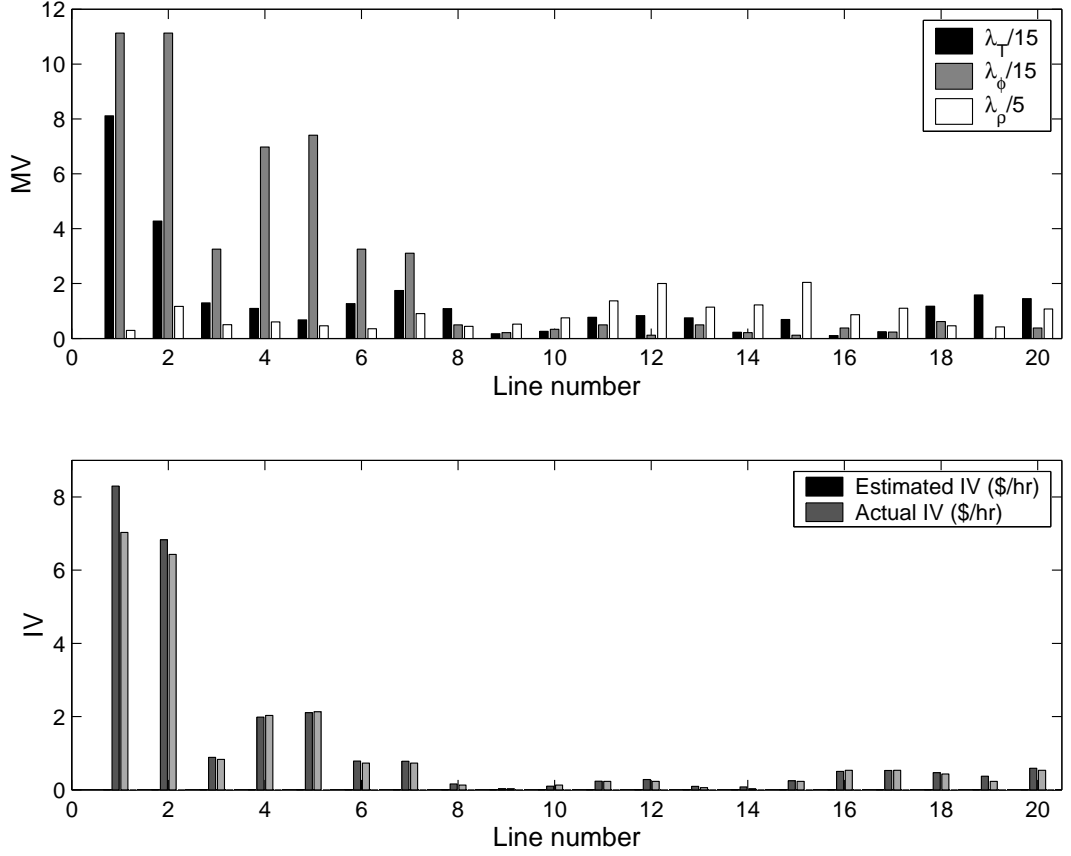


Figure 10.3: Marginal and incremental values for IEEE 14-bus system.

line 1 since it allows more power to be transmitted in under-utilized line 2 while preventing line 1 from overloading. Eventually, no further savings due to UPFC operation can be achieved because of the voltage constraint at bus-2.

Also, reasonable agreement can be observed between the estimated IVs and the actual IVs except line 1 and line 2. The difference between the estimated IV and the actual IV is attributed to the fact that some inequality constraints become binding so that the UPFC cannot be fully utilized. Thus, it is important that the set of binding constraints does not change as x changes in order to obtain a reliable estimated IV. (However, we cannot actually verify this without many additional OPF solutions).

For the 5-bus case, Table 10.1 shows real power generations, transmission line losses and incremental values. Since the generation marginal cost, adjusted for marginal losses at bus 1 is lower than that at bus 2, it is profitable to obtain more

real power from generator 1 as long as its loss-adjusted marginal cost stays lower and no operational limits are reached.

The test results of the IEEE 14-bus system are shown in Figure 10.3. Similar load conditions as in the 5-bus system are used such that the constraint on current in line 1 is binding. As before, the lines with higher MVs produce higher estimated and actual IVs. An important fact to note is that higher voltage lines 1 through 7 are the most suitable locations to install the UPFC. This is because higher voltage lines have lower p.u. impedances and therefore, most of the power will be transferred through those lines and some of the lines may reach their maximum transfer capabilities.

The simulation result for the IEEE 30-bus system is shown in Figure 10.4. Again, lines with low marginal values tend to yield low estimated and actual incremental values, and the most valuable locations tend to be in the high voltage portions of the

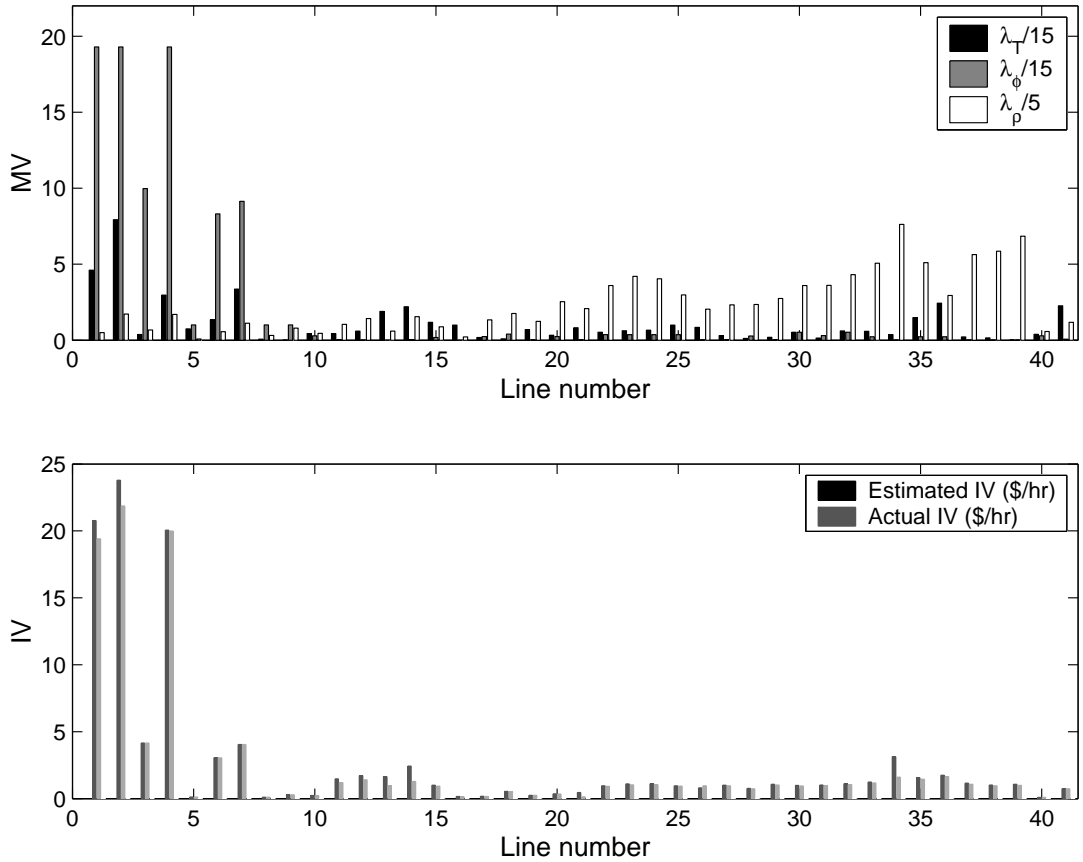


Figure 10.4: Marginal and incremental values for IEEE 30-bus system.

system. Figure 10.4 also shows that estimated IVs are quite close to actual IVs. In addition, we see that locations with large incremental values are also those with large marginal values, thus supporting the idea of using only first-order sensitivity analysis to screen for promising locations for installation of a UPFC.

10.2 Result of GEOPF

This section contains case studies that evaluate the capability of the GEOPF in maximizing social welfare associated with electricity generation cost, gas supply cost, and gas and electricity consumer's benefit. The coefficients of quadratic generation cost and benefit curves are summarized in Appendix C. Since combined nodes are considered as nodes which simply convert gas energy to electric energy, these nodes are not associated with generation cost and gas consumer's benefit. Instead, we will

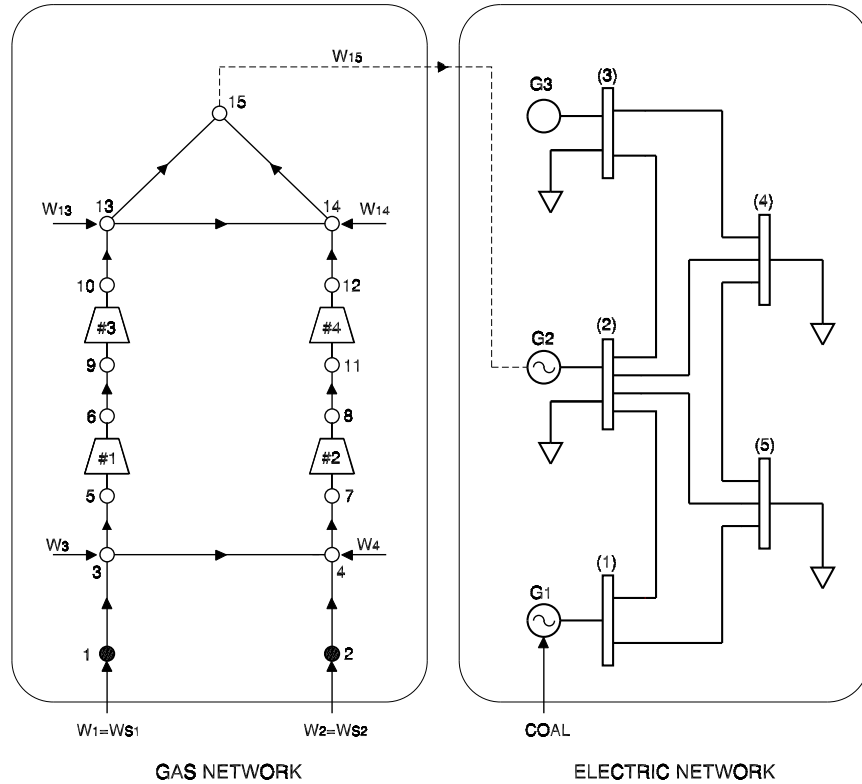


Figure 10.5: Combined gas and electric network

use the coefficients of the fuel rate curve for the gas-fired generator to calculate the amount of gas supplied to the combined node.

10.2.1 Test System I

We will first consider a simple combined network with two real power generators, one of which is a gas-fired generator and the other is a coal-fired generator. Tie-line connections in both natural gas and electricity networks are not considered in this test system. The system analyzed is a combined natural gas and electricity network, which consists of a 5-bus system and a 15-node gas system, as shown in Figure 10.5. The 15-node system is a modification of an example system in [22], plus some made-up benefit and cost functions. The 5-bus electric system obtained by modifying the IEEE 14-bus system has two real power generators at buses 1 and 2, one synchronous condenser at bus 3, and four loads at buses 2 through 5, and bus 1 serves as the reference/slack bus in the electric network. The generator at bus 2 is coincident with gas network node 15. We assume that node 1 is the known-pressure node in the gas system. The gas network has fifteen nodes consisting of five loads at nodes 3, 4, 13, 14, and 15, two sources at nodes 1 and 2, and eight compressor inlet-outlet nodes 5 through 12. We assume that the compressors in the gas network are driven by gas turbines, and the gas is tapped from the outlet node of the compressor station. Appendix C shows the input data for gas and electricity network represented in Figure 10.5.

We assume that generator 1 uses coal with a fixed price, and generator 2 uses natural gas with high price variations.

To study the impact of the wellhead gas prices at source nodes 1 and 2 to the real power generation at combined node 15, three test conditions with different wellhead gas prices are considered as follows:

Case 1:	
Wellhead gas price at node 1 = \$2.07 /($10^6 \times$ BTU)	
Wellhead gas price at node 2 = \$2.12 /($10^6 \times$ BTU)	
Case 2:	
Wellhead gas price at node 1 = \$2.46 /($10^6 \times$ BTU)	
Wellhead gas price at node 2 = \$2.71 /($10^6 \times$ BTU)	
Case 3:	(pipeline branch between nodes 12 and 14 removed)
Wellhead gas price at node 1 = \$2.46 /($10^6 \times$ BTU)	
Wellhead gas price at node 2 = \$2.71 /($10^6 \times$ BTU)	

Wellhead gas prices in cases 2 and 3 are higher than those in case 1. Table 10.2 shows simulation results for the three case studies. In case 1, the gas-fired generator reaches its maximum generation limit due to the low gas price at combined node 15. As noted in Table 10.2, the optimal real power generation P_{G_2} at the combined node is quite sensitive to the wellhead gas prices, and reduced greatly as the wellhead gas prices increase. In case 3, we assume that the pipeline branch between nodes 12 and 14 is unavailable due to a forced-outage. The gas-fired generator reaches its minimum generation limit, which indicates that contingencies occurring in the gas network may result in the significant change of electricity generation patterns. Now, let us compare the social welfare of non-integrated gas and electricity operation with that obtained from the GEOPF for case 2. The social welfare from the GEOPF is \$22,405.83/hr, and the gas price at node 15 is \$2.82/($10^6 \times$ BTU). For non-integrated network operation, let's say that there is a broker who purchases gas from node 15, and sells it to the gas-fired generator at bus 2. He has a long-term contract with the gas-fired generator that he will supply gas at a fixed price. (obviously other contractual arrangements are possible.) But, he will purchase gas from the spot market in the gas network. Thus, the broker can make profit by the price difference

times the amount of gas sold. With the prices of coal and natural gas given, the OPF is implemented to obtain social welfare maximizing solutions in the electric network. Then, the amount of gas transformed to electrical energy at the combined node is used as equality constraint in the OGF problem to calculate the optimal gas network operation scheme. Figure 10.6 shows social welfare losses if we optimize two networks by individually running OPF and OGF with different gas prices at node 15. Since the broker is involved for non-integrated operation, the social welfare is calculated by

$$SW = SW_E + SW_G + B_B, \quad (10.1)$$

where

$$SW_E = \text{electric network social welfare,}$$

$$SW_G = \text{gas network social welfare,}$$

$$B_B = \text{broker's benefit (profit).}$$

Figure 10.6 indicates that the social welfare loss becomes zero when the gas price at node 15 is \$2.82/(10⁶×BTU), which is the same as the marginal cost of gas at node 15 obtained from the GEOPF. Thus, we can verify that the GEOPF returns the social welfare maximizing solutions for the combined gas and electricity network. Since the broker maintains a price difference between the gas price at node 15 and the gas price at the generator at bus 2, the social welfare is reduced even though the difference between payments from the electric system to the gas system exactly cancel out in the overall social welfare, but prices are distorted from their optimal values. Other contractual arrangements with the broker might result in different outcomes.

10.2.2 Test System II

We have seen in Figure 10.6 that we can obtain optimal solutions for the GEOPF by individually running the OPF and the OGF. However, if there are more than one

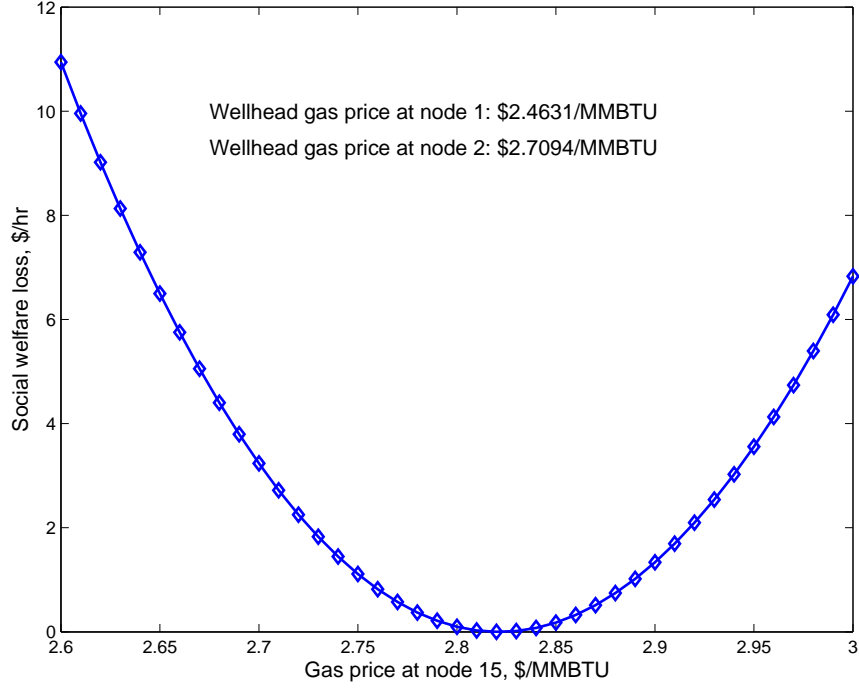


Figure 10.6: Social welfare losses due to non-integrated operation for test system I combined node, optimal solutions cannot be easily obtained by non-integrated network operation. To analyze the electric network with two gas-fired and one coal-fired generators, we will combine the 15-node gas system with WSCC 9-bus system [29]. The WSCC-9 bus system consists of three generators, three loads, and six transmission lines. Network modeling parameters are converted into the IEEE common data format [30] in Appendix C. The generators at buses 2 and 3 are coincident with the gas network at nodes 4 and 15, respectively. The generator at bus 1 is a coal-fired generator with a fixed coal price. Electric loads are located at buses 5, 6, and 8. The coefficients of generator cost curves and consumer benefit curves are given in Appendix C.

We will consider three cases with different wellhead gas prices, and see how they affect the network operation patterns. In case 3, we assume that the pipeline between nodes 12 and 14 is unavailable. The three test cases are given below:

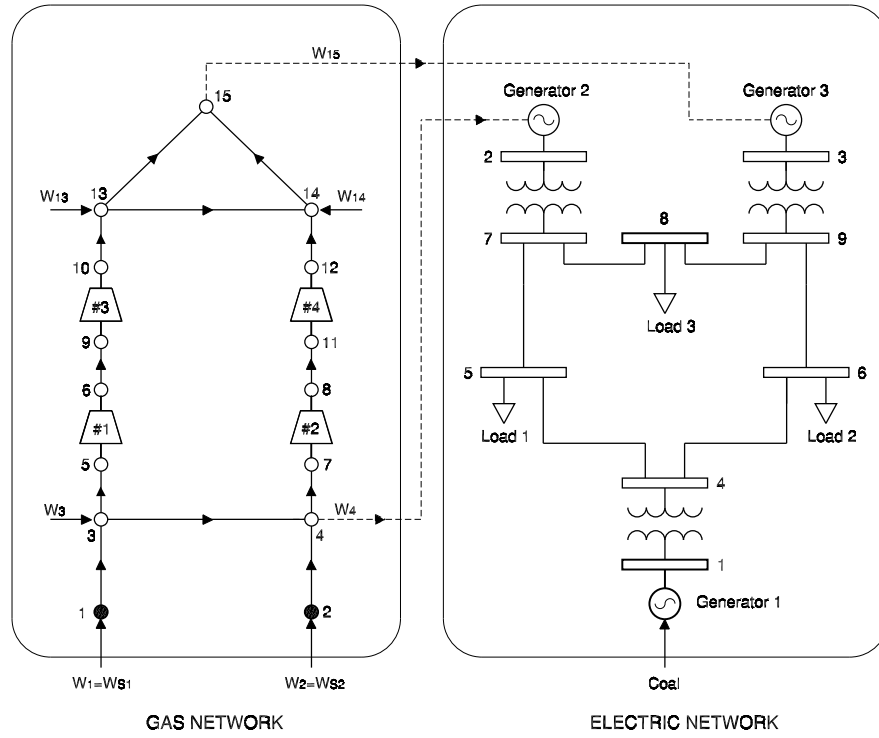


Figure 10.7: Combined gas and electric network

Case 1:	
Wellhead gas price at node 1 = \$2.07 /($10^6 \times$ BTU)	
Wellhead gas price at node 2 = \$2.12 /($10^6 \times$ BTU)	
Case 2:	
Wellhead gas price at node 1 = \$2.51 /($10^6 \times$ BTU)	
Wellhead gas price at node 2 = \$2.51 /($10^6 \times$ BTU)	
Case 3: (pipeline branch between nodes 12 and 14 removed)	
Wellhead gas price at node 1 = \$2.07 /($10^6 \times$ BTU)	
Wellhead gas price at node 2 = \$2.12 /($10^6 \times$ BTU)	

Table 10.3 shows the GEOPF results for three test cases. The coal-fired generator reaches its minimum generation limit since the wellhead gas prices are relatively low in case 1. As the wellhead gas prices increase, the generation patterns are changed noticeably as in case 2. In addition, the amount of gas production at each source node

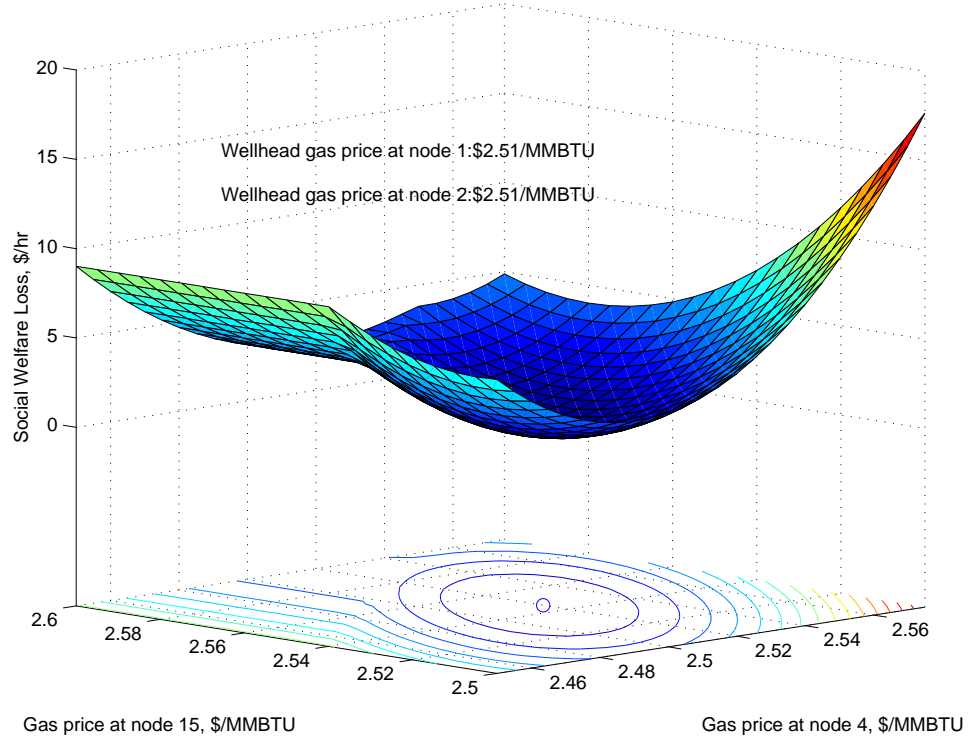


Figure 10.8: Social welfare losses due to non-integrated operation for test system II varies significantly depending on the wellhead gas prices. The electric generation at bus 3 is significantly reduced due to high gas price at node 15. In case 3, we can see that the generation pattern is changed noticeable due to the gas transmission line outage.

Now, we will compare the social welfare of non-integrated gas and electricity operation with that obtained from the GEOPF for case 2. Due to having to guess the gas prices at the two combined nodes for non-integrated gas and electricity operation, the social welfare maximizing solution cannot be easily obtained by individually running OPF and OGF. Figure 10.8 shows the social welfare losses if two networks are operated individually. We can see that the social welfare loss is zero when the gas prices at nodes 4 and 15 are $\$2.52/(10^6 \times \text{BTU})$ and $\$2.55/(10^6 \times \text{BTU})$, respectively. These gas prices are the same gas prices as we obtained from the GEOPF, which verify that the GEOPF can find global solutions which maximize the social welfare for the combined gas and electricity network.

	Case 1	Case 2	Case 3
Gas supply ($10^6 \times \text{SCF/hr}$)			
w_{S_1}	7.2970	8.9047	6.3694
w_{S_2}	10.079	5.1950	6.7761
Source pressure (psia)			
π_1 (slack)	1000.000	1000.000	1000.000
π_2	1200.000	723.167	1057.119
Gas load demand ($10^6 \times \text{SCF/hr}$)			
w_{L_3}	3.8294	3.2460	3.2342
w_{L_4}	3.9981	3.3570	3.3570
$w_{L_{13}}$	4.2388	3.5142	3.1343
$w_{L_{14}}$	4.2474	3.4329	2.9930
$w_{L_{15}}$	0.9891	0.4710	0.3438
Gas price ($\$/ (10^6 \times \text{BTU})$)			
MC_3	2.1238	2.6978	2.7094
MC_4	2.1271	2.7094	2.7094
MC_{13}	2.1872	2.8205	3.1525
MC_{14}	2.1873	2.8205	3.1625
MC_{15}	2.1885	2.8213	3.1578
Real power generation (MW)			
P_{G_1}	132.296	193.713	188.8408
P_{G_2}	150.000	41.786	15.000
Real power demand (MW)			
P_{L_2}	23.1602	18.1988	14.8824
P_{L_3}	99.1564	81.8019	70.4640
P_{L_4}	96.3892	80.6280	70.4423
P_{L_5}	54.0011	45.7602	40.4425
Electricity price ($\$/\text{MWh}$)			
MC_1	11.2170	11.3177	11.3097
MC_2	11.4850	13.6154	15.0395
MC_3	12.4696	14.3126	15.5167
MC_4	12.2137	13.8824	14.9615
MC_5	12.0377	13.5610	14.5447
Social welfare ($\$/\text{hr}$)			
C_E	2161.93	2853.94	2798.81
B_E	4735.93	4129.35	3690.53
C_G	36,994.15	36,548.16	34,557.75
B_G	65,504.01	58,591.45	56,071.87
SW	31,083.86	23,318.70	22,405.83

Table 10.2: GEOPF results for test system I

	Case 1	Case 2	Case 3
Gas supply ($10^6 \times \text{SCF/hr}$)			
w_{S_1}	7.2883	4.3160	6.0010
w_{S_2}	6.8673	7.8251	5.7177
Source pressure (psia)			
π_1 (slack)	1000.000	1000.000	1000.000
π_2	978.630	1200.000	1043.454
Gas load demand ($10^6 \times \text{SCF/hr}$)			
w_{L_3}	3.8377	3.4274	3.8350
w_{L_4}	1.2177	0.8232	1.3102
$w_{L_{13}}$	4.2628	3.8281	3.3177
$w_{L_{14}}$	4.2743	3.7857	3.0599
$w_{L_{15}}$	0.5012	0.2629	0.1212
Gas price ($\$/ (10^6 \times \text{BTU})$)			
MC_3	2.1156	2.5193	2.1182
MC_4	2.1182	2.5197	2.1182
MC_{13}	2.1663	2.5462	2.9922
MC_{14}	2.1663	2.5463	3.1105
MC_{15}	2.1669	2.5465	3.0493
Real power generation (MW)			
P_{G_1}	21.6000	87.3278	30.4071
P_{G_2}	252.8145	171.9092	271.6400
P_{G_3}	102.9182	54.1304	25.0000
Real power demand (MW)			
P_{L_5}	129.2073	122.4114	123.2469
P_{L_6}	112.4537	82.7093	85.8920
P_{L_8}	125.4047	104.5075	109.6712
Electricity price ($\$/\text{MWh}$)			
MC_1	11.5305	12.8552	12.7619
MC_2	10.5436	12.3989	11.8022
MC_3	10.7675	12.5898	12.2628
MC_5	11.5429	12.9922	12.7957
MC_6	11.6100	13.0129	12.8585
MC_8	10.7830	13.0129	12.1386
Social welfare ($\$/\text{hr}$)			
C_E	274.96	1116.37	387.29
B_E	6884.63	6189.05	6305.11
C_G	30,070.20	30,959.73	24,895.15
B_G	49,634.46	46,460.98	43,902.35
SW	26, 173.92	20, 573.94	24, 925.02

Table 10.3: GEOPF results for test system II

CHAPTER 11

CONCLUSIONS AND FUTURE WORK

The objective of this dissertation were:

- to propose an integrated analysis and solution to the GEOPF problem for combined natural gas and electric power transmission networks from a central planning point of view,
- to develop a screening technique to optimally locate UPFCs and other FACTS devices, and
- to introduce a new model for an ideal UPFC to facilitate solution of OPF problems.

The use of an integrated methodology might not seem to make much sense due to the separation of the gas and electricity markets. However, once an integrated methodology is developed, we can then begin work on a distributed or parallel implementation of the centralized problem (which we must already know how to solve if the required data were available). The GEOPF solution is especially important if there are multiple combined nodes (gas-fired generators). Since electric energy and gas prices are so volatile, the GEOPF will significantly contribute to achieving optimal system operation for the combined gas and electric network.

We have also developed a new technique to estimate the UPFC value by using the first- and second-order sensitivities. As demonstrated by several test systems,

transmission lines with higher MVs with respect to the UPFC control parameters yield higher estimated and actual IVs. The estimated IV seems to give a good approximation to the actual IV when the binding inequality set does not change as the UPFC control parameters are relaxed. Simulation results also revealed that lines with low estimated IV yield low actual IV, which adds to the credibility of the sensitivity analyses. We can apply this sensitivity technique to screen for the optimal location of a UPFC in a large power system by ignoring transmission lines with low MV and low estimated IV, and performing a full OPF simulation only with lines with higher estimated IV to obtain the actual IV. Thus, this technique can significantly reduce the computational burden of determining optimal locations of UPFC in a large power system.

To implement the first- and second-order sensitivities of the UPFC to find optimal locations, we developed a unique UPFC ideal transformer model, which consists only of an ideal transformer with a complex turns ratio and a variable shunt admittance. Since this model is embedded in the $\bar{\mathbf{Y}}_{\text{bus}}$ matrix, the size of the $\bar{\mathbf{Y}}_{\text{bus}}$ matrix is not changed, and the MV and estimated IV for each transmission line can be obtained from the solution of the single base case OPF.

Regarding UPFC sensitivity analysis, future work should determine the optimal location x within each line ik should be determined. In addition, λ_T , λ_ϕ and λ_ρ need to be transformed to directly represent the marginal values of the series capacitor and VAR compensator. Loadflow and OPF applications using the UPFC ideal transformer model need to be explored. Inclusion of non-ideal UPFC behavior should also be included in future work.

Note that the GEOPF solution and/or use of proposed UPFC model also provides optional short-term operational solutions, in addition to long-term signals for investment in new facilities.

Future work should be focused on financial tools for valuation of financial derivatives (such as call options) in conjunction with the GEOPF to determine the value of new or existing assets, as well as the role of brokers as intermediaries between gas and electric utilities. The available financial tools have not been combined in the integrated manner needed for proper operation and planning of combined gas and electric systems. The technique for evaluating investments for gas and electric projects in a competitive market are fairly new, and relatively little quantitative data are available on competitive prices and their volatilities. Hence, the valuation of assets in a competitive market is important for future investment decisions in the competitive market. As mentioned above, work on a distributed implementation of the centralized solution-including market design-is also a goal of future work in this area.

BIBLIOGRAPHY

- [1] Michael Klein. Competition in network industries. Technical report, The World Bank Private Sector Development Department, April 1996.
- [2] Harry Singh. The art of market design-what's next for power markets and SMD? *IEEE Power & Energy Magazine*, pages 12–16, September/October 2003.
- [3] Marija Ilić, Francisco Galiana, and Lester Fink. *Power Systems Restructuring (Engineering and Economics)*. Kluwer Academic Publishers, 1998.
- [4] Colin Schauder. The unified power flow controller - a concept becomes reality. In *IEE Colloquium on Flexible AC Transmission Systems-The FACTS(Ref. No. 1998/500)*, pages 7/1–7/6, November 1998.
- [5] L. Gyugyi, C. D. Schauder, S. L. Williams, T. R. Rietman, D. R. Torgerson, and A. Edris. The unified power flow controller: A new approach to power transmission control. *IEEE Transactions on Power Delivery*, 10(2):1085–1097, April 1995.
- [6] M. Noroozian, L. Ängquist, M. Ghandhari, and G. Andersson. Use of UPFC for optimal power flow control. *IEEE Transactions on Power Delivery*, 12(4):1629–1634, October 1997.
- [7] L. Gyugyi. Unified power-flow control concept for flexible AC transmission systems. In *IEE Proceedings C. on Generation, Transmission and Distribution*, volume 139(4), pages 323–331, July 1992.

- [8] Thomas W. Gedra. Power Economics and Regulation. Class notes for ECEN 5193 at Oklahoma State University, 2004.
- [9] J. Duncan Glover and Mulukutla Sarma. *Power System Analysis & Design*. PWS Publishing Company, third edition, 2002.
- [10] John J. Grainger and Jr. William D. Stevenson. *Power System Analysis*. McGraw-Hill, Inc., 1994.
- [11] Allen J. Wood and Bruce F. Wollenberg. *Power Generation, Operation, and Control*. John Wilen & Sons. Inc., second edition, 1996.
- [12] Parnjit Damrongkulkamjorn. *Optimal Power Flow with Expected Security Costs*. PhD thesis, Oklahoma State University, May 1999.
- [13] Stephen J. Wright. *Primal-Dual Interior-Point Methods*. SIAM: Society for Industrial and Applied Mathematics, 1997.
- [14] Seungwon An and Thomas W. Gedra. Estimation of UPFC value using sensitivity analysis. In *Proceedings of the 2002 Midwest Symposium on Circuits and Systems*, Oklahoma State University, Tulsa, OK, August 2002.
- [15] Parnjit Damrongkulkamjorn, Prakash K. Arcot, Peter Dcouth, and Thomas W. Gedra. A screening technique for optimally locating phase shifters in power systems. In *Proceedings of the IEEE/PES Transmission and Distribution Conference*, pages 233–238, April 1994.
- [16] James Danel Weber. Implementation of a newton-based optimal power flow into a power system simulation environment. Master’s thesis, University of Illinois at Urbana-Champaign, 1997.

- [17] K. Ponnambalam, V.H. Quintana, and A. Vannelli. A fast algorithm for power system optimization problems using an interior point method. *IEEE Transactions on Power Systems*, 7(2):892–899, 1992.
- [18] Yu-Chi Wu, Debs, A.S., and R.E. Marsten. A direct nonlinear predictor-corrector primal-dual interior point algorithm for optimal power flows. *IEEE Transactions on Power Systems*, 9(2):876–883, 1994.
- [19] N. Karmarkar. A new polynomial-time algorithm for linear programming. *Combinatorica*, 4:373–395, 1984.
- [20] Stephen G. Nash and Ariela Sofer. *Linear and Nonlinear Programming*. The McGraw-Hill Companies, Inc., 1996.
- [21] Roland W. Jeppson. *Analysis of Flow in Pipe Networks*. ANN Arbor Science, 1976.
- [22] Andrzej J. Osiadacz. *Simulation and Analysis of Gas Network*. Gulf Publishing Company, February 1987.
- [23] Festus Oladele Olorunntwo. *Natural Gas Transmission System Optimization*. PhD thesis, The University of Texas at Austin, May 1981.
- [24] E. W. McAllister. *Pipeline Rule of Thumb Handbook*. Gulf Publishing Company, second edition, 1988.
- [25] T. R Weymouth. Problems in natural gas engineering. *ASME Transactions*, 34:185–234, 1942.
- [26] Lloyd N. Trefethen and III David Bau. *Numerical Linear Algebra*. SIAM (Society for Industrial and Applied Mathematics), 1996.
- [27] Seungwon An and Thomas W. Gedra. UPFC ideal transformer model. In *Proceedings of North American Power Symposium*, pages 46–50, October 2003.

- [28] Hal R. Varian. *Microeconomic Analysis*. New York: Norton, third edition, 1992.
- [29] Peter W. Sauer and M.A. Pai. *Power Systems Dynamics and Stability*. Prentice Hall, 1997.
- [30] Working Group on a Common Format for Exchange of Solved Load Flow Data. Common format for exchange of solved load flow data. *IEEE Transactions on Power Apparatus and Systems*, PAS-92(6):1916–1925, November/December 1973.

APPENDIX A

DERIVATIVES REQUIRED FOR GEOPF

Appendix A includes the Jacobian and Hessian matrixes required to construct mathematical equations to solve the GEOPF.

A.1 Electric Networks

- Voltage Magnitudes and Angles at Each Bus

$$\mathbf{V} = \begin{bmatrix} V_1 \\ V_2 \\ \vdots \\ V_{N_B} \end{bmatrix}, \quad \mathbf{e}^{j\theta} = \begin{bmatrix} e^{j\theta_1} \\ e^{j\theta_2} \\ \vdots \\ e^{j\theta_{N_B}} \end{bmatrix}, \quad \vec{\mathbf{V}} = \begin{bmatrix} V_1 e^{j\theta_1} \\ V_2 e^{j\theta_2} \\ \vdots \\ V_{N_B} e^{j\theta_{N_B}} \end{bmatrix}$$

- Current Injection at Each Bus

$$\vec{I}_i = \left[\sum_{k=1}^{N_B} \mathbf{Y}_{\text{bus}_{ik}} \vec{V}_k \right]^*, \quad i = 1, \dots, N_B$$

$$\vec{\mathbf{I}} = \begin{bmatrix} \vec{I}_1 \\ \vec{I}_2 \\ \vdots \\ \vec{I}_{N_B} \end{bmatrix}$$

- Real and Reactive Power Injection at Each Node

$$h_i = P_{G_i} - P_{L_i} - \text{Re}(\bar{S}_i), \quad i = 1, \dots, N_B$$

$$h_i = Q_{G_i} - Q_{L_i} - \text{Im}(\bar{S}_i), i = 1, \dots, N_B$$

$$\bar{S}_i = \vec{V}_i \vec{I}_i^* = \vec{V}_i \left[\sum_{k=1}^{N_B} \mathbf{Y}_{\text{bus}_{ik}} \vec{V}_k \right]^*$$

$$\frac{\partial h_i}{\partial P_{G_i}} = 1$$

$$\frac{\partial h_i}{\partial Q_{G_i}} = 1$$

$$\frac{\partial h_i}{\partial P_{L_i}} = -1 \quad \text{for real power injection}$$

$$\frac{\partial h_i}{\partial P_{L_i}} = \frac{1}{pf_i} \cdot \sqrt{1 - pf_i^2} \quad \text{for reactive power injection}$$

$$\frac{\partial \bar{S}_i}{\partial V_i} = e^{j\theta_i} \left[\sum_{k=1}^{N_B} \mathbf{Y}_{\text{bus}_{ik}} \vec{V}_k \right]^* + V_i \mathbf{Y}_{\text{bus}_{ii}}^*$$

$$\frac{\partial \bar{S}_i}{\partial V_k} = \vec{V}_i \mathbf{Y}_{\text{bus}_{ik}}^* e^{-j\theta_k}, \quad k \neq i$$

$$\frac{\partial \bar{S}_i}{\partial \theta_i} = j \vec{V}_i \left[\sum_{k=1}^{N_B} \mathbf{Y}_{\text{bus}_{ik}} \vec{V}_k \right]^* - j V_i^2 \mathbf{Y}_{\text{bus}_{ii}}^*$$

$$\frac{\partial \bar{S}}{\partial \theta_k} = -j \vec{V}_i \mathbf{Y}_{\text{bus}_{ik}}^* V_k e^{-j\theta_k}, \quad k \neq i$$

$$\begin{aligned} \mathbf{J}_{S_V} &= \begin{bmatrix} \frac{\partial \bar{S}_1}{\partial V_1} & \frac{\partial \bar{S}_1}{\partial V_2} & \dots & \frac{\partial \bar{S}_1}{\partial V_{N_B}} \\ \frac{\partial \bar{S}_2}{\partial V_1} & \frac{\partial \bar{S}_2}{\partial V_2} & \dots & \frac{\partial \bar{S}_2}{\partial V_{N_B}} \\ \vdots & \vdots & \ddots & \vdots \\ \frac{\partial \bar{S}_{N_B}}{\partial V_1} & \frac{\partial \bar{S}_{N_B}}{\partial V_2} & \dots & \frac{\partial \bar{S}_{N_B}}{\partial V_{N_B}} \end{bmatrix} \\ &= \text{diag}(\vec{\mathbf{V}}) \cdot \mathbf{Y}_{\text{bus}}^* \cdot \text{diag}(\mathbf{e}^{-j\theta}) + \text{diag}(\mathbf{e}^{j\theta}) \cdot \text{diag}(\vec{\mathbf{I}}^*) \end{aligned}$$

$$\begin{aligned}
\mathbf{J}_{S_\theta} &= \begin{bmatrix} \frac{\partial \bar{S}_1}{\partial V \theta_1} & \frac{\partial \bar{S}_1}{\partial \theta_2} & \cdots & \frac{\partial \bar{S}_1}{\partial \theta_{N_B}} \\ \frac{\partial \bar{S}_2}{\partial \theta_1} & \frac{\partial \bar{S}_2}{\partial \theta_2} & \cdots & \frac{\partial \bar{S}_2}{\partial \theta_{N_B}} \\ \vdots & \vdots & \ddots & \vdots \\ \frac{\partial \bar{S}_{N_B}}{\partial \theta_1} & \frac{\partial \bar{S}_{N_B}}{\partial \theta_2} & \cdots & \frac{\partial \bar{S}_{N_B}}{\partial \theta_{N_B}} \end{bmatrix} \\
&= -j \text{diag}(\vec{\mathbf{V}}) \cdot \mathbf{Y}_{\text{bus}}^* \cdot \text{diag}(\vec{\mathbf{V}}^*) + \text{diag}(j\bar{\mathbf{S}}) \\
\mathbf{J}_{P_V} &= \text{Re}(\mathbf{J}_{S_V}) \\
\mathbf{J}_{Q_V} &= \text{Im}(\mathbf{J}_{S_V}) \\
\mathbf{J}_{P_\theta} &= \text{Re}(\mathbf{J}_{S_\theta}) \\
\mathbf{J}_{Q_\theta} &= \text{Im}(\mathbf{J}_{S_\theta}) \\
\mathbf{J}_S &= \begin{bmatrix} \mathbf{J}_{P_V} & \mathbf{J}_{P_\theta} \\ \mathbf{J}_{Q_V} & \mathbf{J}_{Q_\theta} \end{bmatrix} \\
\frac{\partial^2 \bar{S}_i}{\partial V_i^2} &= 2Y_{\text{bus}_{ii}}^* \\
\frac{\partial^2 \bar{S}_i}{\partial V_i \partial V_k} &= e^{j\theta_i} Y_{\text{bus}_{ik}}^* e^{-j\theta_k} \\
\frac{\partial^2 \bar{S}_i}{\partial V_k \partial V_i} &= \frac{\partial^2 \bar{S}_i}{\partial V_i \partial V_k} \\
\mathbf{H}_{S_{iV^2}} &= \begin{bmatrix} \frac{\partial^2 \bar{S}_i}{\partial V_1^2} & \frac{\partial^2 \bar{S}_i}{\partial V_1 \partial V_2} & \cdots & \frac{\partial^2 \bar{S}_i}{\partial V_1 \partial V_{N_B}} \\ \frac{\partial^2 \bar{S}_i}{\partial V_2 \partial V_1} & \frac{\partial^2 \bar{S}_i}{\partial V_2^2} & \cdots & \frac{\partial^2 \bar{S}_i}{\partial V_2 \partial V_{N_B}} \\ \vdots & \vdots & \ddots & \vdots \\ \frac{\partial^2 \bar{S}_i}{\partial V_{N_B} \partial V_1} & \frac{\partial^2 \bar{S}_i}{\partial V_{N_B} \partial V_2} & \cdots & \frac{\partial^2 \bar{S}_i}{\partial V_{N_B}^2} \end{bmatrix} \\
\frac{\partial^2 \bar{S}_i}{\partial \theta_i^2} &= -\bar{S}_i + V_i^2 Y_{\text{bus}_{ii}}^* \\
\frac{\partial^2 \bar{S}_i}{\partial \theta_i \partial \theta_k} &= \frac{\partial^2 \bar{S}_i}{\partial \theta_i \partial \theta_k} = \vec{V}_i Y_{\text{bus}_{ik}}^* \vec{V}_k^* \\
\frac{\partial^2 \bar{S}_i}{\partial \theta_k^2} &= -\frac{\partial^2 \bar{S}_i}{\partial \theta_i \partial \theta_k} = -\vec{V}_i Y_{\text{bus}_{ik}}^* \vec{V}_k^*
\end{aligned}$$

$$\begin{aligned}
\mathbf{H}_{S_{i_{\theta^2}}} &= \begin{bmatrix} \frac{\partial^2 \bar{S}_i}{\partial \theta_1^2} & \frac{\partial^2 \bar{S}_i}{\partial \theta_1 \partial \theta_2} & \cdots & \frac{\partial^2 \bar{S}_i}{\partial \theta_1 \partial \theta_{NB}} \\ \frac{\partial^2 \bar{S}_i}{\partial \theta_2 \partial \theta_1} & \frac{\partial^2 \bar{S}_i}{\partial \theta_2^2} & \cdots & \frac{\partial^2 \bar{S}_i}{\partial \theta_2 \partial \theta_{NB}} \\ \vdots & \vdots & \ddots & \vdots \\ \frac{\partial^2 \bar{S}_i}{\partial \theta_{NB} \partial \theta_1} & \frac{\partial^2 \bar{S}_i}{\partial \theta_{NB} \partial \theta_2} & \cdots & \frac{\partial^2 \bar{S}_i}{\partial \theta_{NB}^2} \end{bmatrix} \\
\frac{\partial^2 \bar{S}_i}{\partial V_i \partial \theta_i} &= \frac{\partial^2 \bar{S}_i}{\partial \theta_i \partial V_i} = j e^{j\theta_i} \left[\sum_{k=1}^{N_B} Y_{\text{bus}_{ik}} \vec{V}_k \right]^* - j V_i Y_{\text{bus}_{ii}}^* \\
\frac{\partial^2 \bar{S}_i}{\partial V_i \partial \theta_k} &= \frac{\partial^2 \bar{S}_i}{\partial \theta_k \partial V_i} = -j e^{j\theta_i} Y_{\text{bus}_{ik}}^* \vec{V}_k^* \\
\frac{\partial^2 \bar{S}_i}{\partial V_k \partial \theta_i} &= \frac{\partial^2 \bar{S}_i}{\partial \theta_i \partial V_k} = j \vec{V}_i Y_{\text{bus}_{ik}}^* e^{-j\theta_k} \\
\frac{\partial^2 \bar{S}_i}{\partial V_k \partial \theta_k} &= \frac{\partial^2 \bar{S}_i}{\partial \theta_k \partial V_k} = -j \vec{V}_i Y_{\text{bus}_{ik}}^* e^{-j\theta_k} \\
\mathbf{H}_{S_{i_{V\theta}}} &= \begin{bmatrix} \frac{\partial^2 \bar{S}_i}{\partial V_1 \partial \theta_1} & \frac{\partial^2 \bar{S}_i}{\partial V_1 \partial \theta_2} & \cdots & \frac{\partial^2 \bar{S}_i}{\partial V_1 \partial \theta_{NB}} \\ \frac{\partial^2 \bar{S}_i}{\partial V_2 \partial \theta_1} & \frac{\partial^2 \bar{S}_i}{\partial V_2 \partial \theta_2} & \cdots & \frac{\partial^2 \bar{S}_i}{\partial V_2 \partial \theta_{NB}} \\ \vdots & \vdots & \ddots & \vdots \\ \frac{\partial^2 \bar{S}_i}{\partial V_{NB} \partial \theta_1} & \frac{\partial^2 \bar{S}_i}{\partial V_{NB} \partial \theta_2} & \cdots & \frac{\partial^2 \bar{S}_i}{\partial V_{NB} \partial \theta_{NB}} \end{bmatrix} \\
\mathbf{H}_{S_{i_{\theta V}}} &= \mathbf{H}_{S_{i_{V\theta}}}^T \\
\mathbf{H}_{P_i} &= \text{Re} \begin{bmatrix} \mathbf{H}_{S_{i_{V^2}}} & \mathbf{H}_{S_{i_{V\theta}}} \\ \mathbf{H}_{S_{i_{\theta V}}} & \mathbf{H}_{S_{i_{\theta^2}}} \end{bmatrix} \\
\mathbf{H}_{Q_i} &= \text{Im} \begin{bmatrix} \mathbf{H}_{S_{i_{V^2}}} & \mathbf{H}_{S_{i_{V\theta}}} \\ \mathbf{H}_{S_{i_{\theta V}}} & \mathbf{H}_{S_{i_{\theta^2}}} \end{bmatrix}
\end{aligned}$$

- Reference Angle Equality Constraint

$$\begin{aligned}
h_i &= \theta_i, & i &= \text{reference bus} \\
\frac{\partial h_i}{\partial \theta_i} &= 1
\end{aligned}$$

- Equality Constraints at Combined Buses

$$h_i = w_{L_i} - (\alpha_{G_i} + \beta_{G_i} P_{G_i} S_{\text{base}} + \gamma_{G_i} P_{G_i}^2 S_{\text{base}}^2) \frac{1}{GHV},$$

$$i = 1, \dots, N_{GE}$$

$$\frac{\partial h_i}{\partial w_{L_i}} = 1$$

$$\frac{\partial h_i}{\partial P_{G_i}} = -(\beta_{G_i} S_{\text{base}} + 2\gamma_{G_i} P_{G_i} S_{\text{base}}^2) \frac{1}{GHV}$$

$$\frac{\partial^2 h_i}{\partial P_{G_i}^2} = -2\gamma_{G_i} S_{\text{base}}^2 \frac{1}{GHV}$$

- Voltage Magnitude Limit

$$g_i = V_{\min_i} - V_i, \quad i = 1, \dots, N_B$$

$$\frac{\partial g_i}{\partial V_i} = -1$$

$$g_i = V_i - V_{\max_i}, \quad i = 1, \dots, N_B$$

$$\frac{\partial g_i}{\partial V_i} = 1$$

- Real Power Generation Limit

$$g_i = P_{G_{\min_i}} - P_{G_i}, \quad i = 1, \dots, N_{PG}$$

$$\frac{\partial g_i}{\partial P_{G_i}} = -1$$

$$g_i = P_{G_i} - P_{G_{\max_i}}, \quad i = 1, \dots, N_{PG}$$

$$\frac{\partial g_i}{\partial P_{G_i}} = 1$$

- Real Power Load Limit

$$g_i = -P_{L_i}, \quad i = 1, \dots, N_{EL}$$

$$\frac{\partial g_i}{\partial P_{L_i}} = -1$$

- Reactive Power Generation Limit

$$\begin{aligned} g_i &= Q_{G \min_i} - Q_{G_i}, & i = 1, \dots, N_{QG} \\ \frac{\partial g_i}{\partial Q_{G_i}} &= -1 \end{aligned}$$

$$\begin{aligned} g_i &= Q_{G_i} - Q_{G \max_i}, & i = 1, \dots, N_{QG} \\ \frac{\partial g_i}{\partial Q_{G_i}} &= 1 \end{aligned}$$

- Line Flow Limit

$$g_i = \vec{I}_{ik} \cdot \vec{I}_{ik}^* - |I_{ik}|^2, \quad i = 1, \dots, N_{EB}$$

$$\begin{aligned} \vec{I}_{ik} &= (\vec{V}_i - \vec{V}_k) Y_{ik} + Y_{\text{shunt}_{ik}} \vec{V}_i \\ \frac{\partial \vec{I}_{ik}}{\partial V_i} &= e^{j\theta_i} Y_{ik} + Y_{\text{shunt}_{ik}} e^{j\theta_i} \\ \frac{\partial \vec{I}_{ik}}{\partial V_k} &= -e^{j\theta_k} Y_{ik} \\ \frac{\partial \vec{I}_{ik}}{\partial \theta_i} &= j \vec{V}_i (Y_{ik} + Y_{\text{shunt}_{ik}}) \\ \frac{\partial \vec{I}_{ik}}{\partial \theta_k} &= -j \vec{V}_k Y_{ik} \\ \frac{\partial \vec{I}_{ik} \vec{I}_{ik}^*}{\partial V_i} &= \vec{I}_{ik} \frac{\partial \vec{I}_{ik}^*}{\partial V_i} + \vec{I}_{ik}^* \frac{\partial \vec{I}_{ik}}{\partial V_i} \\ \frac{\partial \vec{I}_{ik} \vec{I}_{ik}^*}{\partial V_k} &= \vec{I}_{ik} \frac{\partial \vec{I}_{ik}^*}{\partial V_k} + \vec{I}_{ik}^* \frac{\partial \vec{I}_{ik}}{\partial V_k} \\ \frac{\partial \vec{I}_{ik} \vec{I}_{ik}^*}{\partial \theta_i} &= \vec{I}_{ik} \frac{\partial \vec{I}_{ik}^*}{\partial \theta_i} + \vec{I}_{ik}^* \frac{\partial \vec{I}_{ik}}{\partial \theta_i} \\ \frac{\partial \vec{I}_{ik} \vec{I}_{ik}^*}{\partial \theta_k} &= \vec{I}_{ik} \frac{\partial \vec{I}_{ik}^*}{\partial \theta_k} + \vec{I}_{ik}^* \frac{\partial \vec{I}_{ik}}{\partial \theta_k} \\ \frac{\partial^2 \vec{I}_{ik}}{\partial \theta_i^2} &= -\vec{V}_i (Y_{ik} + Y_{\text{shunt}_{ik}}) \\ \frac{\partial^2 \vec{I}_{ik}}{\partial \theta_k^2} &= -j e^{j\theta_k} Y_{ik} \end{aligned}$$

$$\begin{aligned}
\frac{\partial^2 \vec{I}_{ik}}{\partial V_i \partial \theta_i} &= \frac{\partial^2 \vec{I}_{ik}}{\partial \theta_i \partial V_i} = j e^{j\theta_i} (Y_{ik} + Y_{\text{shunt}_{ik}}) \\
\frac{\partial^2 \vec{I}_{ik}}{\partial V_k \partial \theta_k} &= \frac{\partial^2 \vec{I}_{ik}}{\partial V_k \partial \theta_k} = -j e^{j\theta_k} Y_{ik} \\
\frac{\partial^2 \vec{I}_{ik} \vec{I}_{ik}^*}{\partial V_i^2} &= 2 \frac{\partial \vec{I}_{ik}}{\partial V_i} \frac{\partial \vec{I}_{ik}^*}{\partial V_i} \\
\frac{\partial^2 \vec{I}_{ik} \vec{I}_{ik}^*}{\partial V_k^2} &= 2 \frac{\partial \vec{I}_{ik}}{\partial V_k} \frac{\partial \vec{I}_{ik}^*}{\partial V_k} \\
\frac{\partial^2 \vec{I}_{ik} \vec{I}_{ik}^*}{\partial \theta_i^2} &= \vec{I}_{ik} \frac{\partial^2 \vec{I}_{ik}^*}{\partial \theta_i^2} + 2 \frac{\partial \vec{I}_{ik}}{\partial \theta_i} \frac{\partial \vec{I}_{ik}^*}{\partial \theta_i} + \vec{I}_{ik}^* \frac{\partial^2 \vec{I}_{ik}}{\partial \theta_i^2} \\
\frac{\partial^2 \vec{I}_{ik} \vec{I}_{ik}^*}{\partial \theta_k^2} &= \vec{I}_{ik} \frac{\partial^2 \vec{I}_{ik}^*}{\partial \theta_k^2} + 2 \frac{\partial \vec{I}_{ik}}{\partial \theta_k} \frac{\partial \vec{I}_{ik}^*}{\partial \theta_k} + \vec{I}_{ik}^* \frac{\partial^2 \vec{I}_{ik}}{\partial \theta_k^2} \\
\frac{\partial^2 \vec{I}_{ik} \vec{I}_{ik}^*}{\partial V_i \partial \theta_i} &= \frac{\partial^2 \vec{I}_{ik} \vec{I}_{ik}^*}{\partial \theta_i \partial V_i} = \vec{I}_{ik} \frac{\partial^2 \vec{I}_{ik}^*}{\partial V_i \partial \theta_i} + \frac{\partial \vec{I}_{ik}}{\partial V_i} \frac{\partial \vec{I}_{ik}^*}{\partial \theta_i} + \frac{\partial \vec{I}_{ik}^*}{\partial V_i} \frac{\partial \vec{I}_{ik}}{\partial \theta_i} + \vec{I}_{ik}^* \frac{\partial^2 \vec{I}_{ik}}{\partial V_i \partial \theta_i} \\
\frac{\partial^2 \vec{I}_{ik} \vec{I}_{ik}^*}{\partial V_k \partial \theta_k} &= \frac{\partial^2 \vec{I}_{ik} \vec{I}_{ik}^*}{\partial \theta_k \partial V_k} = \vec{I}_{ik} \frac{\partial^2 \vec{I}_{ik}^*}{\partial V_k \partial \theta_k} + \frac{\partial \vec{I}_{ik}}{\partial V_k} \frac{\partial \vec{I}_{ik}^*}{\partial \theta_k} + \frac{\partial \vec{I}_{ik}^*}{\partial V_k} \frac{\partial \vec{I}_{ik}}{\partial \theta_k} + \vec{I}_{ik}^* \frac{\partial^2 \vec{I}_{ik}}{\partial V_k \partial \theta_k} \\
\frac{\partial^2 \vec{I}_{ik} \vec{I}_{ik}^*}{\partial V_i \partial \theta_k} &= \frac{\partial^2 \vec{I}_{ik} \vec{I}_{ik}^*}{\partial \theta_k \partial V_i} = \frac{\partial \vec{I}_{ik}}{\partial V_i} \frac{\partial \vec{I}_{ik}^*}{\partial \theta_k} + \frac{\partial \vec{I}_{ik}^*}{\partial V_i} \frac{\partial \vec{I}_{ik}}{\partial \theta_k} \\
\frac{\partial^2 \vec{I}_{ik} \vec{I}_{ik}^*}{\partial V_k \partial \theta_i} &= \frac{\partial^2 \vec{I}_{ik} \vec{I}_{ik}^*}{\partial \theta_i \partial V_k} = \frac{\partial \vec{I}_{ik}}{\partial V_k} \frac{\partial \vec{I}_{ik}^*}{\partial \theta_i} + \frac{\partial \vec{I}_{ik}^*}{\partial V_k} \frac{\partial \vec{I}_{ik}}{\partial \theta_i}
\end{aligned}$$

A.2 Gas Network

- Gas Pressures and Branch Flow Rates

$$\begin{aligned}\pi &= \begin{bmatrix} \pi_1 & \pi_2 & \dots & \pi_{N_N} \end{bmatrix}^T \\ f &= \begin{bmatrix} f_1 & \dots & f_{N_P} & f_{N_P+1} & \dots & f_{N_P+N_C} \end{bmatrix}^T\end{aligned}$$

- Gas Consumption Rates and Horsepowers at Compressor Stations

$$\begin{aligned}\tau &= \begin{bmatrix} \tau_1 & \tau_2 & \dots & \tau_{N_C} \end{bmatrix}^T \\ H &= \begin{bmatrix} H_1 & H_2 & \dots & H_{N_C} \end{bmatrix}^T\end{aligned}$$

- Weymouth Flow Equation for Pipeline Branches

$$\begin{aligned}h_k &= h_{k_{ij}} = \pi_i^2 - \pi_j^2 - \left(\frac{1}{M_k}\right)^{m1} (S_{ij} f_{k_{ij}})^{m1} S_{ij}, & k = 1, \dots, N_P \\ S_{ij} &= \text{sign}(f_{k_{ij}}) \\ \frac{\partial h_k}{\partial \pi_i} &= 2\pi_i \\ \frac{\partial h_k}{\partial \pi_j} &= -2\pi_j \\ \frac{\partial h_k}{\partial f_{k_{ij}}} &= -m1 \left(\frac{1}{M_k}\right)^{m1} (S_{ij} f_{k_{ij}})^{(m1-1)} \\ \frac{\partial^2 h_k}{\partial \pi_i^2} &= 2 \\ \frac{\partial^2 h_k}{\partial \pi_j^2} &= -2 \\ \frac{\partial^2 h_k}{\partial f_{k_{ij}}^2} &= -m1(m1-1) \left(\frac{1}{M_k}\right)^{m1} f_{k_{ij}}^{(m1-2)} S_{ij}\end{aligned}$$

- Reference Pressure Equality Constraints

$$\begin{aligned}h_i &= \pi_i - \pi_{\text{set}}, & i = \text{reference node} \\ \frac{\partial h_i}{\partial \pi_i} &= 1\end{aligned}$$

- Compressor Operation Equality Constraints

$$h_k = h_{k_{ij}} = H_k - B_k f_k \left[\left(\frac{\pi_j}{\pi_i} \right)^{R_k} - 1 \right], \quad k = 1, \dots, N_C$$

$$R_k = Z_{k_i} \frac{\alpha - 1}{\alpha}$$

$$\frac{\partial h_k}{\partial H_k} = 1$$

$$\frac{\partial h_k}{\partial \pi_i} = R_k B_k f_k \pi_j^{R_k} \pi_i^{-(R_k+1)}$$

$$\frac{\partial h_k}{\partial \pi_j} = -R_k B_k f_k \pi_j^{(R_k-1)} \pi_i^{-R_k}$$

$$\frac{\partial h_k}{\partial f_k} = -B_k \left[\left(\frac{\pi_j}{\pi_i} \right)^{R_k} - 1 \right]$$

$$\frac{\partial^2 h_k}{\partial \pi_i^2} = -R_k(R_k + 1) B_k f_k \pi_j^{R_k} \pi_i^{-(R_k+2)}$$

$$\frac{\partial^2 h_k}{\partial \pi_j^2} = -R_k(R_k - 1) B_k f_k \pi_j^{(R_k-2)} \pi_i^{-R_k}$$

$$\frac{\partial^2 h_k}{\partial \pi_i \partial \pi_j} = \frac{\partial^2 h_k}{\partial \pi_j \partial \pi_i} = R_k^2 B_k f_k \pi_j^{(R_k-1)} \pi_i^{-(R_k+1)}$$

$$\frac{\partial^2 h_k}{\partial f_k \partial \pi_i} = \frac{\partial^2 h_k}{\partial \pi_i \partial f_k} = R_k B_k \pi_j^{R_k} \pi_i^{-(R_k+1)}$$

$$\frac{\partial^2 h_k}{\partial f_k \partial \pi_j} = \frac{\partial^2 h_k}{\partial \pi_j \partial f_k} = -R_k B_k \pi_j^{(R_k-1)} \pi_i^{-R_k}$$

$$h_k = h_{k_{ij}} = \tau_k - \left(\alpha_{T_k} + \beta_{T_k} H_{k_{ij}} + \gamma_{T_k} H_{k_{ij}}^2 \right), \quad k = 1, \dots, N_C$$

$$\frac{\partial h_k}{\partial \tau_k} = 1$$

$$\frac{\partial h_k}{\partial H_{k_{ij}}} = -\beta_{T_k} - 2\gamma_{T_k} H_{k_{ij}}$$

$$\frac{\partial^2 h_k}{\partial H_{k_{ij}}^2} = -2\gamma_{T_k}$$

- Nodal-Flow Balance Equation

$$\begin{aligned}
\mathbf{h} &= (\mathbf{A} + \mathbf{U})f + w - \mathbf{T}\tau, & \dim(\mathbf{h}) &= N_N \times 1 \\
\frac{\partial \mathbf{h}}{\partial f} &= \mathbf{A} + \mathbf{U} \\
\frac{\partial \mathbf{h}}{\partial \tau} &= -\mathbf{T} \\
\frac{\partial \mathbf{h}_i}{\partial w_{S_i}} &= \begin{cases} +1, & \text{if a source is connected to node } i, \\ 0, & \text{otherwise.} \end{cases} \\
\frac{\partial \mathbf{h}_i}{\partial w_{L_i}} &= \begin{cases} -1, & \text{if a load is connected to node } i, \\ 0, & \text{otherwise.} \end{cases}
\end{aligned}$$

- Compressor Inlet-Outlet Pressure Inequality Constraints

$$\begin{aligned}
g_k &= g_{k_{ij}} = \pi_i - \pi_j, & k &= 1, \dots, N_C \\
\frac{\partial g_k}{\partial \pi_i} &= 1 \\
\frac{\partial g_k}{\partial \pi_j} &= -1
\end{aligned}$$

$$\begin{aligned}
g_k &= g_{k_{ij}} = \pi_j - R_{\max_k} \cdot \pi_i, & k &= 1, \dots, N_C \\
\frac{\partial g_k}{\partial \pi_i} &= -R_{\max_i} \\
\frac{\partial g_k}{\partial \pi_j} &= 1
\end{aligned}$$

$$\begin{aligned}
g_k &= g_{k_{ij}} = \pi_i - \pi_j, & k &= 1, \dots, N_C \\
\frac{\partial g_k}{\partial \pi_i} &= 1 \\
\frac{\partial g_k}{\partial \pi_j} &= -1
\end{aligned}$$

- Nodal Pressure Inequality Constraints

$$\begin{aligned} g_k &= \pi_{\min_k} - \pi_k, & k = 2, \dots, N_N \\ \frac{\partial g_k}{\partial \pi_k} &= -1 \end{aligned}$$

$$\begin{aligned} g_k &= \pi_k - \pi_{\max_k}, & k = 2, \dots, N_N \\ \frac{\partial g_k}{\partial \pi_k} &= 1 \end{aligned}$$

- Gas Load Limits

$$\begin{aligned} g_k &= w_{\min_{L_k}} - w_{L_k}, & k = 1, \dots, N_{GL} \\ \frac{\partial g_k}{\partial w_{L_k}} &= -1 \end{aligned}$$

$$\begin{aligned} g_k &= w_{L_{L_k}} - w_{\max_k}, & k = 1, \dots, N_{GL} \\ \frac{\partial g_k}{\partial w_{L_k}} &= 1 \end{aligned}$$

- Gas Source Limits

$$\begin{aligned} g_k &= w_{\min_{S_k}} - w_{S_k}, & k = 1, \dots, N_S \\ \frac{\partial g_k}{\partial w_{S_k}} &= -1 \end{aligned}$$

$$\begin{aligned} g_k &= w_{S_k} - w_{\max_{S_k}}, & k = 1, \dots, N_S \\ \frac{\partial g_k}{\partial w_{S_k}} &= 1 \end{aligned}$$

A.3 Objective Function of GEOPF

$$SW = \sum_{k=1}^{N_{GL}} B_{GL_k} + \sum_{k=1}^{N_{EL}} B_{EL_k} - \sum_{k=1}^{N_S} C_{S_k} - \sum_{k=1}^{N_{NG}} C_{NG_k}$$

$$\begin{aligned} B_{GL_k} &= \alpha_{GL_k} + \beta_{GL_k} w_{L_k} + \gamma_{GL_k} w_{L_k}^2, & k = 1, \dots, N_{GL} \\ \frac{\partial B_{GL_k}}{\partial w_{L_k}} &= \beta_{GL_k} + 2\gamma_{GL_k} w_{L_k} \\ \frac{\partial^2 B_{GL_k}}{\partial w_{L_k}^2} &= 2\gamma_{GL_k} \end{aligned}$$

$$\begin{aligned} B_{EL_k} &= \alpha_{EL_k} + \beta_{EL_k} P_{L_k} S_{\text{base}} + \gamma_{EL_k} P_{L_k}^2 S_{\text{base}}^2, & k = 1, \dots, N_{EL} \\ \frac{\partial B_{EL_k}}{\partial P_{L_k}} &= \beta_{EL_k} S_{\text{base}} + 2\gamma_{EL_k} P_{L_k} S_{\text{base}}^2 \\ \frac{\partial^2 B_{EL_k}}{\partial P_{L_k}^2} &= 2\gamma_{EL_k} S_{\text{base}}^2 \end{aligned}$$

$$\begin{aligned} C_{G_k} &= c_{1_k} \cdot w_{S_k}, & k = 1, \dots, N_S \\ \frac{\partial C_{G_k}}{\partial w_{S_k}} &= c_{1_k} \end{aligned}$$

$$\begin{aligned} C_{E_k} &= \alpha_{G_k} + \beta_{G_k} P_{G_k} S_{\text{base}} + \gamma_{G_k} P_{G_k}^2 S_{\text{base}}^2, & k = 1, \dots, N_G \\ \frac{\partial C_{E_k}}{\partial P_{G_k}} &= \beta_{G_k} S_{\text{base}} + 2\gamma_{G_k} P_{G_k} S_{\text{base}}^2 \\ \frac{\partial^2 C_{E_k}}{\partial P_{G_k}^2} &= 2\gamma_{G_k} S_{\text{base}}^2 \end{aligned}$$

APPENDIX B

DERIVATIVES REQUIRED FOR UPFC SENSITIVITIES

Suppose that a UPFC is installed between bus i and bus k . Then, it can be expressed in a two-port ABCD matrix by

$$\begin{bmatrix} \vec{V}_i \\ \vec{I}_i \end{bmatrix} = \begin{bmatrix} A_{ik} & B_{ik} \\ C_{ik} & D_{ik} \end{bmatrix} \begin{bmatrix} \vec{V}_k \\ -\vec{I}_k \end{bmatrix}, \quad (\text{B.1})$$

where

$$\begin{aligned} A_{ik} &= \bar{T}A_iA_k + j\bar{T}B_iA_k\rho + \frac{1}{\bar{T}^*}B_iC_k, \\ B_{ik} &= \bar{T}A_iB_k + j\bar{T}B_iB_k\rho + \frac{1}{\bar{T}^*}B_iD_k, \\ C_{ik} &= \bar{T}C_iA_k + j\bar{T}D_iA_k\rho + \frac{1}{\bar{T}^*}D_iC_k, \\ D_{ik} &= \bar{T}C_iB_k + j\bar{T}D_iB_k\rho + \frac{1}{\bar{T}^*}D_iD_k. \end{aligned}$$

Equation (B.1) can be converted to Y-parameter representations as

$$\begin{bmatrix} \vec{I}_i \\ \vec{I}_k \end{bmatrix} = \bar{\mathbf{Y}}_{\text{bus}_{ik}} \begin{bmatrix} \vec{V}_i \\ \vec{V}_k \end{bmatrix}, \quad (\text{B.2})$$

where

$$\bar{\mathbf{Y}}_{\text{bus}_{ik}} = \begin{bmatrix} \frac{D_{ik}}{B_{ik}} & C_{ik} - \frac{A_{ik}D_{ik}}{B_{ik}} \\ -\frac{1}{B_{ik}} & \frac{A_{ik}}{B_{ik}} \end{bmatrix},$$

and we define each element of $\bar{\mathbf{Y}}_{\text{bus}_{ik}}$ by

$$Y_{11} = \frac{D_{ik}}{B_{ik}}, \quad Y_{12} = C_{ik} - \frac{A_{ik}D_{ik}}{B_{ik}}, \quad Y_{21} = \frac{-1}{B_{ik}}, \quad Y_{22} = \frac{A_{ik}}{B_{ik}}.$$

The first- and second-order derivatives of each element with respect to the UPFC control variables are written as follows:

$$\begin{aligned}
\frac{\partial Y_{11}}{\partial \rho} &= \frac{jT^4 B_k^2 (A_i D_i - B_i C_i)}{(T^2 A_i B_k + jT^2 B_i B_k \rho + B_i D_k)^2}, \\
\frac{\partial Y_{11}}{\partial T} &= \frac{2TB_k D_k (B_i C_i - A_i D_i)}{(T^2 A_i B_k + jT^2 B_i B_k \rho + B_i D_k)^2}, \\
\frac{\partial^2 Y_{11}}{\partial \rho^2} &= \frac{2T^6 B_i B_k^3 (A_i D_i - B_i C_i)}{(T^2 A_i B_k + jT^2 B_i B_k \rho + B_i D_k)^3}, \\
\frac{\partial^2 Y_{11}}{\partial T^2} &= -2B_k D_k (B_i C_i - A_i D_i) \frac{(3T^2 A_i B_k + j3T^2 B_i B_k \rho - B_i D_k)}{(T^2 A_i B_k + jT^2 B_i B_k \rho + B_i D_k)^3}, \\
\frac{\partial^2 Y_{11}}{\partial \rho \partial T} &= \frac{\partial^2 Y_{11}}{\partial T \partial \rho} = j4T^3 B_i B_k^2 D_k \frac{A_i D_i - B_i C_i}{(T^2 A_i B_k + jT^2 B_i B_k \rho + B_i D_k)^3}, \\
\frac{\partial Y_{12}}{\partial \phi} &= je^{j\phi} \left[TA_k C_i + jTA_k D_i \rho + \frac{1}{T} C_k D_i \right. \\
&\quad \left. - \frac{(TA_i A_k + jTA_k B_i \rho + T^{-1} B_i C_k) (TB_k C_i + jTB_k D_i \rho + T^{-1} D_i D_k)}{TA_i B_k + jTB_i B_k \rho + T^{-1} B_i D_k} \right], \\
\frac{\partial Y_{12}}{\partial T} &= e^{j\phi} \left[A_k C_i + jA_k D_i \rho - \frac{1}{T^2} C_k D_i \right. \\
&\quad - \left(A_i A_k + jA_k B_i \rho - \frac{1}{T^2} B_i C_k \right) \frac{TB_k C_i + jTB_k D_i \rho + T^{-1} D_i D_k}{TA_i B_k + jB_i B_k \rho T + T^{-1} B_i D_k} \\
&\quad - \left(TA_i A_k + jTA_k B_i \rho + \frac{1}{T} B_i C_k \right) \frac{B_k C_i + jB_k D_i \rho - T^{-2} D_i D_k}{TA_i B_k + jTB_i B_k \rho + T^{-1} B_i D_k} \\
&\quad + \left(TA_i A_k + jTA_k B_i \rho + \frac{1}{T} B_i C_k \right) \frac{TB_k C_i + jTB_k D_i \rho + T^{-1} D_i D_k}{(TA_i B_k + jTB_i B_k \rho + T^{-1} B_i D_k)^2} \\
&\quad \left. \times \left(A_i B_k + jB_i B_k \rho - \frac{1}{T^2} B_i D_k \right) \right],
\end{aligned}$$

$$\begin{aligned}
\frac{\partial Y_{12}}{\partial \rho} &= e^{j\phi} \left[jTD_i A_k - jTB_i A_k \frac{TC_i B_k + jTB_k D_i \rho + D_i D_k T^{-1}}{TA_i B_k + jTB_i B_k \rho + T^{-1} B_i D_k} \right. \\
&\quad - j \left(TA_i A_k + jTB_i A_k \rho + \frac{1}{T} B_i C_k \right) \frac{TB_k D_i}{TA_i B_k + jTB_i B_k \rho + T^{-1} B_i D_k} \\
&\quad + j \left(TA_i A_k + jTB_i A_k \rho + \frac{1}{T} B_i C_k \right) \left(TC_i B_k + jTD_i B_k \rho + \frac{1}{T} D_i D_k \right) \\
&\quad \left. \times \frac{TB_i B_k}{(TA_i B_k + jTB_i B_k \rho + T^{-1} B_i D_k)^2} \right], \\
\frac{\partial^2 Y_{12}}{\partial \phi^2} &= -Y_{12}, \\
\frac{\partial^2 Y_{12}}{\partial T^2} &= e^{j\phi} \left[\frac{2}{T^3} D_i C_k - 2B_i C_k \frac{TC_i B_k + jTB_k D_i \rho + T^{-1} D_i D_k}{T^4 A_i B_k + jT^4 B_i B_k \rho + T^2 B_i D_k} \right. \\
&\quad - 2(A_i A_k + jA_k B_i \rho - \frac{1}{T^2} B_i C_k) \frac{B_k C_i + jB_k D_i \rho - T^{-1} D_i D_k}{TA_i B_k + jTB_i B_k \rho + T^{-1} B_i D_k} \\
&\quad + 2(A_i A_k + jA_k B_i \rho - \frac{1}{T^2} B_i C_k) \frac{(TB_k C_i + jTB_k D_i \rho + T^{-1} D_i D_k)}{(TA_i B_k + jTB_i B_k \rho + T^{-1} B_i D_k)^2} \\
&\quad \times \left(A_i B_k + jB_i B_k \rho - \frac{1}{T^2} B_i D_k \right) - 2 \left(TA_i A_k + jTA_k B_i \rho + \frac{1}{T} B_i C_k \right) \\
&\quad \times \left\{ \frac{T^{-4} D_i D_k}{A_i B_k + jB_i B_k \rho + T^{-2} B_i D_k} - \frac{B_k C_i + jB_k D_i \rho - T^{-2} D_i D_k}{(TA_i B_k + jTB_i B_k \rho + T^{-1} B_i D_k)^2} \right. \\
&\quad \times \left(A_i B_k + jB_i B_k \rho - \frac{1}{T^2} B_i D_k \right) \left. \right\} - 2 \left(TA_i A_k + jTA_k B_i \rho + \frac{1}{T} B_i C_k \right) \\
&\quad \times \left\{ \frac{(TB_k C_i + jTB_k D_i \rho + T^{-1} D_i D_k)(A_i B_k + jB_i B_k \rho - T^{-2} B_i D_k)^2}{(TA_i B_k + jTB_i B_k \rho + T^{-1} B_i D_k)^3} \right. \\
&\quad \left. - \frac{TB_k C_i + jTB_k D_i \rho + T^{-1} D_i D_k}{(TA_i B_k + jTB_i B_k \rho + T^{-1} B_i D_k)^2} \frac{1}{T^3} B_i D_k \right\} \Bigg], \\
\frac{\partial^2 Y_{12}}{\partial \rho \partial T} &= \frac{\partial^2 Y_{12}}{\partial T \partial \rho} = -\frac{j e^{j\phi}}{(T^2 A_i B_k + jT^2 B_i B_k \rho + B_i D_k)^3} \left[3T^2 A_k B_i^3 B_k C_i D_k^2 \right. \\
&\quad + A_k B_i^3 D_i D_k^3 - 3T^2 B_i^3 B_k^2 C_i C_k D_k + T^4 A_i B_i^2 B_k^3 C_i C_k + T^6 A_i^3 A_k B_k^3 D_i \\
&\quad - T^4 A_i^2 B_i B_k^3 C_k D_i - T^4 A_i A_k B_i^2 B_k^2 C_i D_k - jT^4 A_i B_i^2 B_k^3 C_k D_i \rho \\
&\quad - 3T^6 A_i A_k B_i^2 B_k^3 D_i \rho^2 + j3T^6 A_i^2 A_k B_i B_k^3 D_i \rho + j3T^2 A_k B_i^3 B_k D_i D_k^2 \rho \\
&\quad + j7T^4 A_i A_k B_i^2 B_k^2 D_i D_k \rho - 3T^4 A_k B_i^3 B_k^2 D_i D_k \rho^2 + 3T^2 A_i B_i^2 B_k^2 C_k D_i D_k \\
&\quad + 4T^4 A_i^2 A_k B_i B_k^2 D_i D_k + jT^4 B_i^3 B_k^3 C_i C_k \rho - jT^4 A_k B_i^3 B_k^2 C_i D_k \rho \\
&\quad \left. - jT^6 A_k B_i^3 B_k^3 D_i \rho^3 \right] + j e^{j\phi} A_k D_i,
\end{aligned}$$

$$\begin{aligned}
\frac{\partial^2 Y_{12}}{\partial \rho^2} &= 2T^5 B_i^2 B_k^2 e^{j\phi} \frac{(B_i B_k C_i C_k + A_i A_k D_i D_k - A_i B_k C_k D_i - A_k B_i C_i D_k)}{(T^2 A_i B_k + jT^2 B_i B_k \rho + B_i D_k)^3}, \\
\frac{\partial^2 Y_{12}}{\partial \phi \partial T} &= \frac{\partial^2 Y_{12}}{\partial T \partial \phi} = j e^{j\phi} \left[A_k C_i + j A_k D_i \rho - \frac{1}{T^2} C_k D_i \right. \\
&\quad - \left(A_i A_k + j B_i A_k \rho - \frac{1}{T^2} B_i C_k \right) \frac{T C_i B_k + j T D_i B_k \rho + T^{-1} D_i D_k}{T A_i B_k + j B_i B_k \rho T + T^{-1} B_i D_k} \\
&\quad - \left(T A_i A_k + j T B_i A_k \rho + \frac{1}{T} B_i C_k \right) \frac{C_i B_k + j D_i B_k \rho - T^{-2} D_i D_k}{T A_i B_k + j B_i B_k \rho T + T^{-1} B_i D_k} \\
&\quad + \left(T A_i A_k + j T B_i A_k \rho + \frac{1}{T} B_i C_k \right) \frac{T C_i B_k + j T D_i B_k \rho + T^{-1} D_i D_k}{(T A_i B_k + j B_i B_k \rho T + T^{-1} B_i D_k)^2} \\
&\quad \times \left(A_i B_k + j B_i B_k \rho - \frac{1}{T^2} B_i D_k \right) \Big], \\
\frac{\partial^2 Y_{12}}{\partial \phi \partial \rho} &= \frac{\partial^2 Y_{12}}{\partial \rho \partial \phi} = j e^{j\phi} \left[j T D_i A_k - j T B_i A_k \frac{T C_i B_k + j T D_i B_k \rho + D_i D_k T^{-1}}{T A_i B_k + j T B_i B_k \rho + T^{-1} B_i D_k} \right. \\
&\quad - j \left(T A_i A_k + j T B_i A_k \rho + \frac{1}{T} B_i C_k \right) \frac{T B_k D_i}{T A_i B_k + j T B_i B_k \rho + T^{-1} B_i D_k} \\
&\quad + j \left(T A_i A_k + j T B_i A_k \rho + \frac{1}{T} B_i C_k \right) \left(T C_i B_k + j T D_i B_k \rho + D_i D_k \frac{1}{T} \right) \\
&\quad \times \frac{T B_i B_k}{(T A_i B_k + j T B_i B_k \rho + T^{-1} B_i D_k)^2} \Big],
\end{aligned}$$

$$\begin{aligned}
\frac{\partial Y_{21}}{\partial \phi} &= \frac{j e^{-j\phi}}{T A_i B_k + j T B_i B_k \rho + T^{-1} B_i D_k}, \\
\frac{\partial Y_{21}}{\partial T} &= \frac{T^2 A_i B_k + j T^2 B_i B_k \rho - B_i D_k}{e^{j\phi} (T^2 A_i B_k + j T^2 B_i B_k \rho + B_i D_k)^2}, \\
\frac{\partial Y_{21}}{\partial \rho} &= \frac{j T B_i B_k}{e^{j\phi} (T A_i B_k + j T B_i B_k \rho + T^{-1} B_i D_k)^2}, \\
\frac{\partial^2 Y_{21}}{\partial \phi^2} &= \frac{e^{-j\phi}}{T A_i B_k + j T B_i B_k \rho + T^{-1} B_i D_k}, \\
\frac{\partial^2 Y_{21}}{\partial T^2} &= -2 B_k \frac{T^2 A_i^2 B_k + 2 j T^2 A_i B_i B_k \rho - 3 A_i B_i D_k - T^2 B_i^2 B_k \rho^2 - j 3 B_i^2 D_k \rho}{T^{-1} e^{j\phi} (T^2 A_i B_k + j T^2 B_i B_k \rho + B_i D_k)^3}, \\
\frac{\partial^2 Y_{21}}{\partial \rho^2} &= \frac{2 T^2 B_i^2 B_k^2}{e^{j\phi} (T A_i B_k + j T B_i B_k \rho + T^{-1} B_i D_k)^3}, \\
\frac{\partial^2 Y_{21}}{\partial \phi \partial T} &= \frac{\partial^2 Y_{21}}{\partial T \partial \phi} = \frac{j}{e^{j\phi} (T^2 A_i B_k + j T^2 B_i B_k \rho + B_i D_k)} \\
&\quad - \frac{2 j (A_i B_k + j B_i B_k \rho)}{e^{j\phi} (T A_i B_k + j T B_i B_k \rho + T^{-1} B_i D_k)^2},
\end{aligned}$$

$$\begin{aligned}\frac{\partial^2 Y_{21}}{\partial \phi \partial \rho} &= \frac{\partial^2 Y_{21}}{\partial \rho \partial \phi} = \frac{T^3 e^{-j\phi} B_i B_k}{(T^2 A_i B_k + jT^2 B_i B_k \rho + B_i D_k)^2}, \\ \frac{\partial^2 Y_{21}}{\partial \rho \partial T} &= \frac{\partial^2 Y_{21}}{\partial T \partial \rho} = -jT^2 B_i B_k \frac{T^2 A_i B_k + jT^2 B_i B_k \rho - 3B_i D_k}{e^{j\phi} (T^2 A_i B_k + jT^2 B_i B_k \rho + B_i D_k)^3},\end{aligned}$$

$$\begin{aligned}\frac{\partial Y_{22}}{\partial \rho} &= \frac{jT^2 B_i^2 (A_k D_k - B_k C_k)}{(T^2 A_i B_k + jT^2 B_i B_k \rho + B_i D_k)^2}, \\ \frac{\partial Y_{22}}{\partial T} &= \frac{2TB_i (A_i A_k D_k - A_i B_k C_k + jA_k B_i D_k \rho - jB_i B_k C_k \rho)}{(T^2 A_i B_k + jT^2 B_i B_k \rho + B_i D_k)^2}, \\ \frac{\partial^2 Y_{22}}{\partial \rho^2} &= \frac{2T^4 B_i^3 B_k (A_k D_k - B_k C_k)}{(T^2 A_i B_k + jT^2 B_i B_k \rho + B_i D_k)^3}, \\ \frac{\partial^2 Y_{22}}{\partial T^2} &= -2B_i (A_i A_k D_k + jA_k B_i D_k \rho - A_i B_k C_k - jB_i B_k C_k \rho) \\ &\quad \times \frac{3T^2 A_i B_k + 3jT^2 B_i B_k \rho - B_i D_k}{(T^2 A_i B_k + jT^2 B_i B_k \rho + B_i D_k)^3}, \\ \frac{\partial^2 Y_{22}}{\partial \rho \partial T} &= \frac{\partial^2 Y_{22}}{\partial T \partial \rho} = -2jTB_i^2 (A_k D_k - B_k C_k) \frac{T^2 A_i B_k + jT^2 B_i B_k \rho - B_i D_k}{(T^2 A_i B_k + jT^2 B_i B_k \rho + B_i D_k)^3}.\end{aligned}$$

Since the UPFC model is embedded into $\bar{\mathbf{Y}}_{\text{bus}}$ matrix, the first- and second- order UPFC sensitivity analysis is only associated with the complex power injections at buses i and k , and the thermal limit of transmission line between the two buses, which are given by

$$\bar{S}_i = \vec{V}_i \vec{I}_i^* = \vec{V}_i \left[\sum_{n=1}^{N_B} \mathbf{Y}_{\text{bus}_{in}} \vec{V}_n \right]^*, \quad (\text{B.3})$$

$$\bar{S}_k = \vec{V}_k \vec{I}_k^* = \vec{V}_k \left[\sum_{n=1}^{N_B} \mathbf{Y}_{\text{bus}_{kn}} \vec{V}_n \right]^*, \quad (\text{B.4})$$

$$\vec{I}_{ik} = \vec{V}_i \mathbf{Y}_{11} + \vec{V}_k \mathbf{Y}_{12}. \quad (\text{B.5})$$

Here, we assume that current flows from bus i to bus k . The first- and second-order derivatives for the above equations are written as follows:

$$\begin{aligned}
\frac{\partial \bar{S}_i}{\partial \phi} &= \vec{V}_i \vec{V}_k^* \left(\frac{\partial Y_{12}}{\partial \phi} \right)^*, \\
\frac{\partial \bar{S}_k}{\partial \phi} &= \vec{V}_k \vec{V}_i^* \left(\frac{\partial Y_{21}}{\partial \phi} \right)^*, \\
\frac{\partial \bar{S}_i}{\partial \rho} &= V_i^2 \left(\frac{\partial Y_{11}}{\partial \rho} \right)^* + \vec{V}_i \vec{V}_k^* \left(\frac{\partial Y_{12}}{\partial \rho} \right)^*, \\
\frac{\partial \bar{S}_k}{\partial \rho} &= \vec{V}_k \vec{V}_i^* \left(\frac{\partial Y_{21}}{\partial \rho} \right)^* + V_k^2 \left(\frac{\partial Y_{22}}{\partial \rho} \right)^*, \\
\frac{\partial \bar{S}_i}{\partial T} &= V_i^2 \left(\frac{\partial Y_{11}}{\partial T} \right)^* + \vec{V}_i \vec{V}_k^* \left(\frac{\partial Y_{12}}{\partial T} \right)^*, \\
\frac{\partial \bar{S}_k}{\partial T} &= \vec{V}_k \vec{V}_i^* \left(\frac{\partial Y_{21}}{\partial T} \right)^* + V_k^2 \left(\frac{\partial Y_{22}}{\partial T} \right)^*, \\
\frac{\partial \vec{I}_{ik}}{\partial \phi} &= \vec{V}_k \frac{\partial Y_{12}}{\partial \phi}, \\
\frac{\partial \vec{I}_{ik}}{\partial \rho} &= \vec{V}_i \frac{\partial Y_{11}}{\partial \rho} + \vec{V}_k \frac{\partial Y_{12}}{\partial \rho}, \\
\frac{\partial \vec{I}_{ik}}{\partial T} &= \vec{V}_i \frac{\partial Y_{11}}{\partial T} + \vec{V}_k \frac{\partial Y_{12}}{\partial T}, \\
\frac{\partial \vec{I}_{ik}}{\partial V_i} &= e^{j\theta_i} Y_{11}, \\
\frac{\partial \vec{I}_{ik}}{\partial \theta_i} &= j \vec{V}_i Y_{11}, \\
\frac{\partial \vec{I}_{ik}}{\partial V_k} &= e^{j\theta_k} Y_{12}, \\
\frac{\partial \vec{I}_{ik}}{\partial \theta_k} &= j \vec{V}_k Y_{12}, \\
\frac{\partial \vec{I}_{ik} \vec{I}_{ik}^*}{\partial \phi} &= \frac{\partial \vec{I}_{ik}}{\partial \phi} \vec{I}_{ik}^* + \frac{\partial \vec{I}_{ik}^*}{\partial \phi} \vec{I}_{ik}, \\
\frac{\partial \vec{I}_{ik} \vec{I}_{ik}^*}{\partial \rho} &= \frac{\partial \vec{I}_{ik}}{\partial \rho} \vec{I}_{ik}^* + \frac{\partial \vec{I}_{ik}^*}{\partial \rho} \vec{I}_{ik}, \\
\frac{\partial \vec{I}_{ik} \vec{I}_{ik}^*}{\partial T} &= \frac{\partial \vec{I}_{ik}}{\partial T} \vec{I}_{ik}^* + \frac{\partial \vec{I}_{ik}^*}{\partial T} \vec{I}_{ik}, \\
\frac{\partial^2 \vec{I}_{ik}}{\partial \phi^2} &= \vec{V}_k \frac{\partial^2 Y_{12}}{\partial \phi^2},
\end{aligned}$$

$$\begin{aligned}
\frac{\partial^2 \vec{I}_{ik}}{\partial \rho^2} &= \left(\vec{V}_i \frac{\partial^2 Y_{11}}{\partial \rho^2} + \vec{V}_k \frac{\partial^2 Y_{12}}{\partial \rho^2} \right), \\
\frac{\partial^2 \vec{I}_{ik}}{\partial T^2} &= \left(\vec{V}_i \frac{\partial^2 Y_{11}}{\partial T^2} + \vec{V}_k \frac{\partial^2 Y_{12}}{\partial T^2} \right), \\
\frac{\partial^2 \vec{I}_{ik}}{\partial V_i \partial \rho} &= \frac{\partial^2 \vec{I}_{ik}}{\partial \rho \partial V_i} = e^{j\theta_i} \frac{\partial Y_{11}}{\partial \rho}, \\
\frac{\partial^2 \vec{I}_{ik}}{\partial V_i \partial T} &= \frac{\partial^2 \vec{I}_{ik}}{\partial T \partial V_i} = e^{j\theta_i} \frac{\partial Y_{11}}{\partial T}, \\
\frac{\partial^2 \vec{I}_{ik}}{\partial V_k \partial \phi} &= \frac{\partial^2 \vec{I}_{ik}}{\partial \phi \partial V_k} = e^{j\theta_k} \frac{\partial Y_{12}}{\partial \phi}, \\
\frac{\partial^2 \vec{I}_{ik}}{\partial V_k \partial \rho} &= \frac{\partial^2 \vec{I}_{ik}}{\partial \rho \partial V_k} = e^{j\theta_k} \frac{\partial Y_{12}}{\partial \rho}, \\
\frac{\partial^2 \vec{I}_{ik}}{\partial V_k \partial T} &= \frac{\partial^2 \vec{I}_{ik}}{\partial T \partial V_k} = e^{j\theta_k} \frac{\partial Y_{12}}{\partial T}, \\
\frac{\partial^2 \vec{I}_{ik}}{\partial \theta_i \partial \rho} &= \frac{\partial^2 \vec{I}_{ik}}{\partial \rho \partial \theta_i} = j \vec{V}_i \frac{\partial Y_{11}}{\partial \rho}, \\
\frac{\partial^2 \vec{I}_{ik}}{\partial \theta_i \partial T} &= \frac{\partial^2 \vec{I}_{ik}}{\partial T \partial \theta_i} = j \vec{V}_i \frac{\partial Y_{11}}{\partial T}, \\
\frac{\partial^2 \vec{I}_{ik}}{\partial \theta_k \partial \phi} &= \frac{\partial^2 \vec{I}_{ik}}{\partial \phi \partial \theta_k} = j \vec{V}_k \frac{\partial Y_{12}}{\partial \phi}, \\
\frac{\partial^2 \vec{I}_{ik}}{\partial \theta_k \partial \rho} &= \frac{\partial^2 \vec{I}_{ik}}{\partial \rho \partial \theta_k} = j \vec{V}_k \frac{\partial Y_{12}}{\partial \rho}, \\
\frac{\partial^2 \vec{I}_{ik}}{\partial \theta_k \partial T} &= \frac{\partial^2 \vec{I}_{ik}}{\partial T \partial \theta_k} = j \vec{V}_k \frac{\partial Y_{12}}{\partial T}, \\
\frac{\partial^2 \vec{I}_{ik}}{\partial \phi \partial \rho} &= \frac{\partial^2 \vec{I}_{ik}}{\partial \rho \partial \phi} = \vec{V}_k \frac{\partial^2 Y_{12}}{\partial \phi \partial \rho}, \\
\frac{\partial^2 \vec{I}_{ik}}{\partial \phi \partial T} &= \frac{\partial^2 \vec{I}_{ik}}{\partial T \partial \phi} = \vec{V}_k \frac{\partial^2 Y_{12}}{\partial \phi \partial T}, \\
\frac{\partial^2 \vec{I}_{ik}}{\partial \rho \partial T} &= \frac{\partial^2 \vec{I}_{ik}}{\partial T \partial \rho} = \vec{V}_i \frac{\partial^2 Y_{11}}{\partial \rho \partial T} + \vec{V}_k \frac{\partial^2 Y_{12}}{\partial \rho \partial T}, \\
\frac{\partial^2 \bar{S}_i}{\partial V_i \partial \phi} &= \frac{\partial^2 \bar{S}_i}{\partial \phi \partial V_i} = e^{j\theta_i} \vec{V}_k^* \left(\frac{\partial Y_{12}}{\partial \phi} \right)^*, \\
\frac{\partial^2 \bar{S}_i}{\partial \theta_i \partial \phi} &= \frac{\partial^2 \bar{S}_i}{\partial \phi \partial \theta_i} = j \vec{V}_i \vec{V}_k^* \left(\frac{\partial Y_{12}}{\partial \phi} \right)^*, \\
\frac{\partial^2 \bar{S}_i}{\partial V_k \partial \phi} &= \frac{\partial^2 \bar{S}_i}{\partial \phi \partial V_k} = \vec{V}_i e^{-j\theta_k} \left(\frac{\partial Y_{12}}{\partial \phi} \right)^*,
\end{aligned}$$

$$\begin{aligned}
\frac{\partial^2 \bar{S}_i}{\partial \theta_k \partial \phi} &= \frac{\partial^2 \bar{S}_i}{\partial \phi \partial \theta_k} = -j \vec{V}_i \vec{V}_k^* \left(\frac{\partial Y_{12}}{\partial \phi} \right)^*, \\
\frac{\partial^2 \bar{S}_i}{\partial V_i \partial \rho} &= \frac{\partial^2 \bar{S}_i}{\partial \rho \partial V_i} = 2V_i \left(\frac{\partial Y_{11}}{\partial \rho} \right)^* + e^{j\theta_i} \vec{V}_k^* \left(\frac{\partial Y_{12}}{\partial \rho} \right)^*, \\
\frac{\partial^2 \bar{S}_i}{\partial \theta_i \partial \rho} &= \frac{\partial^2 \bar{S}_i}{\partial \rho \partial \theta_i} = j \vec{V}_i \vec{V}_k^* \left(\frac{\partial Y_{12}}{\partial \rho} \right)^*, \\
\frac{\partial^2 \bar{S}_i}{\partial V_k \partial \rho} &= \frac{\partial^2 \bar{S}_i}{\partial \rho \partial V_k} = \vec{V}_i e^{-j\theta_k} \left(\frac{\partial Y_{12}}{\partial \rho} \right)^*, \\
\frac{\partial^2 \bar{S}_i}{\partial \theta_k \partial \rho} &= \frac{\partial^2 \bar{S}_i}{\partial \rho \partial \theta_k} = -j \vec{V}_i \vec{V}_k^* \left(\frac{\partial Y_{12}}{\partial \rho} \right)^*, \\
\frac{\partial^2 \bar{S}_i}{\partial V_i \partial T} &= \frac{\partial^2 \bar{S}_i}{\partial T \partial V_i} = 2V_i \left(\frac{\partial Y_{11}}{\partial T} \right)^* + e^{j\theta_i} \vec{V}_k^* \left(\frac{\partial Y_{12}}{\partial T} \right)^*, \\
\frac{\partial^2 \bar{S}_i}{\partial \theta_i \partial T} &= \frac{\partial^2 \bar{S}_i}{\partial T \partial \theta_i} = j \vec{V}_i \vec{V}_k^* \left(\frac{\partial Y_{12}}{\partial T} \right)^*, \\
\frac{\partial^2 \bar{S}_i}{\partial V_k \partial T} &= \frac{\partial^2 \bar{S}_i}{\partial T \partial V_k} = \vec{V}_i e^{-j\theta_k} \left(\frac{\partial Y_{12}}{\partial T} \right)^*, \\
\frac{\partial^2 \bar{S}_i}{\partial \theta_k \partial T} &= \frac{\partial^2 \bar{S}_i}{\partial T \partial \theta_k} = -j \vec{V}_i \vec{V}_k^* \left(\frac{\partial Y_{12}}{\partial T} \right)^*, \\
\frac{\partial^2 \bar{S}_i}{\partial \phi^2} &= \vec{V}_i \vec{V}_k^* \left(\frac{\partial^2 Y_{12}}{\partial \phi^2} \right)^*, \\
\frac{\partial^2 \bar{S}_i}{\partial \rho^2} &= V_i^2 \left(\frac{\partial^2 Y_{11}}{\partial \rho^2} \right)^* + \vec{V}_i \vec{V}_k^* \left(\frac{\partial^2 Y_{12}}{\partial \rho^2} \right)^*, \\
\frac{\partial^2 \bar{S}_i}{\partial T^2} &= V_i^2 \left(\frac{\partial^2 Y_{11}}{\partial T^2} \right)^* + \vec{V}_i \vec{V}_k^* \left(\frac{\partial^2 Y_{12}}{\partial T^2} \right)^*, \\
\frac{\partial^2 \bar{S}_i}{\partial \phi \partial \rho} &= \frac{\partial^2 \bar{S}_i}{\partial \rho \partial \phi} = \vec{V}_i \vec{V}_k^* \left(\frac{\partial^2 Y_{12}}{\partial \phi \partial \rho} \right)^*, \\
\frac{\partial^2 \bar{S}_i}{\partial \phi \partial T} &= \frac{\partial^2 \bar{S}_i}{\partial T \partial \phi} = \vec{V}_i \vec{V}_k^* \left(\frac{\partial^2 Y_{12}}{\partial \phi \partial T} \right)^*, \\
\frac{\partial^2 \bar{S}_i}{\partial \rho \partial T} &= \frac{\partial^2 \bar{S}_i}{\partial T \partial \rho} = V_i^2 \left(\frac{\partial^2 Y_{11}}{\partial \rho \partial T} \right)^* + \vec{V}_i \vec{V}_k^* \left(\frac{\partial^2 Y_{12}}{\partial \rho \partial T} \right)^*, \\
\frac{\partial^2 \bar{S}_k}{\partial V_i \partial \phi} &= \frac{\partial^2 \bar{S}_k}{\partial \phi \partial V_i} = e^{-j\theta_i} \vec{V}_k \left(\frac{\partial Y_{21}}{\partial \phi} \right)^*, \\
\frac{\partial^2 \bar{S}_k}{\partial \theta_i \partial \phi} &= \frac{\partial^2 \bar{S}_k}{\partial \phi \partial \theta_i} = -j \vec{V}_i^* \vec{V}_k \left(\frac{\partial Y_{21}}{\partial \phi} \right)^*,
\end{aligned}$$

$$\begin{aligned}
\frac{\partial^2 \bar{S}_k}{\partial V_k \partial \phi} &= \frac{\partial^2 \bar{S}_k}{\partial \phi \partial V_k} = \vec{V}_i^* e^{j\theta_k} \left(\frac{\partial Y_{21}}{\partial \phi} \right)^*, \\
\frac{\partial^2 \bar{S}_k}{\partial \theta_k \partial \phi} &= \frac{\partial^2 \bar{S}_k}{\partial \phi \partial \theta_k} = j \vec{V}_i^* \vec{V}_k \left(\frac{\partial Y_{21}}{\partial \phi} \right)^*, \\
\frac{\partial^2 \bar{S}_k}{\partial V_i \partial \rho} &= \frac{\partial^2 \bar{S}_k}{\partial \rho \partial V_i} = e^{-j\theta_i} \vec{V}_k \left(\frac{\partial Y_{21}}{\partial \rho} \right)^*, \\
\frac{\partial^2 \bar{S}_k}{\partial \theta_i \partial \rho} &= \frac{\partial^2 \bar{S}_k}{\partial \rho \partial \theta_i} = -j \vec{V}_i^* \vec{V}_k \left(\frac{\partial Y_{21}}{\partial \rho} \right)^*, \\
\frac{\partial^2 \bar{S}_k}{\partial V_k \partial \rho} &= \frac{\partial^2 \bar{S}_k}{\partial \rho \partial V_k} = \vec{V}_i^* e^{j\theta_k} \left(\frac{\partial Y_{21}}{\partial \rho} \right)^* + 2V_k \left(\frac{\partial Y_{22}}{\partial \rho} \right)^*, \\
\frac{\partial^2 \bar{S}_k}{\partial \theta_k \partial \rho} &= \frac{\partial^2 \bar{S}_k}{\partial \rho \partial \theta_k} = j \vec{V}_i^* \vec{V}_k \left(\frac{\partial Y_{21}}{\partial \rho} \right)^*, \\
\frac{\partial^2 \bar{S}_k}{\partial V_i \partial T} &= \frac{\partial^2 \bar{S}_k}{\partial T \partial V_i} = e^{-j\theta_i} \vec{V}_k \left(\frac{\partial Y_{21}}{\partial T} \right)^*, \\
\frac{\partial^2 \bar{S}_k}{\partial \theta_i \partial T} &= \frac{\partial^2 \bar{S}_k}{\partial T \partial \theta_i} = -j \vec{V}_i^* \vec{V}_k \left(\frac{\partial Y_{21}}{\partial T} \right)^*, \\
\frac{\partial^2 \bar{S}_k}{\partial V_k \partial T} &= \frac{\partial^2 \bar{S}_k}{\partial T \partial V_k} = \vec{V}_i^* e^{j\theta_k} \left(\frac{\partial Y_{21}}{\partial T} \right)^* + 2V_k \left(\frac{\partial Y_{22}}{\partial T} \right)^*, \\
\frac{\partial^2 \bar{S}_k}{\partial \theta_k \partial T} &= \frac{\partial^2 \bar{S}_k}{\partial T \partial \theta_k} = j \vec{V}_i^* \vec{V}_k \left(\frac{\partial Y_{21}}{\partial T} \right)^*, \\
\frac{\partial^2 \bar{S}_k}{\partial \phi^2} &= \vec{V}_i^* \vec{V}_k \left(\frac{\partial^2 Y_{21}}{\partial \phi^2} \right)^*, \\
\frac{\partial^2 \bar{S}_k}{\partial \rho^2} &= \vec{V}_i^* \vec{V}_k \left(\frac{\partial^2 Y_{21}}{\partial \rho^2} \right)^* + V_k^2 \left(\frac{\partial^2 Y_{22}}{\partial \rho^2} \right)^*, \\
\frac{\partial^2 \bar{S}_k}{\partial T^2} &= \vec{V}_i^* \vec{V}_k \left(\frac{\partial^2 Y_{21}}{\partial T^2} \right)^* + V_k^2 \left(\frac{\partial^2 Y_{22}}{\partial T^2} \right)^*, \\
\frac{\partial^2 \bar{S}_k}{\partial \phi \partial \rho} &= \frac{\partial^2 \bar{S}_k}{\partial \rho \partial \phi} = \vec{V}_i^* \vec{V}_k \left(\frac{\partial^2 Y_{21}}{\partial \phi \partial \rho} \right)^*, \\
\frac{\partial^2 \bar{S}_k}{\partial \phi \partial T} &= \frac{\partial^2 \bar{S}_k}{\partial T \partial \phi} = \vec{V}_i^* \vec{V}_k \left(\frac{\partial^2 Y_{21}}{\partial \phi \partial T} \right)^*, \\
\frac{\partial^2 \bar{S}_k}{\partial \rho \partial T} &= \frac{\partial^2 \bar{S}_k}{\partial T \partial \rho} = \vec{V}_i^* \vec{V}_k \left(\frac{\partial^2 Y_{21}}{\partial \rho \partial T} \right)^* + V_k^2 \left(\frac{\partial^2 Y_{22}}{\partial \rho \partial T} \right)^*, \\
\frac{\partial^2 \vec{I}_{ik} \vec{I}_{ik}^*}{\partial V_i \partial \phi} &= \frac{\partial^2 \vec{I}_{ik} \vec{I}_{ik}^*}{\partial \phi \partial V_i} = \vec{I}_{ik} \frac{\partial^2 \vec{I}_{ik}^*}{\partial V_i \partial \phi} + \frac{\partial \vec{I}_{ik}}{\partial V_i} \frac{\partial \vec{I}_{ik}^*}{\partial \phi} + \frac{\partial \vec{I}_{ik}^*}{\partial V_i} \frac{\partial \vec{I}_{ik}}{\partial \phi} + \vec{I}_{ik}^* \frac{\partial^2 \vec{I}_{ik}}{\partial V_i \partial \phi},
\end{aligned}$$

APPENDIX C

INPUT DATA FILE FORMAT

The GEOPF program reads natural gas and electricity network data files. IEEE Common Data Format (IEEE CDF) is used to obtain the electric transmission line and bus input data [30]. We created Generation Data Format (GDF) and Load Data Format (LDF) files for the electric network. In a similar way, we created Common Gas Format (CGF) for the natural gas network.

C.1 IEEE Common Data Format

The data file has lines of up to 128 characters. The lines are grouped into sections with section headers. Data items are entered in specific columns. No blank items are allowed, enter zeros instead. Floating point items should have explicit decimal point. No implicit decimal points are used. The IEEE CDF data which has been utilized in the GEOPF program is described below:

◇ **Title Data**

Columns	2-9	Date, in format DD/MM/YY with leading zeros
	11-30	Originator's name
	32-37	MVA base
	39-42	Year
	44	Season (S - Summer, W - Winter)
	46-73	Case identification

◇ **Bus Data**

Columns	1-4	Bus number
	7-17	Bus name
	25-26	Type:
		0=Unregulated (load, PQ)
		1=Hold MVAR generation within voltage limits (PQ)
		2=Hold voltage within VAR limits (PV)
		3=Hold voltage and angle (Swing)
Columns	28-33	Bus voltage (loadflow result)
	34-40	Bus angle (loadflow result)
	41-49	Load MW (loadflow result)
	50-59	Load MVAR (loadflow result)
	60-67	Generation MW (loadflow result)
	68-75	Generation MVAR (loadflow result)
	91-98	Maximum voltage: for only bus type 0
	99-106	Minimum voltage: for only bus type 0
	107-114	Shunt conductance G (per unit)
	115-122	Shunt susceptance B (per unit)

◇ **Line Data**

Columns	1-4	From bus
	6-9	To bus
	19	Line type:
		1=Fixed voltage ratio and/or fixed phase shifter
		2=Fixed phase angle and variable voltage ratio with voltage control
		3=Fixed phase angle and variable voltage ratio with MVAR control
		4=Fixed voltage ratio and variable phase shifter with MW control
	20-29	Branch resistance R, per unit
	30-40	Branch reactance X, per unit
	41-49	Line charging B, per unit
	57-61	Maximum line flow (MVA): for emergency state
	63-67	Maximum line flow (MVA): for normal operating state
	77-82	Transformer tap ratio
	84-90	Phase angle
	91-97	Minimum limit of variable tap ratio or phase shifter
	98-104	Maximum limit of variable tap ratio or phase shifter

C.2 Generator Data

Columns	1-5	Generator bus number
	7-15	Generator name
	17-23	Maximum real power generation
	25-29	Minimum real power generation
	31-38	Maximum reactive power generation
	40-45	Minimum reactive power generation
	40-45	Minimum reactive power generation
	47	Adjustable real power generation: 0=real power generation is not adjustable 1=real power generation is adjustable
	49	Adjustable reactive power generation: 0=reactive power generation is not adjustable 1=reactive power generation is adjustable
	51	Availability: 0=the generator is not available 1=the generator is available
	53-75	Generator cost function: $\alpha_{Gi} + \beta_{Gi}P_{Gi} + \gamma_{Gi}P_{Gi}^2$
	53-59	α_{Gi}
	61-66	β_{Gi}
	68-75	γ_{Gi}
	77-81	Maximum voltage
	83-87	Minimum voltage

C.3 Electricity Load Data

Columns	1-5	Load bus number
	7-13	Load bus name
	15-18	Load type:
		1=residential
		2=industrial
		3=commercial
	20-25	Maximum MW load
	27-32	Minimum MW load
	34-40	Maximum MVAR load
	42-48	Minimum MVAR load
	50	Interruptible load:
		0=not interruptible
		1=interruptible
	52-59	Maximum MW interruptible
	61-87	Customer benefit function: $\alpha_{Li} + \beta_{Li}P_{Li} + \gamma_{Li}P_{Li}^2$
	53-59	α_{Li}
	61-66	β_{Li}
	68-75	γ_{Li}
	77-81	Load power factor

C.4 Natural Gas Common Data Format

◇ Field Data

Columns	1-5	Standard temperature (°R)
	6-12	Standard pressure (psia)
	14-19	Average gas compressibility factor
	20-26	Compressor inlet compressibility factor
	28-31	Gross heating value (BTU/SCF)

◇ Node Data

Columns	1-4	Node number
	7-20	Node name
	23	Type: 0=known-pressure node 1=load node (except combined node) 2=gas-electric combined node 3=compressor inlet node 4=compressor outlet node
	29-37	Pressure, psia (loadflow result)
	39-46	Supply, $10^6 \times \text{SCF/hr}$ (loadflow result)
	48-54	Load demand, $10^6 \times \text{SCF/hr}$ (loadflow result)
	56-60	Minimum pressure (psia)
	62-66	Maximum pressure (psia)

◇ Pipeline Branch Data

Columns	1-4	From node
	6-9	To node
	11-16	Length (mile)
	19-24	Diameter (inch)
	26-30	Efficiency (per unit)
	32-35	Average temperature ($^{\circ}\text{R}$)
	39-40	$m1$ for Weymouth flow equation
	42-49	Pipeline branch flowrate (f_P), $10^6 \times \text{SCF/hr}$ (loadflow result)

◇ **Compressor Branch Data**

Columns	1-4	Compressor number
	6-9	Inlet node
	11-14	Outlet node
	17-23	Compressor branch flowrate (f_C), $10^6 \times \text{SCF/hr}$ (loadflow result)
	26-29	Efficiency (per unit)
	31-34	Maximum compression ratio
	39-42	Compressor suction temperature ($^{\circ}\text{R}$)
	46-69	Fuel consumption rate (SCF/hr): $\alpha_{Ti} + \beta_{Ti}H_i + \gamma_{Ti}H_i^2$
	46-51	α_{Ti}
	53-59	β_{Ti}
	63-69	γ_{Ti}
	71-79	Horsepower (loadflow result)
	83-89	Gas consumption, $10^6 \times \text{SCF/hr}$ (loadflow result)

C.5 Natural Gas Load Data

Columns	1-5	Node number
	7-14	Node name
	17	Load type:
		1=residential
		2=industrial
		3=commercial
		4=generator
	20-22	Generator number if load is a generator.
	24-27	Maximum load ($10^6 \times \text{SCF/hr}$)
	29-33	Minimum load ($10^6 \times \text{SCF/hr}$)
	37	Interruptible load:
		0=not interruptible
		1=interruptible
	39-64	Consumer benefit function (\$/hr): $\alpha_{Li} + \beta_{Li}w_{Li} + \gamma_{Li}w_{Li}^2$
	39-44	α_{Li}
	47-54	β_{Li}
	57-64	γ_{Li}

C.6 Natural Gas Source Data

Columns	1-5	Node number
	7-16	Node name
	19-21	Maximum production rate ($10^6 \times \text{SCF/hr}$)
	23-27	Minimum production rate ($10^6 \times \text{SCF/hr}$)
	28	Availability: 0=not available 1=available
	31-37	Unit price ($\$/ (10^6 \times \text{SCF/hr})$)
	40-45	Maximum pressure (psia)
	48-53	Minimum pressure (psia)

```

=====
12345678901234567890123456789012345678901234567890123456789012345678901234567890
=====

09/25/93 UW ARCHIVE          100.0  1962 W IEEE 14 Bus Test Case
BUS DATA FOLLOWS
1 Bus 1  HV 1 1 3 1.060  0.0  0.0  232.4  -16.9  0.0  1.060  150  -100  0.0  0.0  0
2 Bus 2  HV 1 1 2 1.045  -4.98  21.7  12.7  40.0  42.4  0.0  1.045  50.0  -40.0  0.0  0.0  0
3 Bus 3  HV 1 1 2 1.010  -12.72  94.2  19.0  0.0  23.4  0.0  1.010  40.0  0.0  0.0  0.0  0
4 Bus 4  HV 1 1 0 1.019  -10.33  91.98  -13.64  0.0  0.0  0.0  0.0  1.05  0.95  0.0  0.0  0
5 Bus 5  HV 1 1 0 1.020  -8.78  51.66  14.42  0.0  0.0  0.0  0.0  1.05  0.95  0.0  0.0  0
-999

BRANCH DATA FOLLOWS
1 2 1 1 1 0 0.01938  0.05917  0.0528  155  155  120  0 0 0.0  0.0  0.0  0.0  0.0
1 5 1 1 1 0 0.05403  0.22304  0.0492  110  110  90  0 0 0.0  0.0  0.0  0.0  0.0
2 3 1 1 1 0 0.04699  0.19797  0.0438  95  95  75  0 0 0.0  0.0  0.0  0.0  0.0
2 4 1 1 1 0 0.05811  0.17632  0.0374  95  95  75  0 0 0.0  0.0  0.0  0.0  0.0
2 5 1 1 1 0 0.05695  0.17388  0.0340  95  95  75  0 0 0.0  0.0  0.0  0.0  0.0
3 4 1 1 1 0 0.06701  0.17103  0.0346  95  95  75  0 0 0.0  0.0  0.0  0.0  0.0
4 5 1 1 1 0 0.01335  0.04211  0.0128  95  95  75  0 0 0.0  0.0  0.0  0.0  0.0
-999

LOSS ZONES FOLLOWS
1 IEEE 14 BUS
-99

INTERCHANGE DATA FOLLOWS
1 2 Bus 2  HV 0.0  999.99  IEEE14  IEEE 14 Bus Test Case
-9

TIE LINES FOLLOWS
-999
END OF DATA

```

Figure C.1: IEEE 5-bus system common data format

```

=====
1234567890123456789012345678901234567890123456789012345678901234567890
=====

```

```

BUNUM GENERNAME MX---MW MN--MW MX---MVR MN-MVR P Q A AL_PHA B-E-TA GAM-M--A V-MAX V-MIN MW-UP MW-DN MVARUP MVARDN BETA_R GAMMAR
1 GEN1      250.00 45.0 150.00 -100 1 1 1 692.32 11.0 .000820 1.08 0.950 inf inf inf 0.0 .00000
2 GEN2      150.00 15.0 50.00 -40 1 1 1 692.32 12.0 .000776 1.08 0.950 inf inf inf 0.0 .00000
3 SynCon 1    0.00 0.0 40.00 -40 0 1 1 0.0 0.0 .000000 1.08 0.950 inf inf inf 0.0 .00000

```

Figure C.2: IEEE 5-bus system generator data format

```

=====
1234567890123456789012345678901234567890123456789012345678901234567890
=====

```

```

BUNUM BUSNAME TYPE MX--MW MN--MW MX-MVAR MN-MVAR R MX-MW-IN ALPHA-LD BETA--LD GAMMA--LD ALPHA-IN BETA-IN GAMMA-IN P----F
2 Residen 1 inf 0.0 0.0 inf inf -inf 1 inf 0.00 21.43 -0.2147 0.0 100.0 0.0 0.98
3 Indust1 2 inf 0.0 0.0 inf -inf 1 inf 0.00 23.00 -0.0531 0.0 100.0 0.0 0.98
4 Indust2 2 inf 0.0 0.0 inf -inf 1 inf 0.00 22.48 -0.0531 0.0 100.0 0.0 0.98
5 Commerc 3 inf 0.0 0.0 inf -inf 1 inf 0.00 22.11 -0.0930 0.0 100.0 0.0 0.98

```

Figure C.3: IEEE 5-bus system load data format

```

07/20/94 OSU mods to UW case 100.0 1962 W IEEE14 W/LINE LIMITS, BUS KV
BUS DATA FOLLOWS
14 ITEMS
1 Bus 1 HV 1 1 3 1.0600 .00 .00 232.39 -16.90 230.00 1.0600 150.00 -100.00 .0000 .0000 0
2 Bus 2 HV 1 1 2 1.0450 -4.98 21.70 12.70 40.00 230.00 1.0450 50.00 -40.00 .0000 .0000 0
3 Bus 3 HV 1 1 2 1.0100 -12.72 94.20 19.00 .00 23.39 230.00 1.0100 40.00 .00 .0000 .0000 0
4 Bus 4 HV 1 1 0 1.0186 -10.32 47.80 -3.90 .00 230.00 .0000 1.05 0.950 .0000 .0000 0
5 Bus 5 HV 1 1 0 1.0203 -8.78 7.60 1.60 .00 230.00 .0000 1.05 0.950 .0000 .0000 0
6 Bus 6 LV 1 1 2 1.0700 -14.22 11.20 7.50 .00 12.24 69.00 1.0700 24.00 -6.00 .0000 .0000 0
7 Bus 7 ZV 1 1 0 1.0620 -13.37 .00 .00 .00 161.00 .0000 1.250 0.750 .0000 .0000 0
8 Bus 8 TV 1 1 2 1.0900 -13.37 .00 .00 17.36 138.00 1.0900 24.00 -6.00 .0000 .0000 0
9 Bus 9 LV 1 1 0 1.0563 -14.95 29.50 16.60 .00 69.00 .0000 1.050 0.950 .0000 .1900 0
10 Bus 10 LV 1 1 0 1.0513 -15.10 9.00 5.80 .00 69.00 .0000 1.050 0.950 .0000 .0000 0
11 Bus 11 LV 1 1 0 1.0571 -14.80 3.50 1.80 .00 69.00 .0000 1.050 0.900 .0000 .0000 0
12 Bus 12 LV 1 1 0 1.0552 -15.08 6.10 1.60 .00 69.00 .0000 1.050 0.950 .0000 .0000 0
13 Bus 13 LV 1 1 0 1.0504 -15.16 13.50 5.80 .00 69.00 .0000 1.050 0.950 .0000 .0000 0
14 Bus 14 LV 1 1 0 1.0358 -16.04 14.90 5.00 .00 69.00 .0000 1.050 0.950 .0000 .0000 0
-999

BRANCH DATA FOLLOWS
20 ITEMS
1 2 1 1 1 0 .019380 .059170 .05280 175. 175. 120. 0 0 .0000 .00 .0000 .0000 .0000 .0000
1 5 1 1 1 0 .054030 .223040 .04920 90. 90. 90. 0 0 .0000 .00 .0000 .0000 .0000 .0000
2 3 1 1 1 0 .046990 .197970 .04380 75. 75. 75. 0 0 .0000 .00 .0000 .0000 .0000 .0000
2 4 1 1 1 0 .058110 .176320 .03740 75. 75. 75. 0 0 .0000 .00 .0000 .0000 .0000 .0000
2 5 1 1 1 0 .056950 .173880 .03400 50. 50. 50. 0 0 .0000 .00 .0000 .0000 .0000 .0000
3 4 1 1 1 0 .067010 .171030 .03460 50. 50. 50. 0 0 .0000 .00 .0000 .0000 .0000 .0000
4 5 1 1 1 0 .013350 .042110 .01280 90. 90. 90. 0 0 .0000 .00 .0000 .0000 .0000 .0000
6 11 1 1 1 0 .094980 .198900 .00000 10. 10. 10. 0 0 .0000 .00 .0000 .0000 .0000 .0000
6 12 1 1 1 0 .122910 .255810 .00000 10. 10. 10. 0 0 .0000 .00 .0000 .0000 .0000 .0000
6 13 1 1 1 0 .066150 .130270 .00000 20. 20. 20. 0 0 .0000 .00 .0000 .0000 .0000 .0000
9 10 1 1 1 0 .031810 .084500 .00000 10. 10. 10. 0 0 .0000 .00 .0000 .0000 .0000 .0000
9 14 1 1 1 0 .127110 .270380 .00000 15. 15. 15. 0 0 .0000 .00 .0000 .0000 .0000 .0000
10 11 1 1 1 0 .082050 .192070 .00000 10. 10. 10. 0 0 .0000 .00 .0000 .0000 .0000 .0000
12 13 1 1 1 0 .220920 .199880 .00000 10. 10. 10. 0 0 .0000 .00 .0000 .0000 .0000 .0000
13 14 1 1 1 0 .170930 .348020 .00000 10. 10. 10. 0 0 .0000 .00 .0000 .0000 .0000 .0000
4 7 1 1 1 1 .000000 .209120 .00000 35. 35. 35. 0 0 .9780 .00 .0000 .0000 .0000 .0000
4 9 1 1 1 1 .000000 .556180 .00000 20. 20. 20. 0 0 .9690 .00 .0000 .0000 .0000 .0000
5 6 1 1 1 1 .000000 .252020 .00000 50. 50. 50. 0 0 .9320 .00 .0000 .0000 .0000 .0000
7 8 1 1 1 1 .000000 .176150 .00000 20. 20. 20. 0 0 1.0000 .00 .0000 .0000 .0000 .0000
7 9 1 1 1 1 .000000 .110010 .00000 35. 35. 35. 0 0 1.0000 .00 .0000 .0000 .0000 .0000
-999

```

Figure C.4: IEEE 14-bus system common data format

```

=====
1234567890123456789012345678901234567890123456789012345678901234567890
=====
BUNUM  GENERNAME  MX--GEN  MNGEN  MX---MVR  MN-MVR  P  Q  A  AL--PHA  B-E-TA  GAM---MA  V-MAX  V-MIN  MW-UP  MW-DN  MVARUP  MVARDN  BETA-R  GAMMAR
1 GEN 1      250.00  45.0   150.00  -100  1 1 1  692.32  11.0   .000820  1.080  0.950  inf  inf  inf  inf  inf  0.0 .00000
2 GEN 2      150.00  15.0   50.00   -40  1 1 1  692.32  12.0   .000776  1.080  0.950  inf  inf  inf  inf  inf  0.0 .00000
3 SynCon 1      0.00  0.00   40.00    0  0 1 1      0.00  0.0   .000000  1.080  0.950  inf  inf  inf  inf  inf  0.0 .00000
6 SynCon 2      0.00  0.00   54.00  -50  0 1 1      0.00  0.0   .000000  1.080  0.950  inf  inf  inf  inf  inf  0.0 .00000
8 SynCon 3      0.00  0.00   54.00  -50  0 1 1      0.00  0.0   .000000  1.080  0.950  inf  inf  inf  inf  inf  0.0 .00000
=====

```

Figure C.5: IEEE 14-bus system generator data format

```

=====
1234567890123456789012345678901234567890123456789012345678901234567890
=====
BUNUM  BUSNAME  TYPE  MX--MW  MN--MW  MX-MVAR  MN-MVAR  R  MX-MW-IN  ALPHA-LD  BETA--LD  GAMMA--LD  ALPHA-IN  BETA-IN  GAMMA-IN  P----F
2 Residen      1  inf  0.0   0.0   inf  -inf  1  inf  0.00  21.43  -0.2146  0.0  100.0  0.0  0.98
3 Indust1      2  inf  0.0   0.0   inf  -inf  1  inf  0.00  22.98  -0.0530  0.0  100.0  0.0  0.98
4 Indust2      2  inf  0.0   0.0   inf  -inf  1  inf  0.00  22.45  -0.1021  0.0  100.0  0.0  0.98
5 Commere      3  inf  0.0   0.0   inf  -inf  1  inf  0.00  22.07  -0.6314  0.0  100.0  0.0  0.98
6 Residen      1  inf  0.0   0.0   inf  -inf  1  inf  0.00  22.11  -0.4292  0.0  100.0  0.0  0.98
9 Residen      1  inf  0.0   0.0   inf  -inf  1  inf  0.00  22.41  -0.1652  0.0  100.0  0.0  0.98
10 Residen     1  inf  0.0   0.0   inf  -inf  1  inf  0.00  22.50  -0.5434  0.0  100.0  0.0  0.98
11 Residen     1  inf  0.0   0.0   inf  -inf  1  inf  0.00  22.39  -1.3904  0.0  100.0  0.0  0.98
12 Residen     1  inf  0.0   0.0   inf  -inf  1  inf  0.00  22.51  -0.8022  0.0  100.0  0.0  0.98
13 Residen     1  inf  0.0   0.0   inf  -inf  1  inf  0.00  22.63  -0.3644  0.0  100.0  0.0  0.98
14 Residen     1  inf  0.0   0.0   inf  -inf  1  inf  0.00  23.02  -0.3359  0.0  100.0  0.0  0.98
=====

```

Figure C.6: IEEE 14-bus system load data format

```

=====
1234567890123456789012345678901234567890123456789012345678901234567890
=====

07/20/94 OSU mods to UW case 100.0 1962 W IEEE14 W/LINE LIMITS, BUS KV
BUS DATA FOLLOWS
  1 Bus 1 HV 1 1 3 1.0300 .00 .00 72.000 30.00 230.00 1.0600 150.00 -100.00 .0000 .0000 0
  2 Bus 2 HV 1 1 2 1.0250 8.98 0.000 0.00 163.00 6.41 230.00 1.0450 50.00 -40.00 .0000 .0000 0
  3 Bus 3 HV 1 1 2 1.0250 5.72 0.00 0.00 85.00 -11.9 230.00 1.0100 40.00 .00 .0000 .0000 0
  4 Bus 4 HV 1 1 0 1.0256 -2.32 0.0 0.00 .00 230.00 .0000 1.05 0.955 .0000 .0000 0
  5 Bus 5 HV 1 1 0 0.9900 -4.78 125.0 50.00 .00 230.00 .0000 1.05 0.955 .0000 .0000 0
  6 Bus 6 LV 1 1 0 1.0100 -4.22 90.0 30.00 .00 69.00 1.0700 1.050 0.955 .0000 .0000 0
  7 Bus 7 ZV 1 1 0 1.0220 3.37 .00 .00 161.00 .0000 1.050 0.955 .0000 .0000 0
  8 Bus 8 TV 1 1 0 1.0100 0.37 100.0 35.00 .00 138.00 1.0900 1.050 0.950 .0000 .0000 0
  9 Bus 9 LV 1 1 0 1.0363 2.95 0.00 0.00 .00 69.00 .0000 1.050 0.955 .0000 .1900 0
-999
BRANCH DATA FOLLOWS
  4 6 1 1 1 0 .017000 .092000 .15800 120. 155. 320. 0 0 .0000 .00 .0000 .0000 .0000
  4 5 1 1 1 0 .010000 .085000 .17600 90. 110. 390. 0 0 .0000 .00 .0000 .0000 .0000
  5 7 1 1 1 0 .032000 .161000 .30600 75. 95. 375. 0 0 .0000 .00 .0000 .0000 .0000
  6 9 1 1 1 0 .039000 .170000 .35800 75. 95. 375. 0 0 .0000 .00 .0000 .0000 .0000
  7 8 1 1 1 0 .008500 .072000 .14900 50. 95. 350. 0 0 .0000 .00 .0000 .0000 .0000
  9 8 1 1 1 0 .011900 .100800 .20900 50. 95. 350. 0 0 .0000 .00 .0000 .0000 .0000
  1 4 1 1 1 1 .000000 .057600 .00000 50. 60. 450. 0 0 .9320 .00 .0000 .0000 .0000
  2 7 1 1 1 1 .000000 .062500 .00000 20. 30. 320. 0 0 1.0000 .00 .0000 .0000 .0000
  3 9 1 1 1 1 .000000 .058600 .00000 35. 45. 335. 0 0 1.0000 .00 .0000 .0000 .0000
-999
LOSS ZONES FOLLOWS
  1 IEEE 14 BUS
-99
INTERCHANGE DATA FOLLOWS
  1 2 Bus 2 HV .0 999.99 IEEE14 IEEE 14 Bus Test Case
-9
TIE LINES FOLLOW
-999
END OF DATA

```

Figure C.7: WSCC 9-bus system common data format


```

=====
1234567890123456789012345678901234567890123456789012345678901234567890
=====

BUNUM  GENERNAME  MX---MW  MN---MW  MX---MVR  MN-MVR  P  Q  A  AL__PHA  B-E-TA  GAM-M--A  V-MAX  V-MIN  MW-UP  MW-DN  MVARUP  MVARDN  BETA_R  GAMMAR
1 GEN1      250.00  21.6  150.00 -100 1 1 1 0.0 12.712 .000820 1.040 0.950 50.0 50.0 inf inf 0.0 .00000
2 GEN2      271.64  25.0  50.00 -40 1 1 1 0.0 12.001 .000876 1.045 0.955 35.0 35.0 inf inf 0.0 .00000
3 GEN3      285.00  25.0  50.00 -40 1 1 1 0.0 12.290 .000646 1.045 0.955 35.0 35.0 inf inf 0.0 .00000

=====
1234567890123456789012345678901234567890123456789012345678901234567890
=====

BUNUM  BUSNAME  TYPE  MX---MW  MN---MW  MX-MVAR  MN-MVAR  R  MX-MW-IN  ALPHA-LD  BETA--LD  GAMMA--LD  ALPHA-IN  BETA-IN  GAMMA-IN  P---F
5 Residen  1  125.1  0.00  inf -inf 1 inf 0.00 38.6650 -.1047 0.0 100.0 0.0 0.9285
6 Indust1  2  90.1  0.00  inf -inf 1 inf 0.00 16.8440 -.0231 0.0 100.0 0.0 0.9487
8 Indust2  2  100.1  0.00  inf -inf 1 inf 0.00 21.6300 -.0431 0.0 100.0 0.0 0.9439

=====
1234567890123456789012345678901234567890123456789012345678901234567890
=====

```

Figure C.8: WSCC 9-bus system generator data format

Figure C.9: WSCC 9-bus system load data format

```

=====
01234567890123456789012345678901234567890123456789012345678901234567890123456789
=====
10/26/02 OSU ARCHIVE          1000000.0  GEOPF 15 Node Case
FIELD CONDITION
  520 14.65    0.9 0.955 1015
NODE DATA FOLLOWS              15 ITEMS
  1 Node 1    HP 0      1000.000  7.288  0.000  600 1200
  2 Node 2    HP 0      978.630  6.867  0.000  600 1200
  3 Node 3    HP 1      729.716  0.000  3.838  500 1200
  4 Node 4    HP 2      737.345  0.000  1.218  500 1200
  5 Node 5    HP 3      575.481  0.000  0.000  400 1200
  6 Node 6    HP 4     1035.000  0.000  0.000  400 1200
  7 Node 7    HP 3      607.588  0.000  0.000  400 1200
  8 Node 8    HP 4     1154.400  0.000  0.000  400 1200
  9 Node 9    HP 3      918.628  0.000  0.000  400 1200
 10 Node 10   HP 4      951.000  0.000  0.000  400 1200
 11 Node 11   HP 3      932.810  0.000  0.000  400 1200
 12 Node 12   HP 4      932.810  0.000  0.000  400 1200
 13 Node 13   HP 1      601.554  0.000  4.263  600 1000
 14 Node 14   HP 1      600.778  0.000  4.274  600 1000
 15 Node 15   HP 2      600.000  0.000  0.501  600 1000
-999
BRANCH DATA FOLLOWS              12 ITEMS
  1  3  80.5  19.56  0.90  520  2  7.2883
  2  4  80.3  19.56  0.90  520  2  6.8673
  3  4  55.9  19.56  0.90  520  2 -1.3533
  3  5  81.1  19.62  0.90  520  2  4.8039
  4  7  87.9  19.62  0.90  520  2  4.2963
  6  9  93.5  19.62  0.90  520  2  4.7733
  8 11  99.7  16.69  0.90  520  2  4.2667
 10 13  93.5  16.69  0.90  520  2  4.7716
 12 14  97.9  16.69  0.85  520  2  4.2667
 13 14  86.6  16.69  0.90  520  2  0.2056
 13 15  79.7  16.69  0.90  520  2  0.3032
 14 15  83.5  16.69  0.85  520  2  0.1979
-999
COMPRESSOR STATION DATA FOLLOWS  4 ITEMS
  1  5  6  4.4060  0.83  1.8  520  0.0000  8.3300  0.00000  3667.292  0.0305
  2  7  8  4.2088  0.84  1.9  520  0.0000  8.3300  0.00000  3558.156  0.0296
  3  9 10  4.4060  0.83  1.8  520  0.0000  8.3300  0.00000  203.203  0.0017
  4 11 12  4.2088  0.84  1.9  520  0.0000  8.3300  0.00000   0.000  0.0000
-999
BENEFIT DATA FOLLOWS              5 ITEMS
  3 Load 1  1  0  80  0.0  1  0.0  5980.0 -499.344
  4 Load 2  4  2  90  0.0  0  0.0  5844.8 -460.944
 13 Load 3  2  0  90  0.0  1  0.0  5980.0 -443.520
 14 Load 4  3  0  90  0.0  1  0.0  5571.8 -394.560
 15 Load 5  4  3  30  0.0  0  0.0  5748.6 -496.800
-999
SOURCE DATA FOLLOWS              2 ITEMS
  1 Source 1 200  0.0 1  2550.0 1000.0  600.0
  2 Source 2 200  0.0 1  2550.0 1000.0  600.0
-999
END OF DATA

```

Figure C.10: 15-node natural gas data format

APPENDIX D

MATLAB CODE

D.1 GEOPF

```
% ===== Gas and Electricity Optimal Power Flow =====
% This program returns the solution of the natural gas and electricity optimal
% power flow (GEOPF).
% =====
format compact;
clear all;
nu = 10;
psi = 0.1;
% -----
% Read gas data file
Filename = input('Gas Network Case Name: ','s');
f.cgffile = [ Filename '.cgf' ];

a = ReadGasDF(f);
x = GasDataCon(a);
% -----
% Field Condition
base = x.base; % base unit
To = x.To; % standard temperature, oR
po = x.po; % standard pressure, psia
Za = x.Za; % average gas compressibility factor
Zi = x.Zi; % compressor inlet compressibility factor
G = x.G; % gas specific gravity
GHV = x.GHV; % gross heating value (BTU/ft^3)
CpCv = x.CpCv; % specific heat ratio
m1 = x.m1; % flow equation coefficient
% End of field condition
% -----
% Node Data
NN = x.NN; % # of nodes
loadNode = x.loadNode; % load nodes
combGasNode = x.combGasNode; % gas-electric combined nodes
NGE = x.NGE; % # of gas-elec. combined nodes
GE_load_no = x.GEloadNo; % gas-electric combined load #
NL = x.NL; % # of load nodes
sourceNode = x.sourceNode; % source nodes
refNode = x.sourceNode(1); % ref node
NS = x.NS; % # of source node
Pini = x.Pini; % initial node pressure
Wsrcini = x.Wsrcini; % initial gas supply
Wloadini = x.Wloadini; % initial gas consumption
Pref = x.Pref; % source node pressure
Pmin = x.Pmin; % min. nodal pressure
Pmax = x.Pmax; % max. nodal pressure
N = x.N; % nodal-gas injection incidence matrix
```

```

% End of node data
% -----
% Branch Data
NP = x.NP; % # of pipelines
ppSend = x.ppSend; % pipeline sending end;
ppEnd = x.ppEnd; % pipeline ending end;
lng = x.lng; % pipeline length, in
dia = x.dia; % pipeline diameter,
fpini = x.fp; % pipeline branch flow, 10 x SCF/hr
E = x.E; % pipeline efficiency
Ta = x.Ta; % ave. gas temperature, oR
A = x.A; % nodal-branch incidence matrix
% End of branch data
% -----
% Compressor data
NC = x.NC; % # of compressors
sucNode = x.sucNode; % compressor suction nodes
disNode = x.disNode; % discharge nodes
fcini = x.fc; % initial compressor branch flowrate
eta = x.eta; % compressor efficiency
Smax = x.Smax; % max. compression ratio
Ti = x.Ti; % comp. suction temperature, oR
alphaT = x.alphaT; % alpha
betaT = x.betaT.*10^(-6); % beta
gammaT = x.gammaT; % gamma
HPini = x.HP; % compressor horsepower, HP
tini = x.t; % gas consumption rate, 10 x SCF/hr
U = x.U; % nodal-compressor branch incidence matrix
T = x.T; % nodal-gas turbine tap incidence matrix
% End of Compressor Data Extraction
% -----
% Source node gas price
c1 = x.c1; % $/(10^6 x SCF) at source node
% -----
% Coefficients of industrial consumers benefit functions
betaGLInd = x.betaGLInd; % beta for gas consumers at non-combined nodes
gammaGLInd = x.gammaGLInd; % gamma for gas onsumers at non-combined nodes

Non_com_node = x.non_com_node; % non-combined nodes
combElecBus = x.combElecBus; % combined electric bus
% End of gas data input processing
% -----
% Read electric data file
clear a; % remove structure 'a'
clear x; % remove structure 'x'

Filename = input('Case name: ','s');
x.cdffile = [ Filename '.cdf' ];
x.gdffile = [ Filename '.gdf' ];
x.ldffile = [ Filename '.ldf' ];

a = ReadDF(x);
x = ac_dataread(a);
% -----
% Bus Data
NBus = x.nb; % # of buses
Sbase = x.Sbase; % Sbase

V_MX = x.V_MX; % Vmax
V_MN = x.V_MN; % Vmin
PGini = x.Pg./Sbase; % initial real power generation
QGini = x.Qg./Sbase; % initial reac. power generation
PLini = x.PL./Sbase; % initial real power load
Vini = x.Vmag; % initial bus voltage magnitude
Thetaini = x.Vangle; % initial bus voltage phase angle
% -----
% Branch Data
NLine = x.nl; % # of transmission lines

```

```

I_MX = x.S_MX./Sbase; % max line current
FR = [x.fr ;x.to];
TO = [x.to ;x.fr];
Ybus = x.Y; % Ybus matrix
Y.bran = [x.Y_bran ; x.Y_bran];
Y.shunt = [x.Y_shunt ; x.Y_shunt];
% -----
% Generator Data
PG_MX = x.Pgmax; % Pmax
PG_MN = x.Pgmin; % Pmin
QG_MX = x.Qgmax; % Qmax
QG_MN = x.Qgmin; % Qmin

PgBus = x.Pg_bus; % bus # with real power gen.
QgBus = x.Qg_bus; % bus # with reactive power gen.
NPG = length(PgBus); % total # of real power gen.
NQG = length(QgBus); % total # of reactive power gen.

m=1;
for k=1:NPG
    flag = find(combElecBus == k);
    if flag == [];
        coalGen(m) = k; % non-gas generator
        m=m+1;
    end;
end;
% fuel rate coefficients
alphaGE = x.alpha_c(combElecBus)./2.5; % alpha-GE $2.5/MMBTU
betaGE = x.beta_c(combElecBus)./2.5; % beta-GE $2.5/MMBTU
gammaGE = x.gamma_c(combElecBus)./2.5; % gamma-GE $2.5/MMBTU

% generation cost coefficients
alphaC = x.alpha_c(coalGen); % alpha_cost
betaC = x.beta_c(coalGen); % beta_cost
gammaC = x.gamma_c(coalGen); % gamma-cost
% -----
% Load Data
PEL_MX = x.Plmax; % PELmax
PEL_MN = x.Plmin; % PELmin
PF = x.PF; % power factor

alphaB = x.alpha_b; % alpha
betaB = x.beta_b; % beta
gammaB = x.gamma_b; % gamma

LoadBus = x.Load_bus; % bus # with consumers
NEL = length(LoadBus); % total # of real power consumers
% End of electric data input
% -----
% Weymouth Coefficient (Weymouth Equation:  $P_i^2 - P_j^2 = K * f_k^2$ )
Mk = (E.*433.488./24*10^(-6)*To.*dia.^(8/3))./(po.*sqrt(G*Ta.*lng.*Za));
K = (1./Mk).^m1;
% -----
% Compressor horsepower equation :  $H_k = B_k f_k [ (p_i/p_j)^R - 1 ]$ 
R = Zi.*(CpCv-1)/CpCv;
Bk = 0.08531*24 * Ti./eta.*(CpCv/(CpCv-1));
% -----
% Set up indices for gas newtork decision variables
X.Pi_start = 1;
X.Pi_end = NN;
X.f_start = NN+1;
X.f_end = NN+NP+NC;
X.W_start = NN+NP+NC+1;
X.W_end = NN +NP+NC+NS+NL;
X.t_start = NN +NP+NC+NS+NL+1;
X.t_end = NN +NP+NC+NS+NL+NC;
X.HP_start = X.t_end+1;
X.HP_end = X.t_end+NC;

```

```

X.Pi_source = sourceNode;           % source node pressure index
X.Pi_ref = refNode;                 % ref. node
X.Pi_comp_suc = sucNode;            % comp. suction node pressure index
X.Pi_comp_disc = disNode;          % comp. discharge nodes
X.Pi_load = loadNode;               % load node pressure index
X.Pisnd = ppSend;                   % Pipeline sending nodes
X.Pircv = ppEnd;                    % Pipeline receiving nodes

X.fp = X.f_start:X.f_start+NP-1;    % pipeline branch flowrate
X.fc = X.f_start+NP:X.f_end;        % compressor branch flowrate

X.Wsource = X.W_start:X.W_start+NS-1;
X.Wload = X.W_start+NS:X.W_end;
X.WloadGE = X.Wload(GE_load_no);    % gas and electric combined nodes
X.WloadInd = X.Wload(Non_com_node); % consumers at non-combined nodes

X.Pi = X.Pi_start : X.Pi_end;       % Psia
X.f = X.f_start : X.f_end;          % 10-6 x SCF/hr
X.W = X.W_start : X.W_end;          % 10-6 x SCF/hr
X.t = X.t_start : X.t_end;          % 10-6 x SCF/hr
X.HP = X.HP_start:X.HP_end;         % HP

X.Gaslen = NN+NP+NC+NS+NL+2*NC;     % # of gas network decision variables
% -----
% Set up indices for electric network decision variables
X.Pg_Start = X.Gaslen+1;
X.Pg_End = X.Gaslen+NPG;
X.Qg_Start = X.Pg_End + 1;
X.Qg_End = X.Pg_End + NQG;
X.PL_Start = X.Qg_End + 1;
X.PL_End = X.Qg_End + NEL;
X.V_Start = X.PL_End + 1;
X.V_End = X.PL_End + NBus;
X.Theta_Start = X.V_End + 1;
X.Theta_End = X.V_End + NBus;

X.Pg = X.Pg_Start : X.Pg_End;
X.PgCoal = X.Pg(coalGen);
X.PgGE = X.Pg(combElecBus);
X.Qg = X.Qg_Start : X.Qg_End;
X.PL = X.PL_Start : X.PL_End;
X.V = X.V_Start : X.V_End;
X.Theta = X.Theta_Start : X.Theta_End;

X.ElecLen = NPG + NQG + NEL + 2*NBus;

X.Len = X.Gaslen + X.ElecLen;        % Total # of decision variables
% -----
% Set up indices of 'lambda' for gas network
lmd.Weymouth = 1 : NP;              % Weymouth flow equation
lmd.NodalFlow = NP+1:NP+NN;         % nodal flow balance equation
lmd.TbnHP = NP+NN+1:NP+NN+NC;       % compressor HP required
lmd.TbnFR = NP+NN+NC+1:NP+NN+2*NC;  % turbine Fuel Rate
lmd.P1=NP+NN+2*NC+1;               % reference pressure

lmd.Gaslen = NP+NN+2*NC+1;          % # of gas equality constraints
% -----
% Set up indices for 'lambda' for electric network
lmd.P = lmd.Gaslen+1 : lmd.Gaslen+NBus;
lmd.Q = lmd.Gaslen+NBus+1 : lmd.Gaslen+2*NBus;
lmd.theta = lmd.Gaslen+2*NBus+1;

lmd.Pin = lmd.Gaslen+PgBus;
lmd.Qin = lmd.Gaslen+QgBus + NBus;
lmd.PL_P = lmd.Gaslen+LoadBus;
lmd.PL_Q = lmd.Gaslen+LoadBus + NBus;

lmd.ElecLen = 2*NBus +1;            % # of elec. equa. const.
% -----

```

```

% Set up indices for combined node and bus equality constraints
lmd.GE = lmd.Gaslen+lmd.Eleclen+1:lmd.Gaslen+lmd.Eleclen+NGE;
lmd.GElen = NGE; % NGE = # of gas-electric combined nodes

lmd.len = lmd.Gaslen + lmd.Eleclen + lmd.GElen;
% -----
% Set up indices for 'muG' for gas network
mu.g1 = 1:NC; % Pcompdisc >= Pcompsuc
mu.g2 = NC+1:2*NC; % Pcompdisc <= Pcompsuc x Smax
mu.g3 = 2*NC+1:2*NC+NN; % Pcompsuc >= Pcompmin
mu.g4 = 2*NC+NN+1:2*NC+2*NN; % Pcompdisc <= Pcompmax

mu.Gaslen = 2*NC+2*NN; % # of gas inequality constraints
% -----
% Set up indices for 'muE' for electric network
mu.V_MX_Start = mu.Gaslen+1; % Max. Voltage mag.
mu.V_MX_End = mu.Gaslen+NBus;
mu.V_MN_Start = mu.V_MX_End + 1; % Min. Voltage mag.
mu.V_MN_End = mu.V_MX_End + NBus;
mu.I_MX_Start = mu.V_MN_End+1; % Max. line current mag.
mu.I_MX_End = mu.V_MN_End + 2*NLine;
mu.PgMX_Start = mu.I_MX_End + 1; % Max. Pg
mu.PgMX_End = mu.I_MX_End + NPG;
mu.PgMN_Start = mu.PgMX_End+1; % Min. Pg
mu.PgMN_End = mu.PgMX_End + NPG;
mu.QgMX_Start = mu.PgMN_End + 1; % Max. Pg
mu.QgMX_End = mu.PgMN_End + NQG;
mu.QgMN_Start = mu.QgMX_End+1; % Min. Pg
mu.QgMN_End = mu.QgMX_End + NQG;
mu.PLMN_Start = mu.QgMN_End + 1; % Min. Pload
mu.PLMN_End = mu.QgMN_End + NEL;

mu.V_MX = mu.V_MX_Start : mu.V_MX_End ;
mu.V_MN = mu.V_MN_Start : mu.V_MN_End ;
mu.I_MX = mu.I_MX_Start : mu.I_MX_End ;
mu.PgMX = mu.PgMX_Start : mu.PgMX_End ;
mu.PgMN = mu.PgMN_Start : mu.PgMN_End ;
mu.QgMX = mu.QgMX_Start : mu.QgMX_End ;
mu.QgMN = mu.QgMN_Start : mu.QgMN_End ;
mu.PLMN = mu.PLMN_Start : mu.PLMN_End ;

mu.Eleclen = 2*NBus + 2*NLine + 2*NPG + 2*NQG + NEL;
% -----
% combined node inequality constraints
mu.GE = mu.Gaslen+mu.Eleclen+1 : mu.Gaslen+mu.Eleclen+NGE;
mu.GElen = NGE;

mu.len= mu.Gaslen + mu.Eleclen + mu.GElen;
% -----
% Initial starting values of decision variables for gas network
IVX = sparse(X.len,1);
IVX(X.Pi) = Pini*0.98;
IVX(X.Wsource) = Wsrcini*0.98;
IVX(X.Wload) = Wloadini*0.98;
IVX(X.fp) = fpini*1.08;
IVX(X.fc) = fcini*1.08;
IVX(X.HP) = HPini*1.08;
IVX(X.t) = tini*1.05;
% -----
% Initial starting values of decision variables for electric network
IVX(X.Pg,1) = PGini*0.9;
IVX(X.Qg,1) = QGini*0.9;
IVX(X.PL,1) = PLini*1.1;
IVX(X.V,1) = Vini*1;
IVX(X.Theta) = Thetaini*1.1;
% -----
% Initial starting values of 'lambda' for gas network
lambda = sparse(lmd.len, 1);
lambda(lmd.Weymouth,1) = -1*ones(NP,1);

```

```

lambda(lmd.NodalFlow,1) = 2.5*ones(NN,1);
lambda(lmd.TbnHP,1) = -1*ones(NC,1);
lambda(lmd.TbnFR) = -1*ones(NC,1);
lambda(lmd.P1,1) = 10;
% -----
% Initial starting values of 'lambda' for electric network
lambda(lmd.P) = 10*ones(NBus,1);
lambda(lmd.Q) = 10*ones(NBus,1);
lambda(lmd.theta) = 0;
lambda(lmd.GE) = 10*ones(NGE,1);
% -----
% Initial starting values of 'mu' and 's'
s = ones(mu.len,1);
S = diag(s);
MU = ones(mu.len,1);
M = diag(MU);

Z = [IVX ; lambda ; MU ; s ];      % set of initial values
% -----
Ind.Z_lmd_Start = X.len + 1;
Ind.Z_lmd_End = X.len + lmd.len;
Ind.Z_mu_Start = Ind.Z_lmd_End + 1;
Ind.Z_mu_End = Ind.Z_lmd_End + mu.len;
Ind.Z_S_Start = Ind.Z_mu_End + 1;
Ind.Z_S_End = Ind.Z_mu_End + mu.len;

Ind.Z_lmd = Ind.Z_lmd_Start : Ind.Z_lmd_End;
Ind.Z_mu = Ind.Z_mu_Start : Ind.Z_mu_End;
Ind.Z_S = Ind.Z_S_Start : Ind.Z_S_End;
% -----
% Form matrix dh
df = sparse(X.len,1);

df(X.Wsource,1) = c1;
% Form matrix ddh
ddf = sparse(X.len, X.len);

ddf(X.PgCoal,X.PgCoal) = 2 * diag(gammaC)*Sbase^2;

ddf(X.WloadInd,X.WloadInd) = -diag(2*gammaGLInd);
ddf(X.PL,X.PL) = -2 * diag(gammaB)*Sbase^2;
% -----
% Form matrix dh for gas network
dh = sparse(lmd.len,X.len);

dh(lmd.P1,X.Pi_ref) = 1;          % P1 = Pset

dh(lmd.NodalFlow,X.f) = (A+U) ;
dh(lmd.NodalFlow,X.W) = N;
dh(lmd.NodalFlow,X.t) = -T;

dh(lmd.TbnHP,X.HP) = speye(NC,NC);
dh(lmd.TbnFR,X.t) = speye(NC,NC);
% -----
% Form matrix dh for electric network
dh(lmd.Pin,X.Pg) = speye(NPG,NPG);
dh(lmd.Qin,X.Qg) = speye(NQG,NQG);
dh(lmd.PL_P,X.PL) = -speye(NEL,NEL);
dh(lmd.PL_Q,X.PL) = -diag(1./PF.*sqrt(1-PF.^2));
dh(lmd.theta,X.Theta(1)) = 1;
% -----
% Form matrix dh for gas and electric combined node
dh(lmd.GE,X.WloadGE) = speye(NGE,NGE);
% -----
% Form matrix dg for gas network
dg = sparse(mu.len,X.len);

dg(mu.g1, X.Pi_comp_suc) = speye(NC,NC);
dg(mu.g1, X.Pi_comp_disc) = -speye(NC,NC);

```



```

dg(mu.g2, X.Pi_comp_suc) = -diag(Smax);
dg(mu.g2, X.Pi_comp_disc) = speye(NC,NC);
dg(mu.g3, X.Pi) = -speye(NN,NN);
dg(mu.g4, X.Pi) = speye(NN,NN);
dg(mu.GE, X.WloadGE) = -speye(NGE,NGE);
% -----
% Form matrix dg for real power generation limit
dg(mu.PgMX,X.Pg) = speye(NPG, NPG);
dg(mu.PgMN,X.Pg) = -speye(NPG, NPG);

% Form matrix dg for reactive power generation limit
dg(mu.QgMX,X.Qg) = speye(NQG, NQG);
dg(mu.QgMN,X.Qg) = -speye(NQG, NQG);

% Form matrix dg for Voltage magnitude limit
dg(mu.V_MX,X.V) = speye(NBus,NBus);
dg(mu.V_MN,X.V) = -speye(NBus,NBus);

% Form matrix dg for real power load limit
dg(mu.PLMN,X.PL) = -speye(NEL,NEL);

% Form matrix dg for real power load limit
dg(mu.PLMN,X.PL) = -speye(NEL,NEL);
% -----
N1 = X.len; N2 = lmd.len; N3 = mu.len; N4 = mu.len;
% -----
it = 0; % iteration number
while nu > 1e-13 & it < 200
    it = it+1;
    % -----
    % set up "df" for B and C
    df(X.WloadInd,1)=-(betaGLInd+2*gammaGLInd.*Z(X.WloadInd));
    df(X.PL,1) = -(betaB*Sbase + 2*gammaB.*Z(X.PL)*Sbase^2);
    df(X.PgCoal,1)=(betaC*Sbase+2*gammaC.*Z(X.PgCoal)*Sbase^2);
    % end of construction of the matrix "df" for B and C
    % -----
    % set up "h" for gas network
    h = sparse(lmd.len,1);
    sig = sign(Z(X.fp));
    h(lmd.Weymouth,1) = Z(X.Pisnd).^2 - Z(X.Pircv).^2-sig.*(K.*abs(Z(X.fp)).^m1);
    h(lmd.NodalFlow,1) = (A+U)*Z(X.f) + N*Z(X.W)-T*Z(X.t);
    h(lmd.TbnHP,1) = Z(X.HP)-Z(X.fc).*Bk.*(Z(X.Pi_comp_disc).^R.*Z(X.Pi_comp_suc).^(-R)-1);
    h(lmd.TbnFR,1) = Z(X.t)-(alphaT+betaT.*Z(X.HP)+gammaT.*Z(X.HP).^2);
    h(lmd.P1,1) = Z(X.Pi_ref)-Pref;
    % -----
    % set up "h" for electric network
    theta = Z(X.Theta);
    V = Z(X.V);
    Vph = V.*exp(j*theta);
    I = Ybus*Vph;
    Si = Vph.*conj(I);
    PG = zeros(NBus,1);
    PL = zeros(NBus,1);
    QG = zeros(NBus,1);
    QL = zeros(NBus,1);
    PG(PgBus) = Z(X.Pg);
    QG(QgBus) = Z(X.Qg);
    PL(LoadBus) = Z(X.PL);
    QL(LoadBus) = (PL(LoadBus)./PF).*sqrt(1-PF.^2);
    % set up "h"
    h(lmd.P,1) = PG-PL-real(Si);
    h(lmd.Q,1) = QG-QL-imag(Si);
    h(lmd.theta) = Z(X.Theta(1));
    % -----
    % set up "h" for gas-electric combined node
    h(lmd.GE)=Z(X.WloadGE)-(alphaGE+betaGE.*Z(X.Pg(combElecBus))*Sbase+...
        gammaGE.*Z(X.Pg(combElecBus)).^2*Sbase^2)./GHV(1);
    % end of construction of the matrix "h"
    % -----

```

```

% set up "dh" for gas network
dh(lmd.Weymouth,X.fp) = diag(-m1.*K.*abs(Z(X.fp)).^(m1-1));
dh(lmd.TbnFR,X.HP) = -diag(betaT+2*gammaT.*Z(X.HP));
for m = 1:NP
    dh(lmd.Weymouth(m), X.Pisnd(m)) = 2*Z(X.Pisnd(m));
    dh(lmd.Weymouth(m), X.Pircv(m)) = -2*Z(X.Pircv(m));
end;
dh(lmd.TbnHP, X.Pi_comp_suc) = diag(Z(X.fc).*...
    Bk.*R.*Z(X.Pi_comp_disc).^R.*Z(X.Pi_comp_suc).^(-R-1));
dh(lmd.TbnHP, X.Pi_comp_disc) = -diag(Z(X.fc).*Bk.*...
    R.*Z(X.Pi_comp_disc).^(R-1).*Z(X.Pi_comp_suc).^(-R));
dh(lmd.TbnHP,X.fc) = -diag(Bk.*(Z(X.Pi_comp_disc).^R.*Z(X.Pi_comp_suc).^(-R)-1));
% -----
% set up "dh" for electric network
Jsv = diag(Vph)*conj(Ybus)*conj(diag(exp(j*theta))+diag(exp(j*theta).*conj(I)));
Jst = -j*diag(Vph)*conj(Ybus)*conj(diag(Vph))+diag(j*Si);

dh(lmd.P, X.V) = -real(Jsv);
dh(lmd.Q, X.V) = -imag(Jsv);
dh(lmd.P, X.Theta) = -real(Jst);
dh(lmd.Q, X.Theta) = -imag(Jst);
% end of construction of the matrix "dh"
% -----
% set up "dh" for gas-electric combined node
dh(lmd.GE,X.PgGE) = -diag((betaGE*Sbase+2*gammaGE.*Z(X.Pg(combElecBus))*Sbase^2)/GHV(1));
% -----
% set up "ddh"
DDH = sparse(X.len,X.len);
% set up "ddh" for Weymouth flow equation
for m = 1 : NP
    ddh = sparse(X.len,X.len);
    ddh(X.Pisnd(m),X.Pisnd(m)) = 2*Z(Ind.Z_lmd(m));
    ddh(X.Pircv(m),X.Pircv(m)) = -2*Z(Ind.Z_lmd(m));
    ddh(X.fp(m),X.fp(m)) = -sig(m)*m1(m)*(m1(m)-1)*K(m)*abs(Z(X.fp(m))).^(m1(m)-2)*Z(Ind.Z_lmd(m));
    DDH = DDH + ddh;
end;
% ddh for Turbine Gas Supply
ddh = sparse(X.len,X.len);
ddh(X.HP,X.HP) = -diag(2*gammaT.*Z(Ind.Z_lmd(lmd.TbnFR)));
DDH = DDH + ddh;
% ddh for compressor station horsepower equality constraint
for m = 1:NC
    ddh = sparse(X.len,X.len);
    ddh(X.Pi_comp_suc(m),X.Pi_comp_suc(m)) = -Z(X.fc(m)).*...
        Bk(m)*R*(R+1)*Z(X.Pi_comp_disc(m)).^R.*Z(X.Pi_comp_suc(m)).^(-R-2);
    ddh(X.Pi_comp_disc(m),X.Pi_comp_disc(m)) = -Z(X.fc(m)).*...
        Bk(m).*R*(R-1)*Z(X.Pi_comp_disc(m)).^(R-2)*Z(X.Pi_comp_suc(m)).^(-R);
    ddh(X.Pi_comp_suc(m),X.Pi_comp_disc(m)) = Z(X.fc(m))*Bk(m).*...
        R^2*Z(X.Pi_comp_disc(m)).^(R-1)*Z(X.Pi_comp_suc(m)).^(-R-1);
    ddh(X.Pi_comp_disc(m),X.Pi_comp_suc(m)) = ddh(X.Pi_comp_suc(m),X.Pi_comp_disc(m));
    ddh(X.fc(m),X.Pi_comp_suc(m)) = Bk(m)*R.*Z(X.Pi_comp_disc(m)).^R.*Z(X.Pi_comp_suc(m)).^(-R-1);
    ddh(X.Pi_comp_suc(m),X.fc(m)) = ddh(X.fc(m),X.Pi_comp_suc(m));
    ddh(X.fc(m),X.Pi_comp_disc(m)) = -Bk(m).*R.*Z(X.Pi_comp_disc(m)).^(R-1)*Z(X.Pi_comp_suc(m)).^(-R);
    ddh(X.Pi_comp_disc(m),X.fc(m)) = ddh(X.fc(m),X.Pi_comp_disc(m));
    DDH = DDH + ddh.*Z(Ind.Z_lmd(lmd.TbnHP(m)));
end;
% -----
% set up "ddh" for gas-electric combined node
ddh = sparse(X.len,X.len);
ddh(X.PgGE,X.PgGE) = -diag((2*gammaGE.*Z(Ind.Z_lmd(lmd.GE))*Sbase^2)./GHV);
DDH = DDH + ddh;
% end of construction of the matrix "ddh"
% -----
% set up "ddh"
ddh = sparse(2*NBus,2*NBus);
for m = 1 : NBus
    ddh_V = zeros(NBus,NBus);
    ddh_V(m,:) = exp(j*theta(m))*conj(Ybus(m,:)).*exp(-j*theta');
    ddh_V(:,m) = ddh_V(m,:).';
end;

```

```

ddh_V(m,m)=2*conj(Ybus(m,m));

ddh_theta = zeros(NBus,NBus);
ddh_theta(m,:) = Vph(m)*conj(Ybus(m,:)).*Vph';
ddh_theta(:,m) = ddh_theta(m,:).';
ddh_theta = ddh_theta - diag(ddh_theta(m,:));
ddh_theta(m,m) = -Si(m) + V(m)^2*conj(Ybus(m,m));

ddh_V_theta = zeros(NBus,NBus);
ddh_V_theta(m,:)=-j*exp(j*theta(m))*conj(Ybus(m,:)).*Vph';
ddh_V_theta(:,m)=j*Vph(m)*conj(Ybus(m,:)).'*exp(-j*theta(:));
ddh_V_theta=ddh_V_theta - diag(ddh_V_theta(:,m));
ddh_V_theta(m,m)=j*exp(j*theta(m))*conj(Ybus(m,:))*conj(Vph)-j*V(m)*conj(Ybus(m,m));

ddh_theta_V = ddh_V_theta.';

ddh_S = -[ ddh_V      ddh_V_theta
           ddh_theta_V ddh_theta ];
ddh_P = Z(Ind.Z_lmd(lmd.P(m)))*real(ddh_S);
ddh_Q = Z(Ind.Z_lmd(lmd.Q(m)))*imag(ddh_S);
ddh = ddh + ddh_P + ddh_Q;
end;
DDH(X.V_Start:X.Theta_End,X.V_Start:X.Theta_End)=DDH(X.V_Start:X.Theta_End,X.V_Start:X.Theta_End)+ddh;
% end of construction of matrix ddh
% -----
% set up "g" for gas network
g = sparse(N3,1);
g(mu.g1) = Z(X.Pi_comp_suc)-Z(X.Pi_comp_disc);
g(mu.g2) = Z(X.Pi_comp_disc)-Smax.*Z(X.Pi_comp_suc);
g(mu.g3) = Pmin - Z(X.Pi);
g(mu.g4) = Z(X.Pi)-Pmax;
% -----
% set up "g" for electric network
Iik = (Vph(FR)-Vph(T0)).*Y.bran+Y.shunt.*Vph(FR);

g(mu.V_MX) = Z(X.V) -V_MX;
g(mu.V_MN) =-Z(X.V) + V_MN;
g(mu.I_MX ) = Iik.*conj(Iik) - [ I_MX.^2 ; I_MX.^2 ];
g(mu.PgMX) = Z(X.Pg) - PG_MX/Sbase;
g(mu.PgMN) = -Z(X.Pg) + PG_MN/Sbase ;
g(mu.QgMX) = Z(X.Qg) - QG_MX/Sbase;
g(mu.QgMN) = -Z(X.Qg) + QG_MN/Sbase;
g(mu.PLMN) = -Z(X.PL) + PEL_MN/Sbase;
% -----
% set up "g" for gas-electric combined node
g(mu.GE) = -Z(X.WloadGE);
% -----
% set up "dg" for electric network
% derivatives of Iik w.r.t Voltage magnitude
dI_dVi = exp(j*theta(FR)).*(Y.bran+Y.shunt);
dI_dVk= -exp(j*theta(T0)).*Y.bran;

dIdVi = sparse((1:2*NLine),FR,conj(Iik).*dI_dVi+Iik.*conj(dI_dVi),2*NLine,NBus);
dIdVk = sparse((1:2*NLine),T0,conj(Iik).*dI_dVk+Iik.*conj(dI_dVk),2*NLine,NBus);
dIdV = dIdVi + dIdVk;
dg(mu.I_MX,X.V) = dIdV;

% derivatives of Iik w.r.t Voltage angle
dI_dthetai = j*Vph(FR).*(Y.bran+Y.shunt);
dI_dthetak = -j*Vph(T0).*Y.bran;

dIdthetai = sparse((1:2*NLine),FR,conj(Iik).*dI_dthetai+Iik.*conj(dI_dthetai),2*NLine,NBus);
dIdthetak = sparse((1:2*NLine),T0,conj(Iik).*dI_dthetak+Iik.*conj(dI_dthetak),2*NLine,NBus);
dIdtheta = dIdthetai + dIdthetak;
dg(mu.I_MX, X.Theta) = dIdtheta;
% end of construction of matrix "dg"
% -----
% set up "ddg" for electric network
ddg = zeros(2*NBus,2*NBus);

```

```

for m = 1 : 2*NLine
    ddg_V = sparse(NBus,NBus);
    ddg_V(FR(m),FR(m)) = 2*conj(dI_dVi(m))*dI_dVi(m);
    ddg_V(FR(m),TO(m)) = conj(dI_dVk(m))*dI_dVi(m)+dI_dVk(m)*conj(dI_dVi(m));
    ddg_V(TO(m),FR(m)) = ddg_V(FR(m),TO(m));
    ddg_V(TO(m),TO(m)) = 2*conj(dI_dVk(m))*dI_dVk(m);

    ddg_theta = sparse(NBus,NBus);
    ddI_ddthetaii = -(Y.bran(m)+Y.shunt(m))*Vph(FR(m));
    ddg_theta(FR(m),FR(m)) = Iik(m)'* ddI_ddthetaii+2*...
        conj(dI_dthetai(m))*dI_dthetai(m)+Iik(m)*conj(ddI_ddthetaii);
    ddg_theta(FR(m),TO(m)) = dI_dthetai(m)'*dI_dthetak(m)+dI_dthetai(m)*dI_dthetak(m)';
    ddg_theta(TO(m),FR(m)) = ddg_theta(FR(m),TO(m));
    ddI_ddthetakk = Y.bran(m)*Vph(TO(m));
    ddg_theta(TO(m),TO(m)) = Iik(m)'*ddI_ddthetakk+2*dI_dthetak(m)'*dI_dthetak(m)+Iik(m)*ddI_ddthetakk';

    ddg_V_theta = sparse(NBus,NBus);
    ddI_dVi_dthetai = j*exp(j*theta(FR(m)))*(Y.bran(m)+Y.shunt(m));
    ddg_V_theta(FR(m),FR(m)) = Iik(m)'*ddI_dVi_dthetai+dI_dVi(m)'*...
        dI_dthetai(m)+ dI_dVi(m)*dI_dthetai(m)'+Iik(m)*ddI_dVi_dthetai';
    ddI_dVk_dthetak = -j*exp(j*theta(TO(m)))*Y.bran(m);
    ddg_V_theta(TO(m),TO(m)) = Iik(m)'*ddI_dVk_dthetak+dI_dVk(m)'*...
        dI_dthetak(m)+dI_dVk(m)*dI_dthetak(m)'+Iik(m)*ddI_dVk_dthetak';
    ddg_theta_V = ddg_V_theta.';

    ddg_Iik = [ ddg_V      ddg_V_theta
                ddg_theta_V ddg_theta ];
    ddg = ddg + Z(Ind.Z_mu(mu.I_MX(m)))*ddg_Iik;
end;
DDG = sparse(X.len,X.len);
DDG(X.V_Start:X.Theta_End,X.V_Start:X.Theta_End) = ddg;
% end of construction of matrix "ddg"
% -----
DDFHHG=ddf + DDH + DDG;
J=real([ DDFHHG      dh.'      dg.'      sparse(N1,N3) ;
          dh      sparse(N2,N2)  sparse(N2,N3)  sparse(N2,N3) ;
          dg      sparse(N3,N2)  sparse(N3,N3)  speye(N3,N3) ;
          sparse(N3,N1) sparse(N3,N2)      S      M      ]);

dY = real([-df-dh.'*Z(N1+1:N1+N2)-dg.'*Z(N1+N2+1:N1+N2+N3)
          -h
          -g-Z(N1+N2+N3+1:N1+N2+2*N3)
          nu*ones(N3,1)-M*S*ones(N3,1)]);
dZ = J\dY;
dMU = dZ(Ind.Z_mu);
ds =dZ(Ind.Z_S);
S_Neg_Index = find(ds < 0);
alpha_S = min([1;-s(S_Neg_Index)./ds(S_Neg_Index)]);
MU_Neg_Index = find(dMU < 0);
alpha_MU = min([1;-MU(MU_Neg_Index)./dMU(MU_Neg_Index)]);
alpha = min(alpha_S ,alpha_MU);
Z = Z + 0.9*alpha*dZ;
MU = Z(Ind.Z_mu);
s = Z(Ind.Z_S);
M = diag(MU);
S = diag(s);
if norm(M*s - MU.'*s/N3) <= psi*nu;    % central path
    nu = nu*0.4;
end;
end;
disp('=====');
fprintf('Program converges at %2.0f iteration. \n \n',it);
disp('Nodal Pressure');
P = [[1:NN]; [full(Z(X.Pi))]]';
fprintf('P%1.0f = %2.3f psia \n',P);
disp('Pipeline Branch Flow Rate');
fp = [[1:NP]; [full(Z(X.fp))]]';
fprintf('fp%1.0f = %2.3f MCMCF/hr \n',fp);
fprintf('\nSource Flow Rate\n');

```

```

WS = [[1:NS];[full(Z(X.Wsource))]];
fprintf('WS%1.0f = %2.3f MMCF/hr\n',WS);
fprintf('\nLoad Demand Flow Rate\n');
WL = [[1:NL];[full(Z(X.Wload))]];
fprintf('WL%1.0f = %2.3f MMCF/hr \n',WL);
fprintf('\nCompressor Branch Flow Rate\n');
fc = [[1:NC]; [full(Z(X.fc))]];
fprintf('fc%1.0f = %2.3f MMCF/hr \n',fc);
fprintf('\nTurbine Gas Consumption\n');
t = [[1:NC]; full(Z(X.t))];
fprintf('t%1.0f = %2.3f MMCF/hr \n',t);
fprintf('\nCompressor Horsepower\n');
HP = [[1:NC]; full(Z(X.HP))];
fprintf('HP%1.0f = %2.3f hp \n',HP);
fprintf('\nReal Power Generation\n');
PG = [[1:NPG]; full(Sbase*Z(X.Pg))];
fprintf('PG%1.0f = %2.3f MW \n',PG);
fprintf('\nReal Power Consumption\n');
PL = [[1:NEL]; full(Sbase*Z(X.PL))];
fprintf('PL%1.0f = %2.3f MW \n',PL);
fprintf('\nElec. Marginal Cost\n');
MC = -Z(Ind.Z_lmd(lmd.P))/(Sbase);
MCE = [[1:NBus]; full(MC)];
fprintf('MC%1.0f = %2.3f $/MWh \n',MCE);
fprintf('\nGas Supply Cost\n');
Cg = sum(full(c1.*Z(X.Wsource)));
fprintf('Cg = $%2.2f \n',Cg);
fprintf('\nGas Consumer Benefit\n');
Bg=sum(full(betaGLInd.*Z(X.WloadInd)+gammaGLInd.*Z(X.WloadInd).^2));
fprintf('Bg = $%2.2f \n',Bg);
fprintf('\nElectric Generation Cost\n');
Ce = sum(full((alphaC + betaC.*Z(X.PgCoal)*Sbase + gammaC.*Z(X.PgCoal).^2 *Sbase^2)));
fprintf('Ce = $%2.2f \n',Ce);
fprintf('\nElectric Consumer Benefit\n');
Be=sum(full((betaB.*Z(X.PL)*Sbase+gammaB.*Z(X.PL).^2*Sbase^2)));
fprintf('Be = $%2.2f \n',Be);
fprintf('\nSocial Welfare\n');
SW=Be+Bg- Cg-Ce;
fprintf('SW = $%2.2f \n',SW);
fprintf('\nNodal Price at Load Nodes\n');
MCGload = Z(Ind.Z_lmd(lmd.NodalFlow(loadNode)))/1015;
MCG = [[1:5]; full(-MCGload)];
fprintf('MC%1.0f = %2.3f $/MMBTU \n',MCG);
disp('=====');

```

D.2 Base Case OPF with Sensitivity Analysis

```
% This program returns the solution of optimal power flow. Minimization of system generation
% is the objective function. Sensitivity analysis is performed.
% OPF for SW maximization is used to obtain real power consumptions.
clear all;
nu = 10;
psi = 0.1;
% -----
% Read CDF,GDF and LDF data of the selected ieee file.
Filename = input('Case name: ','s');
x.cdffile = [ Filename '.cdf' ];
x.gdffile = [ Filename '.gdf' ];
x.ldffile = [ Filename '.ldf' ];

a = ReadDF(x);
x = ac_dataread(a);
Sbase = x.Sbase; % S base
NL = x.nL; % # of lines
NB = x.nB; % # of buses
FR = [x.fr ;x.to];
TO = [x.to ;x.fr];
Y.bus = x.Y;
Y.bran = [x.Y_bran ; x.Y_bran];
Y.shunt = [x.Y_shunt ; x.Y_shunt];

PgBus = x.Pg_bus;
QgBus = x.Qg_bus;
LoadBus = x.Load_bus;

NPG = length(PgBus); % total # of real power gen.
NQG = length(QgBus); % total # of reactive power gen.
NEL = length(LoadBus); % total # of real power consumers

PG = zeros(NB,1);
QG = zeros(NB,1);
PL = zeros(NB,1);
QL = zeros(NB,1);

% Real power consumption obtained from OPF with SW maximization
if NB == 5
    PL(LoadBus,1) = [0.2170 0.9406 0.9161 0.5148]';
elseif NB == 14
    PL(LoadBus,1) = [0.2171 0.9420 0.4772 0.0758 0.1118 0.2939 0.0898 0.0350 0.0610 0.1349 0.1489]';
elseif NB == 30
    PL(LoadBus,1) = [0.2360 0.1817 0.0826 1.0609 0.1959 0.3218 0.1483 0.1218 0.1047 0.0883 0.1332...
        0.0975 0.1145 0.0999 0.0762 0.1855 0.1150 0.0867 0.1166 0.0789 0.0897 ]';
end;
QL(LoadBus,1) = (PL(LoadBus)./x.PF).*sqrt(1-x.PF.^2);
% -----
% Set up indices for 'y'
y.Pg_Start = 1;
y.Pg_End = NPG;
y.Qg_Start = y.Pg_End + 1;
y.Qg_End = y.Pg_End + NQG;
y.V_Start = y.Qg_End + 1;
y.V_End = y.Qg_End + NB;
y.Theta_Start = y.V_End + 1;
y.Theta_End = y.V_End + NB ;

y.Pg = y.Pg_Start : y.Pg_End;
y.Qg = y.Qg_Start : y.Qg_End;
y.V = y.V_Start : y.V_End;
y.Theta = y.Theta_Start : y.Theta_End;

y.Length = NPG + NQG + 2*NB ; % Angle at slack bus is not included.
% -----
% Set up indices for 'lamda'
lmd.P = 1 : NB;
```

```

lmd.Q = NB+1 : 2*NB;
lmd.Pin = PgBus;
lmd.Qin = QgBus + NB;
lmd.ref = 2*NB + 1;

lmd.Length = 2*NB + 1;
% -----
% Set up indices for 'mu'
mu.V_MX_Start = 1; % Max. Vave
mu.V_MX_End = NB;
mu.V_MN_Start = mu.V_MX_End + 1; % Min. Vave
mu.V_MN_End = mu.V_MX_End + NB;
mu.I_MX_Start = mu.V_MN_End+1; % Max. line current
mu.I_MX_End = mu.V_MN_End + 2*NL;
mu.PgMX_Start = mu.I_MX_End + 1;
mu.PgMX_End = mu.I_MX_End + NPG;
mu.PgMN_Start = mu.PgMX_End+1;
mu.PgMN_End = mu.PgMX_End + NPG;
mu.QgMX_Start = mu.PgMN_End + 1;
mu.QgMX_End = mu.PgMN_End + NQG;
mu.QgMN_Start = mu.QgMX_End+1;
mu.QgMN_End = mu.QgMX_End + NQG;

mu.V_MX = mu.V_MX_Start : mu.V_MX_End ;
mu.V_MN = mu.V_MN_Start : mu.V_MN_End ;
mu.I_MX = mu.I_MX_Start : mu.I_MX_End ;
mu.PgMX = mu.PgMX_Start : mu.PgMX_End ;
mu.PgMN = mu.PgMN_Start : mu.PgMN_End ;
mu.QgMX = mu.QgMX_Start : mu.QgMX_End ;
mu.QgMN = mu.QgMN_Start : mu.QgMN_End ;

mu.Length = 2*NB + 2*NL + 2*NPG + 2*NQG;
% -----
% Initial guess for Pg,Qg,PLoad,V,theta,lamda,mu and s
z = sparse(y.Length,1);
z(y.Pg,1) = x.Pg./Sbase;
z(y.Qg,1) = x.Qg./Sbase;
z(y.V,1) = x.Vmag;
z(y.Theta) = x.Vangle;

LAMDA = 10*ones(lmd.Length,1);
s = ones(mu.Length,1);
S = diag(s);
MU = 10*ones(mu.Length,1);
M = diag(MU);

Z = [z ; LAMDA ; MU; s];
% -----
% Index of Z
IX.lamda_Start = y.Length + 1;
IX.lamda_End = y.Length + lmd.Length;
IX.mu_Start = IX.lamda_End + 1;
IX.mu_End = IX.lamda_End + mu.Length;
IX.S_Start = IX.mu_End + 1;
IX.S_End = IX.mu_End + mu.Length;

IX.lamda = IX.lamda_Start : IX.lamda_End;
IX.mu = IX.mu_Start : IX.mu_End;
IX.S = IX.S_Start : IX.S_End;
% -----
% Form matrix dh
dh = sparse(lmd.Length,y.Length);

dh(lmd.Pin,y.Pg) = speye(NPG,NPG);
dh(lmd.Qin,y.Qg) = speye(NQG,NQG);

dh(lmd.ref,y.Theta(1)) = -1;
% -----
% Form matrix dg

```

```

dg = sparse(mu.Length,y.Length);

% Form matrix dg for real power generation limit
dg(mu.PgMX,y.Pg) = speye(NPG, NPG);
dg(mu.PgMN,y.Pg) = -speye(NPG, NPG);

% Form matrix dg for reactive power generation limit
dg(mu.QgMX,y.Qg) = speye(NQG, NQG);
dg(mu.QgMN,y.Qg) = -speye(NQG, NQG);

% Form matrix dg for Vage limit
dg(mu.V_MX,y.V) = speye(NB,NB);
dg(mu.V_MN,y.V) = -speye(NB,NB);

% Find inequality value
I_max = [ x.S_MX/Sbase ; x.S_MX/Sbase ];
g0 = [-x.V_MX ; x.V_MN ; -I_max.^2 ; -x.Pgmax/Sbase ; x.Pgmin/Sbase ;
      -x.Qgmax/Sbase ; x.Qgmin/Sbase];
% -----
% Form matrix ddF
ddF = sparse(y.Length,y.Length);
df0 = zeros(y.Length,1);
ddF(y.Pg,y.Pg) = 2 * diag(x.gamma_c)*Sbase^2;

df0(y.Pg) = x.beta_c*Sbase;

N1 = y.Length; N2 = lmd.Length; N3 = mu.Length; N4 = mu.Length;
i = 0;
while nu > 1e-12 & i < 76
    i=i+1;
    % -----
    theta = Z(y.Theta);
    V = Z(y.V);
    Vph = V.*exp(j*theta);
    I = Y.bus*Vph;
    Si = Vph.*conj(I);
    PG(PgBus) = Z(y.Pg);
    QG(QgBus) = Z(y.Qg);
    % set up "h"
    h(lmd.P,1) = PG-PL-real(Si);
    h(lmd.Q,1) = QG-QL-imag(Si);
    h(lmd.ref,1) = -theta(1);
    % end of construction of the matrix "h"
    % -----
    % set up "dh"
    Jsv = diag(Vph)*conj(Y.bus)*conj(diag(exp(j*theta)))+diag(exp(j*theta).*conj(I));
    Jst = -j*diag(Vph)*conj(Y.bus)*conj(diag(Vph))+diag(j*Si);

    dh(lmd.P, y.V) = -real(Jsv);
    dh(lmd.Q, y.V) = -imag(Jsv);
    dh(lmd.P, y.Theta) = -real(Jst);
    dh(lmd.Q, y.Theta) = -imag(Jst);
    % end of construction of the matrix "dh"
    % -----
    % set up "ddh"
    ddh = zeros(2*NB,2*NB);
    for m = 1 : NB
        ddh_V = zeros(NB,NB);
        ddh_V(m,:) = exp(j*theta(m))*conj(Y.bus(m,:)).*exp(-j*theta');
        ddh_V(:,m) = ddh_V(m,:).';
        ddh_V(m,m) = 2*conj(Y.bus(m,m));

        ddh_theta = zeros(NB,NB);
        ddh_theta(m,:) = Vph(m)*conj(Y.bus(m,:)).*Vph'; % w.r.t angles i & k
        ddh_theta(:,m) = ddh_theta(m,:).';
        ddh_theta = ddh_theta - diag(ddh_theta(m,:));
        ddh_theta(m,m) = -Si(m) + V(m)^2*conj(Y.bus(m,m)); % w.r.t angles i & i

        ddh_V_theta = zeros(NB,NB);

```



```

ddh_V_theta(m,:) = -j*exp(j*theta(m))*conj(Y.bus(m,:)).*Vph';
ddh_V_theta(:,m) = j*Vph(m)*conj(Y.bus(m,:)).'*exp(-j*theta(:));
ddh_V_theta = ddh_V_theta - diag(ddh_V_theta(:,m));
ddh_V_theta(m,m) = j*exp(j*theta(m))*conj(Y.bus(m,:))*conj(Vph)-j*V(m)*conj(Y.bus(m,m));

ddh_theta_V = ddh_V_theta.';

ddh_S = [ ddh_V      ddh_V_theta
          ddh_theta_V ddh_theta  ];
ddh_P = Z(IX.lamda(m))*real(ddh_S);
ddh_Q = Z(IX.lamda(m+NB))*imag(ddh_S);
ddh = ddh + ddh_P + ddh_Q;
end;
DDH = sparse(y.Length, y.Length);
DDH(y.V_Start:y.Theta_End,y.V_Start:y.Theta_End) = -ddh;
% end of construction of matrix "ddh"
% -----
% set up "g"
Iik = (Vph(FR)-Vph(TO)).*Y.bran+Y.shunt.*Vph(FR);
gg = zeros(N3,1);
gg(mu.V_MX) = Z(y.V);
gg(mu.V_MN) = -Z(y.V);
gg(mu.I_MX ) = Iik.*conj(Iik);
gg(mu.PgMX) = Z(y.Pg);
gg(mu.PgMN) = -Z(y.Pg);
gg(mu.QgMX) = Z(y.Qg);
gg(mu.QgMN) = -Z(y.Qg);
g = gg + g0;
% end of construction of matrix "g"
% -----
% set up "dg"
% derivatives of Iik w.r.t Voltage magnitude
dI_dVi = exp(j*theta(FR)).*(Y.bran+Y.shunt);
dI_dVk = -exp(j*theta(TO)).*Y.bran;

dIdVi = sparse((1:2*NL),FR,conj(Iik).*dI_dVi+Iik.*conj(dI_dVi),2*NL,NB);
dIdVk = sparse((1:2*NL),TO,conj(Iik).*dI_dVk+Iik.*conj(dI_dVk),2*NL,NB);
dIdV = dIdVi + dIdVk;
dg(mu.I_MX ,y.V) = dIdV;

% derivatives of Iik w.r.t Voltage angle
dI_dthetai = j*Vph(FR).*(Y.bran+Y.shunt);
dI_dthetak = -j*Vph(TO).*Y.bran;

dIidthetai = sparse((1:2*NL),FR,conj(Iik).*dI_dthetai+Iik.*conj(dI_dthetai),2*NL,NB);
dIidthetak = sparse((1:2*NL),TO,conj(Iik).*dI_dthetak+Iik.*conj(dI_dthetak),2*NL,NB);
dIdtheta = dIidthetai + dIidthetak;
dg(mu.I_MX , y.Theta) = dIdtheta;
% end of construction of matrix "dg"
% -----
% set up "ddg"
ddg = zeros(2*NB,2*NB);
for m = 1 : 2*NL
    ddg_V = sparse(NB,NB);
    ddg_V(FR(m),FR(m)) = 2*conj(dI_dVi(m))*dI_dVi(m);
    ddg_V(FR(m),TO(m)) = conj(dI_dVk(m))*dI_dVi(m) + dI_dVk(m)*conj(dI_dVi(m));
    ddg_V(TO(m),FR(m)) = ddg_V(FR(m),TO(m));
    ddg_V(TO(m),TO(m)) = 2*conj(dI_dVk(m))*dI_dVk(m);

    ddg_theta = sparse(NB,NB);
    ddI_ddthetai = -(Y.bran(m)+Y.shunt(m))*Vph(FR(m));
    ddg_theta(FR(m),FR(m)) = Iik(m)'* ddI_ddthetai+2*conj(dI_dthetai(m))*...
        dI_dthetai(m) + Iik(m)*conj(ddI_ddthetai);
    ddg_theta(FR(m),TO(m)) = dI_dthetai(m)'*dI_dthetak(m)+dI_dthetai(m)*dI_dthetak(m)';
    ddg_theta(TO(m),FR(m)) = ddg_theta(FR(m),TO(m));
    ddI_ddthetakk = Y.bran(m)*Vph(TO(m));
    ddg_theta(TO(m),TO(m)) = Iik(m)'*ddI_ddthetakk+2*dI_dthetak(m)'*dI_dthetak(m)...
        +Iik(m)*ddI_ddthetakk';
end;

```

```

ddg_V_theta = sparse(NB,NB);
ddI_dVi_dthetai = j*exp(j*theta(FR(m)))*(Y.bran(m)+Y.shunt(m));
ddg_V_theta(FR(m),FR(m)) = Iik(m)'*ddI_dVi_dthetai + dI_dVi(m)'*dI_dthetai(m)+...
    dI_dVi(m)*dI_dthetai(m)' + Iik(m)*ddI_dVi_dthetai';
ddI_dVk_dthetak = -j*exp(j*theta(TO(m)))*Y.bran(m);
ddg_V_theta(TO(m),TO(m)) = Iik(m)'*ddI_dVk_dthetak+dI_dVk(m)'*dI_dthetak(m)+...
    dI_dVk(m)*dI_dthetak(m)' + Iik(m)*ddI_dVk_dthetak';

ddg_theta_V = ddg_V_theta.';
ddg_Iik = [ ddg_V    ddg_V_theta
            ddg_theta_V ddg_theta    ];
ddg = ddg + Z(IX.mu(mu.I_MX (m)))*ddg_Iik;
end;
DDG = sparse(y.Length,y.Length);
DDG(y.V_Start:y.Theta_End,y.V_Start:y.Theta_End) = ddg;

DDFHG = ddF + DDH + DDG;
J = real([ DDFHG          dh.'          dg.'          sparse(N1,N3) ;
           dh          sparse(N2,N2)    sparse(N2,N3)    sparse(N2,N3) ;
           dg          sparse(N3,N2)    sparse(N3,N3)    speye(N3,N3) ;
           sparse(N3,N1) sparse(N3,N2)    S              M      ]]);
dF = ddF*Z(1:N1) + df0;
dY = real([-dF-dh.'*Z(N1+1:N1+N2)-dg.'*Z(N1+N2+1:N1+N2+N3)
           -h
           -g-Z(N1+N2+N3+1:N1+N2+2*N3)
           nu*ones(N3,1)-M*S*ones(N3,1)]);
dZ = J\dY;
dMU = dZ(IX.mu);
ds = dZ(IX.S);
S_Neg_Index = find(ds < 0);
alpha_S = min([1;-s(S_Neg_Index)./ds(S_Neg_Index)]);
MU_Neg_Index = find(dMU < 0);
alpha_MU = min([1;-MU(MU_Neg_Index)./dMU(MU_Neg_Index)]);
alpha = min(alpha_S ,alpha_MU);
Z = Z + alpha*dZ;
MU = Z(IX.mu);
s = Z(IX.S);
M = diag(MU);
S = diag(s);
if norm(M*s - MU.'*s/N3) <= psi*nu;
    nu = nu*0.4;
end;
end;
%=====
% Find the generation cost
Gen_Cost = x.gamma_c.*Z(y.Pg).^2*Sbase^2 + x.beta_c.*Z(y.Pg)*Sbase + x.alpha_c;
Total_Cost = sum(Gen_Cost);
%=====
% Real Power Loss
Sloss = zeros(NL+1,1);
Sik = Vph(FR).*conj((Vph(FR)-Vph(TO)).*Y.bran+Y.shunt.*Vph(FR));
Sloss(1:N1) = Sik(1:N1) + Sik(N1+1:2*N1);
Ploss = sum(real(Sloss));
Qloss = sum(imag(Sloss));
%=====
Act_List = find(Z(IX.mu)>0.001);
Act_No = length(Act_List);
%=====
disp('Base Case OPF Result');
fprintf('Total Generation Cost = $%2.3f \n',Total_Cost);
disp('Real Power Generation');
Pgen = [[1:NPG]; [full(Z(y.Pg))]]'*Sbase;
fprintf('Pg%1.0f = %2.3f MW \n',Pgen);
fprintf('Real power Loss = %2.3f MW \n',Ploss);
%=====
Flow_Dir = 1;
dist = 0.5;
for (UPFC_POS=1:1:N1)
    BIEQ_No = find(Act_List == (UPFC_POS + 2*N1));

```

```

if isempty(BIEQ_No)
    BIEQ = 0;
else
    BIEQ = 1;
end;
abcd = abcd_const(a,UPFC_POS,Flow_Dir,dist);
Ai = abcd.ABCDi(1,1);
Bi = abcd.ABCDi(1,2);
Ci = abcd.ABCDi(2,1);
Di = abcd.ABCDi(2,2);
Ak = abcd.ABCDk(1,1);
Bk = abcd.ABCDk(1,2);
Ck = abcd.ABCDk(2,1);
Dk = abcd.ABCDk(2,2);

T = 1; phi = 0; rho = 0;
Aik = T*exp(j*phi*pi/180)*Ai*Ak + j*T*exp(j*phi*pi/180)*Bi*Ak*rho+1/T*exp(j*phi*pi/180)*Bi*Ck;
Bik = T*exp(j*phi*pi/180)*Ai*Bk + j*T*exp(j*phi*pi/180)*Bi*Bk*rho+1/T*exp(j*phi*pi/180)*Bi*Dk;
Cik = T*exp(j*phi*pi/180)*Ci*Ak + j*T*exp(j*phi*pi/180)*Di*Ak*rho+1/T*exp(j*phi*pi/180)*Di*Ck;
Dik = T*exp(j*phi*pi/180)*Ci*Bk + j*T*exp(j*phi*pi/180)*Di*Bk*rho+1/T*exp(j*phi*pi/180)*Di*Dk;

Y11 = Dik/Bik;
Y12 = Cik - Aik*Dik/Bik;
Y21 = -1/Bik;
Y22 = Aik/Bik;

Vphi = Vph(FR(UPFC_POS));
Vphk = Vph(TO(UPFC_POS));
Vi = V(FR(UPFC_POS));
Vk = V(TO(UPFC_POS));
thetai = theta(FR(UPFC_POS));
thetak = theta(TO(UPFC_POS));
Iiki = Iik(UPFC_POS);

dY12dphi = j*(Ci*Ak+Di*Ck-(Ai*Ak+Bi*Ck)*(Ci*Bk+Di*Dk)/(Ai*Bk+Bi*Dk));
dSidphi = -Vphi*Vphk'*dY12dphi';

dY21dphi = 1/(-j*Ai*Bk-j*Bi*Dk);
dSkdphi = -Vphk*Vphi'*dY21dphi';

dIikdphi = Vphk*dY12dphi;
dIikIikdphi = dIikdphi*Iiki' + dIikdphi'*Iiki;

dY11drho = j*Bk^2*(Ai*Di-Bi*Ci)/(Ai*Bk+Bi*Dk)^2;
dY12drho = j*Di*Ak-j*Bi*Ak*(Ci*Bk+Di*Dk)/(Ai*Bk+Bi*Dk)-j*(Ai*Ak+Bi*Ck)*Di*Bk/(Ai*Bk+Bi*Dk)...
+j*(Ai*Ak+Bi*Ck)*(Ci*Bk+Di*Dk)/(Ai*Bk+Bi*Dk)^2*Bi*Bk;
dSidrho = -(Vi^2*dY11drho'+Vphi*Vphk'*dY12drho');

dY21drho = j*Bi*Bk/(Ai*Bk+Bi*Dk)^2;
dY22drho = j*Bi^2*(Ak*Dk-Bk*Ck)/(Ai*Bk+Bi*Dk)^2;
dSkdrho = -(Vphk*Vphi'*dY21drho' + Vk^2*dY22drho');

dY11dT = 2*Bk*Dk*(Bi*Ci-Ai*Di)/(Ai*Bk+Bi*Dk)^2;
dY12dT = Ci*Ak-Di*Ck-(Ai*Ak-Bi*Ck)*(Ci*Bk+Di*Dk)/(Ai*Bk+Bi*Dk)-(Ai*Ak+Bi*Ck)*(Ci*Bk-Di*Dk)/...
(Ai*Bk+Bi*Dk)+(Ai*Ak+Bi*Ck)*(Ci*Bk+Di*Dk)/(Ai*Bk+Bi*Dk)^2*(Ai*Bk-Bi*Dk);
dSidT = -(Vi^2*dY11dT' + Vphi*Vphk'*dY12dT');

dY21dT = (Ai*Bk-Bi*Dk)/(Ai*Bk+Bi*Dk)^2;
dY22dT = 2*Bi*(Ai*Ak*Dk-Ck*Ai*Bk)/(Ai*Bk+Bi*Dk)^2;
dSkdT = -(Vphk*Vphi'*dY21dT' + Vk^2*dY22dT');

dIikdrho = Vphi*dY11drho + Vphk*dY12drho;
dIikIikdrho = dIikdrho*Iiki' + dIikdrho'*Iiki;

dIikdT = Vphi*dY11dT + Vphk*dY12dT;
dIikIikdT = dIikdT*Iiki' + dIikdT'*Iiki;

lambda_phi = Z(IX.lamda(lmd.P(FR(UPFC_POS))))*real(dSidphi)+Z(IX.lamda(lmd.Q(FR(UPFC_POS))))*...
imag(dSidphi)+Z(IX.lamda(lmd.P(TO(UPFC_POS))))*real(dSkdphi)+Z(IX.lamda(lmd.Q(TO(UPFC_POS))))*...

```

```

*imag(dSkdphi)+Z(IX.mu(mu.I_MX(UPFC_POS)))*dIikIikdphi;
lambda_rho = Z(IX.lamda(lmd.P(FR(UPFC_POS))))*real(dSidrho) + Z(IX.lamda(lmd.Q(FR(UPFC_POS))))...
*imag(dSidrho)+Z(IX.lamda(lmd.P(TO(UPFC_POS))))*real(dSkdrho)+Z(IX.lamda(lmd.Q(TO(UPFC_POS))))...
*imag(dSkdrho)+Z(IX.mu(mu.I_MX(UPFC_POS)))*dIikIikdrho;
lambda_T = Z(IX.lamda(lmd.P(FR(UPFC_POS))))*real(dSidT) + Z(IX.lamda(lmd.Q(FR(UPFC_POS))))*...
imag(dSidT)+Z(IX.lamda(lmd.P(TO(UPFC_POS))))*real(dSkdT)+Z(IX.lamda(lmd.Q(TO(UPFC_POS))))...
*imag(dSkdT)+Z(IX.mu(mu.I_MX(UPFC_POS)))*dIikIikdT;

lambda = [ lambda_phi lambda_rho lambda_T ]';
% End of first order sensitivity
%=====
% Second-order derivatives for Y11, Y12, Y21, and Y22
ddY11_ddrho = 2*Bi*Bk^3*(Ai*Di-Bi*Ci)/(Ai*Bk+Bi*Dk)^3;
ddY11_ddT = -2*Bk*Dk*(Bi*Ci-Ai*Di)*(3*Ai*Bk-Bi*Dk)/(Ai*Bk+Bi*Dk)^3;
ddY11_drhoT = j*4*Bi*Bk^2*Dk*(Ai*Di-Bi*Ci)/(Ai*Bk+Bi*Dk)^3;

ddY12_ddphi = -Y12;
ddY12_ddT = 2*Di*Ck-2*Bi*Ck*(Ci*Bk+Di*Dk)/(Ai*Bk+Bi*Dk)-2*(Ai*Bk-Bi*Dk)*(Bk*Ci-Di*Dk)/(Ai*Bk+Bi*Dk)...
+2*(Ai*Bk-Bi*Dk)*(Bk*Ci+Di*Dk)/(Ai*Bk+Bi*Dk)^2*(Ai*Bk-Bi*Dk)-2*(Ai*Bk+Bi*Dk)*(Di*Dk/(Ai*Bk+Bi*Dk)...
-(Bk*Ci-Di*Dk)/(Ai*Bk+Bi*Dk)^2*(Ai*Bk-Bi*Dk))-2*(Ai*Bk+Bi*Dk)*((Bk*Ci+Di*Dk)*(Ai*Bk-Bi*Dk)^2/...
(Ai*Bk+Bi*Dk)^3 - (Bk*Ci+Di*Dk)/(Ai*Bk+Bi*Dk)^2*Bi*Dk);
ddY12_ddrho = 2*Bi^2*Bk^2*(Bi*Bk+Ci*Ck+Ai*Bk+Di*Dk-Ai*Bk+Ci*Dk)/(Ai*Bk+Bi*Dk)^3;
ddY12_drhoT = -j/(Ai*Bk+Bi*Dk)^3*(3*Ak*Bi^3*Bk+Ci*Dk^2 + Ak*Bi^3*Di*Dk^3-3*Bi^3*Bk^2*Ci*Ck*Dk+...
Ai*Bi^2*Bk^3*Ci*Ck+Ai^3*Bk^3*Di-Ai^2*Bi*Bk^3*Ck*Di-Ai*Bk+Bi^2*Bk^2*Ci*Dk+3*Ai*Bi^2*Bk^2...
*Ck*Di*Dk+4*Ai^2*Bk*Bi*Bk^2*Di*Dk)+j*Ak*Di;
ddY12_dphidT = j*(Ak*Ci-Ck*Di-(Ai*Bk-Bi*Dk)*(Ci*Bk+Di*Dk)/(Ai*Bk+Bi*Dk)-(Ai*Bk+Bi*Dk)*...
(Ci*Bk-Di*Dk)/(Ai*Bk+Bi*Dk)+(Ai*Bk+Bi*Dk)*(Ci*Bk+Di*Dk)/(Ai*Bk+Bi*Dk)^2*(Ai*Bk-Bi*Dk));
ddY12_dphidrho = j*(j*Di*Bk-j*Bi*Bk*(Ci*Bk+Di*Dk)/(Ai*Bk+Bi*Dk)-j*(Ai*Bk+Bi*Dk)*Bk*Di/...
(Ai*Bk+Bi*Dk)+j*(Ai*Bk+Bi*Dk)*(Ci*Bk+Di*Dk)*(Bi*Bk)/(Ai*Bk+Bi*Dk)^2);

ddY21_ddphi = 1/(Ai*Bk+Bi*Dk);
ddY21_ddT = -2*Bk*(Ai^2*Bk-3*Ai*Bi*Dk)/(Ai*Bk+Bi*Dk)^3;
ddY21_ddrho = 2*Bi^2*Bk^2/(Ai*Bk+Bi*Dk)^3;
ddY21_dphidT = j/(Ai*Bk+Bi*Dk)-2*j*Ai*Bk/(Ai*Bk+Bi*Dk)^2;
ddY21_dphidrho = Bi*Bk/(Ai*Bk+Bi*Dk)^2;
ddY21_drhoT = -j*Bi*Bk*(Ai*Bk-3*Bi*Dk)/(Ai*Bk+Bi*Dk)^3;

ddY22_ddrho = 2*Bi^3*Bk*(Ak*Dk-Bk*Ck)/(Ai*Bk+Bi*Dk)^3;
ddY22_ddT = -2*Bi*(Ai*Bk+Di-Di*Bk)*(3*Ai*Bk-Bi*Dk)/(Ai*Bk+Bi*Dk)^3;
ddY22_drhoT = -2*j*Bi^2*(Ak*Dk-Bk*Ck)*(Ai*Bk-Bi*Dk)/(Ai*Bk+Bi*Dk)^3;

ddSi_ddphi = Vphi*Vphk'*ddY12_ddphi';
ddSi_ddrho = Vi^2*ddY11_ddrho' + Vphi*Vphk'*ddY12_ddrho';
ddSi_ddT = Vi^2*ddY11_ddT' + Vphi*Vphk'*ddY12_ddT';
ddSi_dphidrho = Vphi*Vphk'*ddY12_dphidrho';
ddSi_dphidT = Vphi*Vphk'*ddY12_dphidT';
ddSi_drhoT = Vi^2*ddY11_drhoT' + Vphi*Vphk'*ddY12_drhoT';

ddSi_ddx = [ddSi_ddphi ddSi_dphidrho ddSi_dphidT ;
ddSi_dphidrho ddSi_ddrho ddSi_drhoT ;
ddSi_dphidT ddSi_drhoT ddSi_ddT];

ddSi_dVidphi = exp(j*thetai)*Vphk'*dY12dphi';
ddSi_dthetaidphi = j*Vphi*Vphk'*dY12dphi';
ddSi_dVkdphi = Vphi*exp(-j*thetak)*dY12dphi';
ddSi_dthetakdphi = -j*Vphi*Vphk'*dY12dphi';
ddSi_dVidrho = 2*Vi*dY11drho'+exp(j*thetai)*Vphk'*dY12drho';
ddSi_dthetaidrho = j*Vphi*Vphk'*dY12drho';
ddSi_dVkdrho = Vphi*exp(-j*thetak)*dY12drho';
ddSi_dthetakdrho = -j*Vphi*Vphk'*dY12drho';
ddSi_dVidT = 2*Vi*dY11dT'+exp(j*thetai)*Vphk'*dY12dT';
ddSi_dthetaidT = j*Vphi*Vphk'*dY12dT';
ddSi_dVkdT = Vphi*exp(-j*thetak)*dY12dT';
ddSi_dthetakdT = -j*Vphi*Vphk'*dY12dT';

ddSi_dydx = zeros(y.Length, 3);
ddSi_dydx(y.V(FR(UPFC_POS)), 1) = ddSi_dVidphi;
ddSi_dydx(y.Theta(FR(UPFC_POS)), 1) = ddSi_dthetaidphi;
ddSi_dydx(y.V(TO(UPFC_POS)), 1) = ddSi_dVkdphi;

```

```

ddSi_dydx(y.Theta(TO(UPFC_POS)), 1) = ddSi_dthetakdphi;

ddSi_dydx(y.V(FR(UPFC_POS)), 2) = ddSi_dVidrho;
ddSi_dydx(y.Theta(FR(UPFC_POS)), 2) = ddSi_dthetairho;
ddSi_dydx(y.V(TO(UPFC_POS)), 2) = ddSi_dVkdrho;
ddSi_dydx(y.Theta(TO(UPFC_POS)), 2) = ddSi_dthetakdrho;

ddSi_dydx(y.V(FR(UPFC_POS)), 3) = ddSi_dVidT;
ddSi_dydx(y.Theta(FR(UPFC_POS)), 3) = ddSi_dthetaidT;
ddSi_dydx(y.V(TO(UPFC_POS)), 3) = ddSi_dVkdT;
ddSi_dydx(y.Theta(TO(UPFC_POS)), 3) = ddSi_dthetakdT;
% -----
ddSk_ddphi = Vphi'*Vphk*ddY21_ddphi';
ddSk_ddrho = Vk^2*ddY22_ddrho' + Vphi'*Vphk*ddY21_ddrho';
ddSk_ddT = Vk^2*ddY22_ddT' + Vphi'*Vphk*ddY21_ddT';
ddSk_dphidrho = Vphi'*Vphk*ddY21_dphidrho';
ddSk_dphidT = Vphi'*Vphk*ddY21_dphidT';
ddSk_drhodT = Vk^2*ddY22_drhodT' + Vphi'*Vphk*ddY21_drhodT';

ddSk_ddx = [ddSk_ddphi      ddSk_dphidrho   ddSk_dphidT ;
             ddSk_dphidrho  ddSk_ddrho      ddSk_drhodT ;
             ddSk_dphidT    ddSk_drhodT     ddSk_ddT ];

ddSk_dVidphi = exp(-j*thetai)*Vphk*dY21dphi';
ddSk_dthetaidphi = -j*Vphi'*Vphk*dY21dphi';
ddSk_dVkdphi = Vphi'*exp(j*thetak)*dY21dphi';
ddSk_dthetakdphi = j*Vphi'*Vphk*dY21dphi';
ddSk_dVidrho = exp(-j*thetai)*Vphk*dY21drho';
ddSk_dthetairho = -j*Vphi'*Vphk*dY21drho';
ddSk_dVkdrho = Vphi'*exp(j*thetak)*dY21drho'+2*Vk*dY22drho';
ddSk_dthetakdrho = j*Vphi'*Vphk*dY21drho';
ddSk_dVidT = exp(-j*thetai)*Vphk*dY21dT';
ddSk_dthetaidT = -j*Vphi'*Vphk*dY21dT';
ddSk_dVkdT = Vphi'*exp(j*thetak)*dY21dT'+2*Vk*dY22dT';
ddSk_dthetakdT = j*Vphi'*Vphk*dY21dT';

ddSk_dydx = zeros(y.Length, 3);
ddSk_dydx(y.V(FR(UPFC_POS)), 1) = ddSk_dVidphi;
ddSk_dydx(y.Theta(FR(UPFC_POS)), 1) = ddSk_dthetaidphi;
ddSk_dydx(y.V(TO(UPFC_POS)), 1) = ddSk_dVkdphi;
ddSk_dydx(y.Theta(TO(UPFC_POS)), 1) = ddSk_dthetakdphi;

ddSk_dydx(y.V(FR(UPFC_POS)), 2) = ddSk_dVidrho;
ddSk_dydx(y.Theta(FR(UPFC_POS)), 2) = ddSk_dthetairho;
ddSk_dydx(y.V(TO(UPFC_POS)), 2) = ddSk_dVkdrho;
ddSk_dydx(y.Theta(TO(UPFC_POS)), 2) = ddSk_dthetakdrho;

ddSk_dydx(y.V(FR(UPFC_POS)), 3) = ddSk_dVidT;
ddSk_dydx(y.Theta(FR(UPFC_POS)), 3) = ddSk_dthetaidT;
ddSk_dydx(y.V(TO(UPFC_POS)), 3) = ddSk_dVkdT;
ddSk_dydx(y.Theta(TO(UPFC_POS)), 3) = ddSk_dthetakdT;
% -----
ddIik_ddphi = Vphk*ddY12_ddphi;
ddIik_ddrho = (Vphi*ddY11_ddrho+Vphk*ddY12_ddrho);
ddIik_ddT = Vphi*ddY11_ddT+Vphk*ddY12_ddT;
ddIik_dphidrho = Vphk*ddY12_dphidrho;
ddIik_dphidT = Vphk*ddY12_dphidT;
ddIik_drhodT = Vphi*ddY11_drhodT + Vphk*ddY12_drhodT;

ddIikIik_ddphi = Iiki*ddIik_ddphi' + 2*dIikdphi*dIikdphi'+Iiki'*ddIik_ddphi;
ddIikIik_ddrho = Iiki*ddIik_ddrho' + 2*dIikdrho*dIikdrho'+Iiki'*ddIik_ddrho;
ddIikIik_ddT = Iiki*ddIik_ddT' + 2*dIikdT*dIikdT'+Iiki'*ddIik_ddT;
ddIikIik_dphidrho = Iiki*ddIik_dphidrho'+dIikdphi*dIikdrho'+dIikdphi'*dIikdrho+Iiki'*ddIik_dphidrho;
ddIikIik_dphidT = Iiki*ddIik_dphidT'+dIikdphi*dIikdT'+dIikdphi'*dIikdT+Iiki'*ddIik_dphidT;
ddIikIik_drhodT = Iiki*ddIik_drhodT'+dIikdrho*dIikdT'+dIikdrho'*dIikdT+Iiki'*ddIik_drhodT;

ddIikIik_ddx = [ddIikIik_ddphi      ddIikIik_dphidrho   ddIikIik_dphidT ;
                ddIikIik_dphidrho  ddIikIik_ddrho      ddIikIik_drhodT ;
                ddIikIik_dphidT    ddIikIik_drhodT     ddIikIik_ddT ];

```

```

ddIik_dVidrho = exp(j*thetai)*dY11drho;
ddIik_dVidT = exp(j*thetai)*dY11dT;
ddIik_dVkdphi = exp(j*thetak)*dY12dphi;
ddIik_dVkdrho = exp(j*thetak)*dY12drho;
ddIik_dVkdT = exp(j*thetak)*dY12dT;

ddIik_dthetakdphi = j*Vphk*dY12dphi;
ddIik_dthetakdrho = j*Vphk*dY12drho;
ddIik_dthetakdT = j*Vphk*dY12dT;
ddIik_dthetaidrho = j*Vphi*dY11drho;
ddIik_dthetaidT = j*Vphi*dY11dT;

ddIikIik_dVidphi = exp(j*thetai)*Y11*dIikdphi' + (exp(j*thetai)*Y11)'*dIikdphi;
ddIikIik_dthetaidphi = j*Vphi*Y11*dIikdphi' + (j*Vphi*Y11)'*dIikdphi;
ddIikIik_dVkdphi = Iiki*ddIik_dVkdphi'+exp(j*thetak)*Y12*dIikdphi' + (exp(j*thetak)*Y12)*...
    dIikdphi+Iiki'*ddIik_dVkdphi;
ddIikIik_dthetakdphi = Iiki*ddIik_dthetakdphi'+j*Vphk*Y12*dIikdphi' + (j*Vphk*Y12)'*dIikdphi+...
    Iiki'*ddIik_dthetakdphi;

ddIikIik_dVidrho = Iiki*ddIik_dVidrho'+exp(j*thetai)*Y11*dIikdrho' + (exp(j*thetai)*Y11)* ...
    dIikdrho+Iiki'*ddIik_dVidrho;
ddIikIik_dthetaidrho = Iiki*ddIik_dthetaidrho'+j*Vphi*Y11*dIikdrho' + (j*Vphi*Y11)*...
    dIikdrho+Iiki'*ddIik_dthetaidrho;
ddIikIik_dVkdrho = Iiki*ddIik_dVkdrho'+exp(j*thetak)*Y12*dIikdrho' + (exp(j*thetak)*Y12)* ...
    dIikdrho+Iiki'*ddIik_dVkdrho;
ddIikIik_dthetakdrho = Iiki*ddIik_dthetakdrho'+j*Vphk*Y12*dIikdrho' + (j*Vphk*Y12)* ...
    dIikdrho+Iiki'*ddIik_dthetakdrho;

ddIikIik_dVidT = Iiki*ddIik_dVidT'+exp(j*thetai)*Y11*dIikdT' + (exp(j*thetai)*Y11)* ...
    dIikdT+Iiki'*ddIik_dVidT;
ddIikIik_dthetaidT = Iiki*ddIik_dthetaidT'+j*Vphi*Y11*dIikdT' + (j*Vphi*Y11)'*dIikdT+Iiki'*...
    ddIik_dthetaidT;
ddIikIik_dVkdT = Iiki*ddIik_dVkdT'+exp(j*thetak)*Y12*dIikdT' + (exp(j*thetak)*Y12)'*dIikdT+ ...
    Iiki'*ddIik_dVkdT;
ddIikIik_dthetakdT = Iiki*ddIik_dthetakdT'+j*Vphk*Y12*dIikdT' + (j*Vphk*Y12)'*dIikdT+Iiki'* ...
    ddIik_dthetakdT;

ddIikIik_dydx = zeros(y.Length, 3);
ddIikIik_dydx(y.V(FR(UPFC_POS)),1) = ddIikIik_dVidphi;
ddIikIik_dydx(y.Theta(FR(UPFC_POS)),1) = ddIikIik_dthetaidphi;
ddIikIik_dydx(y.V(TO(UPFC_POS)), 1) = ddIikIik_dVkdphi;
ddIikIik_dydx(y.Theta(TO(UPFC_POS)), 1) = ddIikIik_dthetakdphi;

ddIikIik_dydx(y.V(FR(UPFC_POS)), 2) = ddIikIik_dVidrho;
ddIikIik_dydx(y.Theta(FR(UPFC_POS)), 2) = ddIikIik_dthetaidrho;
ddIikIik_dydx(y.V(TO(UPFC_POS)), 2) = ddIikIik_dVkdrho;
ddIikIik_dydx(y.Theta(TO(UPFC_POS)), 2) = ddIikIik_dthetakdrho;

ddIikIik_dydx(y.V(FR(UPFC_POS)), 3) = ddIikIik_dVidT;
ddIikIik_dydx(y.Theta(FR(UPFC_POS)), 3) = ddIikIik_dthetaidT;
ddIikIik_dydx(y.V(TO(UPFC_POS)), 3) = ddIikIik_dVkdT;
ddIikIik_dydx(y.Theta(TO(UPFC_POS)), 3) = ddIikIik_dthetakdT;
% -----
dydxLik = -real(ddSi_dydx)*Z(IX.lamda(FR(UPFC_POS)))...
    -imag(ddSi_dydx)*Z(IX.lamda(FR(UPFC_POS)+NB))...
    -real(ddSk_dydx)*Z(IX.lamda(TO(UPFC_POS)))...
    -imag(ddSk_dydx)*Z(IX.lamda(TO(UPFC_POS)+NB))...
    +ddIikIik_dydx*Z(IX.mu(mu.I_MX(UPFC_POS)));
% -----
Jx = zeros(lmd.Length+Act_No, 3);
Jx(FR(UPFC_POS),1) = real(dSidphi);
Jx(FR(UPFC_POS),2) = real(dSidrho);
Jx(FR(UPFC_POS),3) = real(dSidT);
Jx(FR(UPFC_POS)+NB,1) = imag(dSidphi);
Jx(FR(UPFC_POS)+NB,2) = imag(dSidrho);
Jx(FR(UPFC_POS)+NB,3) = imag(dSidT);

Jx(TO(UPFC_POS),1) = real(dSkdphi);

```

```

Jx(TO(UPFC_POS),2) = real(dSkdrho);
Jx(TO(UPFC_POS),3) = real(dSkdT);
Jx(TO(UPFC_POS)+NB,1) = imag(dSkdphi);
Jx(TO(UPFC_POS)+NB,2) = imag(dSkdrho);
Jx(TO(UPFC_POS)+NB,3) = imag(dSkdT);
if BIEQ ==1
    Jx(lmd.Length+BIEQ_No,1) = dIikIikdphi;
    Jx(lmd.Length+BIEQ_No,2) = dIikIikdrho;
    Jx(lmd.Length+BIEQ_No,3) = dIikIikdT;
end;
% -----
Hx = -real(ddSi_ddx)*Z(IX.lamda(FR(UPFC_POS)))-imag(ddSi_ddx)*Z(IX.lamda(FR(UPFC_POS)+NB))...
    -real(ddSk_ddx)*Z(IX.lamda(TO(UPFC_POS)))-imag(ddSk_ddx)*Z(IX.lamda(TO(UPFC_POS)+NB))...
    +ddIikIik_ddx*Z(IX.mu(mu.I_MX(UPFC_POS)));
% -----
% Find "W" matrix
JJ = [dh ; dg(Act_List,:)];
W = [DDFHG    JJ.' ;
     JJ       zeros(N2+Act_No, N2+Act_No)];
dz_dx = -real(W\[dydxLik ; Jx]);
dlamda_dx =real([dydxLik ; Jx].'*dz_dx)+Hx;
IV = real(1/2*lambda.'*inv(dlamda_dx)*lambda); % Expected incremental value
fprintf('UPFC installed between bus %1.0f and bus %1.0f \n',x.fr(UPFC_POS), x.to(UPFC_POS));
fprintf('lambda_T = %2.2f, lambda_phi = %2.2f, lambda_rho = %2.2f, IV = %2.4f \n',...
        lambda_T, lambda_phi, lambda_rho, IV);
end

```

D.3 OPF with a UPFC

```
% This program returns the solution of optimal power flow with a UPFC.
% UPFC direct model is used.
clear all;
nu = 10;
psi = 0.1;
% -----
% Read CDF,GDF and LDF data of the selected test system file
Filename = input('Case name: ','s');
x.cdf = [ Filename '.cdf' ];
x.gdf = [ Filename '.gdf' ];
x.ldf = [ Filename '.ldf' ];

a = ReadDF(x);
Sbase = a.Sbase; % System S base
% -----
% UPFC Information
UPFC_POS = input('Type a transmission line number to install a UPFC:');
Flow_Dir = 1;
dist = 0.5;
UPFC_var = 6; % Vp, Vq, Ip, Iq, II and IO
VT = 0.16;
x = upfc_datareadx(a,UPFC_POS,Flow_Dir,dist);
% -----
No_P_GEN = sum(x.Pnumgen); % # of real power generators
No_Q_GEN = sum(x.Qnumgen); % # of reactive power generators
No_LOAD = sum(x.numload); % # of loads
Pg_bus = find(x.Pnumgen > 0); % Locations of real power generators
Qg_bus = find(x.Qnumgen > 0); % Locations of reactive power generators
Load_bus = find(x.numload > 0); % Locations of load
% -----
% Bus Configuration
NB_OLD = x.nb;
NB = x.nb+2;
NL = x.nl;
Ybranch = x.Ybranch;
Yshunt = x.Yshunt;
Ybr = [Ybranch ; Ybranch];
Ysh = [Yshunt ; Yshunt];
Ybus = x.Ybus;
ILmax = x.SL_MX./Sbase; % Max. line currents
V_MX = x.V_MX;
V_MN = x.V_MN;
FR = x.FR;
TO = x.TO;
FR_I = x.FR_I; % UPFC input side bus number
TO_O = x.TO_O; % UPFC output side bus number
% -----
% Load Bus Data Input
PF = zeros(NB_OLD,1);
PF(Load_bus) = x.PF;
PL = zeros(NB_OLD,1);
QL = zeros(NB_OLD,1);
if NB_OLD == 5
    PL = [ 0 ; 0.2170 ; 0.9406 ; 0.9160 ; 0.5148 ];
elseif NB_OLD == 14
    PL(Load_bus,1) = [0.2171 0.9420 0.4772 0.0758 0.1118 0.2939 0.0898 0.0350 0.0610 0.1349 0.1489]';
elseif NB_OLD == 30
    PL(Load_bus,1) = [0.2360 0.1817 0.0826 1.0609 0.1959 0.3218 0.1483 0.1218 0.1047 0.0883 0.1332 ...
        0.0975 0.1145 0.0999 0.0762 0.1855 0.1150 0.0867 0.1166 0.0789 0.0897 ]';
end;
QL(Load_bus) = PL(Load_bus)./x.PF.*sqrt(1-x.PF.^2);
PG = sparse(NB_OLD,1); % PG - PL - Re(Si) = 0;
QG = sparse(NB_OLD,1); % QG - QL - im(Si) = 0;
% -----
% Indices for 'y'
y.Pg_Start = 1;
y.Pg_End = No_P_GEN;
```



```

y.Qg_Start = y.Pg_End + 1;
y.Qg_End = y.Pg_End + No_Q_GEN;
y.V_Start = y.Qg_End + 1;
y.V_End = y.Qg_End + NB;
y.Theta_Start = y.V_End + UPFC_var + 1;
y.Theta_End = y.V_End + UPFC_var + NB - 1;

y.Pg = y.Pg_Start : y.Pg_End;
y.Qg = y.Qg_Start : y.Qg_End;
y.V = y.V_Start : y.V_End;
y.VI = y.V_End - 1;
y.V0 = y.V_End ;
y.Vp = y.V_End + 1;
y.Vq = y.V_End + 2;
y.II = y.V_End + 3;
y.IO = y.V_End + 4;
y.Ip = y.V_End + 5;
y.Iq = y.V_End + 6;

y.Theta = y.Theta_Start : y.Theta_End;
y.thetaI = y.Theta_End-1;
y.theta0 = y.Theta_End;
y.deltaI = y.Theta_End + 1;
y.delta0 = y.Theta_End + 2;

y.Length = y.delta0;
% -----
% Indices for 'lamda'
lamda.P = 1 : NB_OLD;
lamda.Q = NB_OLD+1 : 2*Nb_OLD;
lamda.Pin = Pg_bus;
lamda.Qin = Qg_bus + NB_OLD;
lamda.IIinR = 2*Nb_OLD + 1;
lamda.IIinI = 2*Nb_OLD + 2;
lamda.IOinR = 2*Nb_OLD + 3;
lamda.IOinI = 2*Nb_OLD + 4;
lamda.IR = 2*Nb_OLD + 5;
lamda.II = 2*Nb_OLD + 6;
lamda.VR = 2*Nb_OLD + 7;
lamda.VI = 2*Nb_OLD + 8;
lamda.RP = 2*Nb_OLD + 9;

lamda.Length = lamda.RP ;
% -----
% Indices for 'mu'
mu.V_MX_Start = 1; % Max. Voltage
mu.V_MX_End = NB;
mu.V_MN_Start = mu.V_MX_End + 1; % Min. Voltage
mu.V_MN_End = mu.V_MX_End + NB;
mu.I_MX_Start = mu.V_MN_End+1; % Max. line current
mu.I_MX_End = mu.V_MN_End + 2*(NL+1);
mu.PgMX_Start = mu.I_MX_End + 1; % Max. real power generation
mu.PgMX_End = mu.I_MX_End + No_P_GEN;
mu.PgMN_Start = mu.PgMX_End+1; % Min. real power generation
mu.PgMN_End = mu.PgMX_End + No_P_GEN;
mu.QgMX_Start = mu.PgMN_End + 1; % Max. reactive power generation
mu.QgMX_End = mu.PgMN_End + No_Q_GEN;
mu.QgMN_Start = mu.QgMX_End+1; % Min. reactive power generation
mu.QgMN_End = mu.QgMX_End + No_Q_GEN;

mu.V_MX = mu.V_MX_Start : mu.V_MX_End ;
mu.V_MN = mu.V_MN_Start : mu.V_MN_End ;
mu.I_MX = mu.I_MX_Start : mu.I_MX_End ;
mu.PgMX = mu.PgMX_Start : mu.PgMX_End ;
mu.PgMN = mu.PgMN_Start : mu.PgMN_End ;
mu.QgMX = mu.QgMX_Start : mu.QgMX_End ;
mu.QgMN = mu.QgMN_Start : mu.QgMN_End ;
mu.VT = mu.QgMN_End + 1;

```

```

mu.Length = mu.VT ;
% -----
% Initial guesses for Pg,Qg,PLoad,V,theta,lamda,mu and s
z = sparse(y.Length,1);
if NB_OLD == 5
    z(y.Pg,1) = 1.9847;
    z(y.Qg,1) = 0.7155;
    z(y.V,1) = [1.0800 ; 1.0651 ; 1.0338 ; 1.0292 ; 1.0361 ; 1.03 ; 1.03 ];
    z(y.II,1) = 1.1934;
    z(y.IO,1) = 1.1934;
    z(y.Theta) = [ -0.0681 ; -0.2008 ; -0.1581 ; -0.1348 ; -0.06 ; -0.06 ];
    z(y.deltaI) = 0.05;
    z(y.delta0) = 0.05;
    z(y.Vp) = 0.01;
    z(y.Vq) = 0.05;
    z(y.Ip) = 0.01;
    z(y.Iq) = 0.01;
end; % if

if NB_OLD == 14
    z=IEEE14_initial(y,UPFC_POS);
end;

if NB_OLD == 30
    z(y.Pg,1) = [2.0464    0.4741    0.7209    0.4169    0.1000    0.1000 ]';
    z(y.Qg,1) = [-0.0418    0.0551    0.2553    0.2502    0.1984    0.2660 ]';
    z(y.V,1) = 1.02;
    z(y.II,1) = 1.1934;
    z(y.IO,1) = 1.1934;
    z(y.Theta) = -0.1;
    z(y.deltaI) = 0.05;
    z(y.delta0) = 0.05;
    z(y.Vp) = 0.01;
    z(y.Vq) = 0.05;
    z(y.Ip) = 0.01;
    z(y.Iq) = 0.01;
end;
LAMDA = 10*ones(lamda.Length,1);
s = ones(mu.Length,1);
S = diag(s);
MU = 10*ones(mu.Length,1);
M = diag(MU);

Z = [z ; LAMDA ; MU; s];
% -----
% Indices for "Z"
IX.lamda_Start = y.Length + 1;
IX.lamda_End = y.Length + lamda.Length;
IX.mu_Start = IX.lamda_End + 1;
IX.mu_End = IX.lamda_End + mu.Length;
IX.S_Start = IX.mu_End + 1;
IX.S_End = IX.mu_End + mu.Length;

IX.lamda = IX.lamda_Start : IX.lamda_End;
IX.mu = IX.mu_Start : IX.mu_End;
IX.S = IX.S_Start : IX.S_End;
% -----
% Form matrix dh & DDH with constants
dh = sparse(lamda.Length,y.Length); % Jacobian of equality constraints
DDH = sparse(y.Length,y.Length); % Hessian of equality constraints

dh(lamda.Pin,y.Pg) = speye(No_P_GEN,No_P_GEN);
dh(lamda.Qin,y.Qg) = speye(No_Q_GEN,No_Q_GEN);
% -----
% Form matrix dg & ddgwith constants
dg = sparse(mu.Length,y.Length); % Jacobian of inequality constraints
DDG = sparse(y.Length,y.Length); % Hessian of inequality constraints

dg(mu.PgMX,y.Pg) = speye(No_P_GEN, No_P_GEN); % For real power generation limit

```

```

dg(mu.PgMN,y.Pg) = -speye(No_P_GEN, No_P_GEN);
dg(mu.QgMX,y.Qg) = speye(No_Q_GEN, No_Q_GEN); % For reactive power generation limit
dg(mu.QgMN,y.Qg) = -speye(No_Q_GEN, No_Q_GEN);
dg(mu.V_MX,y.V) = speye(NB,NB); % For voltage limit
dg(mu.V_MN,y.V) = -speye(NB,NB);
% -----
% Find inequality values
g0 = [-V_MX ; V_MN ; -ILmax.^2 ; -x.Pgmax/Sbase ; x.Pgmin/Sbase ;
      -x.Qgmax/Sbase ; x.Qgmin/Sbase ; -VT^2];
% -----
% Form matrix ddF
ddF = sparse(y.Length,y.Length);
df0 = sparse(y.Length,1);

ddF(y.Pg,y.Pg) = 2 * diag(x.gamma_c)*Sbase^2;
df0(y.Pg) = x.beta_c*Sbase;
N1 = y.Length; N2 = lamda.Length; N3 = mu.Length; N4 = mu.Length;
i = 0;
while nu > 1e-11 & i < 100
    i=i+1;
    % -----
    theta = [0 ; Z(y.Theta)];
    V = Z(y.V);
    Vph = V.*exp(j*theta);
    I = Ybus*Vph;
    Si = Vph.*conj(I);
    PG(Pg_bus) = Z(y.Pg);
    QG(Qg_bus) = Z(y.Qg);
    % -----
    % Equality constraints "h"
    h = zeros(lamda.Length,1);
    h(lamda.P,1) = PG-PL-real(Si(1:Nb_OLD));
    h(lamda.Q,1) = QG-QL-imag(Si(1:Nb_OLD));
    IIin = Z(y.II)*exp(j*Z(y.deltaI))+Vph(Nb-1)*(Ybranch(NL)+Yshunt(NL))-Vph(FR_I)*Ybranch(NL);
    IOin = -Z(y.IO)*exp(j*Z(y.delta0))+Vph(Nb)*(Ybranch(NL+1)+Yshunt(NL+1))-Vph(TO_0)*Ybranch(NL+1);
    I_Equ = (Z(y.Ip)+j*Z(y.Iq))*exp(j*Z(y.thetaI))+Z(y.IO)*exp(j*Z(y.delta0))-Z(y.II)*exp(j*Z(y.deltaI));
    V_Equ = Vph(Nb)-Vph(Nb-1)-(Z(y.Vp)+j*Z(y.Vq))*exp(j*Z(y.delta0));
    h(lamda.IIinR) = real(IIin);
    h(lamda.IIinI) = imag(IIin);
    h(lamda.IOinR) = real(IOin);
    h(lamda.IOinI) = imag(IOin);
    h(lamda.IR) = real(I_Equ);
    h(lamda.II) = imag(I_Equ);
    h(lamda.VR) = real(V_Equ);
    h(lamda.VI) = imag(V_Equ);
    h(lamda.RP) = Z(y.VI)*Z(y.Ip)-Z(y.Vp)*Z(y.IO);
    % -----
    % Jacobian of equality constraints "dh"
    % Current injection at regular buses
    Jsv = diag(Vph)*conj(Ybus)*conj(diag(exp(j*theta))+diag(exp(j*theta).*conj(I)));
    Jst = -j*diag(Vph)*conj(Ybus)*conj(diag(Vph))+diag(j*Si);

    dh(lamda.P, y.V) = -real(Jsv(1:Nb_OLD,:));
    dh(lamda.Q, y.V) = -imag(Jsv(1:Nb_OLD,:));
    dh(lamda.P, y.Theta) = -real(Jst(1:Nb_OLD,2:Nb));
    dh(lamda.Q, y.Theta) = -imag(Jst(1:Nb_OLD,2:Nb));

    % Current injection at UPFC input
    dh_IIin = zeros(1,y.Length);
    dh_IIin(1,y.V(FR_I)) = -exp(j*theta(FR_I))*Ybranch(NL);
    dh_IIin(1,y.VI) = exp(j*Z(y.thetaI))*(Yshunt(NL)+Ybranch(NL));
    dh_IIin(1,y.II) = exp(j*Z(y.deltaI));
    if FR_I ~= 1 % Bus 1 is the slack bus.
        dh_IIin(1,y.Theta(FR_I-1)) = -j*Vph(FR_I)*Ybranch(NL);
    end;
    dh_IIin(1,y.thetaI) = j*Vph(Nb-1)*(Yshunt(NL)+Ybranch(NL));
    dh_IIin(1,y.deltaI) = j*Z(y.II)*exp(j*Z(y.deltaI));

    % Current injection at UPFC output

```

```

dh_IOin = zeros(1,y.Length);
dh_IOin(1,y.V(TO_0)) = -exp(j*theta(TO_0))*Ybranch(NL+1);
dh_IOin(1,y.V0) = exp(j*Z(y.theta0))*(Yshunt(NL+1)+Ybranch(NL+1));
dh_IOin(1,y.IO) = -exp(j*Z(y.delta0));
if TO_0 ~= 1 % Bus 1 is the slack bus.
    dh_IOin(1,y.Theta(TO_0-1)) = -j*Vph(TO_0)*Ybranch(NL+1);
end;
dh_IOin(1,y.theta0) = j*Vph(NB)*(Yshunt(NL+1)+Ybranch(NL+1));
dh_IOin(1,y.delta0) = -j*Z(y.IO)*exp(j*Z(y.delta0));

dh(lamda.IIinR,:) = real(dh_IIin);
dh(lamda.IIinI,:) = imag(dh_IIin);
dh(lamda.IOinR,:) = real(dh_IOin);
dh(lamda.IOinI,:) = imag(dh_IOin);

% UPFC current equality
dh_I = zeros(1,y.Length);
dh_I(1,y.II) = -exp(j*Z(y.deltaI));
dh_I(1,y.IO) = exp(j*Z(y.delta0));
dh_I(1,y.Ip) = exp(j*Z(y.thetaI));
dh_I(1,y.Iq) = j*exp(j*Z(y.thetaI));
dh_I(1,y.thetaI) = j*(Z(y.Ip)+j*Z(y.Iq))*exp(j*Z(y.thetaI));
dh_I(1,y.deltaI) = -j*Z(y.II)*exp(j*Z(y.deltaI));
dh_I(1,y.delta0) = j*Z(y.IO)*exp(j*Z(y.delta0));

dh(lamda.IR,:) = real(dh_I);
dh(lamda.II,:) = imag(dh_I);

% UPFC voltage equality
dh_V = zeros(1,y.Length);
dh_V(1,y.VI) = -exp(j*Z(y.thetaI));
dh_V(1,y.V0) = exp(j*Z(y.theta0));
dh_V(1,y.Vp) = -exp(j*Z(y.delta0));
dh_V(1,y.Vq) = -j*exp(j*Z(y.delta0));
dh_V(1,y.thetaI) = -j*Z(y.VI)*exp(j*Z(y.thetaI));
dh_V(1,y.theta0) = j*Z(y.V0)*exp(j*Z(y.theta0));
dh_V(1,y.delta0) = -j*(Z(y.Vp)+j*Z(y.Vq))*exp(j*Z(y.delta0));

dh(lamda.VR,:) = real(dh_V);
dh(lamda.VI,:) = imag(dh_V);

% UPFC real power equality
dh(lamda.RP,y.VI) = Z(y.Ip);
dh(lamda.RP,y.Vp) = -Z(y.IO);
dh(lamda.RP,y.Ip) = Z(y.VI);
dh(lamda.RP,y.IO) = -Z(y.Vp);
% -----
% Hessian of equality constraints "ddh"
% Current injection at regular buses
ddh = zeros(2*Nb-1,2*Nb-1); % Hessian of equality constraints
for m = 1 : Nb_OLD
    ddh_V = zeros(Nb,Nb);
    ddh_V(m,:) = exp(j*theta(m))*conj(Ybus(m,:)).*exp(-j*theta');
    ddh_V(:,m) = ddh_V(m,:).';
    ddh_V(m,m) = 2*conj(Ybus(m,m));

    ddh_theta = zeros(Nb,Nb);
    ddh_theta(m,:) = Vph(m)*conj(Ybus(m,:)).*Vph';
    ddh_theta(:,m) = ddh_theta(m,:).';
    ddh_theta = ddh_theta - diag(ddh_theta(m,:));
    ddh_theta(m,m) = -Si(m) + V(m)^2*conj(Ybus(m,m));

    ddh_V_theta = zeros(Nb,Nb);
    ddh_V_theta(m,:) = -j*exp(j*theta(m))*conj(Ybus(m,:)).*Vph';
    ddh_V_theta(:,m) = j*Vph(m)*conj(Ybus(m,:)).'*exp(-j*theta(:));
    ddh_V_theta = ddh_V_theta - diag(ddh_V_theta(:,m));
    ddh_V_theta(m,m) = j*exp(j*theta(m))*conj(Ybus(m,:))*conj(Vph)-j*V(m)*conj(Ybus(m,m));

    ddh_theta_V = ddh_V_theta.';

```

```

ddh_S = [ ddh_V          ddh_V_theta(:,2:NB)
          ddh_theta_V(2:NB,:) ddh_theta(2:NB,2:NB) ];
ddh_P = Z(IX.lamda(m))*real(ddh_S);
ddh_Q = Z(IX.lamda(m+NB_OLD))*imag(ddh_S);
ddh = ddh + ddh_P + ddh_Q;
end;
DDH1 = sparse(y.Length,y.Length);
DDH1([y.V y.Theta],[y.V y.Theta]) = -ddh;

% Current injection at UPFC input
ddh2 = sparse(y.Length,y.Length);
if FR_I ~= 1
    ddh2(y.Theta(FR_I-1),y.Theta(FR_I-1)) = Vph(FR_I)*Ybranch(NL);
    ddh2(y.V(FR_I),y.Theta(FR_I-1)) = -j*exp(j*theta(FR_I))*Ybranch(NL);
    ddh2(y.Theta(FR_I-1), y.V(FR_I)) = ddh2(y.V(FR_I),y.Theta(FR_I-1));
end;
ddh2(y.thetaI,y.thetaI) = -Vph(NB-1)*(Ybranch(NL)+Yshunt(NL));
ddh2(y.deltaI,y.deltaI) = -Z(y.II)*exp(j*Z(y.deltaI));
ddh2(y.VI,y.thetaI) = j*exp(j*Z(y.thetaI))*(Ybranch(NL)+Yshunt(NL));
ddh2(y.thetaI,y.VI) = ddh2(y.VI,y.thetaI);
ddh2(y.II,y.deltaI) = j*exp(j*Z(y.deltaI));
ddh2(y.deltaI,y.II) = ddh2(y.II,y.deltaI);

DDH2 = real(ddh2)*Z(IX.lamda(lamda.IIinR)) + imag(ddh2)*Z(IX.lamda(lamda.IIinI));

% Current injection at UPFC output
ddh3 = sparse(y.Length,y.Length);
if T0_0 ~= 1
    ddh3(y.Theta(T0_0-1),y.Theta(T0_0-1)) = Vph(T0_0)*Ybranch(NL+1);
    ddh3(y.V(T0_0),y.Theta(T0_0-1)) = -j*exp(j*theta(T0_0))*Ybranch(NL+1);
    ddh3(y.Theta(T0_0-1), y.V(T0_0)) = ddh3(y.V(T0_0),y.Theta(T0_0-1));
end;
ddh3(y.theta0,y.theta0) = -Vph(NB)*(Ybranch(NL+1)+Yshunt(NL+1));
ddh3(y.delta0,y.delta0) = Z(y.IO)*exp(j*Z(y.delta0));
ddh3(y.V0,y.theta0) = j*exp(j*Z(y.theta0))*(Ybranch(NL+1)+Yshunt(NL+1));
ddh3(y.theta0,y.V0) = ddh3(y.V0,y.theta0);
ddh3(y.IO,y.delta0) = -j*exp(j*Z(y.delta0));
ddh3(y.delta0,y.IO) = ddh3(y.IO,y.delta0);

DDH3 = real(ddh3)*Z(IX.lamda(lamda.IOinR)) + imag(ddh3)*Z(IX.lamda(lamda.IOinI));

% UPFC current equality
ddh4 = sparse(y.Length,y.Length);
ddh4(y.thetaI,y.thetaI) = -(Z(y.Ip)+j*Z(y.Iq))*exp(j*Z(y.thetaI));
ddh4(y.deltaI,y.deltaI) = Z(y.II)*exp(j*Z(y.deltaI));
ddh4(y.delta0,y.delta0) = -Z(y.IO)*exp(j*Z(y.delta0));
ddh4(y.II,y.deltaI) = -j*exp(j*Z(y.deltaI));
ddh4(y.deltaI,y.II) = ddh4(y.II,y.deltaI);
ddh4(y.IO,y.delta0) = j*exp(j*Z(y.delta0));
ddh4(y.delta0,y.IO) = ddh4(y.IO,y.delta0);
ddh4(y.Ip,y.thetaI) = j*exp(j*Z(y.thetaI));
ddh4(y.thetaI,y.Ip) = ddh4(y.Ip,y.thetaI);
ddh4(y.Iq,y.thetaI) = -exp(j*Z(y.thetaI));
ddh4(y.thetaI,y.Iq) = ddh4(y.Iq,y.thetaI);

DDH4 = real(ddh4)*Z(IX.lamda(lamda.IR)) + imag(ddh4)*Z(IX.lamda(lamda.II));

% UPFC voltage equality
ddh5 = sparse(y.Length,y.Length);
ddh5(y.thetaI,y.thetaI) = Z(y.VI)*exp(j*Z(y.thetaI));
ddh5(y.theta0,y.theta0) = -Z(y.V0)*exp(j*Z(y.theta0));
ddh5(y.delta0,y.delta0) = (Z(y.Vp)+j*Z(y.Vq))*exp(j*Z(y.delta0));
ddh5(y.VI,y.thetaI) = -j*exp(j*Z(y.thetaI));
ddh5(y.thetaI,y.VI) = ddh5(y.VI,y.thetaI);
ddh5(y.V0,y.theta0) = j*exp(j*Z(y.theta0));
ddh5(y.theta0,y.V0) = ddh5(y.V0,y.theta0);
ddh5(y.Vp,y.delta0) = -j*exp(j*Z(y.delta0));
ddh5(y.delta0,y.Vp) = ddh5(y.Vp,y.delta0);

```

```

ddh5(y.Vq,y.delta0) = exp(j*Z(y.delta0));
ddh5(y.delta0,y.Vq) = ddh5(y.Vq,y.delta0);

DDH5 = real(ddh5)*Z(IX.lamda(lamda.VR)) + imag(ddh5)*Z(IX.lamda(lamda.VI));

% UPFC real power equality
ddh6 = sparse(y.Length,y.Length);
ddh6(y.VI,y.Ip) = 1;
ddh6(y.Ip,y.VI) = 1;
ddh6(y.Vp,y.I0) = -1;
ddh6(y.I0,y.Vp) = -1;

DDH6 = ddh6 * Z(IX.lamda(lamda.RP));

% Construction of total "ddh"
DDH = DDH1 + DDH2 + DDH3 + DDH4 + DDH5 + DDH6;
% -----
% Inequality constraints "g"
Iik = (Vph(FR)-Vph(TO)).*Ybr+Ysh.*Vph(FR);
gg = zeros(N3,1);
gg(mu.V_MX) = Z(y.V);
gg(mu.V_MN) = -Z(y.V);
gg(mu.I_MX) = Iik.*conj(Iik);
gg(mu.PgMX) = Z(y.Pg);
gg(mu.PgMN) = -Z(y.Pg);
gg(mu.QgMX) = Z(y.Qg);
gg(mu.QgMN) = -Z(y.Qg);
gg(mu.VT) = Z(y.Vp)^2 + Z(y.Vq)^2;

g = gg + g0;
% -----
% Jacobian of inequality constraints "dg"
% Line flow inequality
dI_dVi = exp(j*theta(FR)).*(Ybr+Ysh);
dI_dVk = -exp(j*theta(TO)).*Ybr;

dIdVi = sparse((1:2*(NL+1)),FR,conj(Iik).*dI_dVi+Iik.*conj(dI_dVi),2*(NL+1),NB);
dIdVk = sparse((1:2*(NL+1)),TO,conj(Iik).*dI_dVk+Iik.*conj(dI_dVk),2*(NL+1),NB);
dIdV = dIdVi + dIdVk;
dg(mu.I_MX,y.V) = dIdV;

dI_dthetai = j*Vph(FR).*(Ybr+Ysh);
dI_dthetak = -j*Vph(TO).*Ybr;

dIdthetai = sparse((1:2*(NL+1)),FR,conj(Iik).*dI_dthetai+Iik.*conj(dI_dthetai),2*(NL+1),NB);
dIdthetak = sparse((1:2*(NL+1)),TO,conj(Iik).*dI_dthetak+Iik.*conj(dI_dthetak),2*(NL+1),NB);
dIdtheta = dIdthetai + dIdthetak;
dg(mu.I_MX,y.Theta) = dIdtheta(:,2:NB);

% Injected voltage magnitude inequality
dg(mu.VT,y.Vp) = 2 * Z(y.Vp);
dg(mu.VT,y.Vq) = 2 * Z(y.Vq);
% -----
% Hessian of inequality constraints "ddg"
ddg = zeros(2*Nb-1,2*Nb-1);
for m = 1 : 2*(NL+1)
    ddg_V = sparse(Nb,Nb);
    ddg_V(FR(m),FR(m)) = 2*conj(dI_dVi(m))*dI_dVi(m);
    ddg_V(FR(m),TO(m)) = conj(dI_dVk(m))*dI_dVi(m) + dI_dVk(m)*conj(dI_dVi(m));
    ddg_V(TO(m),FR(m)) = ddg_V(FR(m),TO(m));
    ddg_V(TO(m),TO(m)) = 2*conj(dI_dVk(m))*dI_dVk(m);

    ddg_theta = sparse(Nb,Nb);
    ddI_ddthetaii = -(Ybr(m)+Ysh(m))*Vph(FR(m));
    ddg_theta(FR(m),FR(m)) = Iik(m)'* ddI_ddthetaii+2*conj(dI_dthetai(m))*...
        dI_dthetai(m) + Iik(m)*conj(ddI_ddthetaii);
    ddg_theta(FR(m),TO(m)) = dI_dthetai(m)*dI_dthetak(m)+dI_dthetai(m)*dI_dthetak(m)';
    ddg_theta(TO(m),FR(m)) = ddg_theta(FR(m),TO(m));
    ddI_ddthetakk = Ybr(m)*Vph(TO(m));

```

```

ddg_theta(TO(m),TO(m))=Iik(m)'*ddI_ddthetakk+2*dI_dthetak(m)'*dI_dthetak(m)...
+Iik(m)*ddI_ddthetakk';

ddg_V_theta = sparse(NB,NB);
ddI_dVi_dthetai = j*exp(j*theta(FR(m)))*(Ybr(m)+Ysh(m));
ddg_V_theta(FR(m),FR(m)) = Iik(m)'*ddI_dVi_dthetai + dI_dVi(m)'*dI_dthetai(m)+...
dI_dVi(m)*dI_dthetai(m)'+ Iik(m)*ddI_dVi_dthetai';
ddI_dVk_dthetak = -j*exp(j*theta(TO(m)))*Ybr(m);
ddg_V_theta(TO(m),TO(m)) = Iik(m)'*ddI_dVk_dthetak+dI_dVk(m)'*dI_dthetak(m)+...
dI_dVk(m)*dI_dthetak(m)'+Iik(m)*ddI_dVk_dthetak';

ddg_theta_V = ddg_V_theta.';

ddg_Iik = [ ddg_V          ddg_V_theta(:,2:NB)
            ddg_theta_V(2:NB,:) ddg_theta(2:NB,2:NB)];
ddg = ddg + Z(IX.mu(mu.I_MX(m)))*ddg_Iik;
end;
DDG([y.Vp y.Vq],[y.Vp y.Vq]) = Z(IX.mu(mu.VT))*2*speye(2,2);
DDG([y.V y.Theta],[y.V y.Theta]) = ddg;
% -----
H_All = ddF + DDH + DDG;
J = real([ H_All          dh.'          dg.'          sparse(N1,N3) ;
           dh            sparse(N2,N2)      sparse(N2,N3)      sparse(N2,N3) ;
           dg            sparse(N3,N2)      sparse(N3,N3)      speye(N3,N3) ;
           sparse(N3,N1) sparse(N3,N2)          S              M      ]);

dF = ddF*Z(1:N1) + df0;
dY = real([-dF-dh.'*Z(N1+1:N1+N2)-dg.'*Z(N1+N2+1:N1+N2+N3)
           -h
           -g-Z(N1+N2+N3+1:N1+N2+2*N3)
           nu*ones(N3,1)-M*S*ones(N3,1)]);

dZ = J\dY;
dMU = dZ(IX.mu);
ds = dZ(IX.S);
S_Neg_Index = find(ds < 0);
alpha_S = min([1;-s(S_Neg_Index)./ds(S_Neg_Index)]);
MU_Neg_Index = find(dMU < 0);
alpha_MU = min([1;-MU(MU_Neg_Index)./dMU(MU_Neg_Index)]);
alpha = min(alpha_S ,alpha_MU);
Z = real(Z + alpha*dZ);
MU = Z(IX.mu);
s = Z(IX.S);
M = diag(MU);
S = diag(s);
if norm(M*s - MU.'*s/N3) <= psi*nu;
    nu = nu*0.5;
end;
end;
% -----
% Find the generation cost
fprintf('UPFC installed in line %1.0f\n', UPFC_POS);
Gen_Cost = x.gamma_c.*Z(y.Pg).^2*Sbase^2 + x.beta_c.*Z(y.Pg)*Sbase + x.alpha_c;
Total_Cost = sum(Gen_Cost);
% -----
% Real Power Loss
Sloss = zeros(NL+1,1);
Sik = Vph(FR).*conj((Vph(FR)-Vph(TO)).*Ybr+Ysh.*Vph(FR));
Sloss = Sik(1:NL+1) + Sik(NL+2:2*(NL+1));
Ploss = sum(real(Sloss));
Qloss = sum(imag(Sloss));
% -----

```